



Merged Report on In-Depth Case Studies

Partner Institutions:

TU Delft – Chair of Heritage and Technology

Institute of Theoretical and Applied Mechanics of the Czech Academy of Sciences (ITAM)

University of Genoa – School of Architecture

University of Cyprus

Editors: Gabriel Pardo Redondo and Silvia Naldini (TU Delft)

Date: November 19, 2021

Table of Contents

| | |
|---|-----|
| Table of Contents | 1 |
| Introduction..... | 2 |
| In-Need Case Studies | 3 |
| Report on In-Depth Case Study The Fenix II (Rotterdam, The Netherlands, 1920-1922 and 1951-1954)..... | 4 |
| Report on In-Depth Case Study The Henebique Silos (Genoa, Italy, 1899, 1901, 1906, 1924)..... | 26 |
| Report on In-Depth Case Study Fruit and Vegetable market (Genoa, Italy, 1926 to 1930's) | 55 |
| Report on In-Depth Case Study Barrandov Diving Tower (Prague, Czech Republic, 1930)..... | 71 |
| Report on In-Depth Case Study Fuchs restaurant (Prague, Czech Republic, early 1930s) | 98 |
| Report on In-Depth Case Study The Melkonian Education Center (Nicosia, Cyprus, 1924 and 1926) | 129 |
| Report on In-Depth Case Study Old municipal market (Nicosia, Cyprus, 1965)..... | 148 |
| Restored Cases | 172 |
| Report on In-Depth Case Study Case Study: Timmerfabriek (Vlissingen) | 173 |
| Report on In-Depth Case Study Museum of the Treasury of San Lorenzo, Genoa..... | 189 |
| Report on In-Depth Case Study Alexandros Dimitrou Tower (Nicosia, Cyprus, 1966) .. | 210 |
| Discussion and Conclusions | 234 |

Introduction

The concrete used for buildings from the end of the XIX century to the 1960's can be called historic as it had an experimental character. Experimental means that the component materials and their proportions in the mixture varied, the fabrication techniques were entrusted to handicrafts, and the design of the reinforcement was based on other criteria, and on less precise calculations than modern concrete.

In this joint report ten historic concrete buildings are dealt with. This report summarizes the in depth investigations carried out in selected sample of 48 case studies, located in the countries involved in the project. The buildings cover a range of systems and methods by which early concrete buildings were constructed. From the early and massive Hennebique Silos (1901) in Genoa to the residential tower Alexandros Dimitrou Tower (1966) in Nicosia. Two building types are investigated depending on their current condition: (i) a building in need of restoration, to study the damage present and follow the intervention process; (ii) a restored building, to assess the (potential) damage and the restoration possibilities of historic concrete buildings. Some buildings are not entirely in concrete, but include brick infills or natural stone parts. Most buildings are plastered. A coating/paint layer is often present on the concrete or on the plaster.

The investigation and report aim at :

1. Providing an overview of historic concrete buildings in Europe, underlining peculiarities and (technical) developments.
2. Highlighting the challenges related to the renovation of historic concrete buildings.
3. Identifying the aspects contributing to make a renovation project successful from a technical point of view.

In-Need Case Studies

Report on In-Depth Case Study

The Fenix II (Rotterdam, The Netherlands, 1920-1922 and 1951-1954)



Type: In-need of Restoration Case

Partner Institution: TU Delft

Project: **CONSECH 20**

Working Package 2 – Task (iii)

Date: June 15, 2021

By:

Gabriel Pardo Redondo

Silvia Naldini

Barbara Lubelli

Introduction

Characteristics of the Concrete Building and Structure

The Fenix concrete building, formerly known as the San Francisco warehouse - was constructed between 1920 and 1922 and was at the time the largest warehouse in the harbour of Rotterdam – Katendrecht. It disposed of modern techniques for lifting and storing goods, consisting of 12 elevators, high capacity hatches and movable cranes.

It was designed by architect C.N. van Goor. The warehouse served as a storage place for the Holland Amerika Lijn. The luggage was brought to the warehouse by trains, and directly loaded from the trains into the building. Originally the ground floor of the south façade was furnished with an open arcade. On the north façade, the luggage was loaded into the ships.



Figure 1. Fenix II under construction (circa 1920). Source: Holland Amerika Lijn. Loods San Francisco, Rotterdam. Holl. Beton My. 's Gravenhage. Gemeenteluke Archiefdienst Rotterdam 1978-1552.

In 1944, during the second world war, the quay side was bombed and harbour installations were blown up, resulting in damage to the north façade of the building. In 1947, a fire brought more damage to the building, resulting in the splitting of the building in 2 separate halls. The two buildings, named Fenix I and Fenix II, as a reminder of the fact that the building was 'reborn from its ashes', were restored between 1951 and 1954. The restoration included concrete and brick infills and an extension with balconies on the north façade. By then the Fenix also changed its owner: C. Steinweg, a company storing goods for shipping, mainly metal and steel. In the empty space between the two buildings, a cantina was built for the workers.

The Fenix II will soon be restored and transformed into a cultural centre. The building has a historical and social value, recalling harbour activities of the past. The building

was erected in concrete and is a witness of an early use of the material. Concrete fabrication and building techniques have changed substantially in the 1960's. Older concrete materials and techniques should be identified and preserved as much as possible within the transformation process (adaptive re-use).

Relevant interventions on the Fenix II consisted in the addition of a render layer on the external surface of the south facade circa 1980 by the company Vogel. This render varies in thickness (up to 60 mm). On top of the render, an additional thin finish red render layer (+/- 1 mm thick) was applied as part of the process, the material of this finish is [Kristal Cement Graniet](#) (KCG).



Figure 2. North facade of the Fenix II between 1922 and 1944. Source: Holland Amerika Lijn. Loods San Francisco, Rotterdam. Holl. Beton My. 's Gravenhage. Gemeenteluke Archiefdienst Rotterdam 1978-1952.

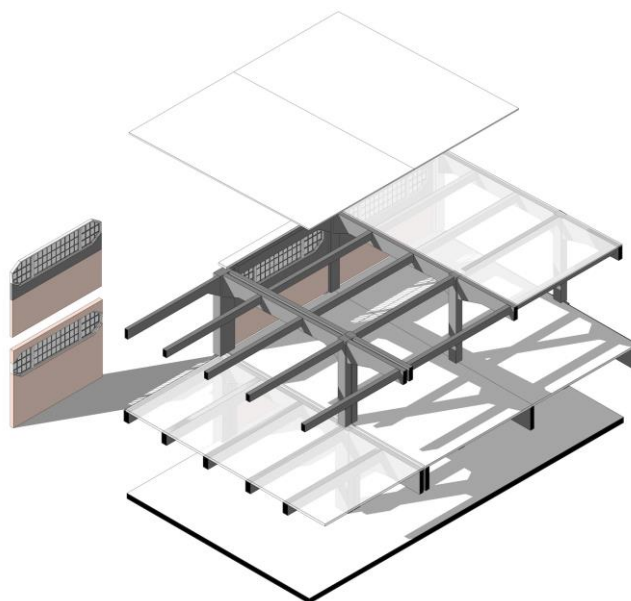


Figure 3. Exploded axonometric view of the building components. Source: source: Report on the state of conservation of Fenix II, Rotterdam. AR0141 CSI – Heritage Conservation, Survey, Investigation of the Built Heritage. (2020). Cher van den Eng, Jonathan Connerney, Mingyu Kim, & Saskia Tideman

Condition of the building

The interior structure of the building is in good state of conservation; there are no general signs of damage in floors and columns. As mentioned before the damage rather concerns specific locations on the external walls and columns.

The exterior of the building concentrates extensive and severe damage, especially the south facade. The north wall, built in 1951, has an open continuous balcony on the first floor. The area of the balcony has extensive biological growth in the upper side and edge, and scattered spalling, cracks and rust layers in the underside of the balcony slab. Some of the columns of the ground floor, especially the ones closer to the expansion joints of the building, also exhibit scattered signs of damage induced by corrosion (spalling and cracks); the water seems to easily drip through the balcony slab and run down to the face of the columns.



Figure 5. Interior view of the building at the northern bay on the first floor (2020).



Figure 5. Corrosion damage in column at the north facade (2020).

In the exterior face of the south façade the following damage were found: Cracks, spalling, and exposed rebar with rust layers. The damage were located in the majority of the columns and under the eaves, and in a lesser extent in the walls of the first floor. The added render from the 1980s did not seem to add protection to the reinforcement, and the visible corrosion is severe, which can affect the structural integrity of the columns. The spalling often affects substantial sections of the concrete, and the loss of steel section, especially in smaller diameters, is beyond safe standards. In one of the columns under restoration at the time of the inspection, signs of pitting corrosion were visible in the rebar (Figure 6). Although, this damage type was only visible after cleaning the rebar with high-pressure water jets to remove the carbonated concrete. The interior

side of the south exterior columns have scattered, local signs of corrosion induced damage, which is not extensive.



Figure 6. Signs of pitting corrosion in one of the exterior columns of the south facade. This picture was taken after cleaning the concrete around the rebar with high-pressure water jets (2020).

Aim of the investigation

The aim of the investigation is to assess the concrete structure of the building and clarify and confirm the causes of the damage. The results and conclusions will be used in WP4 to determine the conservation proposals.

Methods and Results

The following tests were conducted with the aim of defining the causes of the corrosion induced damage:

- Moisture content,
- Carbonation depth,
- Reinforcement layout,
- Concrete cover,
- Compressive strength, and
- Chloride content.

The tests were conducted on 16 columns on July and October, 2020. The columns were selected according to two parameters: exposure (interior and exterior) and age (from 1920 and from 1951)



Figure 7. Picture inside the building

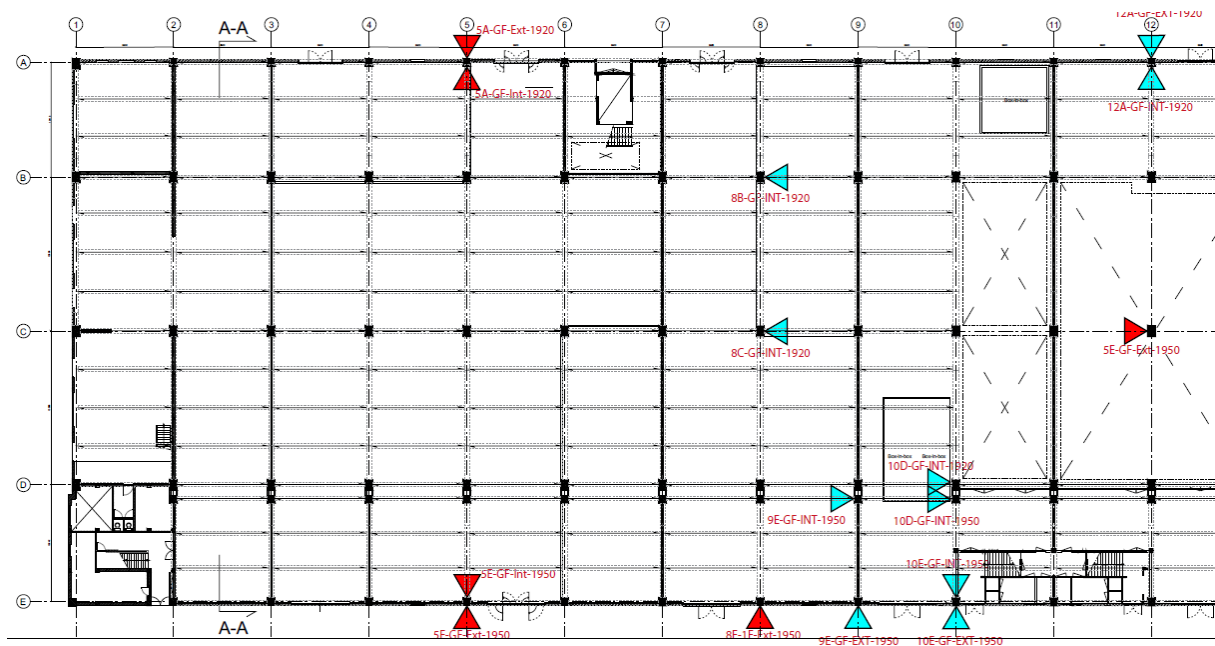


Figure 8. Floor map indicating the columns tested. Red triangles denote columns tested in July and Cyan triangles columns tested in October.

Concrete compressive strength

The rebound hammer Matest C-380 was used to estimate the compressive strength in accordance with NEN-EN 12504-2 [1].

Two exterior columns from 1920 were not tested due to the thick layer of render and/or excessive irregular surface (due to surface preparation to improve bonding with the new render, done in the current restoration works).

In the 1920 and 1951 columns, the average compressive strength of the columns is between 38 and 49 MPa. 1920's interior columns have an average strength of 41.05 MPa (± 2.37) and 1951's interior columns of 45.94 MPa (± 3.62). Exterior 1951's columns have an average of 47.88 MPa (± 1.93). (refer to Table 1).



Figure 9. Exterior south column with render removed.

Carbonation depth

10 mm diameter drills were performed in the selected columns (see Figure 9) at a height of 140 cm (± 10 cm) from the floor. The powder was collected at steps of 10 mm to a total depth of 60 mm. The powder was directly stored in an air tight plastic bags or bottles. Phenolphthalein solution in a concentration of 1% in ethanol was sprayed on the powder in the lab the same day the samples were collected (Figure 10).

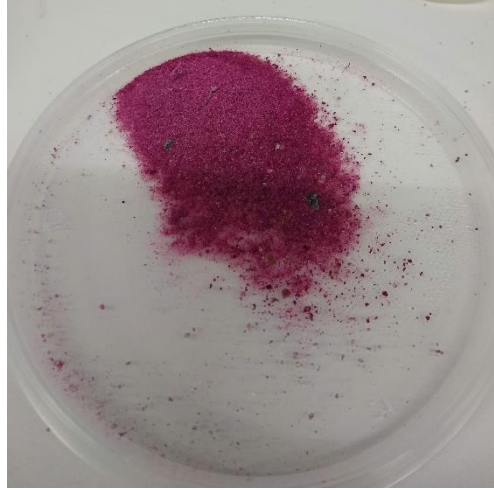


Figure 10. Powder sample in petri dish sprayed with phenolphthalein. The pink colour indicates a pH above 9.

The carbonation front of the 1951's columns was less than 10 mm in both exterior and interior columns. Whereas, the carbonation depth in the 1920's columns was 35 mm in the exterior columns, and 50 mm in interior (see Table 1). To note, the exterior face of column 5A (1920's column) had a 40 mm thick render applied in the 1980s. The carbonation profile revealed that the render was not carbonated, but the concrete from a depth of 50 mm had a slight carbonation, which had obviously occurred before the intervention.

| | | N | Min. Mean concrete cover (mm) | Max. mean carbonation front (mm) | Compressive strength (Mpa) |
|------|----------|----|-------------------------------------|--|----------------------------------|
| 1921 | Interior | 6 | 40,5 ($\pm 17,1$) | 50 ($\pm 6,3$) | 41,05 ($\pm 2,4$) |
| | Exterior | 2 | 58,5 ($\pm 26,2$) | 35 ($\pm 35,4$) | N/A |
| 1951 | Interior | 4 | 22 ($\pm 10,7$) | 10 (± 0) | 45,94 ($\pm 3,6$) |
| | Exterior | 4* | 26,25 ($\pm 12,8$) | 10 (± 0) | 47,88 ($\pm 1,9$) |

Table 1. Results of concrete cover, carbonation depth and compressive strength

Concrete cover

Profoscope cover meter from *Proceq* was used to determine the thickness of the concrete cover. A minimum of 6 readings were taken per column. The concrete cover of the ties (horizontal rebar) and vertical reinforcement of the columns were measured.

On average, the minimum concrete cover in the 1920's columns is about 40 mm, whereas the 1951's columns have a minimum average concrete cover of 22 mm. Exterior columns have between 4 to 16 mm more cover than interior columns. (refer to Table 1).



Figure 11. Exposed reinforcement in 1920's column.

Reinforcement layout and diameter

Proceq Profoscope was used to estimate the reinforcement layout and diameter. At the moment of the inspection, a few columns on the south facade were being repaired. The reinforcement of these columns were visible (Figure 12) and it was possible to confirm the readings obtained with the Profoscope.

The columns are reinforced with vertical round rebar with a diameter ranging from 18 to 32 mm, with a spacing between 150 and 250 mm. The horizontal reinforcement (or ties) has a diameter between 10 to 12 mm with a spacing between 250 to 350 mm on centre.

The main difference between 1920 and 1951's columns is the spacing of the ties. In the 1920s the usual spacing is 350 mm, whereas in the 1951s the maximum spacing is 250 mm.



Moisture content (MC)

Figure 12. Exposed vertical rebar in 1920 ground floor column (exposed side). The white-ish rebar is original (4 in total), the thinner slightly rusty rebar is new.

10 mm drills to obtain concrete powder were performed at 10 mm steps to a maximum of 60 mm depth. Powder was stored immediately in an air-tight plastic bag. The samples were weighed in the same day in a scale with a precision of 0.01g. Samples were placed in oven at 40 degrees Celsius for 48 hours and weighed again.



Figure 13. Samples for the determination of moisture content and chloride content.

MC is below 2% in all columns with the exception of 3 exterior columns that have MC peaks of 2.5, 3 and 8.5%. Average MC in interior columns is 0.62% (+/- 0.40%) and in exterior columns 2.41 (+/- 1.92%) (see Figure 14). Average MC in 1920s columns is 0.45% ($\pm 0.37\%$) for interior, and 1.75% ($\pm 0.51\%$) for exterior. For 1951s columns the average MC is 0.87% ($\pm 0.28\%$) for interior, and 2.73% ($\pm 2.26\%$) for exterior. One of the exterior 1951's columns was soaked wet due to a water infiltration from a drainpipe. Disregarding this column, the average MC of the 1951s exterior columns is 1.39% ($\pm 0.63\%$), which slightly less than for the 1920's exterior columns.

There is not significant difference between MC in exterior columns from 1920 and 1951. However, under the same interior conditions of temperature and humidity, 1951s interior columns tend to have a higher MC than those of the 1920s.

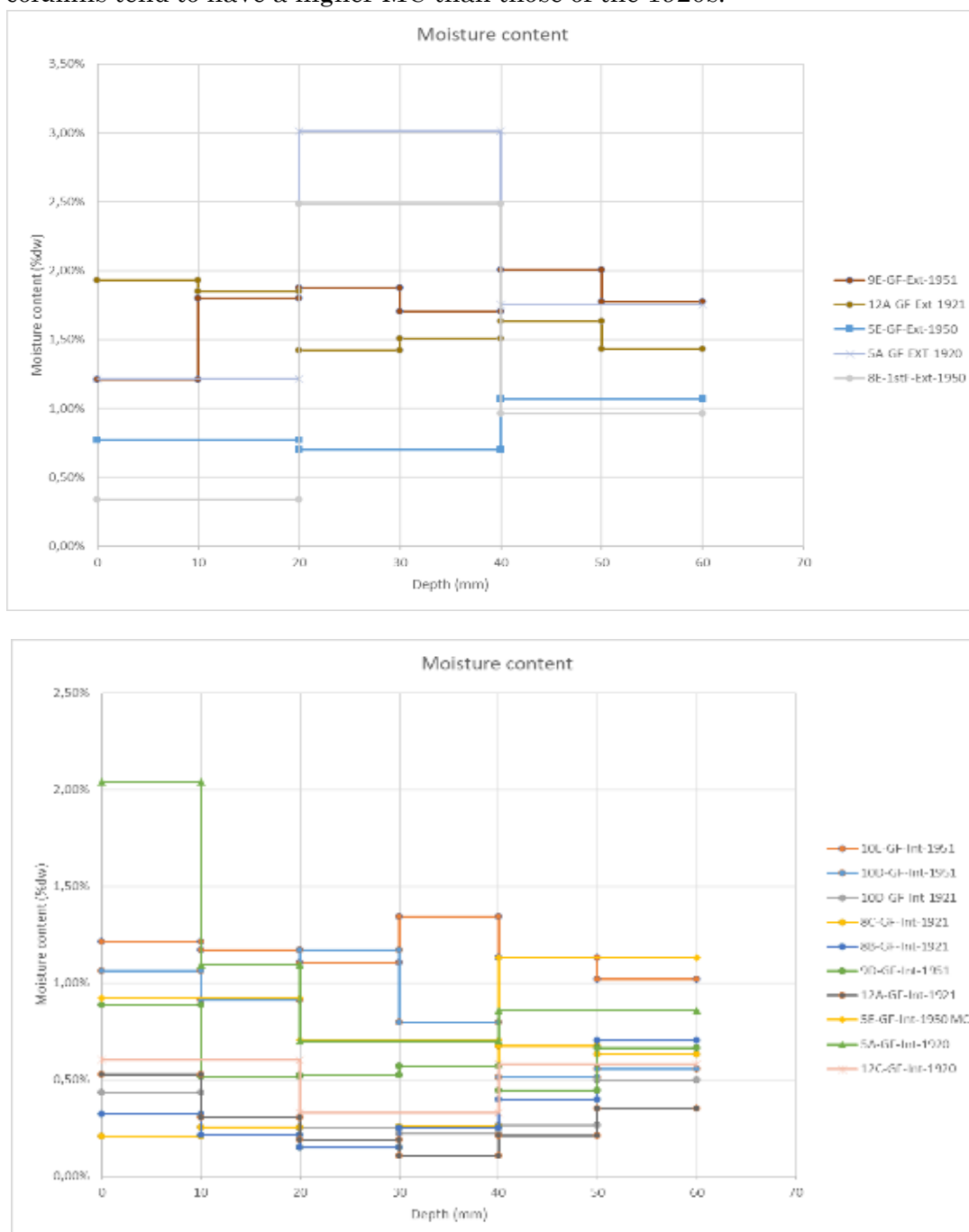


Figure 14. Moisture content of exterior columns (Top) and interior columns (Bottom).

Hygroscopic Moisture content

The dried powder samples of six columns were set in a climatic cabinet at 95% RH and 20°C for 10 days, after which the samples were weighed to determine the hygroscopic moisture content (HMC). The HMC gives an indication of the hygroscopic behaviour of the material and of the presence of soluble salts, and thus of their possible contribution to the measured MC.

HMC is higher than the MC content in all but one case of the sample, column (8E-1st-Ext-1951) (see Figure 15). This means that no moisture source is present in these cases. The increase ranges from 1.67 times in the sample 5A-Int-1920, depth 0-10 mm, to 6.55 times in the sample 5E-GF-Int-1951, depths 20 to 40 mm.

The distribution of the HMC along the depths shows higher values in the deeper intervals (20-60) regardless whether the columns were interior/exterior or dating from the 1920s or 1951s.

The highest HMC were in exterior columns with values from 4% to 5% in depths 20 to 60 mm. The maximum HMC in interior columns was 4.5%.

1920's columns have higher HMC values in depths 40-60 mm. Whereas the 1951's columns have higher values in depths 20 to 40 mm. That gives an indication where the highest concentration of salts might be, which in this case was used to select the samples for a chloride analysis.

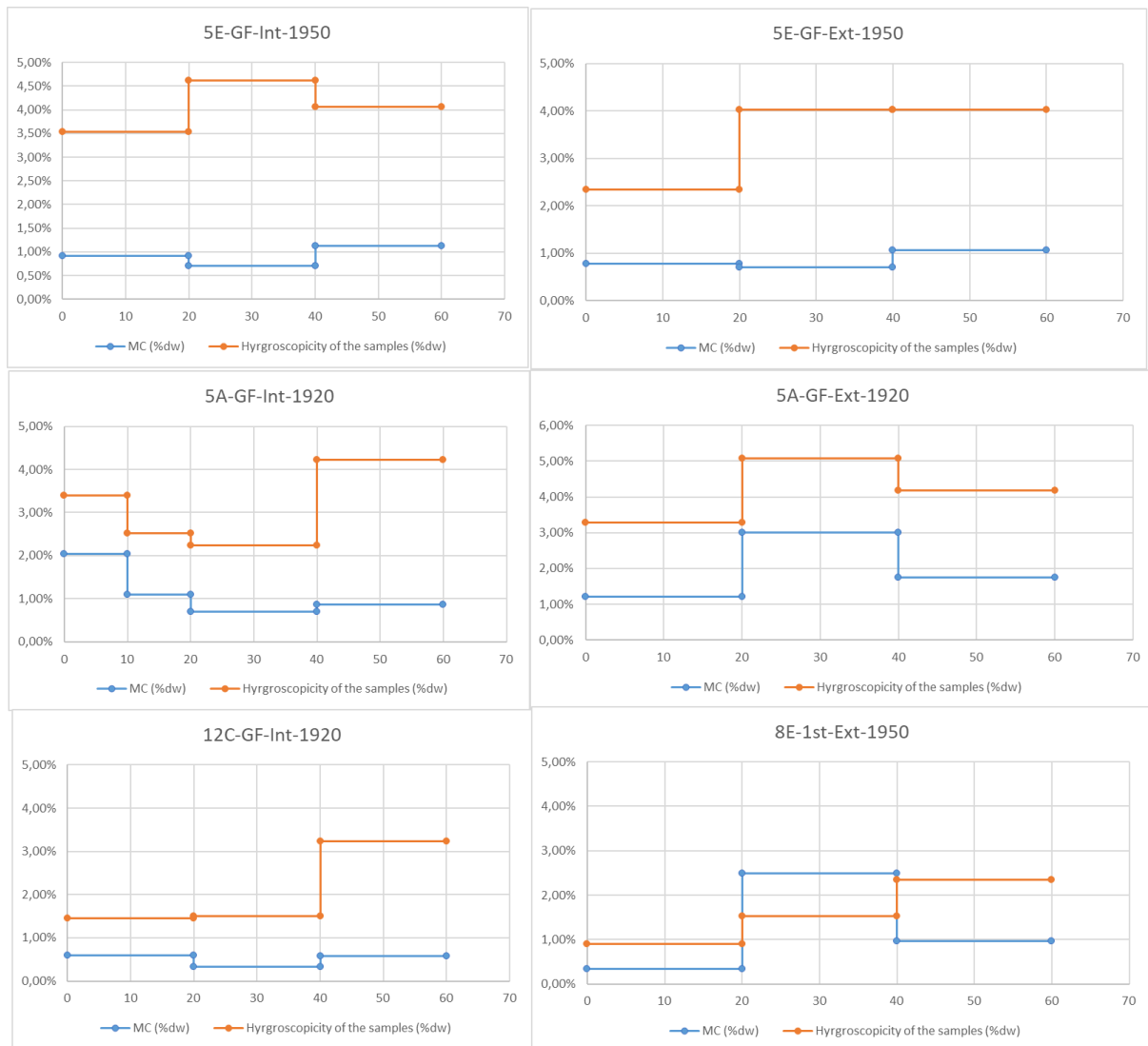


Figure 15. MC and HMC graphs of different samples.

Chloride content and type of cement

Four columns were tested -interior and exterior columns- for both ages, 1920 and 1951. The powder was collected from drills in 10 mm steps until a depth of 60 mm. The goal of the chloride testing was to determine the presence and concentration of chlorides in the concrete surrounding the rebar in order to assess the possible role of chloride-induced corrosion in the observed damage. In addition, the shallower depths in the two interior columns were also determined. The type of cement was also determined, Ordinary Portland Cement.

Both interior columns have similar profile (Figure 16), with a maximum chloride content per quantity of cement of 0.2% in the first 10 mm. In the area where the reinforcement is located (depths 20-40 mm), the chloride content is 0.1% or lower.

In the concrete surrounding the rebar of the exterior columns (30-50 mm), the chloride concentration is 0.3-0.2% in the 1951s, and 0.2-0.1% in the 1920s (Figure 16).

The results indicate that the chloride source comes from external sources and it is not in the concrete mixtures. The concentration decreases as the depth increases.

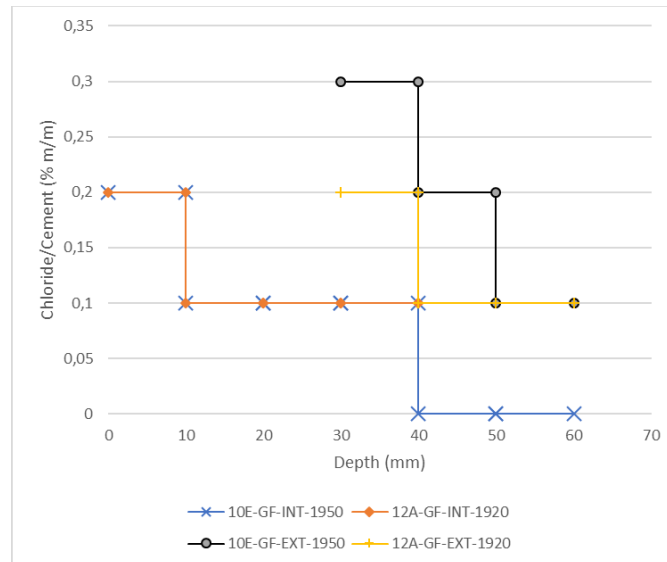


Figure 16. Concentration of chloride content in cement.

Assessment of the corrosion induced damage in the concrete structure

For the assessment of the concrete structures the Simplified Index of Structural Damage (SISD), developed in the project CONTECVET, is used [2]. This method quantifies the degree of corrosion induced damage in the concrete structure based on different parameters. The results of the assessment are used to establish the urgency and the strategy of intervention. The strategy of intervention will not be developed in the current report but in the Work Package 4.

The CONTECVET method uses two levels of assessment. A Simplified and a Detailed Assessment. The Simplified method is based on a qualitative approach related to damage classification methods. The Detailed Assessment is used when the severity of the damage compromises the load-bearing capacity of the structure [3]. In this case study, the load-bearing capacity of the structure was not compromised on a general level –the building has been functioning in the past years and there are no signs of structural damage– thus, only the Simplified Assessment method was performed (Figure 17).

The assessment was performed in the selected columns. Beams and slabs were not assessed due to accessibility constraints. The results show a medium to severe structural damage, all the results are summarized in **Error! Reference source not found.** The ‘medium’ structural damage includes the interior columns and the 1951’s exterior columns. The ‘severe’ structural damage includes the exterior columns from 1920. Respectively, the guidelines recommend to perform a detailed structural assessment

within 5 to 10 years for the ‘medium’ damaged columns, and within 2 to 5 years for the ‘severe’ damaged columns.

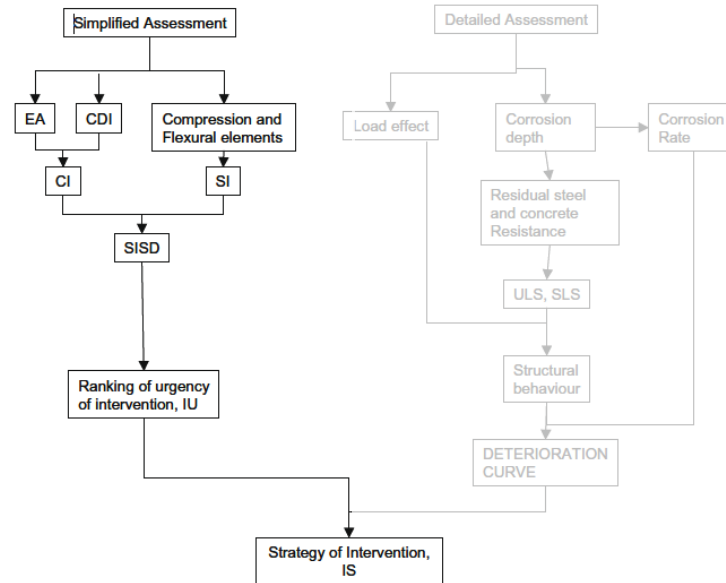


Figure 17. Simplified and detailed procedures for assessment of corrosion-damaged structures (where SISD is the simplified index of structural damage, SCI is the simplified corrosion index, SI is the structural index, EA is the environmental aggressiveness, CDI is the corrosion damage index). Source: CONTECVET Manual [2]

Discussion

The discussion focuses on the difference in the results obtained for the columns of the 1920's and those of the 1951's, and the difference between interior and exterior columns.

The concrete **compressive strength** of the 1951's columns are slightly higher than the 1920's, but there is not a substantial difference (Table 1). Considering the time of construction, 1920's columns have a relative high strength (41 MPa), given the fact that the minimum required compressive strength at the time of construction was 8 MPa [4]. Compressive strength is linked to different characteristics of the concrete, being the most relevant compaction, water/binder ratio and type of binder [5]. The type of binder in all columns is the same, Portland cement, suggesting that both concretes, 1920's and 1951's, may have similar water/cement ratios and compactness. Different works have also proved a correlation between higher compressive strength and higher carbonation resistance as mentioned by in the research of Monteiro et al. [6]. Therefore, it was expected that the 1951's carbonation depth was smaller than in the 1920's columns.

1951's columns have a consistent minimum **carbonation depth** of less than 10 mm. Whereas, 1920's columns have higher carbonation depths, from 10 mm up to 60 mm. This confirms the hypothesis that higher compressive strength have higher carbonation resistance, although this relation does not seem proportional. The difference in compressive strength is around 12%, whereas the carbonation depth can be up to 6 times

larger. The carbonation rate is a parabolic function related to a carbonation coefficient (K), multiplied by the square root of time (\sqrt{t}) according to Fick's first law [2,7]. In the literature, there are not a clear definition how to estimate K in existing buildings, since it is based on concrete composition and environment. Some authors have tried to establish a range of K values based on tests in existing buildings. For example, Monteiro et al. tested 87 concrete buildings up to 99 years old, obtaining values for K between 3.07 and 4.06 for unpainted concrete in relatively humid environments [6]. In the case under study, as the age and carbonation depth is known, the coefficient K can be obtained, resulting $K = 5$ for the 1920's and $K=1.195$ for the 1951's interior concrete columns. Once the coefficient K is obtained, the carbonation rate can be plotted to estimate when the carbonation front may reach the reinforcement (Figure 19).

Following this line of thought, identical concrete composition under similar environmental conditions should have similar carbonation rate. However, there is a substantial difference in carbonation between the interior and the exterior columns from the 1920s, there is not difference in the 1951's columns though. One explanation for the difference in carbonation rates of the 1920's columns is that, based on historical pictures, there was an original render, of about 10 mm, applied in the exterior face of the columns (Figure 18). Applying an additional render reduces the carbonation depth by increasing the cover. Another explanation is the difference of MC between interior and exterior columns. High MC can slow down the carbonation rate due to the fact that the water blocks the pores [8]. The difference of MC between the interior and exterior may not be substantial nowadays, but in the past, when the building was in use, the MC of the exterior columns was possibly higher due to splashes, and water run-offs when loading and unloading containers.



Figure 18. Part of the original 1920's north façade after the bombing in 1944. The red arrow points out the render applied over the exterior concrete columns. Retrieve from: <https://pt.slideshare.net/Consoslide/fenixlofts-presentatie-201113/3?smtNoRedir=1>

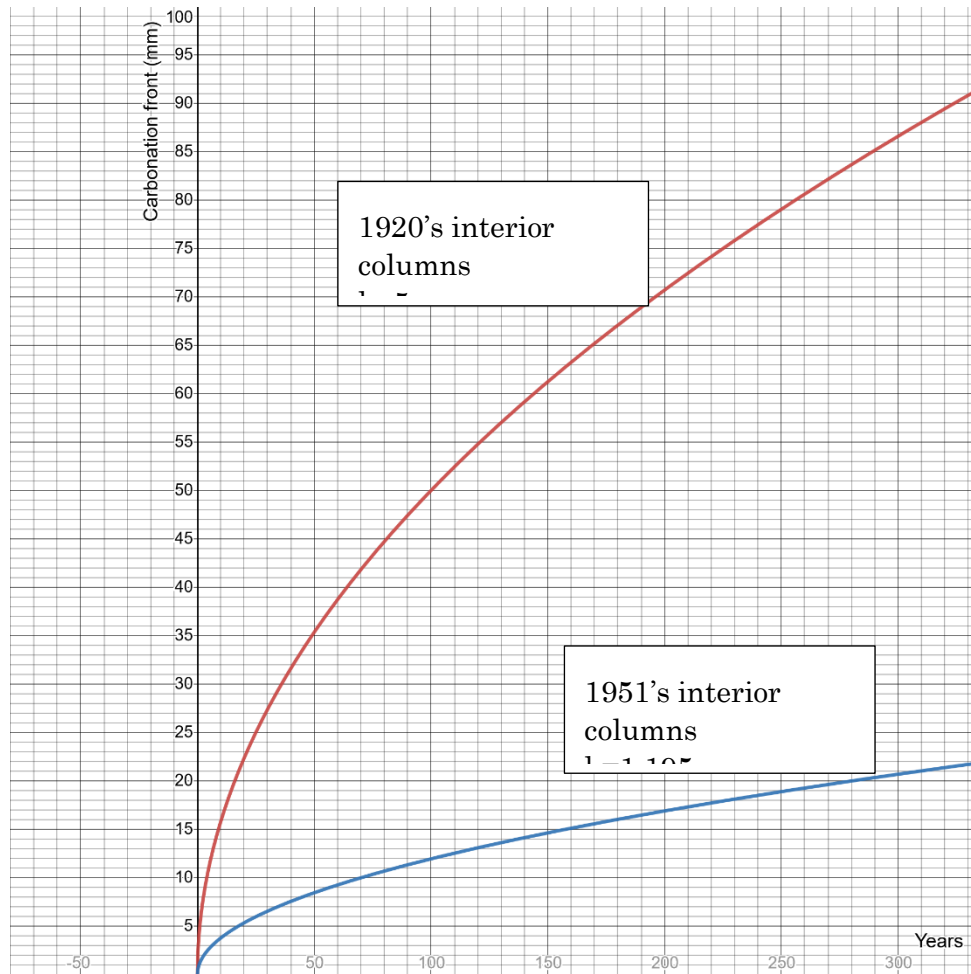


Figure 19. Estimated carbonation rates of 1920's and 1951's interior concrete columns according to Fick's first law.

Concrete cover is on average thicker in the 1920's columns than in the 1951's. This is in contradiction with the general idea that older concrete have thinner concrete covers (15 mm in the 1912 concrete code [4] and 30 mm in the 1951 code [9]). Exterior columns have more concrete cover than interior columns, but there was not a special requirement for thicker covers in exterior columns according to the codes of the time [4,9,10]. It seems that the design engineers took into account the location of the columns to add extra protection in the exterior columns. It is also probable that, given the fact that the building was in close contact with water, a thicker cover than the minimum was desired.

The **spacing of ties** (horizontal reinforcement) in 1920's and 1951's columns exceed the minimum standards according to the codes of the time [4,11], which set larger spacing. For instance, the 1912's concrete code [4], stated that the maximum distance between ties in a columns was the smallest side of the column or 30 times the diameter of the longitudinal reinforcement, in this case study that that is 700 mm and 840 mm respectively. In fact, the spacing of the ties used in both ages would satisfy the

requirements of current standards according to Eurocode 2 [12]. These results align with the theory that the design engineers of the construction did not stay in the minimum requirements but went beyond to provide a higher strength and durability to the concrete structure.

The **moisture content (MC)** in 1951's interior columns is considerable higher than in 1920's interior columns. The reason why 1951's columns have higher MC is not clear but it is likely related to the concrete characteristics since both columns are in the same environment. Concretes with higher water/cement ratios tend to be more permeable, although other factors like aggregate type or compaction methods can also influence. MC can vary in concrete by the relative humidity [13], but in this case the relative humidity was similar in both testing campaigns (60% to 70%). Higher MC in concrete can reduce the rate of carbonation, but in this case the difference in MC between interior and exterior columns does not seem enough to make a substantial difference in the carbonation rate. In summary, there are different factors that can explain why the MC in 1951's columns is higher than 1920's but there are not enough data to confirm the hypothesis made.

In addition, a higher MC in carbonated concrete has higher corrosion probability than dryer concretes. One study performed by two universities in Brazil estimated a MC threshold around 0.6% by weight to achieve a corrosion probability beyond 50% [14]. The explanation is linked to the increase of conductivity of the concrete resulting in more electronegative values of corrosion potential. Considering the threshold of 0.6%, the interior columns from 1920 would be on the verge of corrosion probability beyond 50%, and the exterior columns will be in high risk of corrosion in the columns where concrete in contact with the reinforcement is carbonated. This theory confirms the damage seen in the exterior columns but not in the interior ones.

No relevant difference in **HMC** at 20°C /95%RH between 1920 and 1951 were found. Exterior columns have higher HMC than interior, having its peaks in depths between 20 to 40 mm. HMC is higher than MC in general, this confirms that there is not moisture sources, and it may indicate the presence of salt laden materials, although for accurate results the HMC of the material without the salt should be compared with the values obtained. It is likely that one of these salts may contain chlorides, which can cause chloride-induced corrosion in the reinforcement if enough moisture is present. The highest chloride concentration is located in depths 20 to 40, which overlaps with the zone of the highest HMC. However, the results of the chloride analysis do not reveal a deleterious amount of total chlorides. Although this is a subject of discussion.

The European standard EN 206-1 [15] restricts the **chloride content** to 0.2 to 0.4% chloride by mass of binder. These limits, however, are guidelines for the production of fresh concrete. In a review paper analysing the results of over 50 chloride test experiments [16], Angst et al. [2009] observed a large variability with respect to the threshold of chloride content in concrete, ranging from 0.04 to 8.34% total chloride by weight of cement. The chloride threshold is influenced by many factors, the most relevant being the pH of the surrounding concrete, steel potential, conditions of the steel-concrete interface, type of binder, chloride binding capacity, mineral admixtures, water-binder ratio, moisture content, and surface condition of the steel. Also, the testing method to determine chloride content can give different results. The selected method

used in this report (ISESAM Method) may provide values between 70 to 90% of the true total chloride content because ‘acid extraction techniques cannot completely dissolve all the chlorides from the powder samples’ [16]. In any case, in the tested sample, the maximum total chloride concentration is 0.3% of the binder weight, located in one of the 1951 exterior columns, which do not exhibit signs of chloride-induced corrosion damage. This means that the damage related to chloride found is local and not severe. Therefore, chloride-induced corrosion is not likely to be a threat.

The structural assessment by the **CONTECVET** method provided results aligned with initial assessments. The exterior columns from 1920 were ‘severely’ damaged, with a need of intervention in the short term. The rest of the columns were ‘medium’ damaged, and should be assessed again within the next 5 to 10 years to monitor the evolution of the damage. By comparison, the rest of the interior concrete structure had a similar condition as the interior concrete columns; thus, it can be considered as ‘medium’ damaged.

Conclusions

The Fenix II building was built in two different periods, one part built in 1920 and the other in 1951. Sixteen columns were investigated to assess the properties of the historic concrete and to make an in-depth analysis of its characteristics related to the visible damage.

Concrete from both ages showed similar results in terms of compressive strength ($>40\text{MPa}$), reinforcement layout (appropriate layout, and tie distribution) and total chloride content (0.1 to 0.3% of cement weight). The substantial differences appear in terms of concrete cover, carbonation depth and moisture content. The rate of carbonation from 1920 is faster than that of 1951. Based on the literature, the carbonation rate decreases in time as a function of square root of time. This suggests that the permeability of the 1920's is much higher than 1951's. This is in line with the expectation that older concrete is more permeable as younger concrete due most likely to compaction methods and concrete composition. The low carbonation rate of the 1951 columns, less than 10 mm in 70 years, also suggests that historic concrete do not necessarily are more permeable than modern concrete and can be as durable. The results also suggest that the concrete designers of the building did not stay in the minimum standards of the time but provided a higher level of quality.

The damage types found are related to corrosion processes and are mainly located in the exterior 1920 columns. The causes of the damage are linked to carbonation of the concrete, thin original concrete cover (before the render was applied) and moisture content. There is not clear signs of chloride-induced corrosion and the levels of chloride found do not represent a hazard for the structure.

The rest of the structure showed scattered and localized corrosion-related damage which can be expected in a building of this age.

Bibliography

- [1] NEN-EN 12504-2. Testing concrete in structures - Part 2: Non- destructive testing - Determination of rebound number, 2019.
- [2] Eduardo Torroja Institute, Geocisa, CONTECVET: A validated users manual for assessing the residual service life of concrete structures. Manual for assessing corrosion-affected concrete structures, CBI on behalf of the CONTECVET partners, 2001. <http://www.diva-portal.org/smash/record.jsf?pid=diva2%3A960698&dswid=-9170> (accessed June 15, 2019).
- [3] C. Andrade, I. Martínez, Use of indices to assess the performance of existing and repaired concrete structures, *Constr. Build. Mater.* 23 (2009) 3012–3019. <https://doi.org/10.1016/j.conbuildmat.2009.04.009>.
- [4] Koninklijk Instituut van Ingenieurs, Gewapend Beton Voorschriften 1912, 1912.
- [5] H.A. Heinemann, *Historic Concrete. From concrete repair to concrete conservation*, TU Delft, 2013. <https://doi.org/9789052694115>.
- [6] I. Monteiro, F.A. Branco, J. De Brito, R. Neves, Statistical analysis of the carbonation coefficient in open air concrete structures, *Constr. Build. Mater.* 29 (2012) 263–269. <https://doi.org/10.1016/j.conbuildmat.2011.10.028>.
- [7] C. Van Steen, L. Koptopoulou, E. Verstrynge, Historical and Structural Analysis of a Deteriorated Reinforced Concrete Structure: Student Residence Camilo Torres in Leuven (Belgium), in: *RILEM Bookseries*, 2019: pp. 2304–2313. https://doi.org/10.1007/978-3-319-99441-3_247.
- [8] L. Czarnecki, P. Woyciechowski, Modelling of concrete carbonation : is it a process unlimited in time and restricted in space ?, (2013). <https://doi.org/10.2478/bpasts-2013-0016>.
- [9] Koninklijk Instituut van Ingenieurs; Nederlands Normalisatie-instituut; N 1009 Gewapend-Betonvoorschriften 1950, (1950).
- [10] 1940 Gewapend Beton voorschriften, (n.d.).
- [11] K. Instituut, V. Ingenieurs, Gewapend Beton, (1940).
- [12] Euroopan Concrete Platform, EuroCode 2 Commentary, Brussels, 2008.
- [13] J. Pazderka, P. Reiterman, CZECH WW2 CONCRETE FORTIFICATIONS: CORROSION PROCESSES AND REMEDIATION METHOD BASED ON CRYSTALLIZING COATING, *Acta Polytech.* 59 (2019) 358–370. <https://doi.org/10.14311/AP.2019.59.0358>.
- [14] M.H.F. Medeiros, F.C. Rocha, R.A. Medeiros-JUNIOR, P. Helene, Corrosion potential: influence of moisture, water-cement ratio, chloride content and concrete cover, *Rev. IBRACON Estruturas e Mater.* 10 (2017) 864–885.

<https://doi.org/10.1590/s1983-41952017000400005>.

- [15] European Standard, NEN-EN 206:2014+A1:2016 Concrete - Specification, performance, production and conformity, 2016.
- [16] U. Angst, B. Elsener, C.K. Larsen, Ø. Vennesland, Critical chloride content in reinforced concrete — A review, *Cem. Concr. Res.* 39 (2009) 1122–1138. <https://doi.org/10.1016/j.cemconres.2009.08.006>.
- [1] NEN-EN 12504-2. Testing concrete in structures - Part 2: Non- destructive testing - Determination of rebound number, 2019.
- [2] Eduardo Torroja Institute, Geocisa, CONTECVET: A validated users manual for assessing the residual service life of concrete structures. Manual for assessing corrosion-affected concrete structures, CBI on behalf of the CONTECVET partners, 2001. <http://www.diva-portal.org/smash/record.jsf?pid=diva2%3A960698&dswid=-9170> (accessed June 15, 2019).
- [3] C. Andrade, I. Martínez, Use of indices to assess the performance of existing and repaired concrete structures, *Constr. Build. Mater.* 23 (2009) 3012–3019. <https://doi.org/10.1016/j.conbuildmat.2009.04.009>.
- [4] Koninklijk Instituut van Ingenieurs, Gewapend Beton Voorschriften 1912, 1912.
- [5] H.A. Heinemann, Historic Concrete. From concrete repair to concrete conservation, TU Delft, 2013. <https://doi.org/9789052694115>.
- [6] I. Monteiro, F.A. Branco, J. De Brito, R. Neves, Statistical analysis of the carbonation coefficient in open air concrete structures, *Constr. Build. Mater.* 29 (2012) 263–269. <https://doi.org/10.1016/j.conbuildmat.2011.10.028>.
- [7] C. Van Steen, L. Koptopoulou, E. Verstrynge, Historical and Structural Analysis of a Deteriorated Reinforced Concrete Structure: Student Residence Camilo Torres in Leuven (Belgium), in: RILEM Bookseries, 2019: pp. 2304–2313. https://doi.org/10.1007/978-3-319-99441-3_247.
- [8] L. Czarnecki, P. Woyciechowski, Modelling of concrete carbonation ; is it a process unlimited in time and restricted in space ?, (2013). <https://doi.org/10.2478/bpasts-2013-0016>.
- [9] Koninklijk Instituut van Ingenieurs; Nederlands Normalisatie-instituut; N 1009 Gewapend-Betonvoorschriften 1950, (1950).
- [10] 1940 Gewapend Beton voorschriften, (n.d.).
- [11] K. Instituut, V. Ingenieurs, Gewapend Beton, (1940).
- [12] Europan Concrete Platform, EuroCode 2 Commentary, Brussels, 2008.
- [13] J. Pazderka, P. Reiterman, CZECH WW2 CONCRETE FORTIFICATIONS:

CORROSION PROCESSES AND REMEDIATION METHOD BASED ON
CRYSTALLIZING COATING, *Acta Polytech.* 59 (2019) 358–370.
<https://doi.org/10.14311/AP.2019.59.0358>.

- [14] M.H.F. Medeiros, F.C. Rocha, R.A. Medeiros-JUNIOR, P. Helene, Corrosion potential: influence of moisture, water-cement ratio, chloride content and concrete cover, *Rev. IBRACON Estruturas e Mater.* 10 (2017) 864–885.
<https://doi.org/10.1590/s1983-41952017000400005>.
- [15] European Standard, NEN-EN 206:2014+A1:2016 Concrete - Specification, performance, production and conformity, 2016.
- [16] U. Angst, B. Elsener, C.K. Larsen, Ø. Vennesland, Critical chloride content in reinforced concrete — A review, *Cem. Concr. Res.* 39 (2009) 1122–1138.
<https://doi.org/10.1016/j.cemconres.2009.08.006>.

Report on In-Depth Case Study

The Henebique Silos (Genoa, Italy, 1899, 1901, 1906, 1924)



Type: In need of restoration

Partner Institution: Unige

Project: **CONSECH 20** *Working Package 2 – Task (iii)*

Date: 30/09/2021

By: Author 1 Stefano F. Musso

Author 2 Stefano Podestà

Author 3 Luca Pedrazzi

Author 4 Giovanna Franco

Introduction

The grain silos in the port of Genoa, first designed in 1899, are the most complex in reinforced concrete construction project in Italy and perhaps in the world, dating to the beginning of 20th century.

The huge artefact was designed by the Milanese engineers A. Carissimo and G. Crotti, with engineer G.B. De Cristoforis who contributed to solve some doubts that still existed at the time about the innovative adopted constructive system. In fact, the work belongs in a period when the construction technique of the reinforced concrete conglomerate was not yet universally accepted and positively assessed.

It was a period in which the reinforced concrete construction techniques was still in a pioneering phase, characterised by the presence of different patents, of studies and theories in progressive and open development, of calculation methods in progress and experimentations, with no official national and even less international regulations in place.

The architectural complex is now protected by the Italian Ministry of Cultural Goods and Activities and Tourism, according to the Italian Code of Cultural Goods and Landscape (D. Lgl. 42/2004) as an outstanding example of architectural value, for historical, aesthetic, constructive and economic-social reasons.

A Technical Record, as required by current legislation, has been prepared to be part of the “Feasibility economical and technical project” for the restoration and reuse of the complex, indicating among others contents, the duties of conservation and the available margins for the modification of the Silos. This document has been approved by the local Superintendency and constituted the basis of a recent international Call for Interest, spread off by the owner of the complex, in order to choose a private entrepreneur able to present a definite-executive project for its restoration/reuse in a co-financing partnership with the public body in charge of it. The foreseen possible new uses are linked to the social-economic needs of the City and the local community and comprehend: hotels, temporary residences, commercial spaces, services related to the cruises and tourism, social activities, offices and spaces devoted to activities of social interest.

The former Silos, due to their location and size, are a characteristic element of the entire old port, within which the testimonies of the port's material history have been enhanced through significant restoration, rehabilitation and even new construction work, determining the contemporary layout and the new relationship with the historic city.

The closure of the Silos towards the city is due to the nature of the building, which had an exclusive functional relationship with the port. Similarly, the constituent elements of the Silos are perceptible from a number of significant points of view in the public space; in particular, from the Commenda di Pré, the Maritime Station, the Cotton Warehouses, the pedestrian routes in the Old Port, the urban public transport routes along the port arch and the causeway.

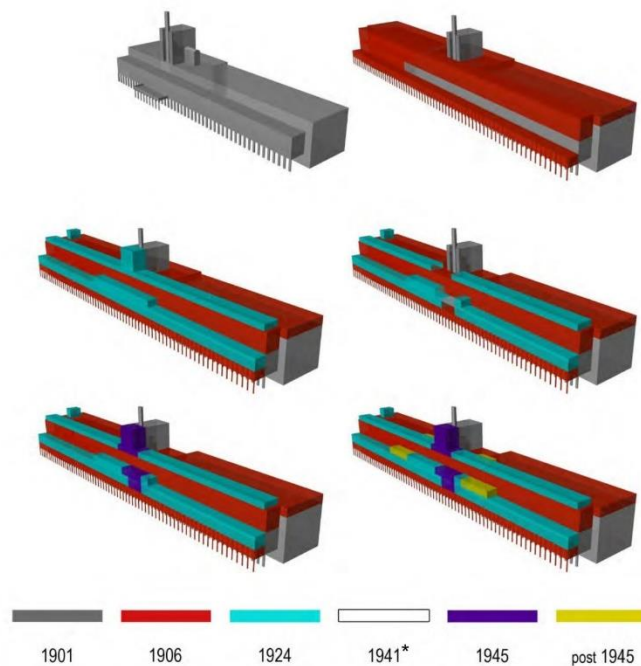
The size of the building is out of scale with respect to the historic city, but at the same time it is an emergency capable of dialoguing with the large cruise ships that today change the coastal landscape of the harbour.

The roof terrace of the Silos provides an exceptional panoramic view of both the waterfront of the Porto Antico (Old Harbour) and the surrounding urban landscape of the city.



Constructive phases of the Silos

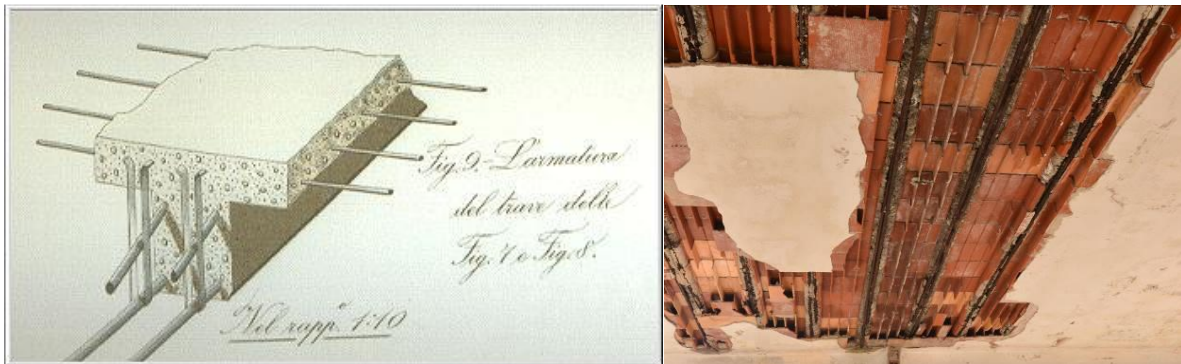
- - 1899-1901 construction of east silo, main building, portion of west silo and wharf
- - 1906 completion of west silo, elevation, portico on sea front
- - 1924-1929 extension
- - 1945 repair of bomb damage and extensions
- - Post 1945 extensions
- - 2008 demolition of the wharf



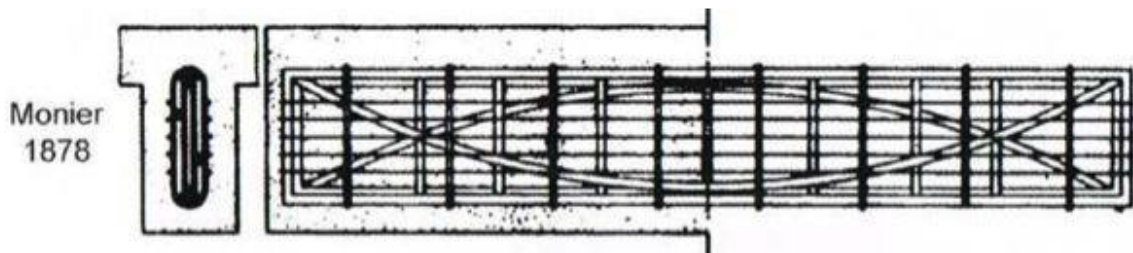
Characteristics of the Concrete Building and Structure

Materials

The whole complex is constructed with reinforced concrete structures and elements. Although many modifications occurred in the construction methods and techniques over the years after its first design, conception and partial construction (“Hennebique” patent, “Monier” patent, “Tirrex” type brickwork system, and so on.), the reinforced concrete is used for all its vertical load-bearing, for parts of its horizontal bearing elements and for the external closure system, as well as for the main partitions of its inner spaces, in particular for those used for the grain storage cells.



Detail of reinforcement in Hennebique patent and of the floors



Typical reinforced beam in the Monier patent

The remaining internal partitions among spaces are made of solid, perforated or semi-filled bricks, or with hollow core concrete.

Lastly, some secondary additions subsequent to the two main construction phases (1901-1906), such as the electrical transformation cabin and the external emergency stairs, were made with steelwork. Some of the parapets and most of the pipes and machinery, still present within the complex, are made of iron and can be considered an integral part of the building due to its peculiar functional characteristics. Others machineries and installations linked to the original function of the Silos have been unfortunately completely removed from the site or even destroyed, thus provoking a painful loss of historical testimonies about the economic and social history of the Harbor and of the City.

A large part of the surface of the façades is finished with faux blocks in plaster, with continuous horizontal bands of approximately 50 cm in height, with alternating striped plaster (parts in relief) and smooth plaster, to enhance the chiaroscuro effect. There is the

presence of mainly metal artefacts of different nature and with different value and documentary significance.



South and east facades

Type of structure

As the building belongs to the period of development of reinforced concrete construction techniques, different types of structures coexist within it, for conception, geometries, shapes and consistency or constructive characters:

- The first part of the complex, completed in 1901 has a reinforced concrete structure bearing based on the Hennebique patent. It is characterized by square, rectangular or polygonal cross-section pillars, by rectangular cross-section beams, often warped in both directions and monolithically connected to the slabs of the ceilings, longitudinally reinforced in the lower limb with straight round bars and open at U-shaped, by stirrups made of flat iron sections or round bars for supporting shear stresses and brackets near the beam-pillar joints. There is also the presence, in some floors, of flat counter-flaps, with little reinforcement, whose original function was to obtain a flat soffit but which had anyway a full structural function and of pillars with little or no reinforcement at all (e.g. first portico facing the sea hosting the loading railway wagons) with tie brackets of two irons at the top.
- The extension of the previously described first part of the complex, completed in 1906 (and probably also its second extension realized in 1924) has a reinforced concrete structure based on Monier's patent, characterized by reinforced beams with large straight longitudinal bars, placed one next to the others, and other curved bars bent in correspondence with the "inversion of the flexing moment", at the supports, and closed stirrups with a constant pitch, along the length of the beams, and thickened at the supports; square or rectangular cross-section pillars with a variable number of bars placed on the perimeter and stirrups with round bars (but also with a plate that binds two bars, as in the Hennebique system).
- Other construction techniques are mainly linked to the reconstruction of the section damaged by English Royal Navy bombing in 1941 and to the new additions and modifications realized after World War II show a succession of different constructive solutions, consistent with the contemporary development of technological knowledge of the employed materials. The locker rooms, for example, have in-situ reinforced beams

and brick pinions to lighten them and the new electric transformation room has a structure in metalwork and an in-situ realized reinforced concrete slab.

The Hennebique silos are a complex work due to the extension of the building, the large number of typological sections present and the profound transformations it has undergone since its construction. The presence of a mixed structural system that combines within it characteristic aspects of different structural concepts (industrial-residential), applied in different ways by the two companies that built the work in its two main phases (1901-1906) constitutes the complex aspect of the analysis.



Other relevant characteristics

The first element characterizing the building is the mix of different construction techniques adopted during the successive additions and reconstructions, even though the materials used are substantially the same. This succession and partial overlapping of different constructive interventions over times represents an interesting case study and, at the same time, a reason of inner vulnerability of the building, due to the different static behavior of the new added parts compared with that of the pre-existing ones and to the reciprocal connection modalities among all those components.

The second important feature is the prediction, already on stage since the preliminary project, of the subsequent main expansions of the original building.

Finally, the persistent and continuous use of this complex, from its construction to its abandonment, even if with the changes in equipment's and movement methods of the grain over times, is another important feature.

Condition of the building

Since it was disused as a granary silo and as a venue of the management offices for its activities, at the end of the eighties of the past century, together with the adjacent new silo built in the early sixties and demolished in the nineties, the complex Hennebique has been in a state of total neglect for thirty years. During this time it has suffered various types and processes of degradation, ranging from those due to anthropogenic causes to those related to the intrinsic characteristics of the materials employed in its construction

and successive modifications and their exposition to environmental aggressive agents, from the normal action of atmospheric agents to its pathological increasing, registered in the more recent periods, linked to the global climate change.

The uncontrolled infiltrations and percolation of rain waters inside the complex and the vulnerability of some construction elements and of their materials made some parts of the building unrecoverable and on the verge of local and luckily limited collapses, especially in the more recent and poorest expansion and additions

The dismantling of the technological equipment, with the removal of technical apparatus and of inner piping and the voluntary demolition of portions of the floor, including the roof, to allow machinery to be transported out of the building, the subsequent vandalism and the improper uses that the building underwent since its abandonment, have seriously affected the integrity and in some cases even the legibility of the spaces, and have allowed widespread weathering of the interior spaces as well.

The exteriors of the building, on the other hand, retains substantial integrity, formal and constructive, especially taking into the due account the total absence of maintenance that it suffered for so many years.

Moreover, in historic reinforced concrete buildings, in general, the possible shortcomings in structural design are combined with those in construction details. Often, in fact, we find ourselves faced with very slender, poorly reinforced pillars supporting large, strongly reinforced beams.

The lack of structural ductility and hierarchy of resistances leads to the verification of these structures in terms of resistance, in order to identify which structural elements, if any, could enter into crisis first even for limited increases in stress, such as a change of use, and therefore all the more so for an exceptional event such as an earthquake.

Damage types

The prevailing degradation of reinforced concrete structures relates to: corrosion and shearing of the reinforcement bars, cracking, detachment and expulsion of the concrete cover, crumbling of the floors, salt efflorescence, patina and biological colonization, missing structural parts.

The others constructive components (like frames and surface treatments, for example) suffer for many others degradation phenomena, among which are.

- Degradation of anthropogenic origins and causes. Location: all rooms. Particularly sensitive to changing rooms, offices, doors and windows on all floors, stairwells. Causes: lack of access control. During the dismantling phase of the installations, numerous slots were opened in the horizons to allow the dismantling and movement of the machinery to be removed. Dynamics: use of the premises for bivouacking and incongruous use of the materials and spaces. Effects: demolition of many internal partitions, damage to internal and external doors and windows, sanitary fittings, architectural surfaces, removal of materials (e.g. staircase coverings), furniture and documents still present in the complex. Possible developments: At present, together with the closure of all possible access points, periodic monitoring of the interiors by security personnel is also

accompanied; the combination of these conditions should allow this kind of damage to be stopped.



Example of anthropogenic degradation

- Corrosion of iron and cast iron structures. Location: iron parapets at the solar pavilions, external doors and windows, boat mooring bollards, various metal items inside and outside the complex. Causes: condition of exposure of the element to atmospheric agents and chemical composition of the metal alloy. Dynamics: The processes are mainly of two types: chemical (contact with a compound such as oxygen or carbon dioxide) and electrochemical (processes of an electrical nature induced by the humid environment) and consist in the transformation of steel into "rust" (ferric oxides $\text{Fe}(\text{OH})_2$, $\text{Fe}(\text{OH})_3$, etc.). The process is particularly fast in the presence of atmospheric pollutants (hydrochloric acid, hydrogen sulphide, etc.). Effects: loss of mechanical strength of the material, which gradually detaches in the form of flakes and dust, thus allowing the phenomenon to be triggered in the inner layers. The conditions of exposure and the characteristics of the chemical composition of the artefact lead to different types of corrosion: uniform, disuniform, ulcer/crater, penetrating, cavernous, intergranular. Possible evolution: gradual reduction of the section of the artefact.



- Corrosion of internal concrete reinforcement. Location: the phenomenon is particularly evident in all the roof slabs, on the internal slabs of the central body, near the most exposed pillars (e.g. in the railway wagon loading gallery on the sea side and in the central body). Causes: condition of exposure of the element, inherent in it or generated by environmental alterations (e.g. water infiltration, exposure to marine aerosol due to damage to protection systems such as windows and doors). At a chemical level, this causes: advancement of the carbonation process which destroys the oxide film and with it the conditions of passivity; exceeding of a critical chloride content. Other causes: presence, in the case of structures affected by electric fields, of currents interfering with the reinforcement. Dynamics: Under normal conditions, the reinforcements inside the concrete passivate, i.e. they are covered with a thin, compact, coherent and uniform layer of protective oxide which blocks the advance of the corrosion process of the same. The chemical process consists in the transformation of steel into rust (ferric oxides Fe(OH)_2 , Fe(OH)_3 , etc.). Effects: Internal compressive stresses on the concrete and tensile stresses on the surface, due to the increase in volume of 2 to 6 times that of the iron from which they originate. These in turn generate surface cracks running parallel to the reinforcement rods, which increase progressively and culminate in the total expulsion of the cover. At the structural level, corrosion of the reinforcements leads to a reduction in the resistant section of the reinforcements, a reduction in their adherence, which may also cause a loss of anchorage. Possible developments: detachment of the cover and surface finishing layers; advanced states of corrosion may contribute to the collapse of structural parts.



- Detachment/expulsion of concrete cover. Location: the phenomenon is particularly evident in all the roof slabs, on the internal slabs of the central body, near the most exposed pillars (e.g. railway wagon loading tunnels and central body). Causes: freeze-thaw cycles, sulphate attack, chloride attack, corrosion of the reinforcements Dynamics: increase in volume of the reinforcements due to corrosion causes detachment of the outermost material. Effects: loss of the cortical layer, which also has a

protective function for the reinforcement iron; loss of the covering plaster; worsening of the exposure conditions of the reinforcement. Possible evolutions: the worsening of the exposure conditions of the reinforcement causes an acceleration of the corrosion process of the reinforcement; it exposes the deeper layers of the concrete to degradation agents. The process leads to the progressive deterioration of the performance of the structural element until it collapses.



- Lack of plastering. Location: exterior elevations, interior surfaces in several areas. Causes: water run-off due to malfunctioning of rainwater collection and disposal systems; action of the concrete substrate; action of saline efflorescence (particularly in interiors), erosion, anthropogenic mechanical actions, freeze-thaw cycles, etc. Dynamics: absence is the final stage in the evolution of degradation phenomena due to erosion, efflorescence, disintegration, detachment caused by water infiltration or the action of the increase in volume due to corrosion of the underlying reinforcements and is therefore to be related to the other items. Effects: absence of plaster coating, even decorated (e.g. external facades). Possible evolution: the deterioration, without prejudice to the condition of the building, is likely to increase.



North facade

- Erosion. Location: external facades, internal walls near openings.
Causes: percolation of rainwater, wind action. Dynamics: mechanical and chemical action due to water run-off as a result of surface exposure conditions or, in more serious cases, damage to structures protecting the surfaces (cornices, eaves, etc.) and/or abrasion of windblown dust.
Effects: gradual. Possible evolution: In the absence of protective measures, degradation will continue to extend.

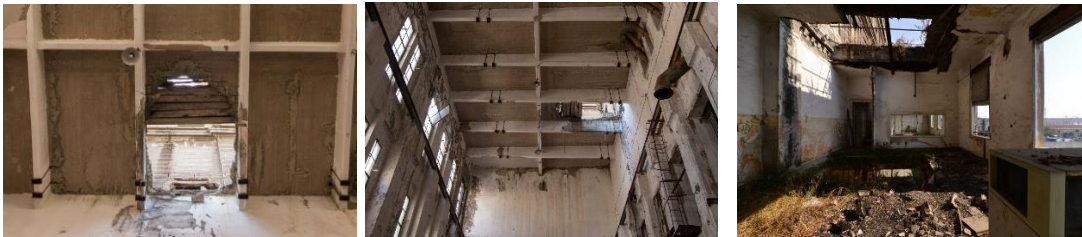


Noth Facade

- Salt efflorescence. Location: various portions of internal and external plaster, structural elements in contact with the ground (in particular sea tunnel for loading railway wagons). Causes: exposure to atmospheric agents, capillary rise from the ground, wind action. The phenomenon is caused by the crystallisation of salts, particularly chlorine and sulphur brought in by marine aerosols and rainwater. Dynamics: formation of substances with a crystalline appearance inside the material, causing the most superficial parts to detach (crypto-efflorescence). Effects: gradual loss of material and/or impoverishment of its strength characteristics (disintegration). In the case of concrete, this is related to the phenomena of corrosion of the reinforcement (in particular chlorides) and therefore to the detachment of the iron covers and the formation of swelling, expulsion of material, chalking in the case of sulphates. Possible evolutions: the phenomenon is destined to evolve over time.



- Lacking parts in floor structures. Location: roof and floor slabs of the pump room, mainly in the sea area (offices, changing rooms), internal slabs of the main building, first floor slab (slab of the railway track portico). Causes: mechanical actions (anthropogenic, by falling portions of the floor above), collapse due to corrosion of the reinforcement rods and degradation of the concrete. Dynamics: the deterioration of the concrete and reinforcement causes a loss of strength which leads to the element collapsing even under its own weight. The fall of the mass of the portion of the slab can cause damage to the one below. In some slabs, slots have been intentionally opened to allow materials to be removed and dropped to the ground. Effects: formation of rainwater ingress paths, loss of functionality of the floor. Possible evolutions: the advancement of the deterioration phenomena is destined to amplify the phenomenon. Several horizons are in a state of imminent collapse.



Hypothesis on damage processes

Degradation of anthropogenic origins and causes: during the dismantling phase of the inner technological installations linked to the movement of grain, numerous holes were opened in the horizontal structures to allow the dismantling and movement of the machinery to be removed. The lack of access control to the complex, further, allowed the spoliation of the most valuable surviving materials (stone slabs, wrought iron parapets), the use of the spaces as bivouacs by homeless people and outright vandalism, with consequent heavy damages.

Oxidation and corrosion of iron and cast iron items: this is linked to their conditions of exposure to the aggressive environmental agents and lack of maintenance and renewal of protective paints (caused by carbonation or chloride) be ruled out, especially in the case of particularly damaged elements.

Oxidation and corrosion of the reinforcements inside the concrete: as the effect of the carbonation of the concrete and the action of chlorides brought upon them by marine aerosols.

Sulphate attack of the cement matrix causes a reaction between the sulphate ion SO_4 and the components of the cement matrix.

Freeze-thaw cycles due to 92% saturated capillary pores at low temperatures cause delamination of the concrete (scaling).

Detachment/expulsion of the concrete cover: this phenomenon is particularly evident in all the structures most subject to the carbonating action of atmospheric agents and chlorides brought in by the marine aerosol, such as the roofs slabs, the internal slabs of the central part of the complex, the most exposed pillars (e.g. in the tunnel exposed to the sea, hosting the loading and downloading railway wagons of the grain). The phenomenon can also be related to the mix composition of the concrete, the binder used as well as the metal alloy employed for the inner reinforcement, and cracks created by critical stresses, movements or deformations of the structures.

Lack of render: particularly evident on the external and internal elevations, due to deterioration caused by erosion, sulfating, freeze/thaw cycles and to anthropogenic action.

Erosion: widespread on all external surfaces and in particular those below the damaged water collection systems (gutters, downpipes, etc.), as well as on the parts of the elevations most exposed to wind.

Saline efflorescence: present above all on the surfaces most exposed to the aggression of the atmospheric agents, in particular with water stagnation, or the action of marine aerosols and on the structures directly in contact with the ground (pillars and masonry)

Lacking parts in the floor structures: it is mainly the effect of the above mentioned dismantling of inner machineries and installations. There are also some limited portions of the complex that have collapsed due to localized deterioration of the structures.

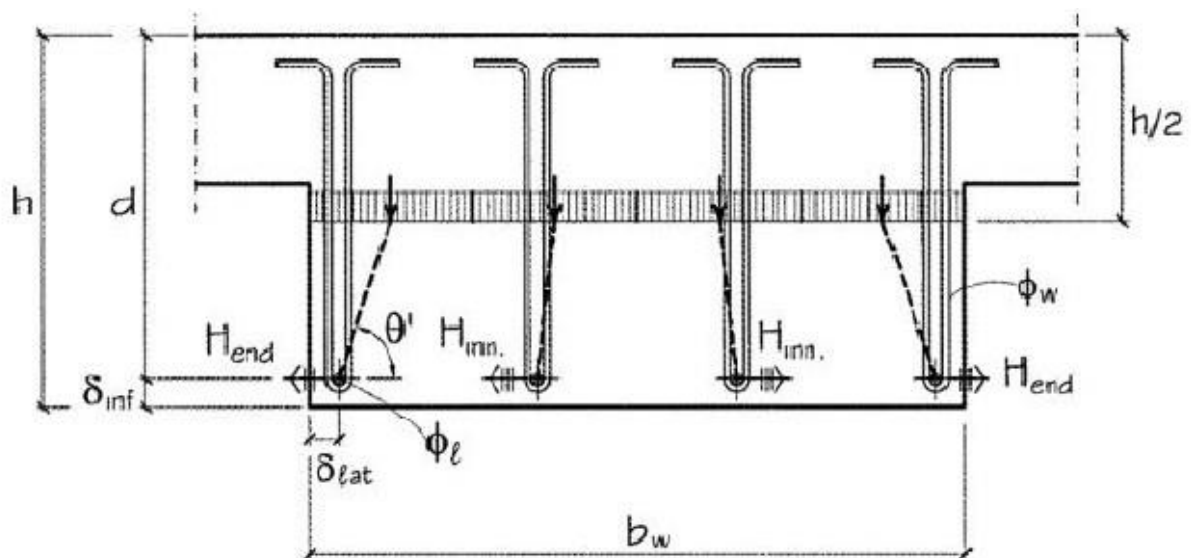


With regard to the degradation of the constructive elements, and not only of the material, the problems are mainly related to the shear reinforcement of the structural elements. The presence of open stirrups and U-shaped connectors leads to a fragile behaviour (shear failure of the beams and failure of the nodes) since an effective confinement of the concrete is not guaranteed. In this regard, the evaluation of the shear behaviour of the deflected elements is a problematic aspect of the construction type under consideration.

The causes are due to:

- reinforcing steel with a low carbon content, which gives the cracks typical of elements reinforced with high ductility steel;
- the transversal reinforcing bars (open U-shaped stirrups made of iron plates or rods) which are not able to provide adequate confinement to the concrete struts of the resistant truss.

Both aspects undermine the assumptions on which the model of the truss with variable inclination proposed by the current Technical Standard is based: in particular, due to the high ductility of the steels used, the core reinforcement is not able to limit the crack openings formed at the time of the first shear crack. This results in large deformations and the relative crack pattern is characterised by lesions which do not allow the crossing of compressed connecting rods with inclinations smaller than those corresponding to the yield crack.



Model of analysis of the transversal behaviour of a beam with U connectors

Aim of the investigation

A complete understanding of the structural behaviour and characteristics of the materials is essential for any project of functional rehabilitation, which sees in the eventual structural recovery an added value such as to allow a more conscious design.

This knowledge must refer to the structure in its original condition, to the construction techniques of the time, to the alterations it has undergone, to the phenomena that have occurred from time to time and that have transformed the work into its present state. Knowledge was based on qualitative and quantitative approaches.

The qualitative aspects were researched by reading the bibliographic sources, but above all by "reading" the only direct source, which is the artefact itself, analysing structural instabilities and the deterioration of the materials through inspections.

The quantitative aspects were obtained by checking the dimensional survey, on indirect surveys of the materials, and on structural analyses.

The path identified is fully harmonised with what has been proposed in the recent 'Guidelines for the evaluation and reduction of seismic risk of cultural heritage' (Prime Ministerial Decree of 9 February 2011), to which explicit reference is made in the analysis procedure adopted and implemented. The fact of being faced with a historical concrete structure has obviously determined inevitable differences (for example in the type of investigation or in the analysis model carried out - the Guidelines are in fact specifically addressed to the cultural heritage of masonry and wood structures). However, the knowledge path identified in the Guidelines was the basis for our work, as was the adoption of a simplified model to assess the seismic vulnerability of the Silos complex. The structural analysis, however, was not limited to the seismic risk of the complex, but went as far as analysing the static suitability of the building.

In the case of listed buildings, such as the Hennebique Silos, the Guidelines have correlated the confidence factor on several parameters, defining partial confidence factors FC_k ($k=1.4$) related to four categories of investigation (geometric survey, identification of the historical and construction specificities of the building, mechanical properties of materials, soil and foundations). The confidence factors are to be used as additional partial safety coefficients that take into account deficiencies in the knowledge of the parameters of the model. According to these categories of investigation, and to the level of detailing reached in them, the overall confidence factor is defined.

This approach takes into account the need to deal with an architectural artefact characterised by multiple construction phases, different materials and techniques, for which the systematic application of investigations, most of which are destructive or semi-destructive, can undermine the material integrity that must be the basis of any recovery and conservation intervention. Although, in theory, the problems encountered in historical concrete buildings are those described above, it should be noted that, following the inspections and surveys carried out on the Hennebique Silos, construction solutions other than those generally adopted have emerged. For this reason, in order to assess the structural safety of the Hennebique silos, it is necessary to investigate the construction details adopted and assess the characteristics to be taken into account in the structural analyses.

The various inspections carried out made it possible to inspect, in varying degrees of depth, the different areas of the building, in order to be able to locate and make a preliminary identification of the parts that can be restored and those that, on the contrary, will have to be demolished, due to the structural criticalities affecting them.

A subdivision into four macro-areas is considered, characterised by common criticalities, in order to highlight the state of deterioration and give indications on possible interventions.

Methods

The general procedure for assessing the safety of an existing building involves an indispensable knowledge phase which can be divided into the following stages

- historical-critical analysis
- survey of the state of affairs
- mechanical characterisation of the materials;
- experimental tests,
- structural analysis.

Although in a simplified manner, two main elements can be identified which cause the poor durability of concrete structures: intrinsic factors of the material (amplified in the case of uncontrolled mixes) and environmental factors (related to the exposure of the concrete). With regard to the first aspect, it is clear that the construction of silos in reinforced concrete did not have a construction tradition consolidated over time, so as to be able to make use of reliable concrete preparation procedures; furthermore, the intrinsic vulnerability of the steel-concrete system leads to "physiological" micro-cracking which provides a preferential route of penetration for external aggressive agents, which cause oxidation of the reinforcement rods and the progressive deterioration of the structural elements. This phenomenon is conditioned by exposure and is more aggressive in relation to the environment in which the structure is located. In this sense, the marine environment in which the Hennebique Silos are located has been an additional factor in favouring the progression of the chemical-physical degradation phenomena.

The identification and recognition of the construction techniques and materials used in the complex has been carried out through archive researches and the characterization of their compositions with specific chemical-physical analysis in laboratory.

The evaluation of the evolution of the degradation phenomena has been obtained through comparison of archive images of the same elements over the years, as well as through the comparison between the behaviors of similar elements in different exposure.



The characterization and evaluation of the technical qualities of the concrete parts and elements has been carried out through many tests of mechanical nature.

The mechanical characterisation of the materials necessarily involves a campaign of on-site and laboratory diagnostics, in order to identify the mechanical (strength, deformability, etc.), physical (porosity, etc.) and chemical (composition, etc.) characteristics of the materials.

In the case of the Hennebique Silos, it was possible to make use of the data obtained during a diagnostic campaign carried out in 2002 by the Structural and Geotechnical Engineering Department of the University of Genoa (head of research Prof. Ing. Vladimiro Augusti). First of all, therefore, the available data were analysed and only later was a new investigation plan prepared and carried out. It should be noted that reference was made to the data from the 2002 diagnostic campaign, but the data was completely reworked.

The new diagnostic campaign involved the same points of investigation as in 2002, since the intention was to assess any decay in the characteristics of the materials about ten years later, but also new structural elements that were not considered in 2002 and were considered to be particularly decisive in the behaviour of the building. The new plan of investigation was therefore based on a preliminary, albeit approximate, interpretation of the characteristics and structural behaviour of the structure, so that it could be addressed where the data to be acquired could make a significant contribution to knowledge.

Five types of experimental tests were carried out as part of the 2002 diagnostic campaign:

- Sclerometric tests, performed on site with a Controlsmod. 58-C181/N instrument - Percussion energy 2,207 Joule.
- Ultrasonic tests, performed on site with a Controls instrument - Ultrasonic Pulse Velocity Tester - mod. 58-E48, 54 kHz probes with an accuracy of 0.1µs.
- Sonreb method: the combined SONREB method was developed to reduce the errors committed with the methods described above; it was noted that the moisture content underestimates the sclerometric index and overestimates the ultrasonic speed and that, as the age of the concrete increases, the sclerometric index increases while the ultrasonic speed decreases. The combined use of the two tests therefore makes it possible to partially compensate for the errors made by using the two methods individually. The application of the Sonreb method requires the evaluation of the local values of the ultrasonic velocity V and the rebound index S , from which the strength of the concrete R_c can be obtained.
- Compression tests, performed in the laboratory on cylindrical concrete specimens (cores), with a diameter of 74 mm and a height of approximately 150 mm, with automatic detection of axial displacements under load performed with equipment designed in the DISEG Laboratory.
- Tensile tests carried out in the laboratory on steel bars obtained from reinforcements emerging from partially demolished or tampered structural elements.
- Open porosity tests for water absorption, performed at the Laboratory of the Department of Building, Urban Planning and Materials Engineering (DEUIM), in collaboration with Prof. Marino Giordani.



Punto di prova C1.1 e C1.2



Punto di prova P2.1



Punto di prova P1.1 e P1.2



Punto di prova C5.1A e C5.1B



Punto di prova P26/2.1A e P26/2.2B



Punto di prova TH1.1



Punto di prova PS1.1



Punto di prova PT1.2

Two types of experimental tests were carried out as part of the 2013 diagnostic campaign:

- Sclerometric tests, performed on site with a Controlsmod. 58-C181/N instrument - Percussion energy 2,207 Joules;
- Ultrasonic tests, performed on site with a CMS instrument from Boviarsrl - UltrasonicPulseVelocity Tester - mod. 58-E48, 54 kHz probes with an accuracy of 0.1µs.



Punto di prova K1



Punto di prova K2



Punto di prova K3



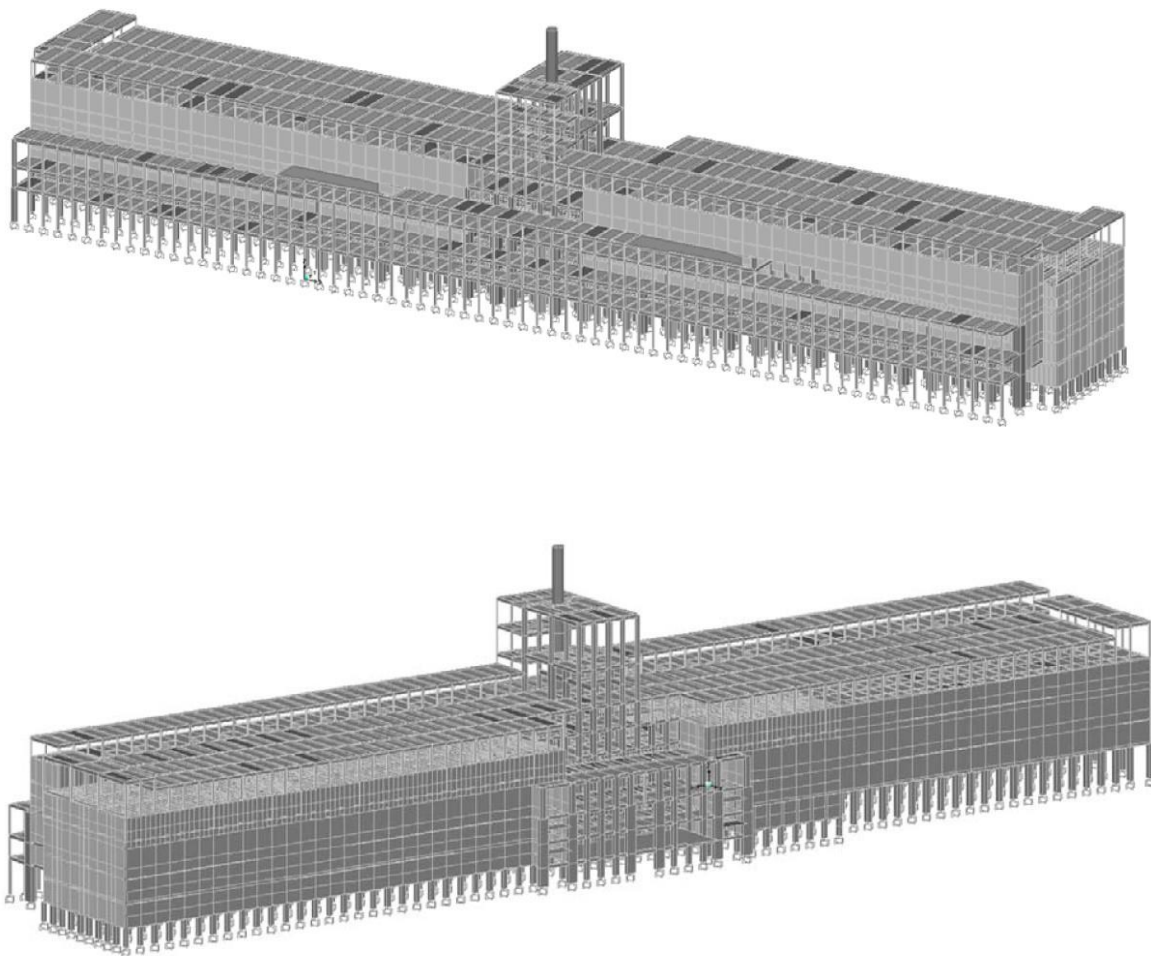
Punto di prova K4

For the structural analysis, a three-dimensional finite element model was defined to evaluate the structural response under different loading conditions. The evaluations reported in this document, deduced from a detailed global model, must, however, be assumed as a preliminary assessment of structural safety also in relation to seismic hazard. The verifications were, in fact, conducted for the types of structural elements most frequently and most stressed in relation to the different load conditions. The result must

therefore always be taken as a preliminary assessment in the same way as a simplified analysis, but with greater reliability on the calculation model (which was carried out as if a detailed analysis had to be performed) and easily extended to all the structural elements that characterise the model itself.

The model, carried out using the SAP2000 calculation code, was created using mainly "Frame" objects to represent beams and columns and "Area" objects to represent cell horizons and walls. These elements were then assigned the corresponding geometries of the cross-sections obtained from the inspections carried out or from archive documentation. Unambiguous mechanical properties, obtained from the reprocessing of the core compression tests (2002), were associated with the material assigned to the model elements.

The overall model is composed of 8689 frames, 12752 nodes and 15135 areas.



In order to take into account the finite dimension of the beam-pillar node, the terminal portions of the elements were considered rigid (respecting the geometry of the elements converging in the node) so as not to have unnatural values of the bending moment.

With regard to the thickness of the "Area" elements associated with the cells, a value of 40 cm was assigned for the perimeter walls and 13 cm for the interior walls.

The floor slabs were not modelled with finite elements, but with geometric elements designed only to transfer the vertical loads to the conglomerate walls and to the beams and columns. Since the stiffness in the floor plane is very high (full slabs), a rigid plane condition (diaphragm) was imposed on all the nodes belonging to the same horizon, diversifying it in relation to the height and construction phases.

The structure, due to the completion that occurred in 1906, has a joint that is visible only in some portions of the structure and that has not been maintained in subsequent extensions.

In order to understand the structural behaviour of the complex and to assess its seismic safety margins, also in relation to a possible seismic improvement intervention, two different models were carried out: the first (MODEL A) considering the ordinary working loads as defined by the original use, which also included the weight of the grain in the silos (specific weight of 7.50 kN/m³); the second (MODEL B) assuming a constant variable overload as a reference and representative of the future uses with a view to a functional redevelopment. The first model was also carried out to assess whether the quality of the original structural design and its realisation did not present, already in an initial situation, criticalities or structural deficiencies such as to compromise its safety in a static condition.

Results

First diagnostic campaign. With regard to ultrasonic testing, the results obtained were as follows:

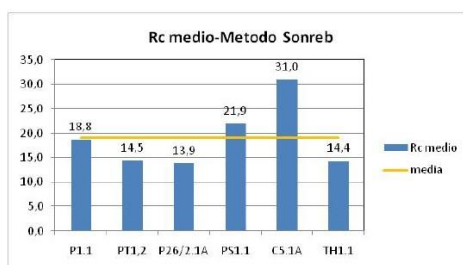
| | Punti di prova | t medio | d | v | v |
|-----------------|----------------|---------|------|---------|-------|
| | [Nome] | [μs] | [cm] | [cm/μs] | [m/s] |
| PILASTRI | P1.1 | 276 | 90,5 | 0,328 | 3279 |
| | PT1.2 | 247,6 | 81 | 0,327 | 3271 |
| | P26/2.1A | 206 | 66 | 0,320 | 3204 |
| | PS1.1 | 80,5 | 26,5 | 0,329 | 3292 |
| CELLE | C5.1A | 70,35 | 28 | 0,398 | 3980 |
| TRAVI | TH1.1 | 81,4 | 25 | 0,307 | 3071 |

The results of the sclerometric tests were as follows

| | Punti di prova | Indice sclerometrico medio |
|-----------------|----------------|----------------------------|
| | [Nome] | [-] |
| PILASTRI | P1.1 | 34 |
| | P2.1 | 37 |
| | PT1,2 | 28 |
| | PT2.1A | 31 |
| | P26/2.1A | 28 |
| | PS1.1 | 38 |
| | PS2.1B | 35 |
| CELLE | C4.1A | 24 |
| | C5.1A | 36 |
| TRAVI | TH1.1 | 31 |
| | TH2.1 | 28 |

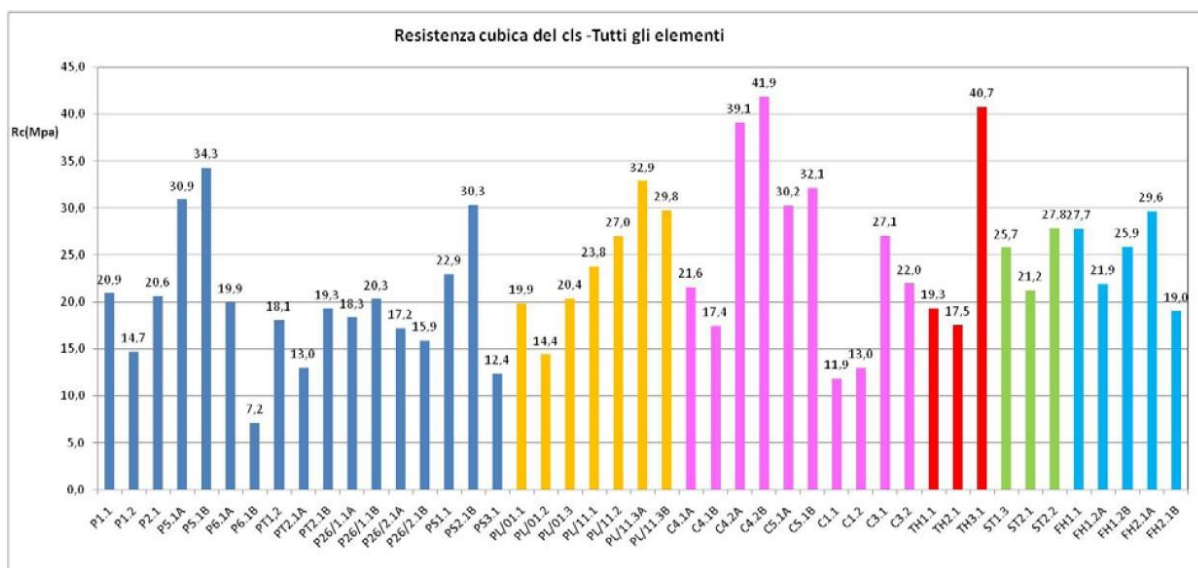
The application of the Sonreb methodology therefore led to the calculation of the cubic compressive strength values of the concrete.

| | | Punti di prova | Indice sclerometrico medio | v | R _c (Giacchetti, Lacquaniti (1980)) | R _c (Gašparik (1984)) | R _c (Di Leo, Pascale (1994)) | R _c (Arioğlu, Köylüoğlu (1996)) | R _c (Del Monte et al.(2004)) | Media cubica | Media cilindrica |
|----------|------|----------------|----------------------------|-------|---|-------------------------------------|--|---|--|--------------|------------------|
| | | [Nome] | [-] | [m/s] | [Mpa] | [Mpa] | [Mpa] | [Mpa] | [Mpa] | [Mpa] | [Mpa] |
| PILASTRI | 1901 | P1.1 | 34 | 3279 | 14,8 | 20,8 | 19,9 | 17,9 | 20,5 | 18,8 | 15,6 |
| | | PT1.2 | 28 | 3271 | 11,2 | 16,3 | 16,1 | 12,5 | 16,4 | 14,5 | 12,0 |
| | 1926 | P26/2.1A | 28 | 3204 | 10,6 | 15,7 | 15,3 | 11,8 | 15,8 | 13,9 | 11,5 |
| | 1906 | PS1.1 | 38 | 3292 | 17,5 | 24,1 | 22,6 | 22,1 | 23,4 | 21,9 | 18,2 |
| CELLE | 1901 | C5.1A | 36 | 3980 | 26,6 | 32,0 | 34,0 | 31,9 | 30,3 | 31,0 | 25,7 |
| | | TH1.1 | 31 | 3071 | 11,0 | 16,4 | 15,4 | 12,9 | 16,5 | 14,4 | 12,0 |



The data and results of the simple compression tests carried out in the laboratory on the cores taken from the various structural elements of the building are shown below.

| | | Campione | D | h | h/D | C _{n/d} | C _d | C _p | σ _r | σ _r | σ _{r,corr} | σ _{r,cub} | σ _{r,cub,corr} | | |
|----------|------|----------|------|------|------|------------------|----------------|----------------|----------------|----------------|---------------------|--------------------|-------------------------|-------|------------|
| | | [Nome] | [mm] | [mm] | [-] | [-] | [-] | [-] | [Kg/cm²] | [Mpa] | [Mpa] | [Mpa] | [Mpa] | Media | Deviazione |
| PILASTRI | 1901 | P1.1 | 74 | 159 | 2,15 | 1,02 | 1,03 | 1,20 | 140,74 | 13,8 | 17,4 | 16,6 | 20,9 | 18,7 | 3,5 |
| | | P1.2 | 74 | 151 | 2,04 | 1,00 | 1,03 | 1,20 | 100,03 | 9,8 | 12,2 | 11,8 | 14,7 | | |
| | | P2.1 | 74 | 150 | 2,03 | 1,00 | 1,03 | 1,20 | 140,74 | 13,8 | 17,1 | 16,6 | 20,6 | | |
| | 1911 | P5.1A | 74 | 158 | 2,14 | 1,02 | 1,03 | 1,20 | 208,20 | 20,4 | 25,7 | 24,6 | 30,9 | 23,1 | 12,2 |
| | | P5.1B | 74 | 150 | 2,03 | 1,00 | 1,03 | 1,20 | 233,79 | 22,9 | 28,4 | 27,6 | 34,3 | | |
| | | P6.1A | 74 | 155 | 2,09 | 1,01 | 1,03 | 1,20 | 134,93 | 13,2 | 16,5 | 15,9 | 19,9 | | |
| | | P6.1B | 74 | 150 | 2,03 | 1,00 | 1,03 | 1,20 | 48,85 | 4,8 | 5,9 | 5,8 | 7,2 | | |
| | 1901 | PT1.2 | 74 | 150 | 2,03 | 1,00 | 1,03 | 1,20 | 123,16 | 12,1 | 15,0 | 14,6 | 18,1 | 16,8 | 3,4 |
| | | PT2.1A | 74 | 147 | 1,99 | 1,00 | 1,03 | 1,20 | 88,80 | 8,7 | 10,7 | 10,5 | 13,0 | | |
| | | PT2.1B | 74 | 129 | 1,74 | 0,96 | 1,03 | 1,20 | 136,84 | 13,4 | 16,0 | 16,2 | 19,3 | | |
| | 1926 | P26/1.1A | 74 | 105 | 1,42 | 0,91 | 1,03 | 1,20 | 138,42 | 13,6 | 15,2 | 16,4 | 18,3 | 17,9 | 1,9 |
| | | P26/1.1B | 74 | 121 | 1,64 | 0,95 | 1,03 | 1,20 | 146,92 | 14,4 | 16,9 | 17,4 | 20,3 | | |
| | | P26/2.1A | 74 | 132 | 1,78 | 0,97 | 1,03 | 1,20 | 121,21 | 11,9 | 14,3 | 14,3 | 17,2 | | |
| | | P26/2.1B | 74 | 148 | 2,00 | 1,00 | 1,03 | 1,20 | 108,97 | 10,7 | 13,2 | 12,9 | 15,9 | | |
| | 1911 | PS1.1 | 74 | 148 | 2,00 | 1,00 | 1,03 | 1,20 | 157,03 | 15,4 | 19,0 | 18,6 | 22,9 | 21,9 | 9,0 |
| PS2.1B | | 74 | 116 | 1,57 | 0,94 | 1,03 | 1,20 | 221,84 | 21,8 | 25,2 | 26,2 | 30,3 | | | |
| PS3.1 | | 74 | 124 | 1,68 | 0,95 | 1,03 | 1,20 | 88,74 | 8,7 | 10,3 | 10,5 | 12,4 | | | |
| PLATEA | 1901 | PL/01.1 | 74 | 148 | 2,00 | 1,00 | 1,03 | 1,20 | 136,09 | 13,4 | 16,5 | 16,1 | 19,9 | 18,2 | 3,3 |
| | | PL/01.2 | 74 | 161 | 2,18 | 1,02 | 1,03 | 1,20 | 96,54 | 9,5 | 11,9 | 11,4 | 14,4 | | |
| | | PL/01.3 | 74 | 158 | 2,14 | 1,02 | 1,03 | 1,20 | 137,25 | 13,5 | 16,9 | 16,2 | 20,4 | | |
| | 1911 | PL/11.1 | 74 | 154 | 2,08 | 1,01 | 1,03 | 1,20 | 161,45 | 15,8 | 19,8 | 19,1 | 23,8 | 28,4 | 3,9 |
| | | PL/11.2 | 74 | 184 | 2,49 | 1,05 | 1,03 | 1,20 | 175,64 | 17,2 | 22,4 | 20,8 | 27,0 | | |
| | | PL/11.3A | 74 | 186 | 2,51 | 1,05 | 1,03 | 1,20 | 213,55 | 20,9 | 27,3 | 25,2 | 32,9 | | |
| | | PL/11.3B | 74 | 162 | 2,19 | 1,02 | 1,03 | 1,20 | 199,36 | 19,6 | 24,7 | 23,6 | 29,8 | | |



Total graphic of the resistance to compression of all the pieces

As can be seen from the graph below, the compressive strength values of the concrete obtained using the Sonreb method are not very different from those identified using the core compression test. Except in the case of specimen C5.1A, the values obtained using the Sonreb methodology tend to underestimate the compressive strength of the concrete compared to the direct compression test.

| Campione | Diametro del provino | Sezione resistente | Snervamento unitario | Rottura unitaria | Allungamento % |
|----------|----------------------|--------------------|----------------------|----------------------|----------------|
| n° | [mm] | [mm ²] | [N/mm ²] | [N/mm ²] | Ap5 |
| 1 | 10 | 78,5 | 242 | 293 | 25 |
| 2 | 10 | 78,5 | 223 | 293 | 26 |
| 3 | 10 | 78,5 | 229 | 286 | 25 |
| 4 | 13 | 132,7 | 279 | 373 | 23 |
| 5 | 13 | 132,7 | 271 | 376 | 24 |
| 6 | 13 | 132,7 | 279 | 373 | 23 |

As regards the characterisation of the reinforcing steel, tensile tests were carried out on plain steel bars taken from the site. The results are shown in the following table.

| Campione | Diametro del provino | Sezione resistente | Snervamento unitario | Rottura unitaria | Allungamento % |
|----------|----------------------|--------------------|----------------------|----------------------|----------------|
| n° | [mm] | [mm ²] | [N/mm ²] | [N/mm ²] | Ap5 |
| 1 | 10 | 78,5 | 242 | 293 | 25 |
| 2 | 10 | 78,5 | 223 | 293 | 26 |
| 3 | 10 | 78,5 | 229 | 286 | 25 |
| 4 | 13 | 132,7 | 279 | 373 | 23 |
| 5 | 13 | 132,7 | 271 | 376 | 24 |
| 6 | 13 | 132,7 | 279 | 373 | 23 |

2013 campaign

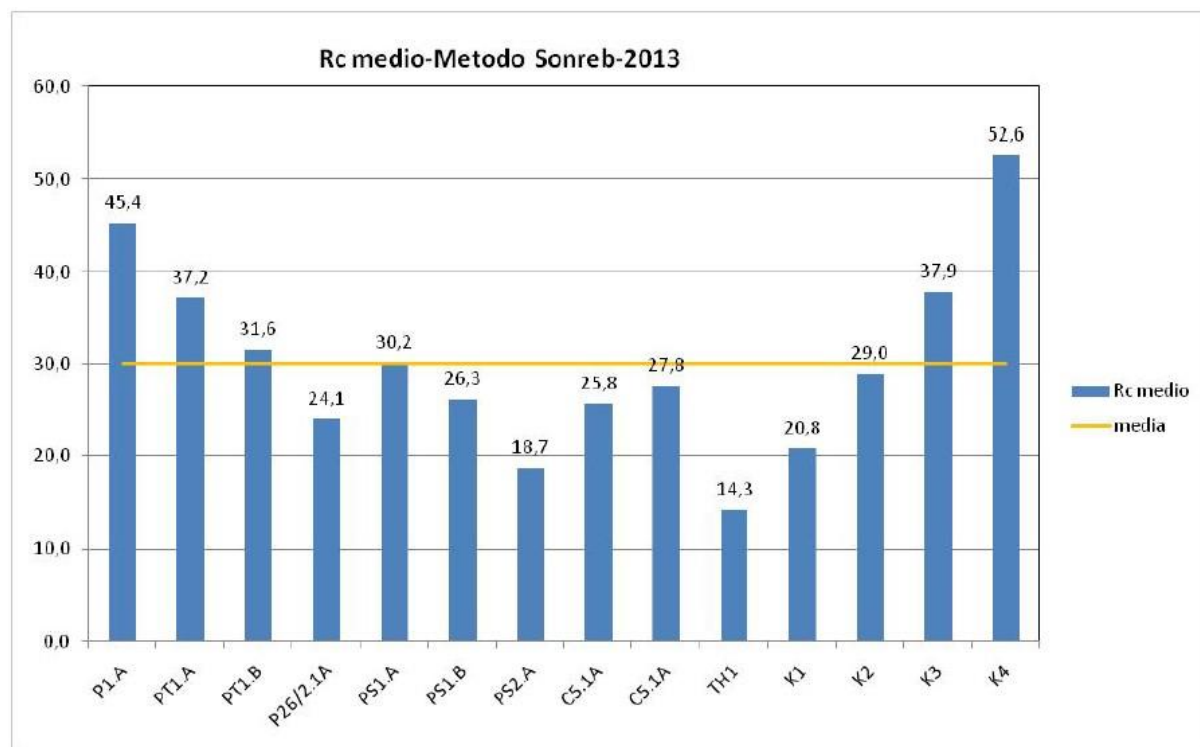
The results of the ultrasonic tests were as follows

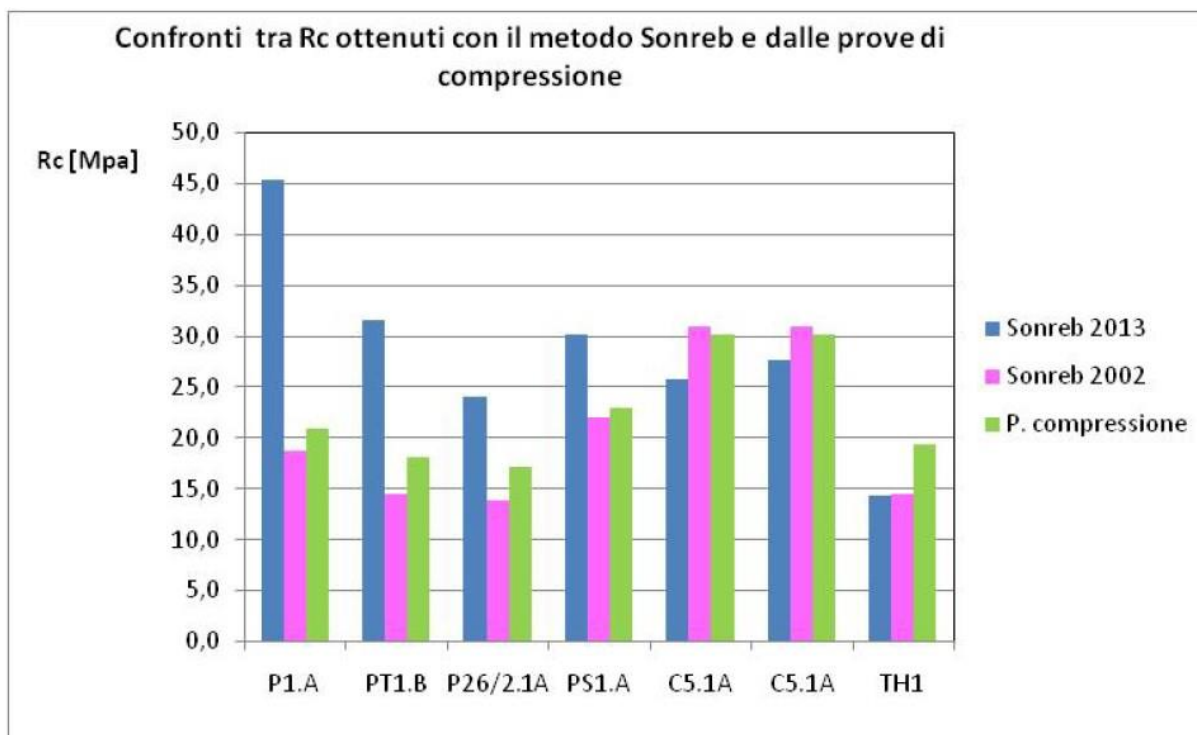
| | | Punti di prova | V [m/s] | dev.st [m/s] |
|----------|------|----------------|---------|--------------|
| | | [Nome] | [-] | [-] |
| PILASTRI | 1901 | P1.A | 3831 | 43 |
| | | PT1.A | 4001 | 18 |
| | | PT1.B | 3865 | 24 |
| | 1926 | P26/2.1A | 3381 | 77 |
| | | P26/2.1B | 3294 | 28 |
| | 1906 | PS1.A | 3401 | 76 |
| | | PS1.B | 3151 | 20 |
| | | PS2.A | 2901 | 73 |
| | | PS2.B | 3364 | 36 |
| CELLE | 1901 | C5.1A | 3304 | 76 |
| | | C5.1A | 3419 | 40 |
| TRAVI | 1901 | TH1 | 2856 | 38 |
| PILASTRI | 1906 | K1 | 3204 | 21 |
| | | K1_2 | 2740 | 47 |
| | | K2 | 3384 | 78 |
| | 1901 | K3 | 3941 | 24 |
| | | K3_2 | 3730 | 26 |
| | | K4 | 4095 | 42 |
| | | K4_2 | 3842 | 23 |

With regard to the sclerometric tests, the results were as follows:

| | | Punti di prova | Indice sclerometrico medio |
|----------|------|----------------|----------------------------|
| | | [Nome] | [-] |
| PILASTRI | 1901 | P1.A | 51 |
| | | P2.A | 46 |
| | | PT1.A | 41 |
| | | PT1.B | 38 |
| | | PT2 | 40 |
| | 1926 | P26/2.1A | 39 |
| | | P26/2.1B | 38 |
| | 1906 | PS1.A | 46 |
| | | PS1.B | 47 |
| | | PS2.A | 41 |
| CELLE | 1901 | C5.1A | 43 |
| TRAVI | 1901 | TH1 | 35 |
| | | TH2 | 34 |
| PILASTRI | 1906 | K1 | 38 |
| | | K2 | 45 |
| | 1901 | K3 | 43 |
| | | K4 | 51 |

The application of the Sonreb methodology thus led to the calculation of the cubic compressive strength values of the concrete, as previously described.





Comparison graph between the concrete compressive strength values obtained using the Sonreb methodology during the 2002 and 2013 tests, the 2002 tests and the 2013 tests. The last column refers instead to the compressive strength value of the concrete obtained with the simple compression test of the cores (2002 survey campaign)

Discussion

From a purely structural point of view, the analyses have shown that the Hennebique Silos complex was optimally designed, even though it was built at a pioneering time for reinforced concrete structures. The verifications carried out demonstrate, in fact, how the characteristics of the materials and elements allow an adequate level of safety to be achieved, even considering the actions induced by the load combinations foreseen by the current technical standards. The evaluation of the trusses against bending, carried out with the methods imposed by the current NTC 2018 and using the calculation stresses indicated in the standard of 1907, has validated the design of the structural elements that are verified for gravitational loads. Despite the inconsistencies in the pre-dimensioning model introduced by engineer François Hennebique, the section of a beam has a good behaviour in relation to bending stresses, thanks to the presence of the solid reinforced slab of considerable thickness; the reinforcement of the slab, in fact, contributes to the resistance with a contribution of compressed metal area. As far as shear is concerned, the construction details revealed inadequate stirrups (open U-shaped stirrups), particularly in the elements made according to the Hennebique patent. However, no problems related to this aspect were found, thanks to the presence of the counter-batten which prevents lateral shear mechanisms in the main and secondary beams. A further analysis of the structural behaviour of the building was the evaluation of the tensional state of the columns on the ground floor, considering the axial stresses resulting from the combination of vertical loads foreseen in the original design. The pure compressive stress, evaluated for each type of section, assumes maximum values in the order of 7 MPa, lower than the tension threshold dictated by the Standard.

Conclusions

General principles to be followed in future reuse and redevelopment interventions are considered:

- a. The substantial preservation of the building, its volumetry and its fundamental architectural, constructional and stylistic characteristics as testimony to the 'material culture' of a pioneering era for the construction of reinforced concrete structures.
- b. The conservation of part of the granary cells as evidence of the building's original storage function.
- c. The conservation of elements representative of its function as an industrial machine for handling grain, also envisaging the valorisation in situ of any recoverable elements of the parts and accessory mechanisms.
- d. The historical-cultural valorisation and public use of a significant part of the complex. Aspetto statico-strutturale

Since the structural static aspect, with the use of the then innovative construction technology of reinforced concrete, represents a fundamental element of the complex and its historical value and contributes, in no small way, to determining its material and cultural identity, the redevelopment project must guarantee

- the preservation of the original structural conception of the complex, compatibly with the 'structurally' acceptable transformations on the basis of the attached technical report;
- the compatibility of the materials used for the redevelopment, with the original materials, so as not to cause damage to the existing structures;
- the durability of the materials and technologies used, which will be such as to guarantee subsequent ordinary or extraordinary maintenance operations that are easy and sustainable, without altering the architectural complex

With regard to the determination of the degree of modifiability of the Hennebique granary silo, it was possible, by means of finite element modelling, to examine the structure subject to transformations, associated with a maximum level (MODEL 1) and an intermediate level (MODEL 2), and to process the data obtained from the analyses. As might be expected, the application of a plausible overload of 3 kN/m², referring to the category of rooms susceptible to crowding, leads to lower normal stresses from the static action; it should be remembered that the range of values of the vertical variable loads of the primary design is between 3kN/m², imposed on the floors of the offices and corridors, and a maximum of 35kN/m² in the boiler room and the coal cellar. The difference between MODEL 1 and MODEL 2 is found in terms of the redistribution of loads on the load-

bearing elements, an effect due to the different conformation resulting from the choice of cells to be demolished.

The dynamic analyses revealed some criticalities which are related to particular cases within the section types examined at the base of the Silos. The most problematic elements are located at the central body and the innermost portico.

The sections of the pillars at the base (Pyl,D1 and Pyl,E) in the central part of the building are not verified because they have a reinforcement diameter of Ø12 which is not sufficient to counteract the bending moments in both directions and they have a low normal load. The elements constituting the seaward part on the ground floor, on the other hand, have no reinforcement and therefore the bending resistance is minimal. In the group belonging to the same section, some elements of the side wings do not satisfy the verification; the safety coefficient ρ assumes, however, values not much greater than unity (except in some limited cases).

The assumptions, however, adopted for this verification are cautious both in the definition of the seismic response spectrum, with the choice of soil category C, and in the use of an approximate rupture domain, implying a good margin of safety; it is presumable that a supplementary geological and geophysical investigation (with a more confident assignment of the soil class) will reduce the number of unverified elements. The top pillars of the ribbon room do not present any criticalities at the level of structural verification in both models; however, they need localised consolidation work to remedy the state of deterioration described above.

In conclusion, it is possible to state that the granary silos have a good structural behaviour towards static action (gravitational loads), which improves considering a future use different from the original function. In terms of structural recovery, the precarious conditions of degradation, however limited to certain portions of the building, require in some cases demolition and in others immediate consolidation, to avoid further deterioration and local collapse. The critical points found in the dynamic analysis carried out on the new hypothetical configurations are not such as to prejudice the redevelopment and functional reuse of the building. In particular, the transformability index achieved through the imposed modifications has determined positive results in both models, providing two possible solutions that can be adopted in view of future projects for the rebirth of Silos Hennebique.

Bibliography

- Carissimo A., Crotti G., De Cristoforis G.B., **Silos granario del porto di Genova. Progetto degli ingegneri A. Carissimo, G. Crotti, G.B. De Cristoforis.**, ed. Capriolo e Massimino, Milano, 1899 [Berio - Misc GEN D.1.14]
- Rotondo Terminiello G., Carbona D., **Porto di Genova, Palazzo San Giorgio, Aeroporto**, Sagep, Genova, 1986, pag. 38 [Berio - L GE A387.10]
- Tonizzi M.E., **Merci, strutture e lavoro nel Porto di Genova tra '800 e '900**, Franco Angeli, Milano, 2000 [Berio L GE C 387.1 TON]
- Carbona D., **Consorzio Autonomo del Porto di Genova: archivio storico** (6 volumi)
- Voce **Silo** in "Enciclopedia Italiana Treccani"
- Consorzio Autonomo del Porto di Genova, **Le opere del Porto di Genova nell'ultimo venticinquennio**, Stabilimento Arti Grafiche Drocchi Martinelli & C., Settembre 1931, [N. Carboneri, Scuola Politecnica, coll. Misc. R216y7]
- Ronco N., **Il Porto di Genova – conferenza tenuta a Milano il giorno 12 marzo 1911 all'Associazione Nazionale per i Congressi di Navigazione**, [N. Carboneri, Scuola Politecnica, coll. Misc. R114]
- AA.VV., **Nove opere del Porto Vecchio. La Costruzione del Porto di Genova tra Otto e Novecento. Catalogo della mostra, Genova, Palazzo S. Giorgio 23 novembre/13 dicembre 1987**, Sagep Editrice, Genova, 1987
- Rollandi M. S., **Merci e capitali: evoluzione e funzione dei magazzini del porto di Genova fra Otto e Novecento**, estratto da "il patrimonio industriale marittimo in Italia e Spagna. Strutture e territorio", a cura di Di Vittorio A., Barciela C., Massa P., De Ferrari Editore, Genova, 2009
- Rosso Del Brenna G., **Archeologia industriale e architettura contemporanea nel Porto di Genova**, Sagep, Genova, 2014
- AA.VV. "**Beton als gestalter (cemento armato: ideologie e forme da Hennebique a Hibelheimer)**", in Rassegna, anno XIV, 49/1, marzo 1992
- Festa C., **Guida pratica del porto di Genova**, 1^a edizione, a cura di Gazzetta Marittima, Genova, 1908
- Regio Ispettorato Generale delle Strade Ferrate, **Gli impianti e l'esercizio del porto di Genova, relazione compilata per cura del Circolo Ferroviario di Genova**, Tipo-litografia del Genio Civile, Roma 1902
- Poleggi E., Timossi G., **Porto di Genova, storia e attualità**, Sagep, Genova, 1977

| <u>Archives</u> | |
|--|--|
| a. Archivio Impresa Porcheddu, c/o Politecnico di Torino, biblioteca del Dipartimento di Ingegneria dei Sistemi Edilizi e Territoriali (DISET), Corso Duca degli Abruzzi, 24 – Torino | |
| - | Progetto dei Silos Granari nel Porto di Genova. Coll. 177 - anno 1900/1901 e coll. 177/3573 - anno 1900/1901 |
| b. Archivio Autorità Portuale di Genova, c/o Autorità di Sistema Portuale del Mar Ligure Occidentale, Palazzo S. Giorgio, via della Mercanzia, 2 – Genova | |
| - | Fondo Direzione Lavori, coll. DL 126, fascicolo 43 |
| c. Archivio Storico Comune di Genova - piazza G. Matteotti 10, | |
| - | Fondo "Amministrazione municipale", scatola 1952 |

Report on In-Depth Case Study

Fruit and Vegetable market (Genoa, Italy, 1926 to 1930's)



Type: undergoing restoration

Partner Institution: UniGe

Project: **CONSECH 20**

Working Package 2 – Task (iii)

Date: 28/09/2021

By:

Author 1 Rita Vecchiattini

Author 2 Giovanna Franco

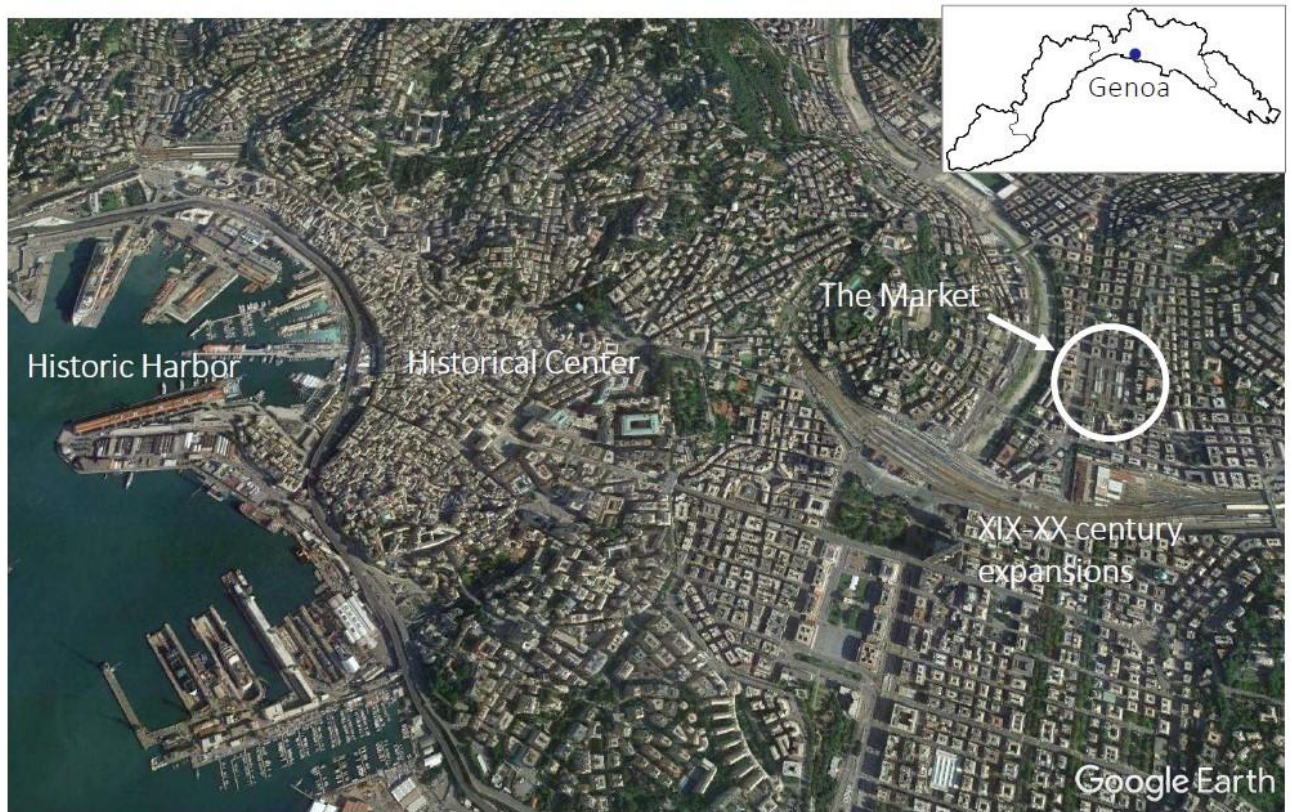
Author 3 Stefano F. Musso

Introduction

The fruit and vegetable market is located in Genoa in S. Fruttuoso district.

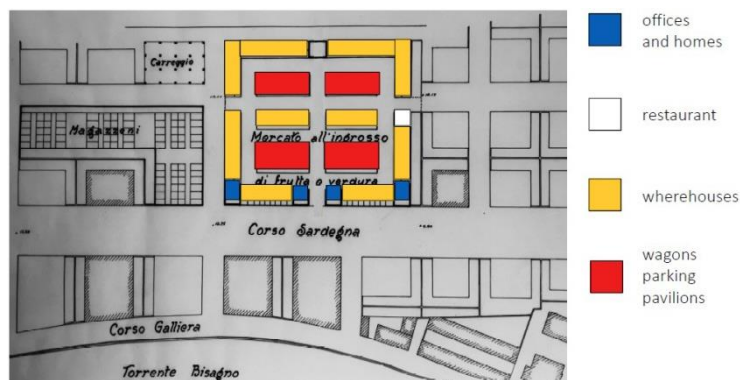
The complex was designed by the Technical Office of the Municipality in the late 1920s on a plot of 25,000 square meters by designers Ing. Mario Braccialini, Ing. Tomaso Badano and Arch. Giulio Zappa.

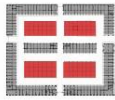
The building has been analyzed by the University of Genoa as part of a degree thesis in engineering-architecture. This report exposes part of the material produced.



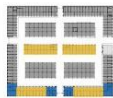
The market consists of four perimeter buildings organized on a single level with flat roof that defines a central rectangular space. Near the corners and the main entrance, however, these buildings are on two floors.

In the central space are located four double-height canopies with two-pitched roof originally intended for the parking of wagons, and two rectangular buildings on one level with flat roof used as warehouses.





Central pavilions for wagons parking



offices and residences



restaurant

Buildings for warehouses, offices and restaurants



One floor perimeter buildings

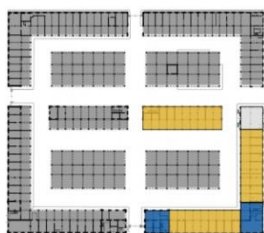
The construction work was entrusted to the company Giacomo Borneto & Figli, owner of a part of the lot.

The complex is the result of a repeated scheme, of a unified and coherent vision, although it was built in successive lots, from 1926 to 1930.

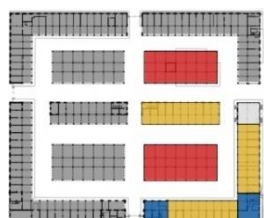


View of the market complex, Google Earth

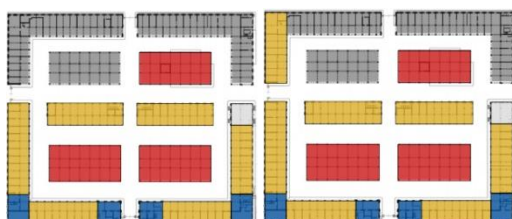
The construction of the complex took place for subsequent lots:



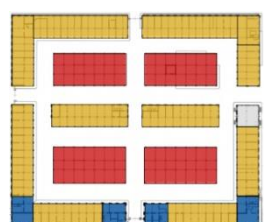
1926. Building of warehouses, offices and restaurant



1927. Construction of the first two central pavilions



1928 and 1930. Construction of other warehouses and pavilions



1931. Completion of the market complex

The construction is the result of a cultural period characterized by the rapid evolution of technical standards on reinforced concrete.

The executive project was then guided by four different regulations, published a few years later.

The buildings built in 1926 and 1927 follow the requirements of DP 15/05/1925, those built in 1928 the RDL 4/09/1927, the building built in 1930 the RDL¹ 4/04/1929 while the last parts, built after 1930, are in line with the RDL 18/07/1930.

1925:

- Tensile strength of reinforcements between 38 and 50 kg/mm².

¹ RDL= Royal Legislative Decree - D. Lgl. = Legislative Decree

- The longitudinal reinforcement shall not have a total section less than 1% of that of the conglomerate.
- The transverse tying of the bars and rods which arm the pillar must be effective and at a distance considerably less which the lateral bending of the bars and rods may occur, considered as insulated.

1927:

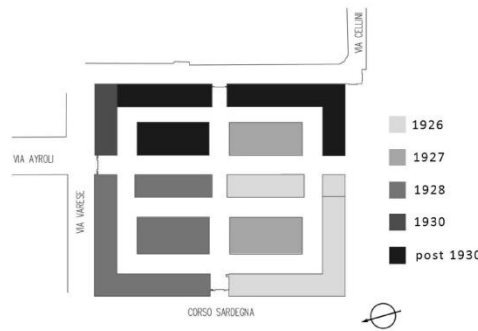
- Tensile strength of reinforcements between 38 and 50Kg/mm².
- The longitudinal reinforcement shall not have an overall section less than 1% or 0,50% of that of the conglomerate, when the latter is not greater than 1600 cmq or not less than 6400 cmq respectively. For intermediate conglomerate sections the iron section will vary linearly between the above limits.
- The transverse ligatures of the irons which arm the pillar must be distributed at a distance of 10 times the diameter of the irons.

1929:

- Tensile strength of reinforcements between 38 and 50 kg/mm².
- The longitudinal reinforcement shall not have a total section less than 1% or 0.70% of that of the conglomerate, when the latter is not more than 1600cmq or not less than 6400cmq, respectively. For intermediate conglomerate sections the iron section will vary linearly between the above limits.
- The transverse ligatures of the irons which arm the pillar must be distributed at a distance of 10 times the diameter of the irons.

1930:

- Tensile strength of reinforcements between 38 and 50 kg/mm².
- The longitudinal reinforcement shall not have a total section less than 1% or 0.70% of that of the conglomerate, when the latter is not more than 1600cmq or not less than 6400cmq, respectively. For intermediate conglomerate sections the iron section will vary linearly between the above limits.
- The transversal ligatures of the irons which arm the pillar must be distributed at a short distance never exceeding the minor dimension of the section of the pillar.



Legislation applied in the different stages of the construction of the complex

On part of the artifact was placed an architectural constraint. It is in fact stated that "it has a particularly important historical and artistic interest, pursuant to art. 10 comma 1 D. Lgs January 22, 2004 n. 42, because the two "L" bodies of the market overlooking Corso Sardegna and the two indoor pavilions are representative of the construction and typological characteristics of the complex, built in the first thirty years of the twentieth century".

For simplicity and accessibility reasons, we consider only the four canopies for this study: two in 1927, one in 1928 and one in 1930.

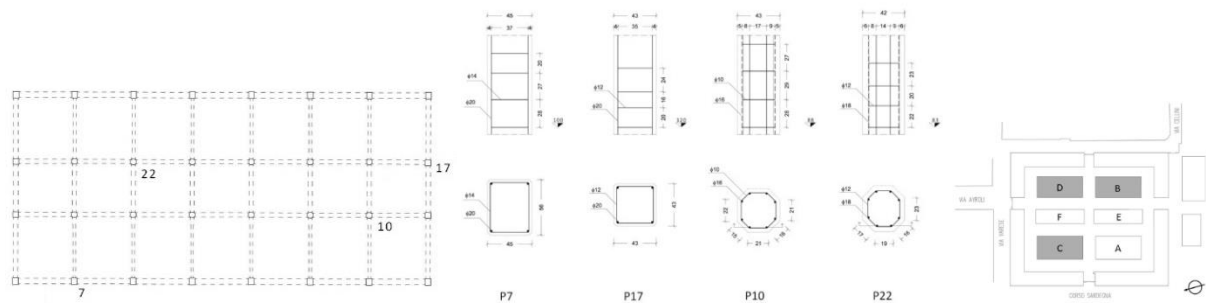
Characteristics of the Concrete Building and Structure

Materials

The concrete that forms the structure of the pavilions (pillars and beams) is made of a mixture of lime and cement with sea sand, gravel and crushed bricks. The lithotypes, recognised under the stereoscopic optical microscope, in some samples of material from three of the four pavilions are ophiolites, marly limestone and calcite spatica. The aggregate is strongly angular, for the fine fraction, and sub-rounded for the coarse. The mixture used in the roof structure, built in 1928, differs from the others in the absence of crushed stones and a greater presence of fine fraction (max 5-6 mm). Beams and pillars are covered with a thick layer of aerial lime and sea sand plaster.

Type of structure

The four rectangular pavilions divided into three "aisles" consist in a structure of reinforced concrete pillars and beams. The pillars have different cross-sections depending on their position in the plan: on the transversal sides, they are square, on the longitudinal ones, they are rectangular, and in the inner space, they are octagonal.



Pillars reinforcement roof B

At mid-height, the pillars are connected one to each other by beams. In the case of the pavilions built in 1927 and 1928, the beams are made of steel, to support the glazing or the light slabs of the external surfaces. In the pavilion built after 1930, the beams are made of reinforced concrete and support an intermediate floor, as well of reinforced concrete.



Connecting steel beams at half height of the pillars.



Connecting concrete beams at half height of the pillars.

The roof of the two side "naves" is flat and made with reinforced alveolar floors, while the roof of the central "nave" is double-pitched and has a supporting structure in reinforced concrete. In addition, in the roofs built in 1927 and 1928, there is a secondary warp in steel and transverse joists in wood, while in the roof built after 1930 there is a secondary warp in reinforced concrete and transverse joists in steel.

The roof covering is in all cases in Eternit (asbestos cement slabs).



Double-pitched roof of the central "nave".

Other relevant characteristics

The four pavilions belong to a single project but and were built at different times, less than 5 years apart each other. This has led to small differences in their constituent materials, dimensions and structures, even following the same plan, shape and conception structural.

Condition of the building

Several modifications to the pavilions have been realized over time, after their construction, in an uncontrolled way by the responsible of the single sales areas of the market: addition of steel beams, removal of glass partitions, insertion of technical installation in the reinforced concrete floors, anchoring of windows and doors to the pillars, new paintings etc .



The complex has been closed and abandoned since about ten years (precisely, since 2009, when the market was transferred in the western part of the city) and this has provoked a progressively degradation mainly due to huge and diffused water infiltration from the roofs and the broken or lacking windows.

An urban regeneration project is currently underway, which has foreseen the restoration/rehabilitation of the protected buildings, the substitution of the metal canopies with new ones in structural glasses, and the demolition of two pavilions (one from 1927 and one from 1930), to give space to a park and others functions of social interest for the neighborhood.

Damage types

The prevailing degradation of reinforced concrete structures relates to: corrosion and shearing of the reinforcement bars, cracking, detachment and expulsion of the concrete cover, crumbling of the floors, salt efflorescence, patina and biological colonisation, missing structural parts (columns and beams). The others constructive components (like frames and surface treatments, for example) suffer for many others degradation phenomena like: lacking parts, erosion, loss of cohesion, surface depots (coherent and incoherent), fissures and cracks, among others.

Hypothesis on damage processes

The main causes of this degradation are:

- infiltration of water into the roof covering which covers a large part of the intrados of the roof slab of buildings and sections of the roof beams.
- capillary ascent that affects the bricks infill present in the perimeter buildings because the market rises on soil of alluvial origin, little permeable, consisting of sand and clay.

These two causes are favored by the damage caused by the anchoring of doors and windows on the primary structure and the passage of the systems.

- presence of chlorides in concrete.

The main effects on the artifact are:

- saline efflorescences in the form of whitish substances with irregular diffusion and geometry.
- organic patina in the form of green deposit. The areas concerned could indicate both the presence of an excess of water and a poor quality of the conglomerate in terms of porosity.
- plaster breaks in continuity between the coating layers with respect to the substrate. The phenomenon could also be attributed to the structural changes and interventions made over time to the constructive elements.
- expulsion of ferris covers probably due to the depassivant action of chloride present in the material.
- static-constructive failures and deficiencies of slabs and inflexible elements due to corrosion of the irons placed on the underside of the reinforced concrete joists and the addition of slabs on the perimeter beams (canopy D).



Saline efflorescences



Biological patina



Expulsion of the iron cover



Detachment of plaster

Aim of the investigation

The investigations carried on and still ongoing have two main objectives:

- to understand the small/large differences in materials and structures relating to pavilions built at different times (1927-1928 and after 1930), if they exist;
- to estimate the resistance of the reinforced concrete parts, as far as possible in non-destructive ways.

Methods

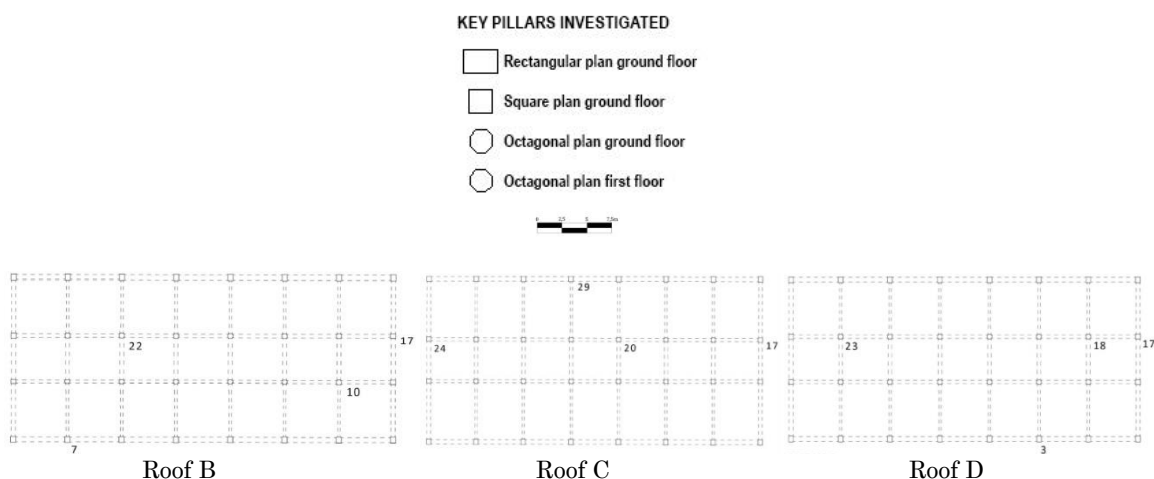
The adopted non-destructive diagnosis methods are as following:

- Non-destructive “pacometer” investigations, based on the principles of electromagnetic induction (BS 1881:204), performed with an “Elcometer 331” instrument, with maximum survey capacity corresponding to a depth of 10 cm.
- Non-destructive ”Sclerometer” tests, based on the rebound velocity (UNI-EN 12504-2, UNI-EN 13791, ASTM C 805), carried out with the "C181/N" instrument.
- Non-destructive “Ultrasound” tests, based on the propagation speed of electromagnetic waves (UNI-EN 12504-4), which have been afterwards compared with the “Sclerometric” tests, by using the “SonReb” method.
- Non-destructive investigations with "Leeb Hardness" tester of the reinforcements, based on rebound velocity (DIN 50156), carried out with the "EPX300" instrument.
- Destructive compression tests carried out on extracted specimens according to UNI 6131-2003 and UNI-EN 12504-1 regulations and standards

Further, the following analysis have been executed:

- Carbonation level analysis with “Phenolphthalein” method.
- Mineralogical-petrographic analysis of the samples of concrete extracted from different structural components of the market, carried out with “Stereoscopic Optical Microscope”, used in reflected light.
- “Infrared Spectrophotometry” analysis of several salts’ efflorescence samples.

Results



Pacometric investigations (Appendix A, Figure 1):

- there are three types of pillars divided by shape in plan.
- in the three roofs the pillars are differently armed.

- staple pitch is different in all three roofs investigated.

Sclerometric tests (Appendix A, Figures 2, 3):

- Different compressive strength of a few units for the two roofs examined.

Non-destructive investigations with Leeb durometer (Appendix A, Figure 4,5):

- Low tensile strength values were found in roofs.
- Roof D has lower values than C.

Destructive compression tests (Appendix A, Figure 6,7):

- Two different mix designs for the presence of bricks in the canopy C.
- Different compressive strength values of the two roofs.
- In roof C as the h/D increases, the resistance decreases, while in roof D this does not occur.

Non-destructive ultrasound tests combined with sclerometric tests using the SonReb method (Appendix A, Figure 8,9):

- Values of cubic resistance are more homogeneous than those found in the individual tests.
- Roof C has higher resistance values than other buildings.

Analysis of carbonation level with phenolphthalein (Appendix A, Figure 10,11):

- Carbonation depth increases by about 1 cm every 10 years. In general, carbonation values are consistent with the time coherent since construction.
- Although more recently constructed, the depth of carbonation is on average greater in roofing D.

Mineralogical-petrographical analysis (Appendix A, figure 12):

- The samples analysed have the same characteristics although they differ in the size of the aggregates.
- Abnormal presence of broken bricks in roofs B and C.

Infrared spectrophotometric analysis of saline efflorescences (Appendix A, Figure 13):

- Presence of chlorides, sulphates and nitrates.

Conclusions

From the verifications carried out according to the regulations of 1925, 1927-e 1930 it is found that in general the roof D has been planned in compliance with the requirements of the regulations in force, while the canopy C and the perimeter building deviate more.

The verification showed that the roof differ from each other. Both do not meet the shear test in the most stressed beam and this is due to the fact that the regulations of the time did not require the transverse reinforcement steps such as to avoid shear breakage, in particular in the supports where there is greater stress.

Focus on pillar stability verification: in roof D the verification is satisfied for a value of slinness equal to about the half of that limit, while in roof C the slinness value of the pillar is very close to that of slinness limit this because the free light of inflection is very high (double of roof D).

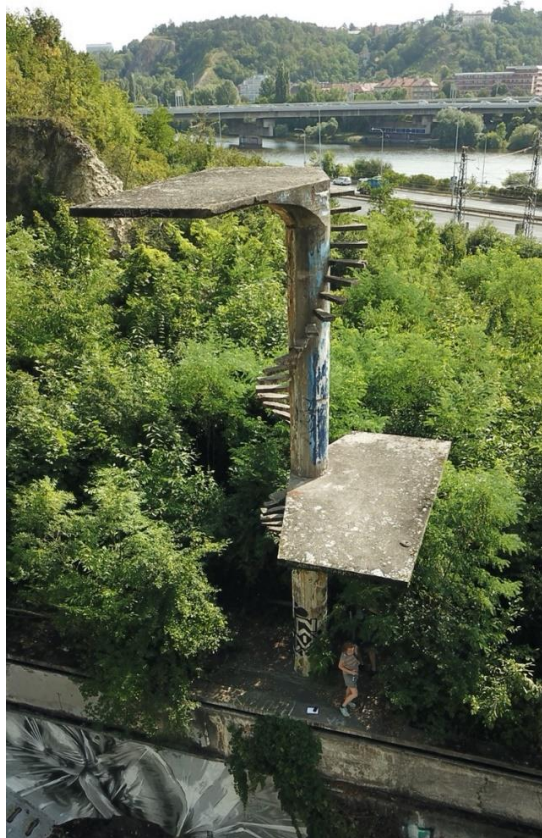
Bibliography

Il mercato Ortofrutticolo di Corso Sardegna a Genova. Analisi della struttura e dei materiali in rapporto alle normative sul calcestruzzo armato dei primi anni del Novecento. University of Genova, Polytechnic School, Ingegneria Edile-Architettura. Eugenia Repetto, Supervised: Prof. Rita Vecchiattini, Co-supervised: Ing. Chiara Romano, Arch. Gerolamo Stagno, a.a. 2015-2016.

Le nuove frontiere del restauro. Trasferimenti, contaminazioni, ibridazioni. Scienza e Beni Culturali, XXXIII. Convegno Internazionale 2017, Giornate di Studi Bressanone 27-30 giugno 2017, Arcadia Ricerche Edition.

Report on In-Depth Case Study

Barrandov Diving Tower (Prague, Czech Republic, 1930)



CONSECH20 – WP2 (iii)

Ondřej Dušek

Cristiana Nunes

Hanna Hasníková

Konstantinos Sotiriadis

Zuzana Slížková

October 5, 2021

Introduction

Background

The Barrandov swimming stadium, located in the outskirts of Prague (Praha 5 Hlubočepy), is an iconic sports modernist construction in the Czech Republic. It was designed by the architect Václav Kolář and built in 1930 on the left bank of the Vltava river in Prague, at a former limestone quarry site. It was part of the development of the area encompassing residencies, film studios, and a restaurant. The dominant feature of the complex is a concrete functionalist diving tower with two platforms resting on a cast-in-place pillar with a spiral staircase. The peculiar diving tower soon became an emblem of water sports constructions in the country. The swimming complex was in use since its inauguration in 1931 until 1955. In 1993, the complex was declared a cultural monument. The swimming pool and the diving tower are currently in a state of ruin and surrounded by overgrown vegetation. However, it is accessible to the public and, during summer, it has been used as a place for cultural events.

The diving tower has been selected as a case study for in-depth analysis within the project because of its historical importance, poor conservation condition (including the absence of documentation), and significance to the local community and tourism.

Research aims

This report aims to complete the architectural documentation and the condition assessment of the Barrandov diving tower, which entails the following tasks:

- Documentation of the structure,
- Information about the current condition of the structure and materials, and
- Planning of tests and analyses.

Brief history

Urban Context

The stadium's complex and, in particular, its diving tower is valuable as a peculiar architectural design in its detail. Nevertheless, it also has a special significance in its urban context because it was created as an integral part of the garden city of Barrandov, growing in the southwest of Prague since 1928. This urban development has a unique position in the history of Prague city planning, as the first one of this kind - a result of activities carried out by a single private entrepreneur, Václav Maria Havel (father of the former Czechoslovak/Czech president Václav Havel). We could find other examples of

progressive development projects in Prague of the interwar period (e.g., Baba settlement), but cooperatives or the Municipality ran these.

Diverse influences mark the concept and the implementation of the development plan. During his stay in the USA in the early '20s, Václav M. Havel, the son of a prominent Prague family and a person of cosmopolitan nature, visited the residential garden districts of San Francisco (in particular Ingleside). This experience is considered to be the initial inspiration for the Barrandov development project. The other crucial moments had been: his visit to Stuttgart Weissenhof Colony in 1928 and the work of Czech functionalist architects (Max Urban, Vladimír Grégr, Jaromír Krejcar, and Jaroslav Fragner)[1].

The initial part of the settlement, designed almost entirely in a progressive, modernist style, was built during a decade starting in 1928. The master plan outlined the structure of the garden city, composed mainly of detached gardens surrounded by residences. The Barrandovské Terasy Restaurant was planned as a genuine key point of the new district. Its location on the edge of a Vltava River cliff offered an extraordinary view; a lighthouse-like tower dominated its architecture. Built extremely rapidly within 1929, it suddenly became a rather popular place within the context of the entire city. Another important neighborhood element soon rose on the opposite side of the district: the Barrandov film studios run by Václav M. Havel's brother Miloš. Due to the film industry's presence, all the neighbourhood soon acquired the nickname "Czech Hollywood."

The empty area of an abandoned quarry below the restaurant's terrace naturally caught the planners' attention. The idea to place a swimming pool there was soon to be tested by the first designs of the architects. As Andrea Turjanicová points out in her work [2], the notable presence of a sports facility in the newly developing area corresponds with the importance of sports and health for the "modern lifestyle" of the period. The construction of a swimming pool concluded the development of the area, both in spatial and functional meanings. After this intervention, the Barrandov neighbourhood was ready to be presented as an expression of modern lifestyle. The stadium and the restaurant were closely connected. The busy life of the swimming pool could have been easily watched from the terraces and garden of the restaurant (Figure 1, 2).

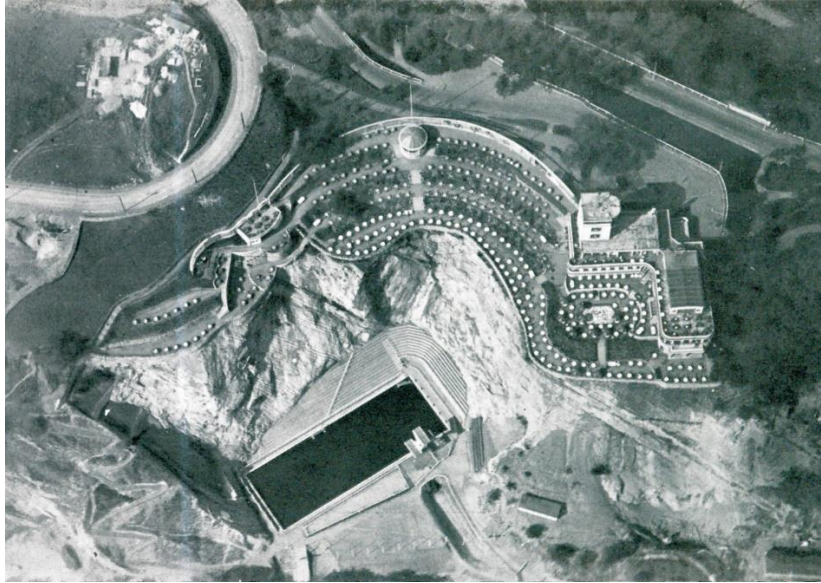


Figure 20. Aerial view of the Swimming Stadium and the Barrandovské Terasy restaurant [3]

The Construction of the Stadium

A partnership with the Czech Swimming Club had soon been established. According to the agreement, the entrepreneur would offer the plot for free. In addition, the Swimming Club would build a swimming stadium there to host professional athletes and the general public. The consortium also negotiated a subsidiary of the Public Health Ministry and the Municipality to cover the building costs.

The construction works were provided by Brázdil & Ješ, a company that previously executed the structure of the Barrandovské Terasy Restaurant. Master Carpenter J. Ulrych constructed the wooden structure to serve as changing chambers and club. The stadium's construction started in 1929, but soon the progress was delayed by the Great Depression. Also, the building costs rose over the initially agreed budget. Despite the debts, the stadium's construction was finished and inaugurated in 1931[4].

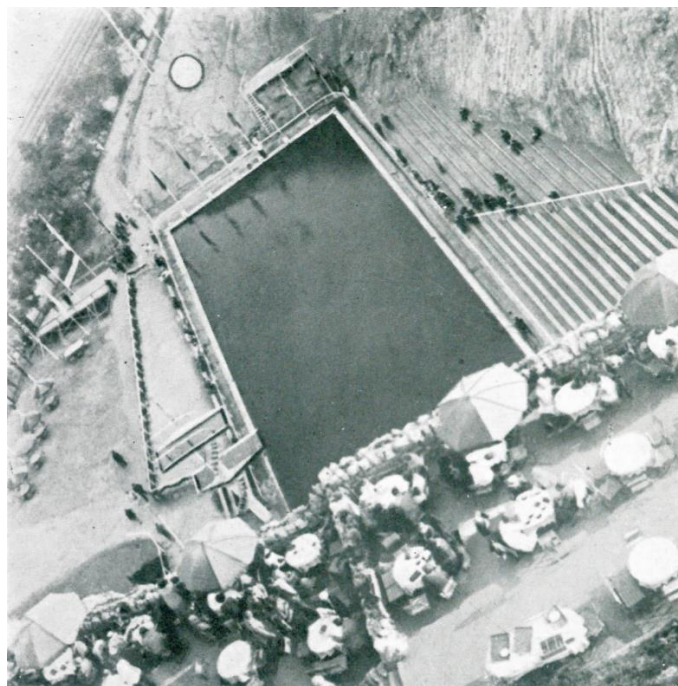


Figure 2. View from the Restaurant towards the Swimming Stadium [3]

The Architect and the Design

The complex was based on the design by Václav Kolátor (1899-1983), an architect and a member of the Czech Swimming Club; Kolátor was a specialist within the field, a professional swimmer, a promoter of water sports, and co-author of the book on bath and swimming pool architecture (Figure 3). During his career he designed several swimming and bath facilities (e.g. Volary, Česká Třebová, Litomyšl, Chrudim and Piešťany) [2].

Kolátor created an elegant functionalist design complying with the parameters for international sports competitions. The stadium comprised a pergola and a building with changing rooms plus a club – a simple geometric volume with a flat roof used for sunbathing. The tribunes were built at the foot of the cliff, using its natural topography. The 50/18 m swimming pool's depth varied from 0.9 to 4.5 m. The pool walls were made of reinforced concrete, and the bottom was carved in the rock. The swimming pool water was pumped from a well drilled in sandy soil close to the Vltava Riverbank. The swimming pool had six swimming lanes, and its front was equipped with starting blocks, and the long side with a springboard and a diving tower — the most significant architectural element of the stadium. On the one hand, the surroundings of the swimming stadium, a ca. 45m high limestone-shale massive cliffs with the tower of the restaurant at the top, contributed to a unique genius locus. On the other hand, it caused one notable disadvantage: direct sunshine reached the area only in the morning hours; otherwise, it was hidden behind the cliffs.

The Diving Tower

The diving tower was designed as a reinforced concrete cast-in-place structure, based on one single structural element: a round pillar (height 9.75 m, perimeter 1.2 m, foundation depth: 4.5 m). Two diving platforms and a helix-shaped circular staircase were cantilevered from the pillar, each step being an independent cantilever separated from others. The last step under both of the platforms is atypical, the volume of the step is integrated ("submerged") into the platform's volume, and the step is more profound. There are 18 stair steps between the ground level and the lower diving platform and 19 stair steps between the lower and the upper. The diving platforms were cantilevered asymmetrically from the pillar, one in the height of 4.75 m and the other in the height of 9.75 m high (5 and 10 m above the pool water level). A simple metal tube handrail highlighted the geometry of the structure, copying the form of the helix. The metal-tube columns of the handrail were fixed to the sides of the stairs and the platforms [5], [6].

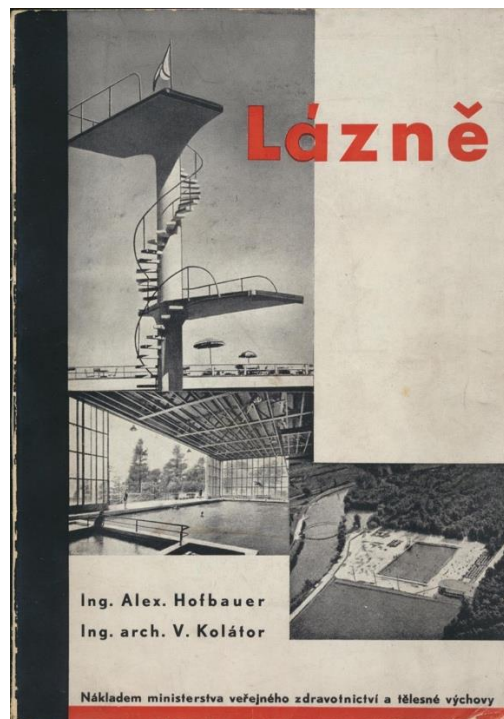


Figure 3. Cover of the book *Lázně (Baths)* by Václav Kolátor and Alex. Hoffbauer [6]

The Fame and Decline of the Stadium

Even before the opening, the swimming stadium was burdened with the debts caused by the higher construction costs and deepened by the impacts of the financial crisis (the expected subventions and provisions were lower than counted). On top of that, a fire destroyed the wooden buildings containing the changing rooms in 1934, and it had to be restored.

Despite these problems, the swimming stadium became a favourite leisure time destination and a centre of professional sports. In addition, the diving tower was frequently used as an object of interest of the Avant-Garde arts and photography (e.g., Karel Teige, Josef Sudek, and Eugen Wiškovský, Figure 4) as well as of popular media

(lifestyle magazines and cinematography) [2], [7]. A collection of photographs documenting the stadium's sports events can be found in the Photobank of the Czech Press Agency (ČTK).



Figure 4. Karel Teige, Collage Number 196, 1941.

During the Stalinist regime that came to power after 1948, the stadium and the restaurant were expropriated and "nationalised." The complex started to suffer due to insufficient maintenance. In the 1960s, as a new swimming stadium was built on the opposite side of the river, in Podolí, the Barrandov stadium was closed.

Since then, the facility has been abandoned. The swimming pool wall has been broken in the middle; the tribunes have been deteriorating and covered with vegetation. The handrail and the lower stair steps of the diving tower have been removed, most likely for safety reasons (to avoid access from visitors). In the 1990s, the stadium was returned to the heirs of its original owner, the Havel brothers.

Recently, the site has been empty, but the vegetation is being taken care of, and some pathways have been marked. The public can access the site and, during the summer, it has been used as a venue for cultural events. The restaurant's building on the top of the cliff is being restored as new buildings are being constructed in the area of its original terraces. We can ask whether these new activities would stimulate any favourable change in the neighbouring swimming stadium.

Documentation and condition assessment

Visual assessment

The visual inspection of the structure was performed on 21.7.2020 when the vegetation was flourishing (Figure 5.a) and on 27.2.2020 when the vegetation surrounding it was naked (Figure 5.b). The description of the damage types was done according to the MDCS atlas [8].

The structure of the diving tower and the swimming pool are in a state of ruin, i.e., it is virtually impossible to restore its original state without discarding most of the original materials.



Figure 5. General view of the diving tower and its surroundings: a) Photo taken on 21.7.2020, b) Photo taken on 27.2.2020.

Four main categories of material damage were registered:

- i) Surface discoloration: soiling, graffiti
- ii) Biological colonization of concrete
- iii) Corrosion of the steel reinforcement
- iv) Detachment and features induced by material loss, mainly disintegration

The pillar of the diving tower is the only element that does not show signs of structural damage, though higher plants with roots adjacent to the pillar might grow, affecting its stability (Figure 6.a). Apart from the almost complete loss of the original surface coats that once covered the pillar, the most common deterioration patterns registered on the pillar are surface discoloration due to soiling and graffiti (Figure 6.a,b).

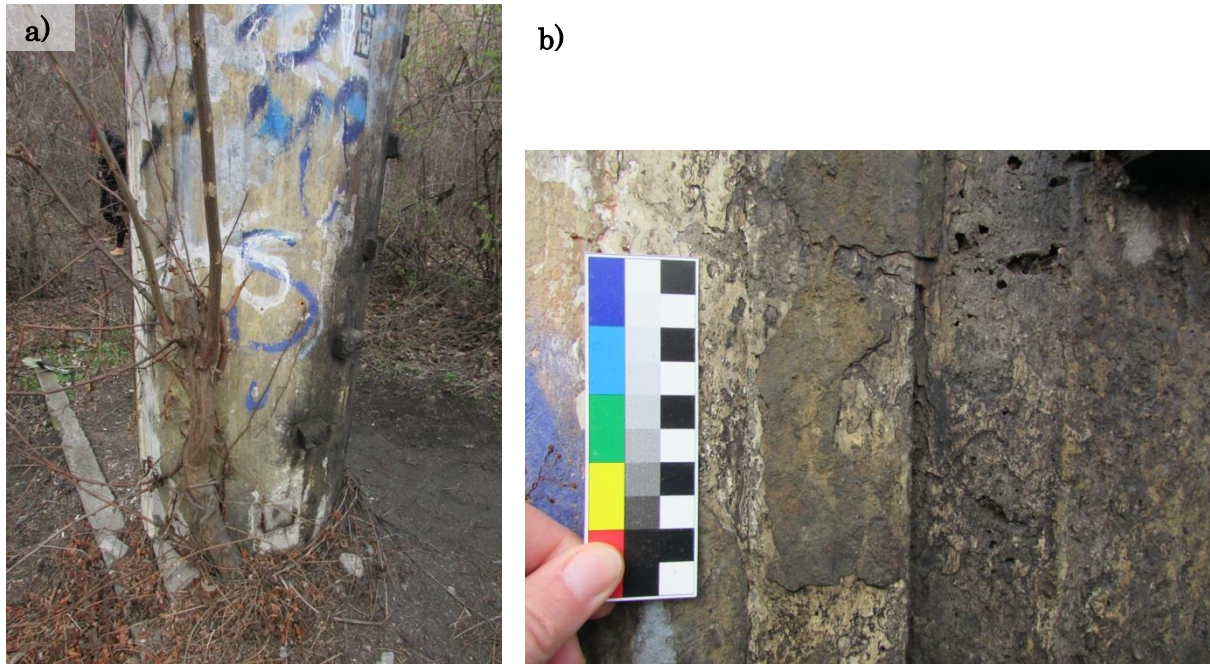


Figure 6. Detail of the pillar at the ground level: a) Graffiti and higher plant growing adjacent to the pillar, b) Reminiscences of finishing coats (blistering) and soiling.

The stair steps have lost most of the concrete cover triggered by the corrosion of the reinforcement (Figure 7.a). In general, the concrete surface layers remain only on the top of the steps (Figure 7.b). The handrail that once spiraled along the stairs is absent. The first ten stair steps from the ground level have been removed for safety reasons since the complex is accessible to the public.

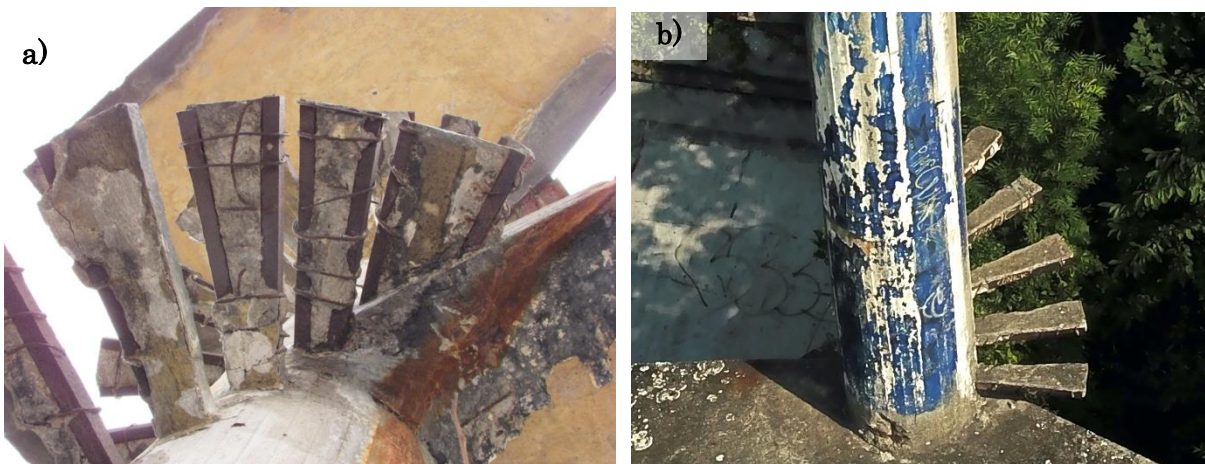


Figure 7. Details of the stair steps: a) View below the steps to the lower platform, b) Top view of the steps to the highest platform.

The diving platforms show biological colonization on the top of the concrete cover (e.g., lichens, cyanobacteria, mosses) (Figure 8.a) and corrosion of the reinforcement mostly visible underneath the platforms (Figure 8.b, d), enabling the visualization of its radial structure (Figure 8.c).

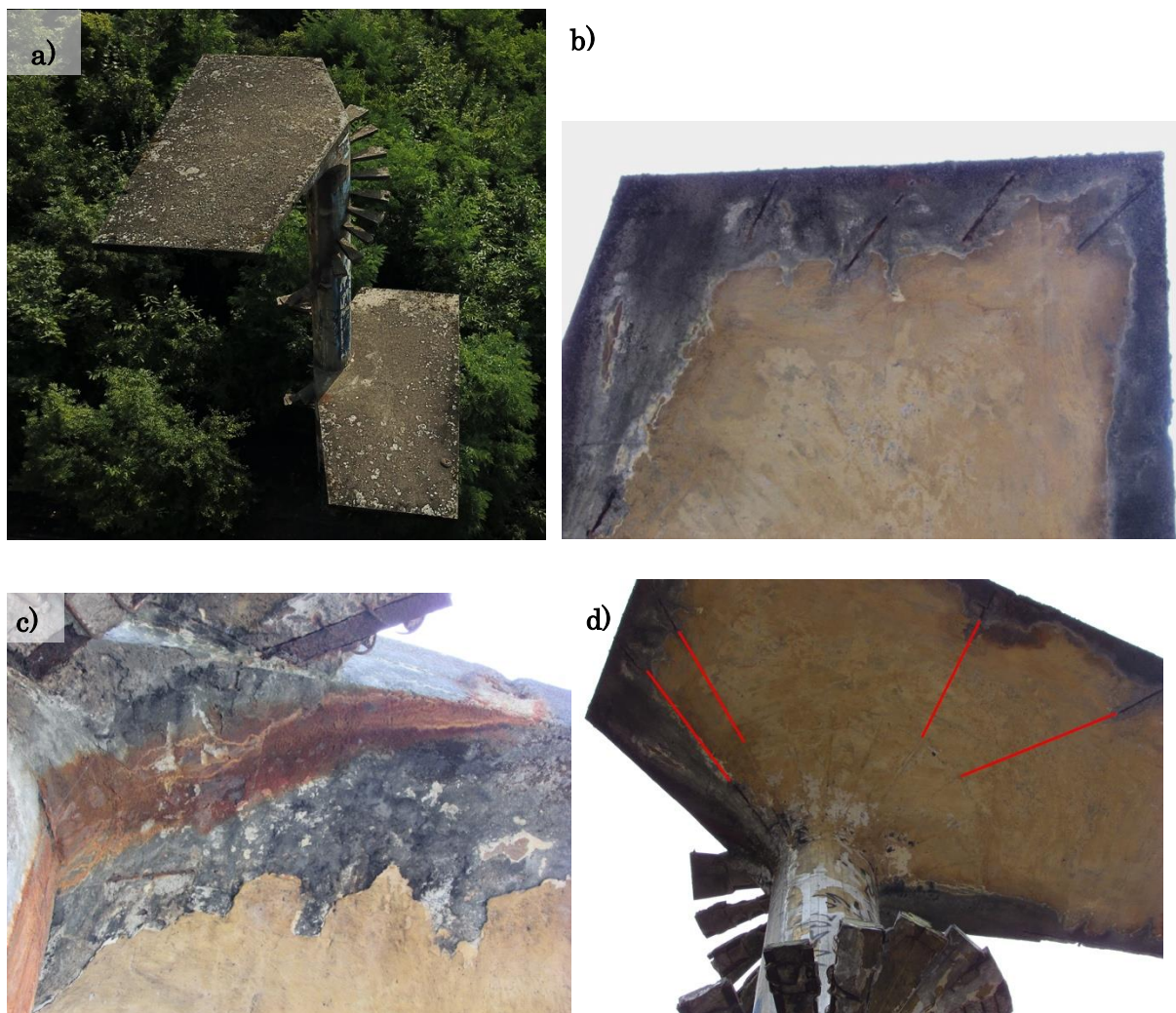


Figure 8. Aspects of the platforms: a) Top view of the platforms showing biological colonization, b) Detail of the corrosion of the reinforcement in the highest platform, c) Detail of the staining resulting from the corrosion of the reinforcement in the lower platform, d) Bottom view of the highest platform with the indication of the structure of the reinforcement (red lines).

The possible sources of the deterioration patterns observed are a combination of factors mostly related to water and aerosols: carbonation-induced corrosion, frost action, acid chemical pollution attack (proximity to high traffic roads), and biological colonization. Special analyses are required to assess the causes of damage accurately, which are detailed in Chapter 4.

The documentation of the structure

The old and the new drawing documentation

Although the swimming stadium and its diving tower have already been a point of interest for research [1], [2], [5], [7], almost nothing of the original drawing documentation had been revealed. The main places to archival search, such as the Municipal archive of Prague 5, the architect Kolátor's fonds in the National Technical Museum, or the Havel Family archive, had no documents. The construction history of

the stadium, as described in Václav M. Havel's memories [4], pointed out another possible source. The Archive of Architecture of the National Technical Museum (NTM) contains a collection of documents of the constructor of the stadium, the Brázdil & Ješ Construction Company. This archive remained inaccessible for more than one year. Still, finally, after reopening in summer 2021, it revealed precious materials linked to the Barrandov Swimming Stadium, including parts of the executive project drawings. The new findings are described in a separate paragraph.

Although the historic plans offer a lot of useful information, two sets of new drawings had to be processed for the next steps of the research project:

- a) The current state – containing the location of the damages, samples, etc.
- b) The drawing documentation reconstructing the original state of the structure – including the parts that are nowadays missing (the handrails, the flagpole) and redefining the precise geometry that became unclear due to decades of deterioration (e.g., the edges of the cantilevered stairs).

The Brázdil & Ješ Construction Company fonds in the Archive of Architecture of the National Technical Museum

The fonds of the Brázdil & Ješ Construction Company contains three files of documents relevant to the project and construction of the Swimming Stadium pod Barrandovskými terasami.*

The collection represents a mixture of documents from different project phases: the quotation budgets, internal communication of the company with contracted craftsmen, structural calculations, executive project drawings (the reinforcement and formwork plans of the swimming stadium, the diving tower, and the shat installation), construction accounting, etc. The documents are often incomplete, in many cases only in fragments. A clear description and dates are often missing.

Several factors caused the loss of documentation. The fonds are composed of the inheritance of Eng. Pavel Brázdil and of the remnants of the company archive. The Construction Company Brázdil & Ješ existed from 1928 until 1948. After the communist coup, the company was integrated into a state-owned construction enterprise, and Štěpán Ješ was persecuted due to his previous political activities. In 2002, the fonds were damaged during the great flood as other collections of the NTM's archive of architecture.

Only a small part of the documents refers to the structure of the diving tower. This structure is drafted in two drawings of the executive project: the reinforcement and formwork plan of the diving tower (Figure 9.a) and the reinforcement plan of its foundation (Figure 9.b). Three fascicles of the structural calculations are devoted to the structure of the diving tower. Three different proposals for the finishing of the diving tower surfaces are described in the preliminary budget.

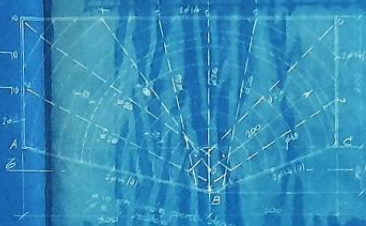
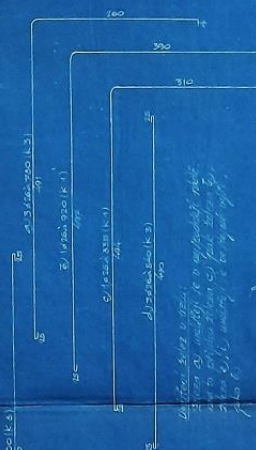
The items with the most important references to the diving tower are given in Appendix 1.

PLAVECKÝ STADIÓN POD BARRANDOVEM. SÁDOVACÍ A ARMOVACÍ PLÁN VĚŘE PRO SKOK 1:25

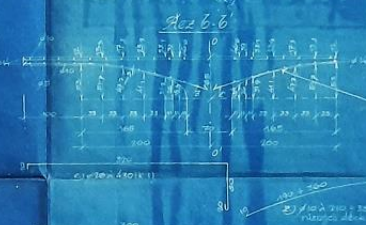
SLoup

HORNÍ PODESTA

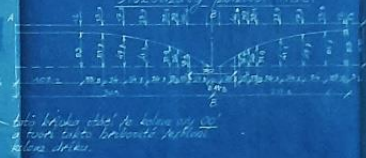
Rez A-A



Rez B-B



Pozitivní pohled ABC



DOLNÍ PODESTA

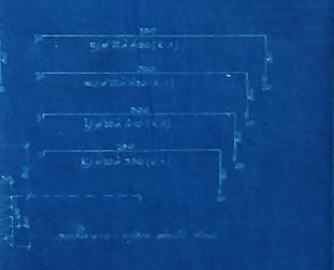
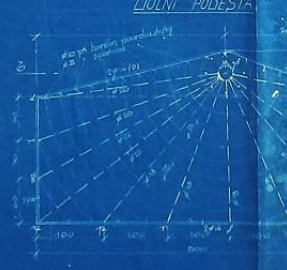


Figure 9.a) The reinforcement and formwork plan of the diving tower.



Figure 9.b) The reinforcement plan of the diving tower foundation.

Other Historic Sources

Besides the documents found in the Brázdil & Ješ company fonds, only a few simple drawings of the swimming stadium can be found in contemporary books and reviews. The complex's general situation plan and axonometry (Figure 10.a, b) were published in the Stavba review [3] in 1931. The same situation plan is also reprinted in the book "Lázně" (Bath) mentioned below.

Detailed text descriptions linked to the diving tower appear in different historic publications:

- In the book "Lázně" ("Baths") [6] written by the architect of the swimming stadium Václav Kolátor and by the Eng. Alex. Hoffbauer, the normative dimensions of the diving towers are suggested: the horizontal dimensions of the platforms as 5 x 2 m and their heights as 5 and 10 m above the water level.
- The swimming stadium was represented in the catalogue of the exhibition Czech functionalism 1920-1940 organised in the Museum of Applied Arts in Prague in 1978. [5] The dimensions of the platforms, their height, and the width of the staircase are described in the text accompanying the photograph of the diving tower. The catalogue was made during Václav Kolátor's lifetime, and the information was probably obtained directly from him.

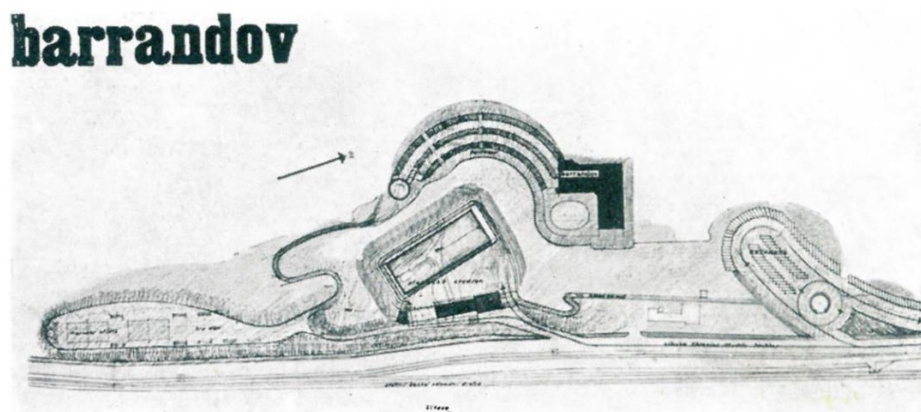


Figure 10.a) The general situation plan of the Swimming Stadium and the Barrandovské Terasy Restaurant
Klikněte nebo klepněte sem a zadejte text.



Figure 10.b) Collage of the Axonometrics the Swimming Stadium and the photo of the Restaurant

The historic photographs of the swimming stadium, both artistic and popular, are a precious source of information on the original state of the diving tower, on its original surface finishing, as well as on the forms of the disappeared elements, the handrail, and the flagpole. Concerning other vanished structures of the site, the building of the changing rooms, the club, etc. the historic photographs and film shots remain the only visual representation (particular sources are described in paragraph 2.5)

Close-Range Photogrammetry

The lack of drawing documentation required a new survey. Many constraints limit the methods of the measured survey: the state of the structure does not allow to climb the upper parts, its surroundings are covered with vegetation, and hardly accessible for a lift platform. Due to these reasons, the method of close-range photogrammetry was chosen. A drone was used to shoot over 600 photos to document the state of the inaccessible parts of the structure and serve as the input data for the photogrammetric 3D image. The photos were processed in the Agisoft Photoscan software. A 3D image composed of a point-cloud was generated (Figure 11.a).

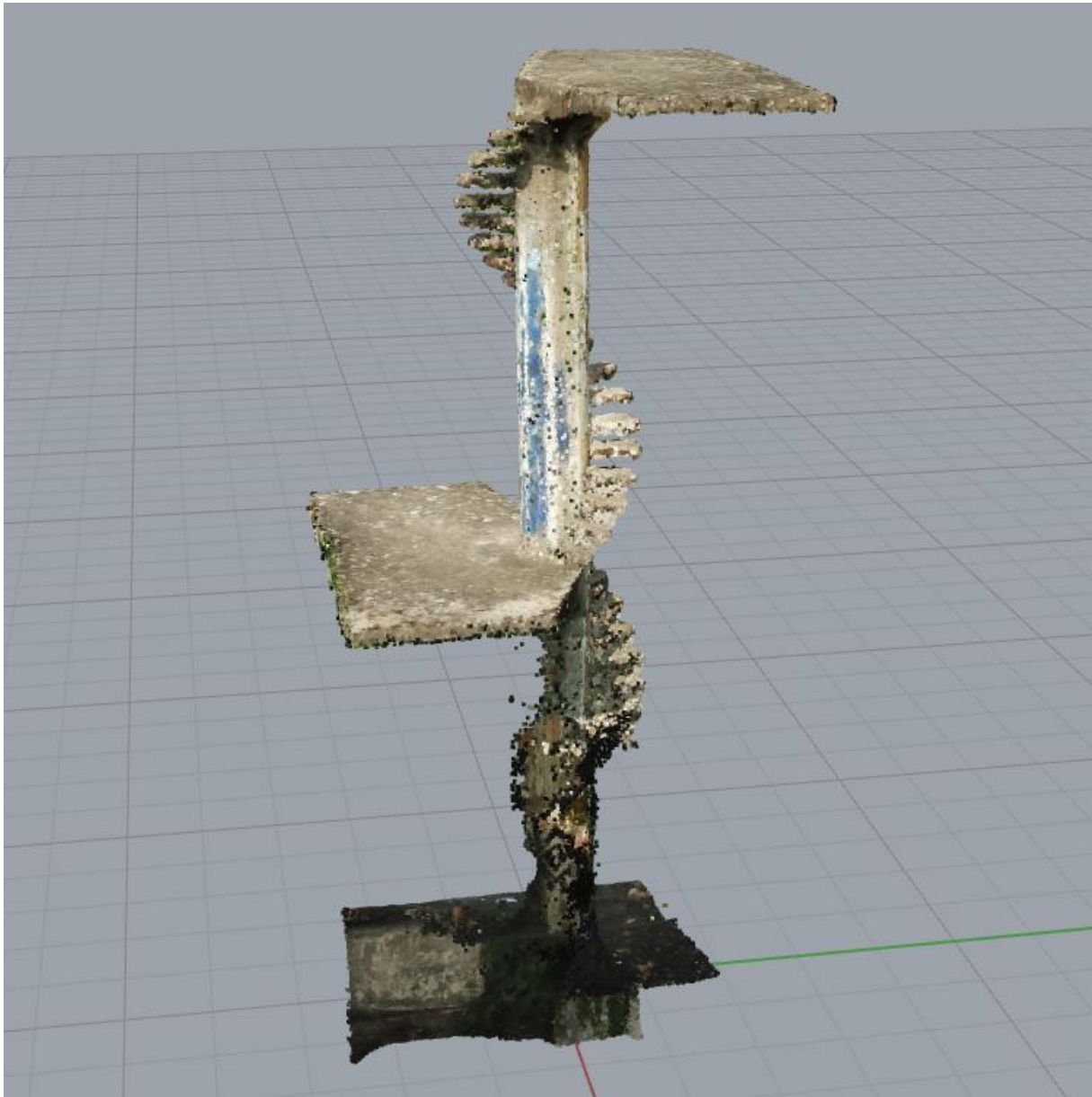


Figure 11.a) Point cloud 3D image generated by the photogrammetry software.

Drawings of the recent and original state

The recent and original drawings (Figure 11.b, c, d) were elaborated using all the information sources mentioned.

The executive–project drawings and the photogrammetric survey were taken as the primary source for reconstructing the original state. The executive–project drawings describe precisely the shapes and the dimensions of the principal elements of the structure: pillar, platforms, and foundations. The circular staircase is not drawn, but described hereafter.

The measured survey does not entirely reveal the staircase's original geometry due to the difficult access and the state of deterioration: the stairs are the most damaged part of the structure. The lower ten stairs are missing, the upper ones have lost their original

shape, the concrete surface layer has crumbled off, the reinforcement bars and wires are exposed, and almost no original edges of the stairs have been preserved. Nevertheless, the photogrammetry-generated point cloud gave approximate information about the shapes of the stairs, in particular about the atypical shapes of the highest stairs below each of the platforms.

The basic dimensions of the stairs are mentioned in the structural calculations and the preliminary budgets. Still, when confronted with the geometry of the pillar and the platforms, their precise geometry remains unclear.

The reconstruction of the missing elements – the handrails and the flagpole – is limited due to the lack of documentation: there is no evidence about any drawings of the handrails preserved to our days, except the hand-drawn sketch in one of the executive project blueprints marking the positions of its columns on the sides of the upper platform. The 3D geometry of the handrail was derived from the original photographs; the positions of the anchoring points of the handrail columns remain visible on the platforms. In 1929's preliminary budget, the handrail material was specified as a D42 steel "gas" pipeline. This material is still present in other elements on the site– the access ladders on the sides of the swimming pool are made of steel pipes of this diameter.

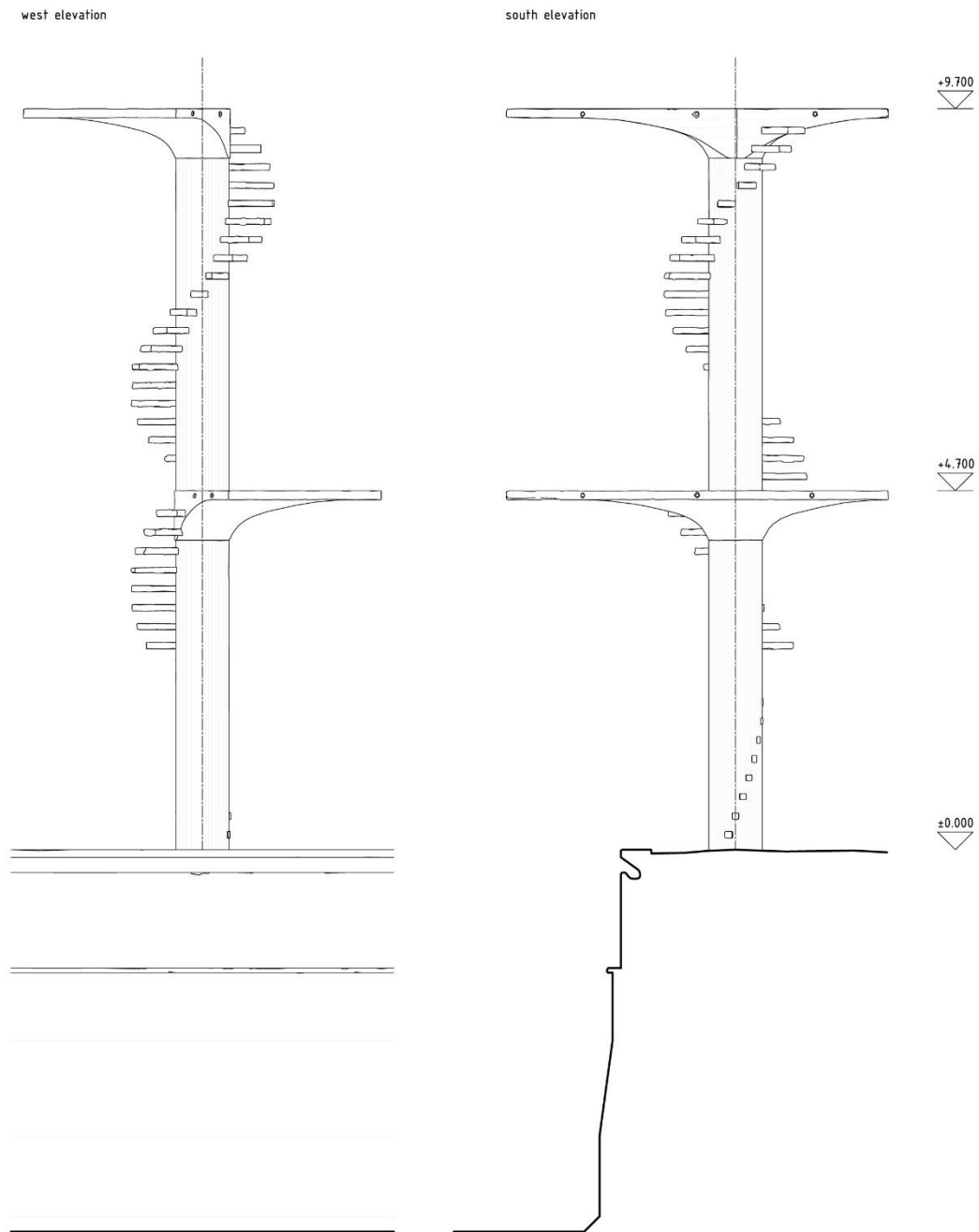


Figure 11.b) Recent state of the tower – elevations.

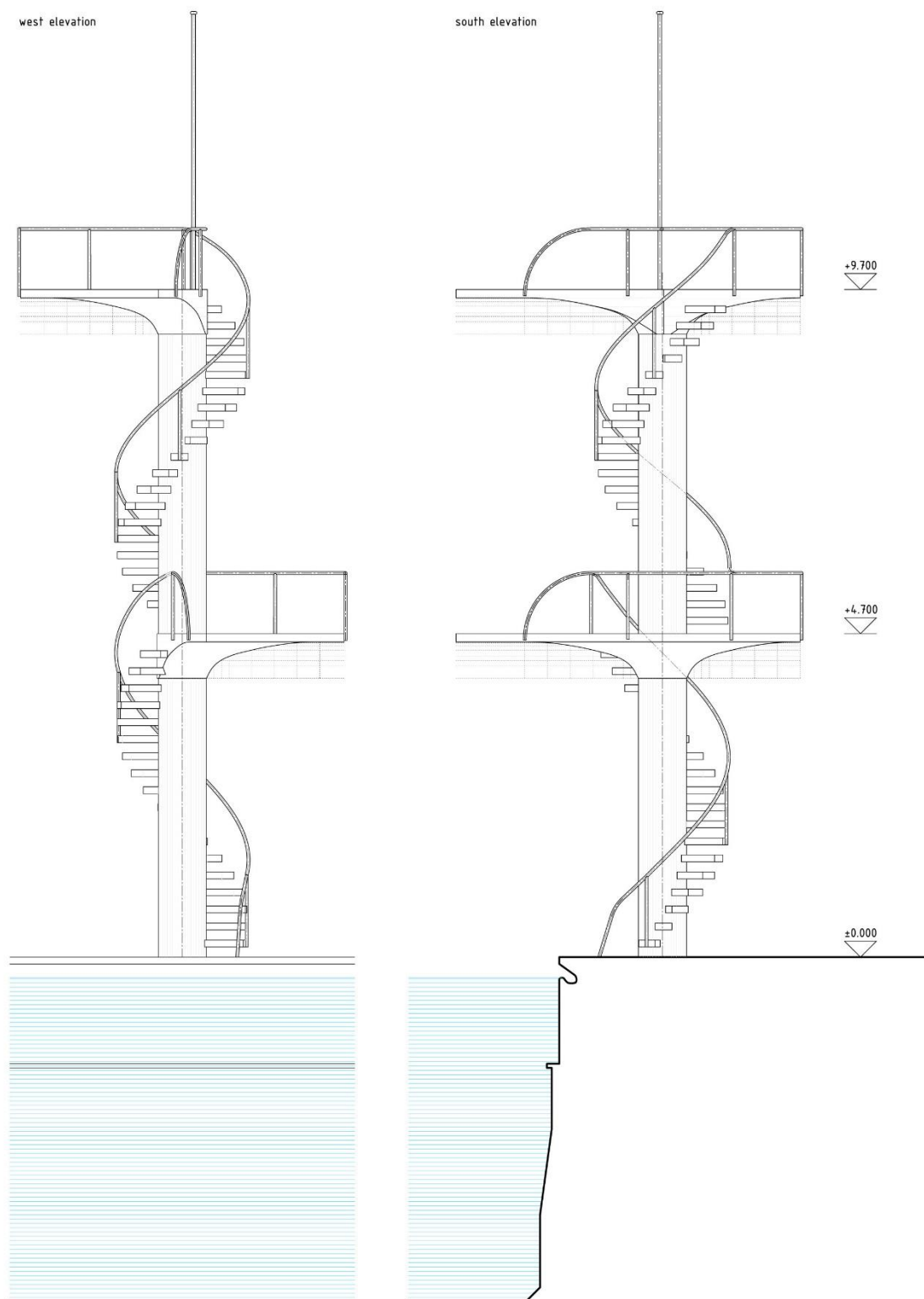


Figure 11.c) Reconstruction of the original state of the tower – elevations.

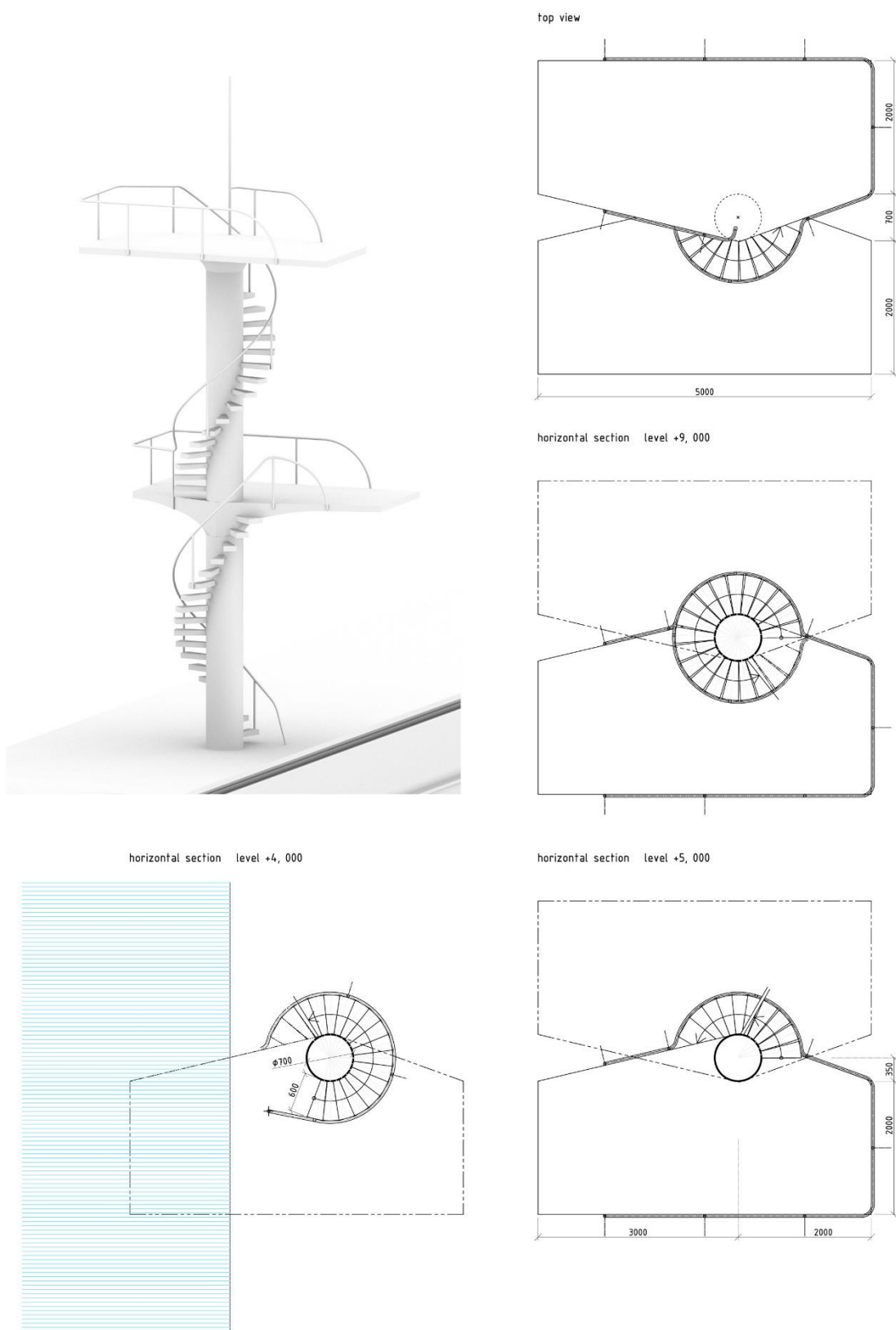


Figure 11.d) Reconstruction of the original state – horizontal sections, 3D sketch.

Plan of material and structural analyses

Finishing coats

The entire concrete surface of the diving tower was covered with a finishing coat. The finishing coat was only closely observed on the pillar at the ground level and seemed composed of at least three layers with different colours (Figure 12.a): (1) white, (2) orange, and (3) yellow layer. The finishing coat system was thin enough, so the texture of the traces resulting from the cast-in-place construction was visible (Figure 12.b).

The characterization of the finishing coat system should be assessed by analysing its stratigraphy, microstructure, and chemical-mineralogical composition using microscopic methods (LM, SEM-EDS, and Raman microscopy) and FTIR. However, sampling of the entire cross-section of the coats might prove complicated. The collection of samples by scratching can be an option. Still, there is a risk of contamination between the different layers, complicating the assessment of the original composition of the already degraded coats. Hence, a larger number of samples should be collected with this sampling method to enable a reliable statistical analysis. In addition, onsite analysis with a portable X-ray fluorescence device could help analyse the composition of the finishing coats.

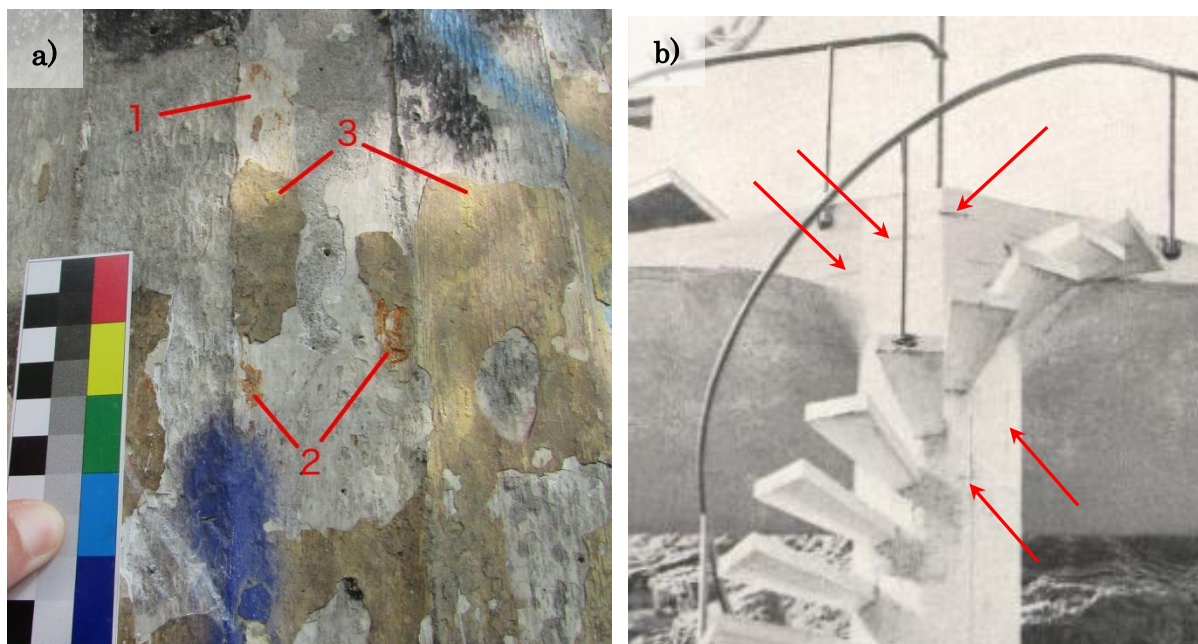


Figure 12. Finishing coats: a) Aspects of the finishing coats on the pillar at the ground level where three layers can be detected (marked in red in a sequence of application), b) Detail of a photo from 1932 where it is possible to see the traces of the texture remaining from the cast-in-place coated constructive system [9].

Concrete

The concrete composition and its conservation condition can be best assessed by sampling, which has to be representative. Cores and powder extraction will be considered, depending on the analysis required and/or the allowed extent of intervention

on the structure. Further samples can be easily obtained from the crumbling parts of the structure (e.g., stairs). It should be noted that the original concrete composition would hardly be retrieved without core sampling. This limitation has to be carefully considered when deciding which amount of information is needed for restoration purposes. Nevertheless, the degraded concrete cover analysis at areas where an advanced state of degradation is observed is also of value for documenting and planning a conservation proposal.

An idea for sampling the concrete at both the stairs and the pillar without causing extensive damage – assuming that the same type of cement paste was used for both elements – is by drilling in depth through the remaining "openings" of the steps that were removed in the past for safety reasons (Figure 13). In this way, both deteriorated and sound concrete can be sampled.

The main analyses that have to be performed for characterizing the hardened concrete include the determination of cement, aggregate and water content, as well as of chlorides, sulfates, and alkalis. Considering the cement technology of those times, a rough approximation of the type of aggregate and cement used will also be considered. Assessment of the crystalline and amorphous part of the samples will be investigated with X-ray diffraction and nuclear magnetic resonance spectroscopy, providing extensive information about the extent of damage and the phases formed. The presence and the quality of chemical admixture will be studied with infrared spectroscopy. Further information will be obtained from analysing the composition of the coatings and determining the carbonation depth.

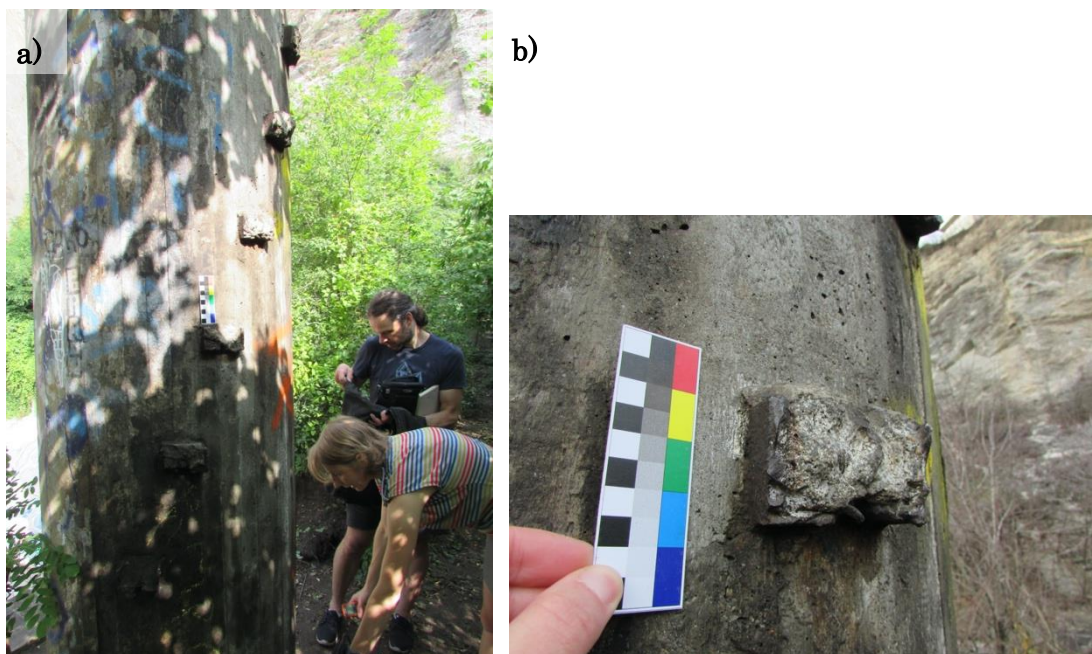


Figure 13. Step "openings" that remained after the removal of the steps for safety reasons: a) View of the pillar at the ground level showing the step "openings," b) Detail of a step "opening."

Samples obtained will be investigated to determine the quality of the historic concrete layer (used cement, amount of cement, ratio aggregate: binder, composition,

microstructure, cohesion, homogeneity) and to assess the mechanical characteristics of the material.

Reinforcement

Platforms

The platforms' thickness varies from 80mm to 600mm (the largest part is less than 200mm), so it is suitable for analysis using ground-penetrating radar or X-ray radiography. These non-destructive methods of analysis can provide valuable data on the structure of the reinforcement. In addition, moisture mapping with a microwave sensing device would also be helpful, though this device requires sampling for calibrating the moisture content [9].

Stairs

The reinforcement structure of the stair steps is currently visible due to the loss of the concrete cover (Figure 7). However, the part of the reinforcement embedded in the pillar remains unknown, i.e., up to which depth the reinforcement penetrates the pillar. Ultrasound pulse velocity may provide some data on this structural aspect.

Pillar

The pillar is the most complicated element to assess the structure of the reinforcement given its large diameter, thus rendering useless scanning tools such as ground-penetrating radar. Ultrasound pulse velocity may also be used to

Structural analysis

After assessing the composition of the concrete, reinforcement, and respective degree of corrosion, a structural capacity assessment focusing on snow loads and wind should be performed.

Discussion

The Question of the Context:

The diving tower is part of the abandoned swimming stadium complex. The owners' will for the restoration of its original function is highly improbable. Therefore, a proposal for converting the entire complex should be defined before defining the conservation/restoration plan. The type of usage and the accessibility to the site are also crucial for the restoration strategy, mainly regarding safety issues. Currently, the

swimming pool site is in a state of ruin, and its ground is accessible. Its deepest part under the diving tower is occasionally used for theatre and art performances, during which the diving tower became part of the scene.

The Possibilities of Conservation/ Restoration

It is necessary to address the intervention of the dire state of the tower (conservation/restoration) as a part of the reuse project of the entire complex of the swimming stadium. This report outlines the possible ways of conserving/restoring this particular structure, focusing on its architectural and technical aspects.

The analysis of the current state of the tower and the 1930's photos indicate that the pillar's surface was simply made of cast concrete covered with a finishing coat to smooth up the marks of the wooden formworks, which are visible in the historical photos (Figure 12).

There are two principal concepts for future interventions: (i) Restoration of the original state and (ii) Conservation of the state of ruin. Besides these two extreme concepts, other restoration approaches like thematizing the aging and the roughness of the structure (e.g., conserving the marks of time left on its surface, leaving the concrete uncovered without a unifying finishing coat). The choice of the approach depends on various factors, particularly on the reuse plan for the entire site

Restoration of the original state

The restoration of the original state means the replacement of a large part of the original materials. For example, all the stair steps would have to be replaced, and probably also the diving platforms, thus resulting in a highly invasive intervention on the pillar where these elements rest. The entire new finishing coat should also, as best as possible, reproduce the composition and texture of the original coats. Still, it would be virtually impossible to preserve the original coats if a new unifying finishing coat was applied to restore the original aspect of the tower. Examples of this type of intervention are given in Figures 14 and 15.



Figure 14: Example of the reconstruction of the original state of the Oskar Pořízka tram stop at Obilní trh in Brno (1928-1929); restoration intervention by Tomáš Rusín and Ivan Wahla (Atelier RAW) in 2012-17.



Figure 15: Example of the "invisible" repair with a material of identical visual qualities. Statue of a musician by Alois Šutera, Přerov, 1965, restored by Josef Červinka and Vladislava Říhová in 2019.

Conservation of the state of ruin.

The conservation of the state of ruin is a particular approach known in the heritage protection practice commonly applied on older structures (e.g., stone structures such as fortifications and castles). The intervention focuses on conserving the state of the structure as it is and mitigating the ongoing degradation processes. It is a question of how this concept usually applied on massive stone structures can be used on a small reinforced concrete structure. The conservation would mean cleaning the structure from the biological agents, recovering the exposed reinforcement, stabilizing the deteriorated parts (e.g., stairs) and surfaces. There would be demands on the aesthetics' repairs on all the visual qualities of the newly added material (colour, composition, etc.). It is in question if the repairs should be "invisible," i.e. if the visual attributes of the new stabilizing materials should be identical to the old ones like in the example given in Figure 15. In this approach, a slight difference between the old and the new materials may be relevant, as in the example shown in Figure 16.

The work with the existing surface of the structure has various forms besides the concept of the "conservation of a ruin" approach. For example, the fragments of the historic paints can be left intentionally as the marks of the time, thematizing the aging of the structure as in the example given in Figure 17. On the other hand, if the intention is to outline the roughness of the cast-in-place concrete, the surface layers can be removed and the structure revealed in its fundamental materiality.

In the Barrandov diving tower case, the reconstruction of the handrail and the missing stairs is also in question, though not in the sense of the restoration of the original architecture but as its interpretation. The accessibility of the structure goes hand in hand with the restoration of the load-bearing function of the structure (the stairs and the platforms).



Figure 16: Example of restoration intervention preserving the material's patina intentionally and leaving the patch repairs visible. Zdeněk Plesník, vila Zikmund in Zlín (1953); restoration by Petr Všečka, Transat architekti (2000- 07).



Figure 17: Example of a restoration intervention thematizing the rough concrete with age marks and visible patch repairs; conversion of a cement plant in Bratislava, Atelier GutGut 2015-17.

Conclusions

The Barandov diving tower is an iconic sports modernist construction in the Czech Republic. It has been selected as a case study for in-depth analysis within the project

because of its historical importance, poor conservation condition, and significance to the local community and tourism. This report added new architectural documentation of the structure and the condition assessment of its current state for planning an intervention. Two conservation approaches were considered and discussed: i) Restoration of the original state and (ii) Conservation of the state of ruin. Further analyses for both options were given.

References

- [1] M. Bártová, J. Hájek, Z. Poliačiková, Z. Mladá, and J. Baláček, “Odborné podklady pro zpracování plánu ochrany památkové zóny Barrandov, mimořádný úkol MK ČR č. 11./2009,” Prague, 2009.
- [2] Václav Kolátor, “Plavecký stadion v Praze na Barrandově,” *Stavba, měsíčník pro stavební umění*, vol. IX., pp. 167–168, 1931.
- [3] A. Turjanicová, “Koupaliště jako architektonický úkol. Venkovní koupaliště v české architektuře dvacátých až čtyřicátých let 20. století (The Swimming Pool as an Architectural Task. Open-air Swimming Pools in Czech Architecture of the 1920s–1940s),” Prague, 2009.
- [4] V. M. Havel, *Mé vzpomínky*. Prague: Lidové noviny, 1993.
- [5] A. Vondrová, “Český funkcionalismus 1920–1940 (architektura).” the Museum of Applied Arts, Prague, 1978.
- [6] V. Kolátor and A. Hoffbauer, *Lázně, stavba lázní, koupališť a plováren, jejich stavba a zařízení*. Prague: Ministerstvo veřejného zdravotnictví a tělesné výchovy, 1935.
- [7] R. Švácha *et al.*, *Naprej!: Česká sportovní architektura 1567-2012*. Prague: Prostor - architektura, interi, 2012.
- [8] Monument Diagnosis and Conservation System.
<https://mdcs.monumentenkenis.nl/> (retrieved on July 2020)
- [9] Magazín Světozor, Vol. 32 (1931-1932)
- [10] J. Válek, S. Kruschwitz, J. Wöstmann, T. Kind, J. Valach, C. Köpp, J. Lesák, Non-destructive investigation of wet building materials: multi-methodical approach, *J. Perf. Constr. Fac.* 24 (5) (2010) 462–472, [http://dx.doi.org/10.1061/\(asce\)cf.1943-5509.0000056](http://dx.doi.org/10.1061/(asce)cf.1943-5509.0000056).

Report on In-Depth Case Study

Fuchs restaurant (Prague, Czech Republic, early 1930s)



CONSECH20 – WP2 (iii) – Draft Report

Ondřej Dušek

Cristiana Nunes

Jan Válek

Marek Eisler

Petr Kozlovcev

June 14, 2021



Introduction

The Fuchs restaurant from the early 1930s was designed by Josef Fuchs and Bohumil Steigenhöfer. Built in 1932 with reinforced concrete, it functioned as a restaurant and an entrance to the ice ring stadium. The stadium was demolished in 2011, but the restaurant building was spared and nowadays, it is a protected and listed building waiting for repair.

The city of Prague has expressed interest in repairing the building with the idea of embracing the modern architecture of the original construction. This work would include removing many of the added elements of the building that are not original.

The building is an example of progressive functionalist architecture. The building is significant for its cubic shapes and use of progressive elements such as horizontal windows, cantilevered slab shelters over the doors on the terrace, a flat slab over the main entrance beared by simple round columns, horizontal steel tube guardrails with details similar to those in other buildings by the same author, e.g. the Trade Fair Palace - J.Fuchs,O.Tyl, currently the National Gallery.

The building is located in one of the islands of central Prague, in an area traditionally dedicated to sports and leisure. The building is adjacent to the bridge and can be reached by public transport - the tram station (Stvanice) is in front of the building facade. In the opposite side of the building there is a wide empty field (place of the demolished stadium), which is nowadays used for biking. The building is currently being used as a disco, bar, and bike workshop.

The aim of this report is to analyse existing documentation on the Fuchs building and performing the condition assessment of the its recent state to back up the plan for a conservation proposal.

Brief History

The Ice-Hockey in the Czech Lands

The game of Ice-Hockey first appeared in the Czech lands in the late 19th century, firstly in the form of Bandy Ice-Hockey, played with a round ball. The Canadian version, played with a rubber puck, was brought to the Czech lands in 1908, and soon it had replaced the Bandy style game.

The sport was practiced on frozen lakes, rivers and on ice rinks. The first ice rinks in Prague were built at Letná plain and later in Holešovice. Soon the game reached a professional level, the Czechoslovak National Ice-Hockey Team won the European

Championship in 1922, 1925 and 1929. In 1925, Prague was supposed to host the Championship but due to an unexpected ice thaw it had to be moved to the Vysoké Tatry Mountains in Slovakia. This issue meant that the construction of a modern winter stadium with artificial ice rink became a necessity. [1]

The Urban Context

Various location for the new stadium had been considered since late 1920s, and finally the Štvanice Island on the Vltava River, within the limits of inner city of Prague was chosen (Figure 1). The island was frequently flooded and for this reason mostly only temporary structures were built there. For centuries the island has been a place for leisure activities. A cruel entertainment of hunting wild animals with dogs in an arena gave the island its name. Later, in the 19th and early 20th century it hosted restaurants, a cabaret, a swimming pool and lawn tennis courts. In 1911 a new bridge connected the island with both sides of the river and its importance rose. [2]



Figure 1 The urban context. Aerial photo 1945, highlighted objects: the Prague Castle, the Charles Bridge, the National Museum, the Winter Stadium.

The Project and the Construction

Although the project of the new winter stadium at Štvanice Island was initiated by the Municipality, it was not conceived as a public work. The development of the project and the construction of the stadium was contracted to a private company who would afterwards profit from its operation of the stadium. The deal has been made with the Prague Sample Trade Fairs Company, who had already been operating the ice rink in Prague- Holešovice, on a site next to its recently built Trade Fair Palace (nowadays the seat of the National Gallery). The Municipality contributed by offering the plot of land for free. The project was planned with the aim of hosting the world championship in 1932.

The first designs of the Winter Stadium had been supposedly made by Josef Fuchs, the architect who had regularly worked for the Prague Sample Trade Fairs Company, and who had, together with the architect Oldřich Tyl, already designed for them the building of Trade Fair Palace.

Josef Fuchs finalized the executive project in 1930 and the construction company of ing. Dr. Tomáš Keclík was chosen. The works had already started when the impact of the Great Depression hit. The Prague Sample Trade Fairs Company went bankrupt, partly due to the debts incurred during the construction of the Trade Fair Palace. The construction works were interrupted, and architect Fuchs stopped his involvement as he no longer received his fees. A new consortium was established to finish the construction, bringing together the municipality, the construction company and the Brno Machine-Works, supplying the technology. This partnership issued in an agreement about the future ownership of the stadium:

According to the amount of their individual investments, the structure would afterwards belong to the construction company. Bohumil Steigenhöfer, an architect and professional hockey-player, was contracted to modify the original project. The construction works have recommenced. Anyway, Czechoslovakia was forced to cancel the hosting of the Ice-Hockey Championship in March 1932. The construction works were finished in autumn 1932 and the stadium was opened on the 6th of November 1932. Due to mention that the first Match between the Manitoba and the Prague team took place at the stadium under construction, in January 1931, with the concrete structure of the restaurant building covered with scaffolding in the background (Figure 2). [2]



Figure 2 The Stadium in the state of construction, 1931- 1932 (?)



Figure 3 The completed Winter Stadium, 1932

The Design, the Built Structure and Its Documentation

It is difficult to reconstruct the development of the project from the preliminary study to the executed version, because only the fragments of the particular project phases has been preserved to our days (Figure 4, 5). Even concerning the built structure, many aspects remain unclear— there are almost no plans nor photos documenting the original state of the interiors of the restaurant building. Other parts of the stadium, the ice rink and the tribunes has been transformed by series of adaptations during decades and finally demolished in 2011. Only the restaurant building remains in its materiality. The list of the preserved original drawings is being annexed. [2]

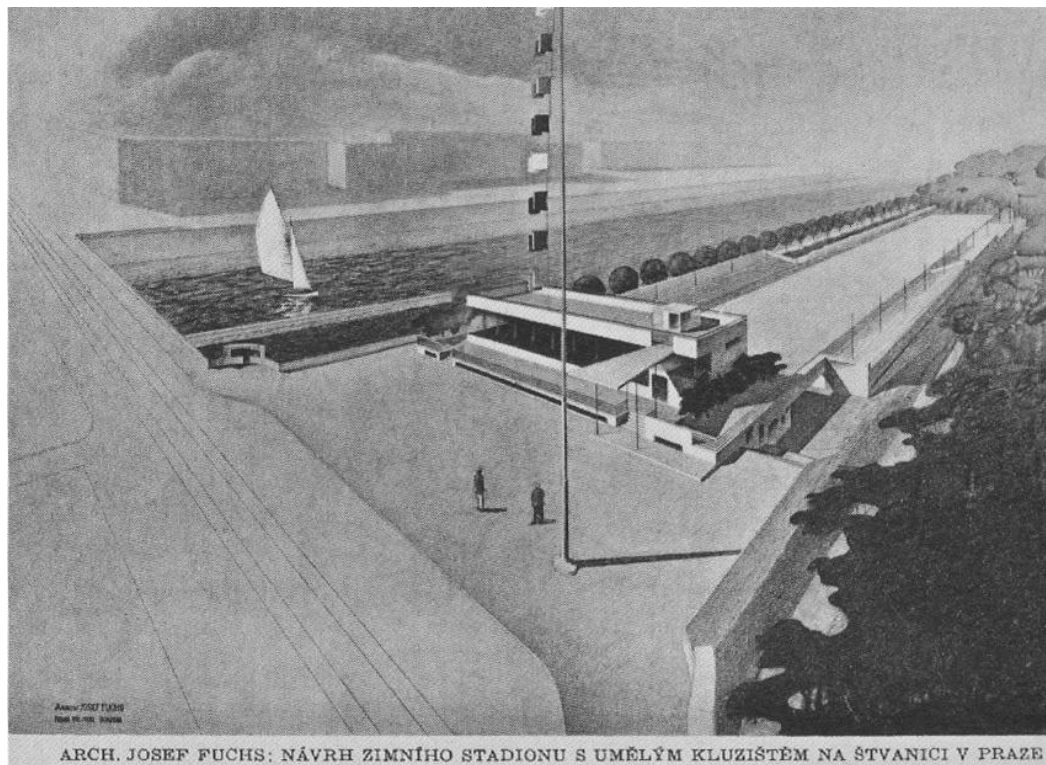


Figure 4: The perspective drawing by Josef Fuchs, 1930.

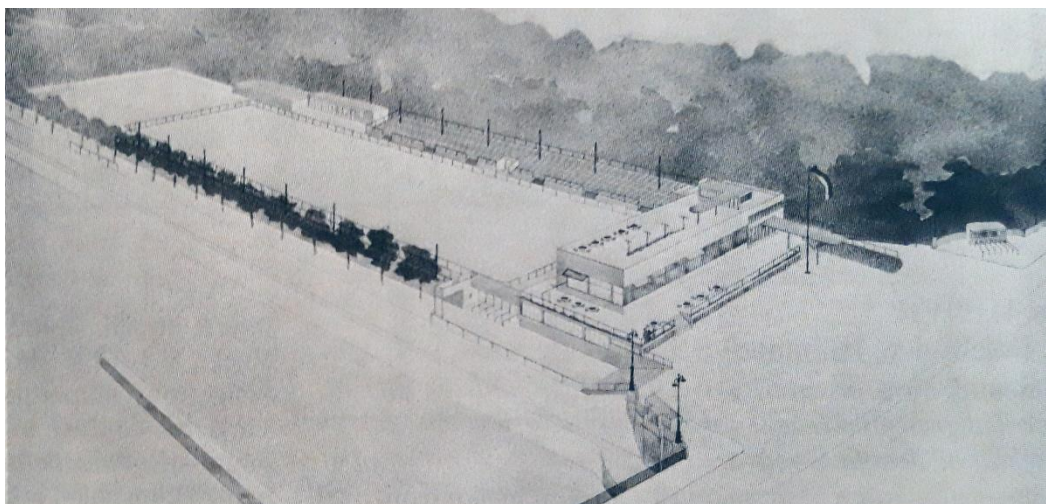


Figure 5 The perspective drawing by Bohumil Steigenhöfer (?), 1932.

The original state of the stadium, as it was completed in 1932, contained an open-air ice rink (92x32 m) surrounded by tribunes from three sides (Figure 3). The building of the restaurant was attached from the east side, between the stadium and the bridge. Two large stairways were placed from both sides of the building, descending from the bridge level to the island ground with the ice rink. There was another building with the freezing technology placed on the north side of the stadium (Figure 3, 5) The technology was manufactured by the Brno Machine Works according to the patent of an Austrian expert Dr. Schmidt.

The only preserved part of the stadium is the restaurant building. On its original design contained the characteristic signs of the functionalist style. A composition of basic geometric volumes was towered by a penthouse with a flagpole placed asymmetrically on the roof terrace. The design of the façades no longer reflected the system of tectonic elements. The bear-loading structure of the building, a reinforced concrete frame, was hidden inside the interior of the building, detached from the façade. This solution allowed using stripe windows and tinny walls, so the exteriors gained a look of a lightweight envelope. Enormous stripe windows and the entrance door were placed asymmetrically on the east façade, the entrance from the bridge level was marked with a canopy in the form of a long and tiny concrete slab supported by round columns (Figure 6). Two superposed horizontal windows all over the east façade offered a view towards the stadium and the Prague Castle (Figure 7).

The restaurant occupied a 5 meters-high space accessible from the terrace above the bridge level. The space was punctuated by two rows of columns, a gallery was attached to the west façade. The lower floor under the restaurant on the island level contained the restaurant kitchen, technical equipment and the sportsmen's changing rooms.

The load-bearing structure of the building is a reinforced concrete frame with the columns inside the interior. The slabs between the principal beams are made of reinforced concrete using permanent ceramic formworks. The exterior walls are composed of a sandwich structure with a principal reinforced-concrete layer on the exterior side. [3]–[5]

The shape of the building, its position on the island, the stripe windows, tube handrails and a flagpole, all these motives refers to the contemporary naval architecture, a popular inspiration among modernist architects (Figure 4). [2], [6]



Figure 6 The completed Stadium, east façade, access from the bridge level, original state, 1932.



Figure 7 the completed Stadium, west façade, original state, 1932.

The Architects

Josef Fuchs (1894- 1979) was a student of Josip Plečnik at the School of Applied Arts in Prague. Since 1921 he had created many temporary structure- and exhibition designs for the Sample Trade Fairs Company. The same company was also the investor of the most important project of his career, the Trade Fair Palace (designed and built between 1924-1928, Figure 8). In it's time it was one of the biggest structures built in the progressive constructivist style. Besides the Winter Stadium at Štvanice, Fuchs designed several villas in Prague, the buildings and the master plan of the Prague ZOO. After 1950 he worked in the Prague Project Institute, where he realized for example the design for the rendering plant in Tišice. [1], [7]–[9]



Figure 8: Josef Fuchs and Oldřich Tyl, Trade Fair Prague Holešovice, 1924-1928.

Bohumil Steigenhöfer (1905-1989) was a Czech architect and at the same time a professional ice-hockey player. He didn't finish the studies at the Czech Technical University, and he started to work in studios of prestigious modernist architects (Jaromír Krejcar and František Kavalír). As an employee, he participated in the creation of several iconic buildings of the functionalist era. Thanks to this practice he became an expert on the economy of construction, in budgeting. He subscribed to the School of Architecture of the Academy of Fine Arts, led by Josef Gočár, where he graduated in 1932. As an independent architect he continued redesigning the tribunes of the Winter Stadium Štvanice until the 1950s, the Novina Printing Works in Prague- Na Poříčí. Since 1948 he worked on the projects of several industrial plants, but together with Václav Krásný and Stanislav Tobek he designed the new winter stadium in Prague Holešovice (1959- 1962, Figure 9). [1], [7], [10]

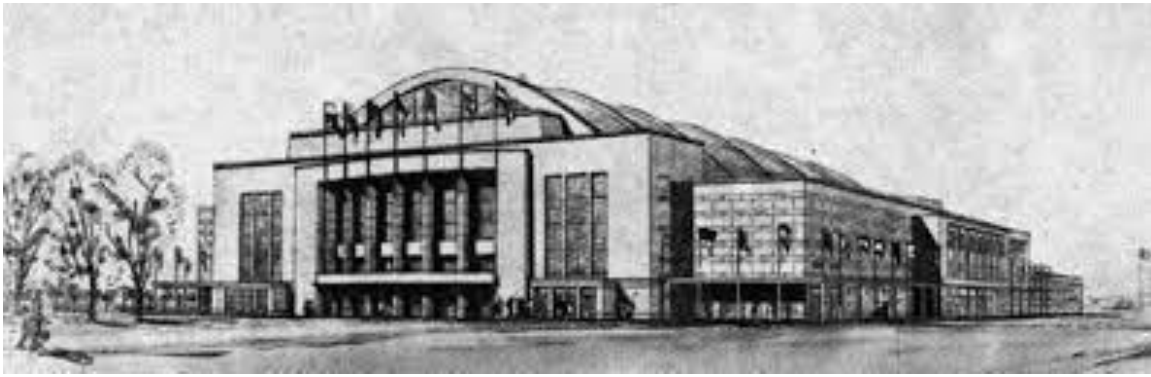


Figure 9 : Václav Krásný, Stanislav Tobek and Bohumil Steigenhöfer, Winter Stadium Prague Holešovice 1959- 1962.

Later Interventions

The building hosted four World Ice-Hockey Championships (1933, 1938, 1947 and 1959) and many other ice-hockey and figure skating events. Among the Prague inhabitants, it became popular for its public ice-skating sessions. In 1948, it was expropriated from Mr. Keclík and administrated by the Czech Physical Education Union. The importance of the Stadium was crucial— around 1950 the Stadium was used by five Prague ice-hockey teams.

The structure of the Stadium changed in many ways during its lifetime. The tribunes grew and the shelters over them were added stepwise since the 30s (Figure 8, 9). According to the drawing documentation, the interiors of the restaurant building were reorganized and a new entrance to the tribunes was made in the middle of the east façade in 1949. The service facilities were placed under the tribunes. Around 1950, the steep tribunes protected by cantilevered shelters surrounded the ice-rink from all four sides. The ice rink remained uncovered (Figure 10). [2], [6]



Figure 10: Development of the structure of the tribunes, 1938, 1951.

In 1956 the Stadium underwent another reform related to the upcoming World Championship; the ice rink and the tribunes were covered with a new structure, designed by the civil engineer Josef Zeman. Its principal structure was made of steel

bars, covered with a timber envelope. This intervention changed completely the meaning and the importance of the former restaurant building, originally a dominant structure of the stadium (Figures 11 and 12).

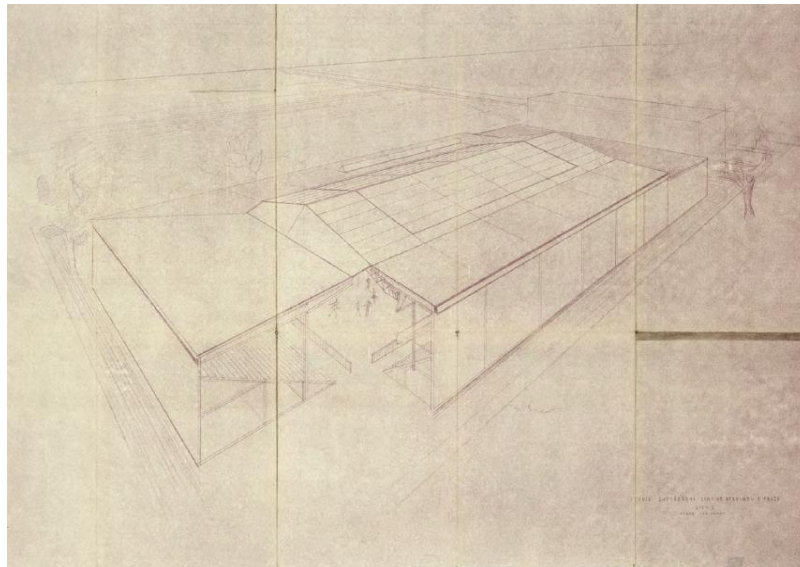


Figure 11: Josef Zeman, project of the new roof over the ice rink (1956).



Figure 12: The Stadium after the reform in 1956.

The stadium was continually in use for decades. Besides the winter sports, it hosted basket-ball, boxing and other sports and cultural events. Its importance started to diminish with the construction of the new Winter Stadium in Prague Holešovice (completed in 1962). The stadium was closed in the late 1980s, due to financial reasons—the public skating sessions were the only source of regular incomes. In 1997, the stadium was hired by a private firm and the ice-rink was reopened. The restaurant building was

adapted to a disco- “Music Club” and many inappropriate changes were made, especially in the interiors of the restaurant building. In 2000, the building was listed as a cultural monument. The stadium was seriously damaged by the enormous flood in the summer of 2003. This led to another closure for restoration followed by its reopening. However, the disagreement about sharing the restoration costs lead to the decision of the Municipality to demand the tenant to leave. Meanwhile, the lack of maintenance issued several damages in the timber envelope and in the secondary structure. In 2011, the demolition of the stadium (except the restaurant building) was ordered. The demolition occurred in the regime of emergency, without an ordinary administration procedure, despite the protests of the heritage protection experts and other professionals (Figure 13). Criticisms pointed out that the rapidness of the demolition did not correspond to the severity of damages, because the principal structure of the roof remained safe and without a risk of collapse. [1], [2]



Figure 13: The stadium before its demolition in 2011.

The Present and the Future

After the demolition of the main part of the stadium, the restaurant building remained empty and closed. In 2018, when a new city mayor was elected, the building was hired by a cultural promoter. Since then the building has been offering space for independent culture and community life. The upper floors, the interiors of the former restaurant, host an alternative music club named Fuchs2. The lower floor open to the island side is occupied by two independent spaces relied on to city biking (a bar and music club *Bike Jesus* and a communitarian bike-repair workshop *Bike Kitchen*). The area of the demolished building remains empty, the field has been adapted to a bike motocross track. The site has become a remarkable point on the cultural map of the city (Figure 14).

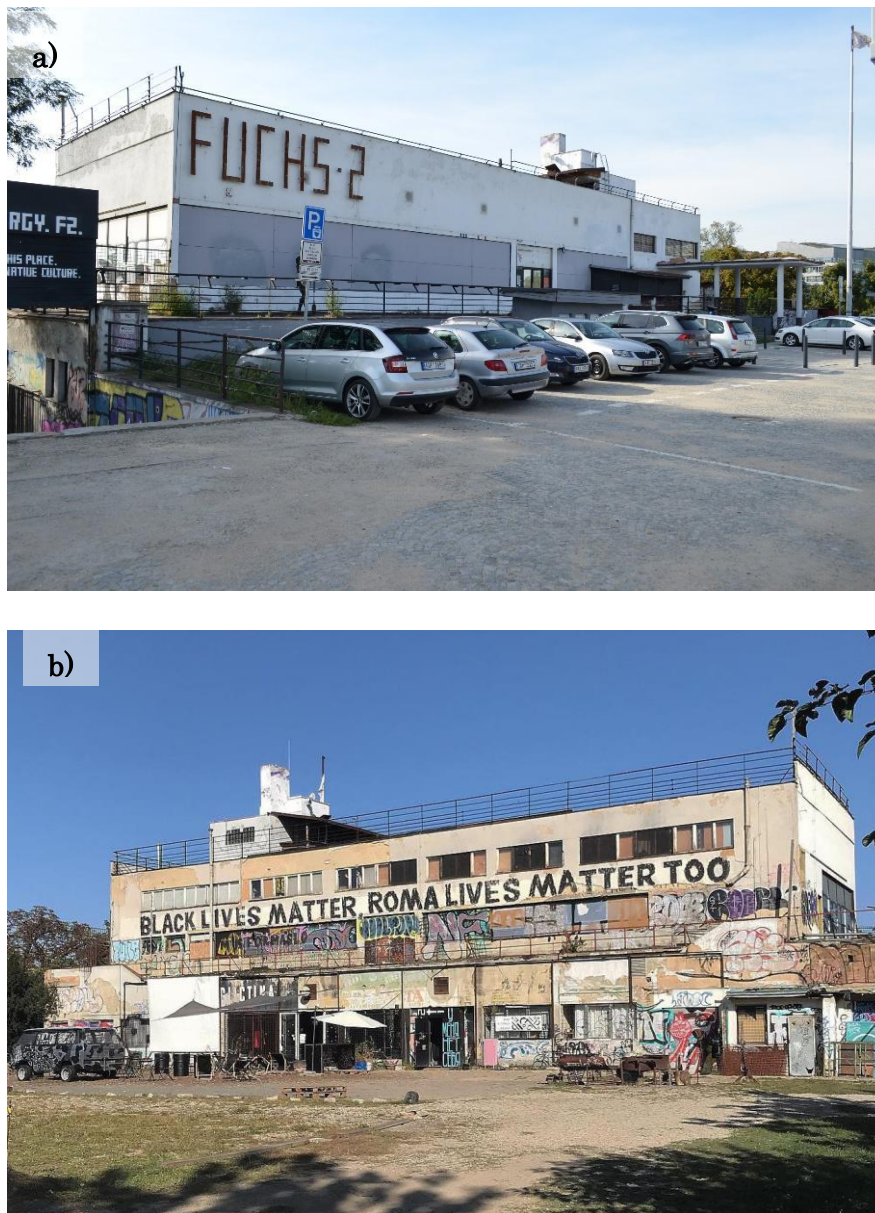


Figure 14: The recent state of the restaurant building: a) main façade, b) Western façade.

Despite reopening for public activities, the building remains in a poor state, only the most urgent repairs and the basic maintenance are being applied. Independently of the recent usage, a restoration of the building is being planned, a structural and historical survey of the building has been performed [2]–[6] and an architectural reuse plan has been proposed [1]. It follows the idea of the restoration of the building to the original 1930's state, removing the later interventions (Figure 15). It is in question if this approach is relevant as the original ice rink is missing.



Figure 15: Jiří Javůrek, Vladimír Thiele (SGL PROJEKT s.r.o.), restoration study, 2015.

We can suppose that the restoration would be followed by an ordinary selection procedure to choose the new tenant. Regarding other similar cases (e.g. the City Market in Nicosia – another case study of this project) certain preoccupations are relevant that the spontaneous and communitarian activities of the temporary usage will be replaced by something much more conventional due to the rules of the bureaucratic process. A way to preserve some aspects of the recent usage should be investigated and other alternative approaches to the restoration should be considered.

Condition Assessment

Brief Description of the Structure

The main vertical and lateral supporting structure consists of monolithic concrete frames (Figure 16). These frames act in the transverse direction of the building (Figure 17). There are two rows of columns that extend the full building height, identified as such as column lines A and B. Additionally, one row of columns reaches level 1NP, column line C. From there, there are concrete beams between these columns at levels 1NP and 3NP. There are also beams on level 2NP on the north side of the building. The frames are typically spaced at 3.6 meters. Spanning between the frame beams on each level are concrete slabs. [11]

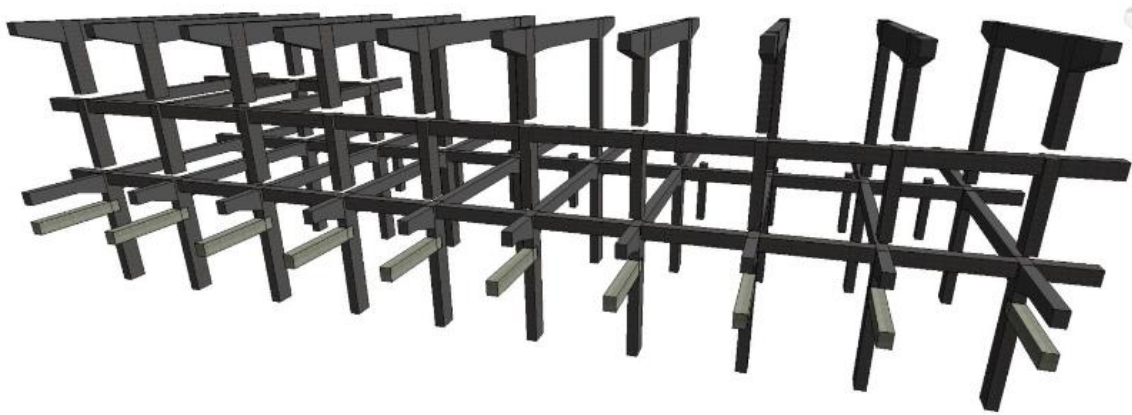


Figure 16: Isometric view of the internal frame structure (view from the Southwest) [12].

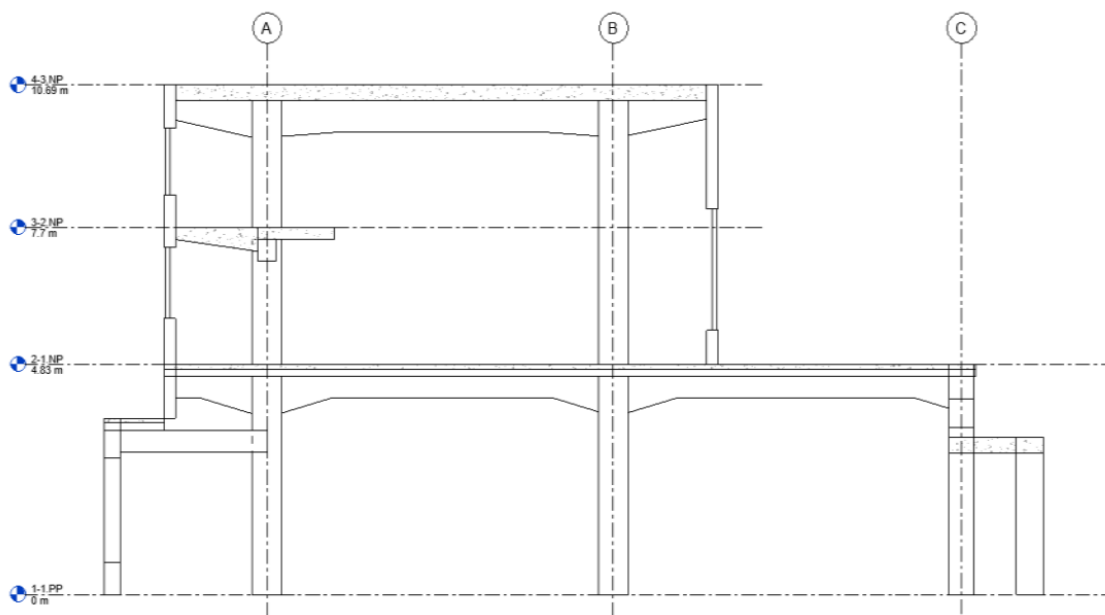


Figure 17: Transverse frame cross section (North view) [11].

The columns are monolithically cast-in-place with continuous vertical reinforcement and stirrups. The full height columns are 35 cm by 65 cm, while the single-story columns are 35 cm by 55 cm. All columns have the strong axis in the transverse direction of the building [1].

In the longitudinal direction the full height columns create continuous frames (Figure 18). At level 1NP, the beams of the frame occur at both full height columns, lines A and B, while at level 2NP, there is only one line of beams creating framing action at column line A. There are no frame beams at level 3NP so the columns cantilever above the frame beams to resist longitudinal lateral loads at the roof level. [11]

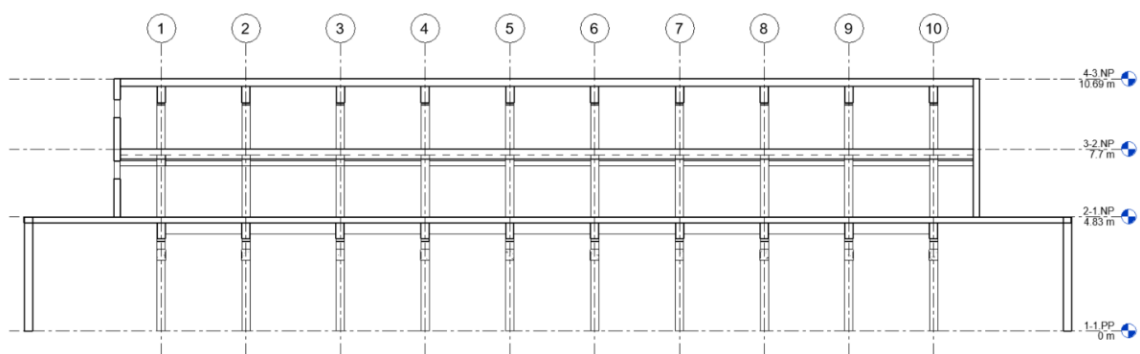


Figure 18: Longitudinal frame cross section – East view. Frame beams exist at levels 1NP and 2NP [11].

The load path of the walls is unknown. The two possibilities are that the walls are supported or hung from the slabs at each level, acting like a curtain wall. The alternative is that the walls act in a load bearing manner with the total self-weight of the wall bearing at the base of the wall. Many of the windows on the east, west and south are very large and apparently lack any interior support. The window above level 2NP on the west exterior wall is over 34 meters long. This condition makes the bearing wall load path unlikely. However, if the exterior walls are supported by the slab on each level, this means that the ceramic composite slabs are supporting the wall self-weight, which also seems like a flawed method, but the lesser of two evils. Additionally, with the intention to reopen all the original windows that have been infilled, it is possible that the original load path has changed through all the alterations. Additionally, at the intersection of the south wall and east wall, the windows extend to almost all the way to the corner leaving a 24 cm by 32 cm post. The function of the post is unknown, whether is it loaded and behaves like a post or whether it acts as a mullion for which the windows attach. [11]

The balcony area of level 2NP was originally constructed with a concrete parapet railing between the balcony and level 1NP below. However, during one of the renovations, possibly in 2007, where the mirrored balcony was installed, a small section of the parapet was demolished. It is probable that the reinforcing bars in the slab bent up within the parapet to provide bending strength for lateral railing loads. If this

reinforcing was removed with the parapet, it likely removed the bent bar development capacity that was allowing the slab to function properly. This would mean that the slab might not have any tensile resistance from the steel. The exact reinforcement position will have to be investigated. [11]

Main Damages

The visual inspection of the structure was performed on 15.5.2020. The description of the damage types was done according to the MDCS atlas [12]. A comprehensive survey was conducted in 2015 [5], in which material samples were collected and tested to identify the composition of various structural elements. The sampled areas were not repaired and, in some elements, the steel reinforcing is exposed (Figure 19).



Figure 19: Sampled areas in 2015: a) Aspect of a sampled beam, b) Aspect of sampled column.

The exterior of the building is covered with a cement plaster, but only in the Western facade the plaster is original, but it is peeling off in many areas (Figure 20.a). The non-original plasters also show disintegration (delamination) in several areas (Figure 17.b).

a)

b)



Figure 20: Aspect of the cement plasters showing lacunas resulting from delamination: a) Detail of the original plasters preserved in the Western facade, b) Non-original plasters in the main façade.

The load-bearing RC structures are generally in good condition, but there are local failures due to water infiltration triggering the corrosion of the reinforcement (Figure 21).



Figure 21: Corrosion of the reinforcement of a cantilevered beam due to water infiltration (basement – 2PP level).

The condition of the ceramic ceilings is generally poor due to the corrosion of the reinforcement (loss of rebar diameter) leading to crumbling of the ceramic formwork. This is most severe in the slab of the terrace area (level 1NP). This is probably due to water infiltration since the top of the slab is exposed to the exterior of the building. Moreover, this slab spans further than the typical interior bay, over 5.5 meters, which could cause more substantial deflection and ponding of water above. There is severe damage to the concrete, steel reinforcing, and ceramic material. The area is currently shored with wood posts and beams (Figure 22.a). The steel reinforcing is visible between the ceramic from below, showing of corrosion of the reinforcement. Adjacent to the temporary shoring, there is an area of the ceiling that has been repaired, possible using

a textile reinforced mortar or a steel reinforced grout system (Figure 22.b). In some areas, the structure is beyond repair and need to be replaced as also stated in the 2015 report [5].



Figure 22: Aspect of the ceilings made of ceramic formworks (level INP): a) Corrosion of the reinforcement due to water infiltration leading to failure of the ceramic material with temporary shoring of the slab, b) Recent repair of composite slab damage.

3D Structural Finite Element Model

Scheuer [11] performed a 3D structural finite element model of the building within the scope of the project and the information provided here was taken from Scheuer's thesis. The data on material properties from the survey conducted in 2015 [5] was used for the description of the elements of the building.

The purpose of the model is twofold, to assist in spatially understanding the composition of the building and to then to convey the results and recommendations in the form of drawings.

An ample amount of information was available to create the model. The previous reports completed in 2015 articulated the different building systems and components. Included in this data are the sizes of specific beams and columns, thicknesses of main floor slabs and other non-structural segments of those elements. In addition to the reports, CAD files were available showing plan layouts and cross sections of the building in various locations. These CAD files were prepared in the as built condition, therefore showing the reality of the current condition, including non-square corners and sloped slabs. This indicates that they were possibly created using photogrammetry or laser scanning.

Creating a model, essentially constructing the building from scratch digitally, was incredibly helpful in understanding the connectivity and load path of the structural elements. The perspective and thought process of the original designer was taken into account during the model construction in order to recognize how all the individual elements function. The layout of the main structural frames is clear from pictures and drawings, however the load path from different elements is less clear. Specifically, the support and bearing conditions of the exterior walls difficult to ascertain. Additionally,

longitudinal beams are not clearly shown on drawings and are often obscured in pictures especially on level 2NP, therefore the existence and size needed to be.

To perform the static analysis of the building, RAM Elements, by Bentley Systems, was used. It is a 3D finite element analysis program popular program in the United States and other locations. It is an easy to use program with powerful capabilities. It provides highly customizable materials and shapes. The user interface is simple and intuitive to use

Prior to running the analysis, the finite elements were discretized. Quadratic elements were used to create a more refined analysis. Various sizes were meshed to create a balance between realistic behaviour and model computing size and time. In the end, a maximum node spacing of 50 cm was used (Figure 23). This size fit well with the size of the wall shells and opening interfaces (Figure 24).

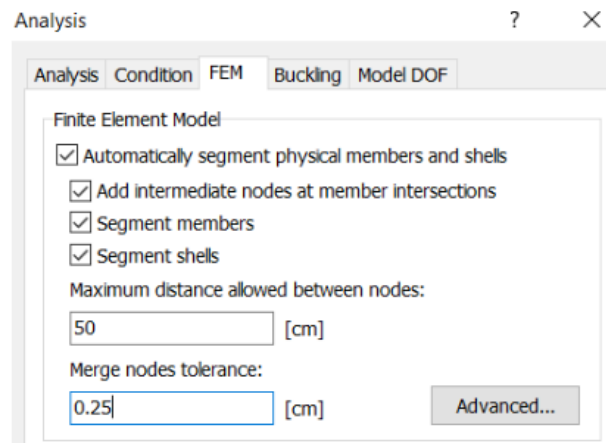


Figure 23: Finite Element input table from RAM Elements

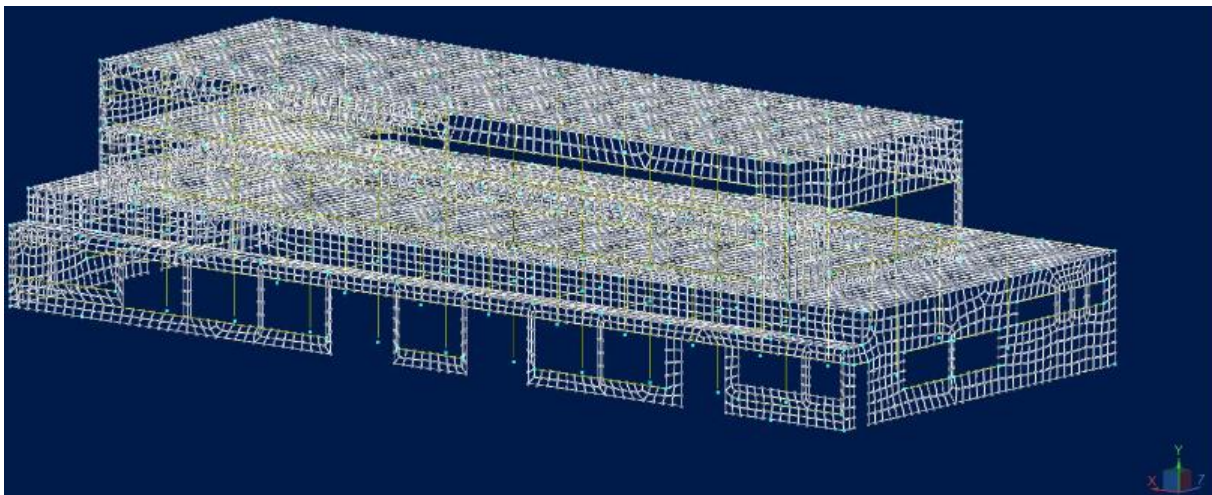


Figure 24: Finite elements in RAM Elements (view from the southwest).

The analysis provides reasonable and expected results. Upon performing verification procedures to confirm that the model is behaving properly. All loads are accounted for and hand checked moments and shears provided confirmation. Deflections of the members seemed reasonable.

Looking at the deflected shape, it is clear how the load from the wall affects the behavior of the entire structure (Figure 25). The most significant behaviour relates to how the balcony area on level 2NP supports the wall on the western wall while that support does not exist at the eastern wall. Therefore, significant weight of the wall on the eastern side of the building is concentrated on the roof framing, while it is distributed more evenly on the west side. This disproportionate loading causes the entire building to rotate. The maximum deflection of the center of the roof edge due to this rotation is less than 5 mm.

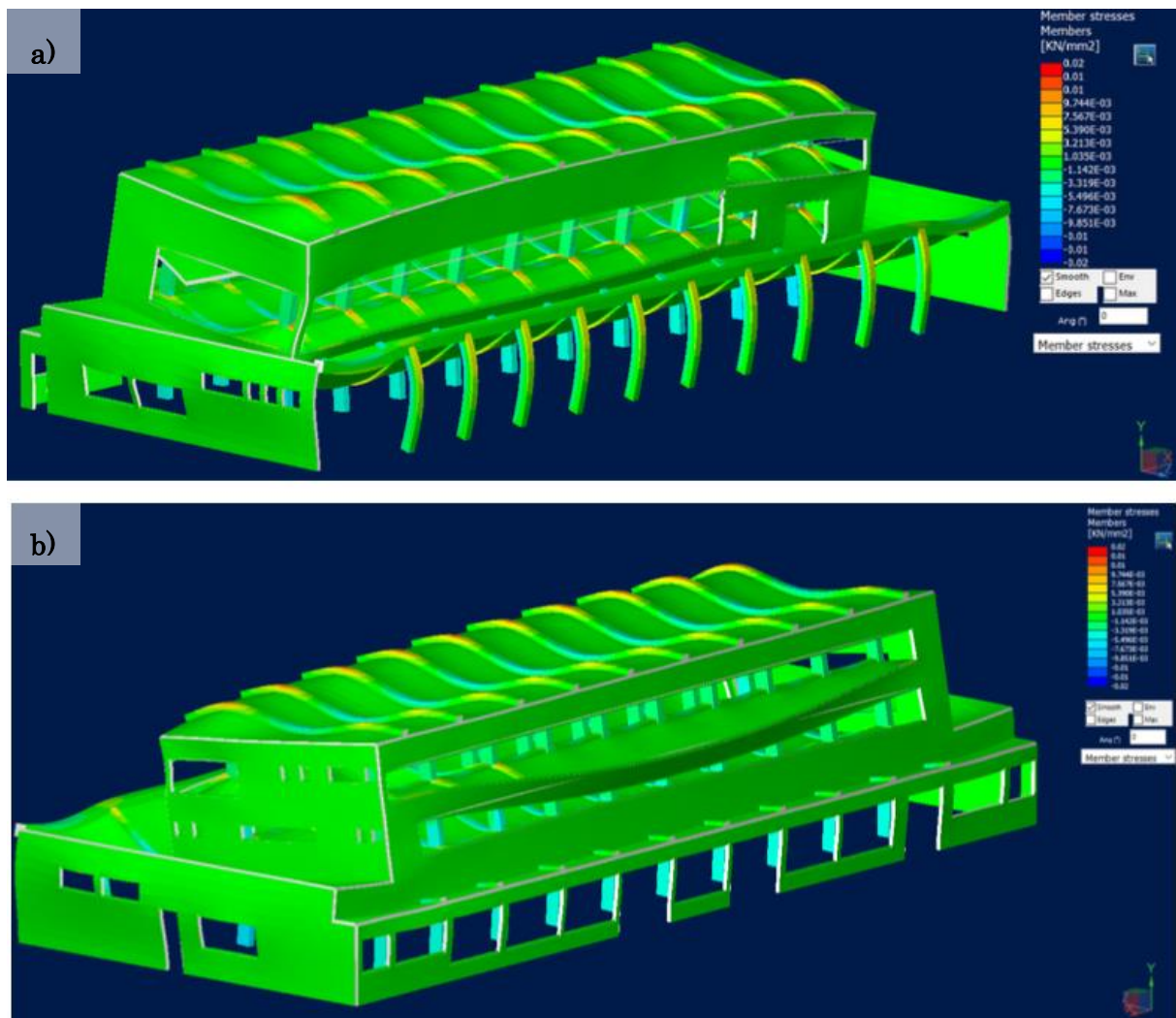


Figure 25: a) Member stresses for controlling load combination in the deformed shape from the southeast b) Member stresses for controlling load combination in the deformed shape from the northwest.

Since the window openings are so long, it allows the walls at each level of the building to behave independently of the other wall areas. The downside of this is that the elements that connect the different wall areas are typically slender and transfer a large amount of load. This is most obvious example of this is the post between windows at the southeast corner of the building between levels 1NP and 3NP (Figure 26). These concentration of force and stresses could cause cracking and damage. This is something that should be inspected in greater detail and would also be a candidate for more in-depth non-linear analysis. The other result of this load transfer is that the slab below has to support all the load. There is no beam directly below the wall in this area, so the slab is supporting it. This cause a significant amount of relative deflection at about 6 mm. The bearing conditions and reinforcement of this slab should be examined further to verify the adequacy of this condition.

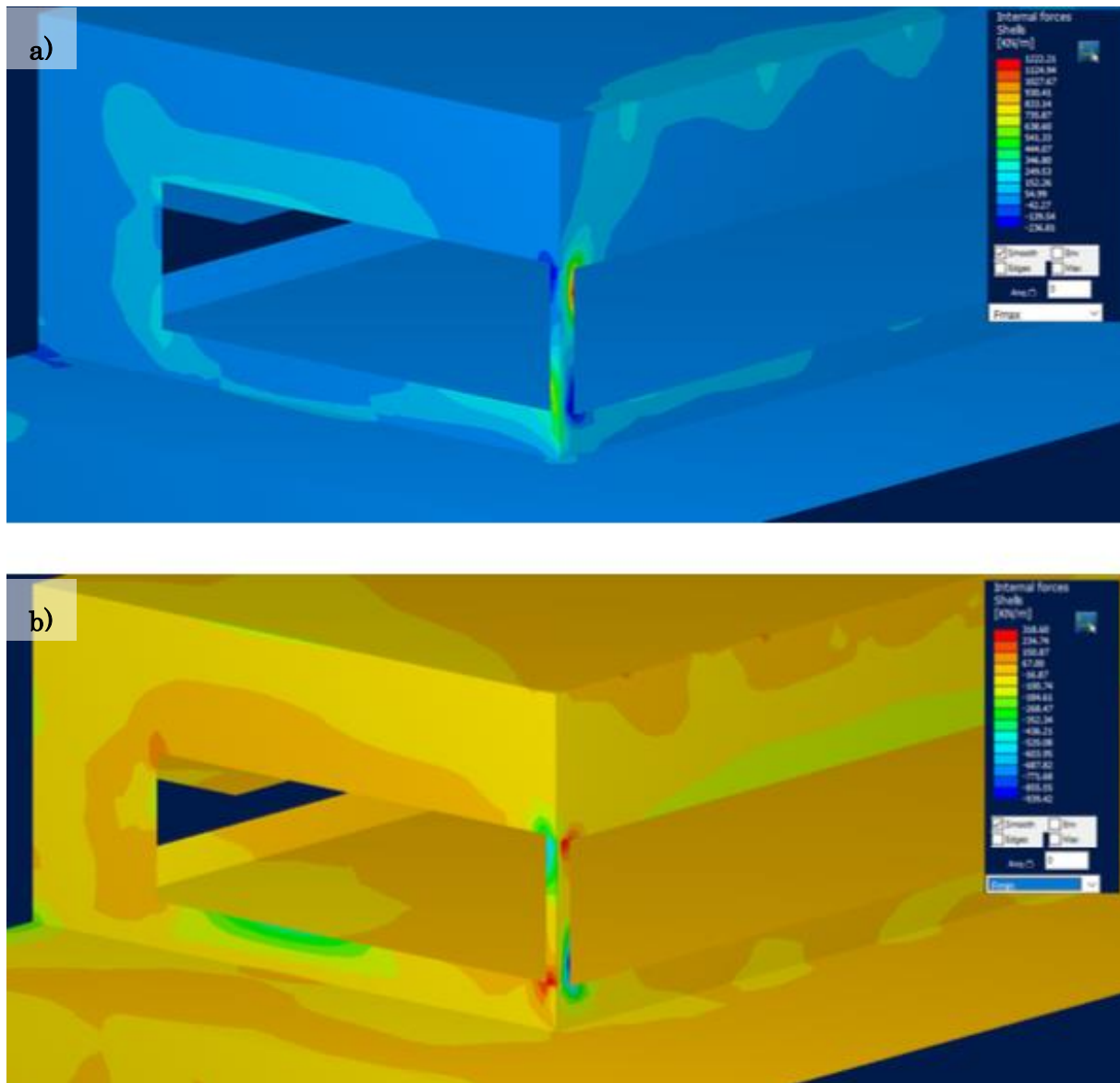


Figure 26: a) Maximum internal force envelope of southeast corner post b) Minimum internal force envelope of southeast corner post.

In the area of the balcony on level 2NP where it is the torsional resistance of the longitudinal beams that stabilize the level, the entire wall and slab rotate, though the maximum deflection there is only 5 mm, which is below the limit. This further shows that the walls are likely supported at each level as the slabs have the capacity to resist it.

GPR Survey of the Reinforcement

The aim of the survey was to assess the use of Ground Penetration Radar (GPR) for the reinforcement position detection. For this case study a potentially critical section of a façade above the app. 16 m long horizontal window was selected, Figure 27. GPR from IDS company equipped with 2 GHz high frequency antenna was used. The survey was carried out on April 30, 2021.

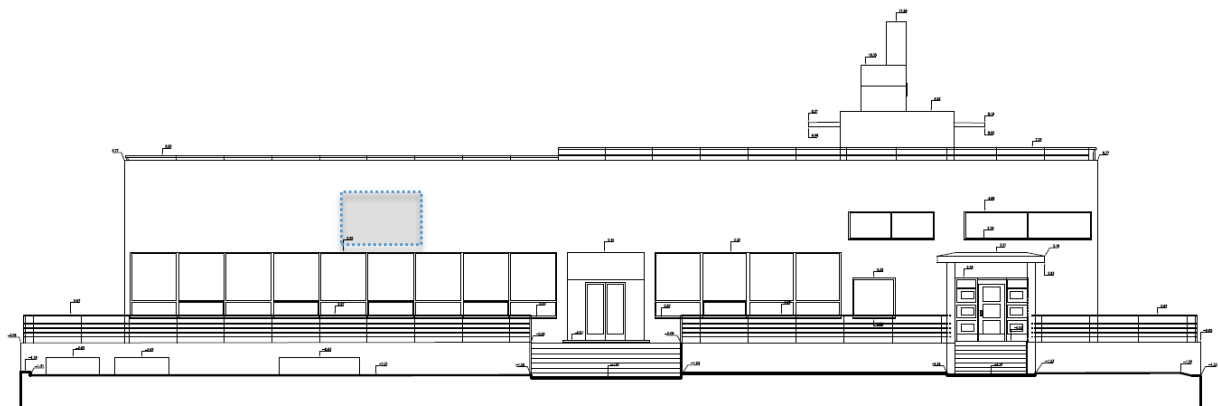


Figure 27: East elevation with approximate position of the surveyed area.

Methods used and procedure

Georadar, Ground Radar, or GPR (Ground Penetrating Radar) is a device that uses a radar signal to survey and then display the internal structure beneath a surface being examined. It is a geophysical method that can be used for a wide range of non-destructive reconnaissance tasks from foundation engineering, through archaeology to detailed exploration of subsurface defects in buildings. The basic principle of the measurement is pulse transmission of electromagnetic waves (< 1 ns), which passes through a given environment (the material under investigation). In engineering-building applications, frequencies ranging from 300 MHz to 2.5 GHz are used. The reflected waves are received by the antenna and displayed according to the arrival time and in relation to the antenna position. A reflection or signal change occurs when it passes through environments with different permittivity (e.g. a stone-to-air threshold) and conductivity (e.g. the presence of iron fasteners). The measured parameter is time. If the wave propagation speed of a given material or materials is known, then the depth at which the signal changes or is reflected can be determined. For measurement, it is most common to use antenna motion along a line in the surface plane. If within the material

environment being studied there is an object or a cavity, a so-called inhomogeneity, from which the emitted waves are reflected, as the antenna approaches it, the distance showing its depth is shortened and subsequently extended as the distance between the object and the antenna then increases. In radargrams, these reflections create hyperbolas. For subsequent interpretation and localization of any findings it is necessary to know the position of the antenna during the measurement. The antenna feed is most often recorded by a measuring wheel that measures the linear distance from a starting point.

Survey Specifications

The survey was conducted from both interior and exterior faces of the wall. The interior is partially lined with decorative panels, and a gallery is built in with a floor level at the height of app. 30 cm under the horizontal window lintel.

The wall structure from exterior to interior is the following: a render of varying thickness (15–30 mm), a reinforced concrete wall (150 mm), thermal insulation (45 mm) and unreinforced concrete (45 mm). This was determined at the position of a hole made to build in a ventilator. There it was also possible to detect the remains of metal bars that were cut away, Figures 28 and 29. Only 6 mm wires were found present in this section.

The wall above the horizontal window is most probably supported by cantilevers of transverse frames spaced 3.6 m. An area covering the section around the axis of the support was selected and surveyed from both interior and exterior faces.

The interior part of the wall was divided into the sections above the lining and on the lining. Only the results from the section above the lining are presented here. The air gap between the lining and the wall made the radargrams less informative. The selected area above the lining was divided into 4 longitudinal (horizontal) and 19 transversal (vertical) mutually perpendicular line profiles, Figure 30. The longitudinal profiles **LLL20005–LLL20008** (referred to as L5–8) are 0.3 m apart. The distance between the transverse profiles **TTT20001–TTT20019** (referred to as T1–19) is also 0.3 m. The starting points of L and T1-6 profiles are shown in Figure 31.

The exterior part of the wall was accessed from a ladder. The profiles were scanned following the same grid as set out in the interior but the profiles do not match in length and numbers (Figure 32). For T profiles **TTT10001–TTT10010** (referred to as T1–10) it was possible to start at the bottom part of the wall (starting position of the antenna was 70 mm from the edge) and continue some cm above the interior ceiling level. The L profiles **LLL10001–LLL10007** and **LLL10011–LLL10017** (referred to as L1–7 and L11–17) cover together approximately 2.8 m and finish at the point where the L profiles start.

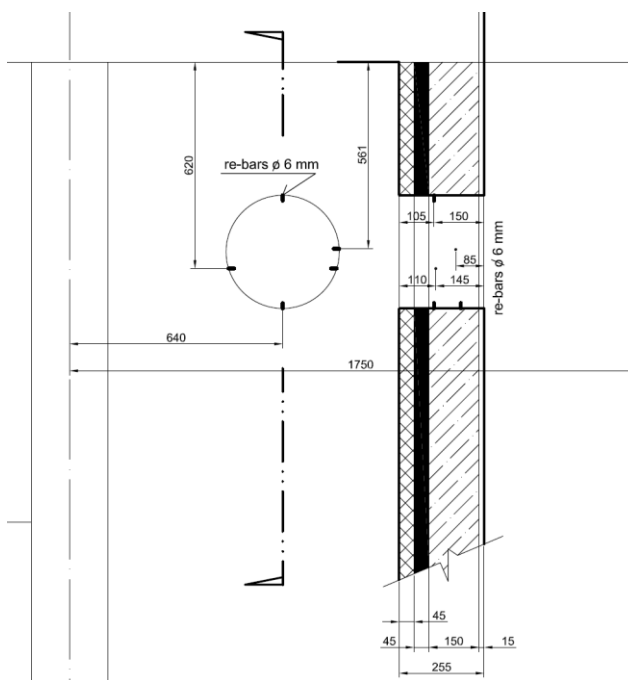


Figure 28: Structure of the wall in the position of a secondarily placed ventilation.



Figure. 29: Photo of the wall breakthrough.



Figure 30: The surveyed area in the interior includes the section between two supporting frames.



Figure 31: Origin of the coordinate system above the lining. Horizontal L and vertical T profiles are spaced 300 mm.



Figure 32: The surveyed area on the exterior facade. The T1–10 and L1–7 and L11–17 scenes match the grid from the interior but not the length of the interior profiles. The spacing is 300 mm. Dashed and dotted lines – profiles on the interior side and hidden structures (frames, ceiling, floor) respectively.

Procedure

For this task a ground radar from the IDS company was used. Considering the resolution and assumed depth range, a 2 GHz antenna was used. The linear displacement distance of the antenna over the profile was measured by a wheel. Following initial verification, the following system setup was selected: a depth resolution of 1024 samples / scan was selected to capture the radar scans, the time limit was 16 ns, the rate of signal propagation was estimated to be 140 -150 mm / ns, and the signal was read at 10 mm intervals in the direction of the antenna movement (Figures 33 and 34).

Slice software was used for the evaluation. To make the reflections visible, the signal was amplified (gained) linearly depth-wise, an interval of displayed frequencies was selected, and the distance between the antenna and the surface was subtracted, a process called filtration. From the course of the hyperbolic reflections, the rate of signal propagation was confirmed. It was 140 mm / ns and was considered average for the given environment. In general, the depth of the reflected signal shown in radargrams based on an average is only approximate since it is dependent on the actual velocity of the signal passing through the material, which is to some extent always inhomogeneous both depthwise and along the profile. The degree of simplification for the given resolution is usually adequate. The radargrams obtained are presented in **Appendix A**.

The measurements do not provide information on the diameter or quality of the reinforcements. The reported depths and dimensions are merely indicative.

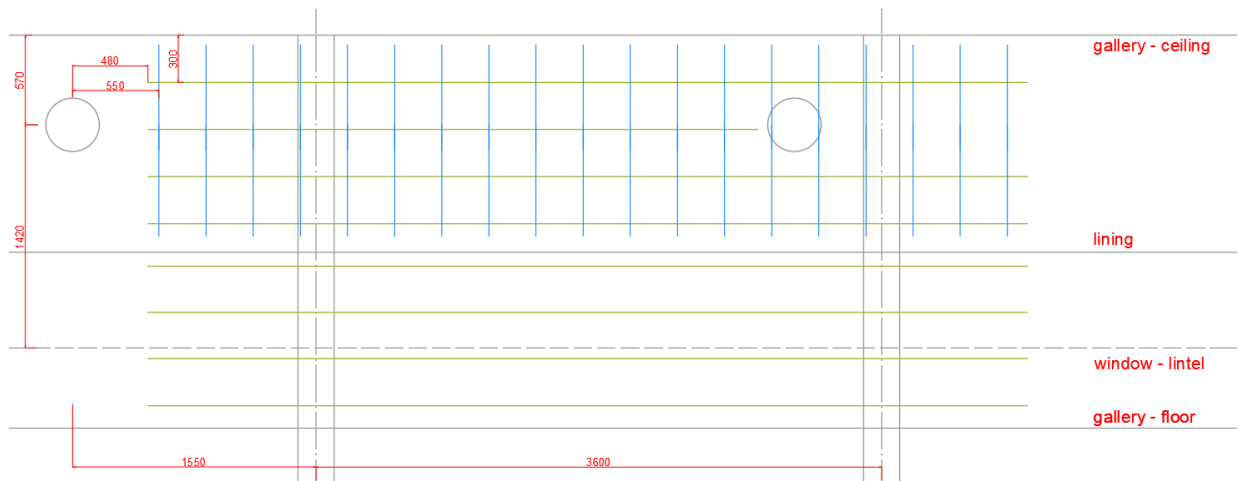
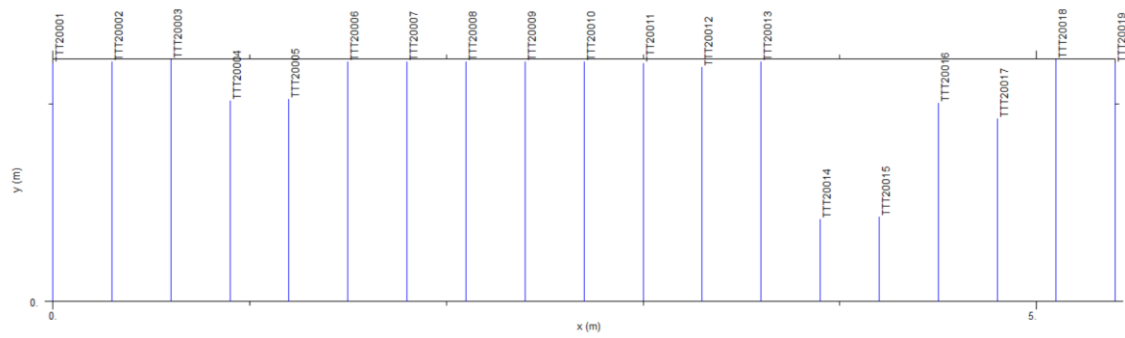
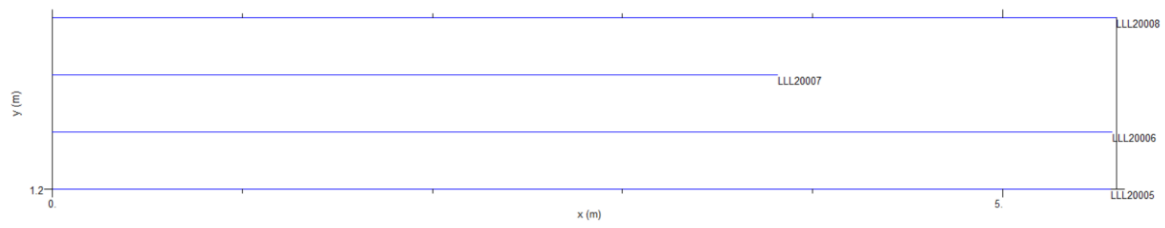


Figure 33: Marking and positioning of longitudinal and transverse profiles on the interior part of the wall. The origin point of the coordinate system is 1.0 m from the frame axis and 1.4 m from the ceiling. Not to a specific scale.

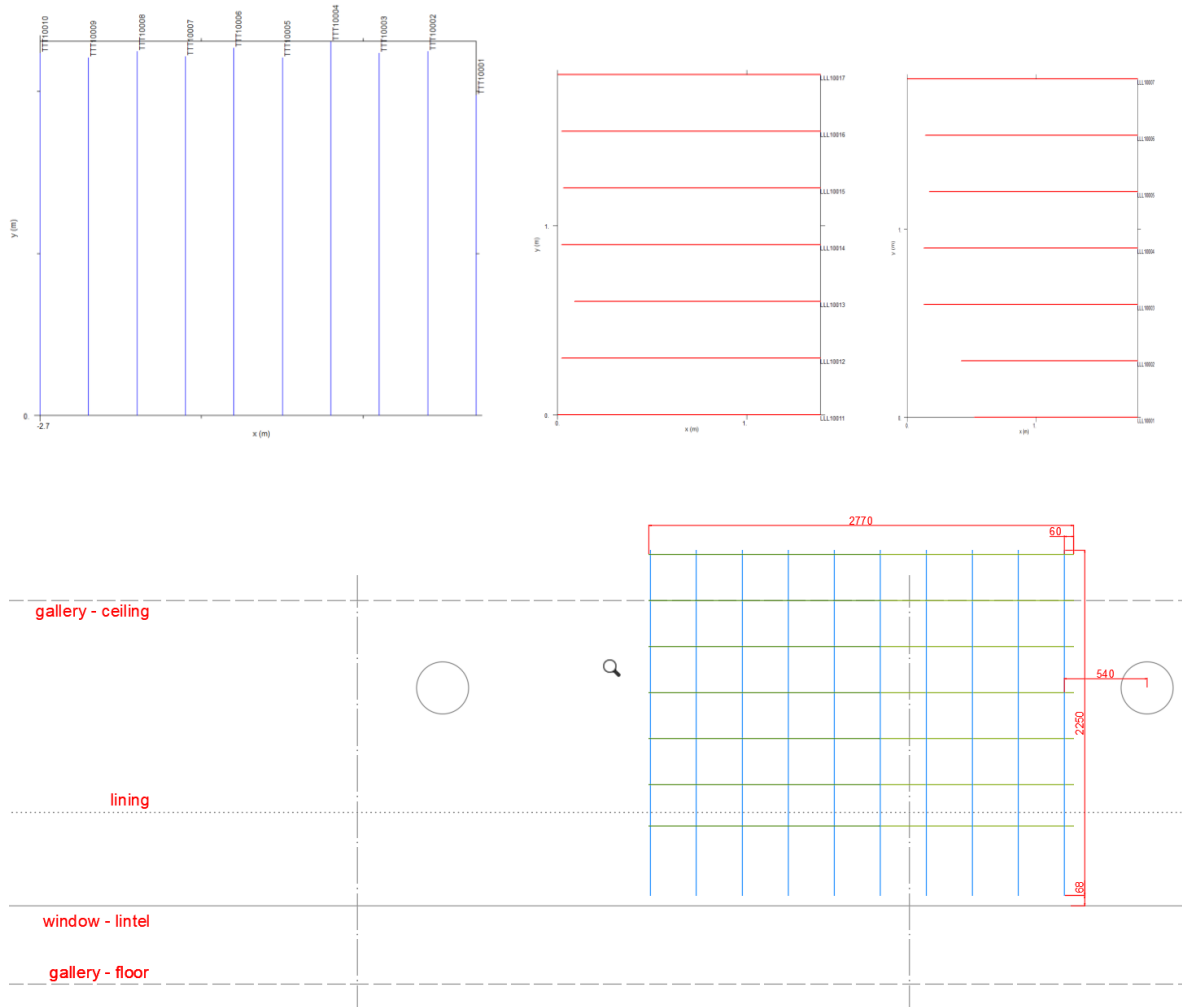


Figure 34: Marking and positioning of longitudinal and transverse profiles on the exterior part of the wall. Not to a specific scale.

Summary interpretation of the survey results

Appendix A shows the radargrams for the L and T profiles on both sides of the façade wall. The radargrams are presented after background removal and filtration of extreme frequencies (noise). The measured radargrams are not described and interpreted individually but as a set of L or T scans.

The wall is composed of the reinforced concrete and additional layers as described above. The propagation of the radar waves seems to differ between the additional layers (insulation layers) and the concrete. This resulted into the following: (i) propagation speed is not constant across the thickness of the structure thus the determined depth can be less accurate, especially when scanned from the interior side, (ii) reflection of the radar waves from the back side of the wall are not clear when scanned from the exterior side, (iii) scanning from the interior side was in general less informative.

The most informative are scans from the exterior side. The T1-10 profiles show the reflection hyperbolas from the reinforcement which is expected to be perpendicular or possibly also oblique to the profile. The reinforcement is detected at two depth levels under the surface, at app. 80–120 mm and 150–160 mm, called upper and lower reinforcement respectively; regarding the depth of reinforcement placement, it should be noted that the cement based render varies in thickness from app. 15 to 30 mm. The distance along the scans T1 and T6, and the spacing between the re-bars is given in table 1 in the **Appendix A**. There are repeating hyperbolas on the parallel scans at similar positions, and thus this is interpreted as horizontal reinforcement bars with spacing varying between 290–360 mm for the upper re-bars, see the drawing in the **Appendix B**. The lower re-bars are not always clearly detectable on all ten profiles but it seems that they are also placed in a similar manner. In addition, there are also single reflections in some profiles that do not repeat at the same distances as in the others. These can be interpreted as some oblique re-bars, ends of follow-up re-bars or secondary re-bars.

The L 1–7 and L11–17 profiles also show reflection hyperbolas from the reinforcement. In this case we expected to detect vertically placed reinforcement. As can be seen from the radargrams, the detected positions where the scanned profile crossed a re-bar do not exactly repeat in the parallel profiles. Many are shifted to the left or right. Also the spacing is less regular than in the case of the horizontal reinforcement. Due to this uncertainty, the position of re-bars at the profile were marked by dots (black upper re-bars, grey lower re-bars), see Appendix B, without the estimation of the re-bars position. The reinforcement is detected at two depth levels below the surface, at app. 60-70 mm and 140–150 mm. There are other re-bars added at around the position of the profile L5 running upwards that are about 40 mm deep, while the re-bars running from the lower parts are inclined inside into the structure. The spacing between re-bars varies between 170 to 200 mm. There are also additional re-bars inserted in between at certain positions.

The geometrical imperfection of the vertical re-bars and also the horizontal ones to a lower extent is probably due to deformation during casting of concrete and reflects the way how the re-bars were fixed in their position and together. It can partially be caused by the movement of the antenna during the measurement. The horizontal profiles were scanned from a ladder and had to be divided in to two sections with a certain overlap. During the post processing it was found that the overlapped sections did not match. In such a case the profiles L11-L17 were preferred.

Discussion

The 3D structural finite element analysis indicated that the fundamental structure of the Fuchs building is adequate if all assumptions are validated. Pending further investigation and analysis, the building appears to be suitable for use in modern day. The building has some locations of damage, but these tend to be localized and simple to

resolve. In particular a complete damage assessment must be completed on the shell of the building to identify all damage that is currently hidden.

The radar survey made it possible to non-destructively identify the reinforcement of a section of concrete façade wall above the horizontal window. The surveyed section included the part around the supporting frame which is most probably bearing the load of this part of the facade. The surveying fulfilled the objective of obtaining overview information on the structure of the façade wall and its reinforcement by the GPR. The results of the survey are detailed in the previous text and appendixes. The GPR survey uncovered certain limits that relate to the used method and procedure. The method does not allow to determine the diameter to the reinforcement (a shortcoming which can be overcome by the complementary use of a re-bar scanner). The results can be improved by a denser measuring grid and by better access from the exterior side. The GPR with 2GHz antenna is less suitable in the parts where there is a number of re-bars close to each other and overlap at different depths and angles. This GPR analysis provides basic information and background for evaluation with regard to the use of GPR IDS with 2GHz antenna on this site. It serves as an example of the possible use of this methods for subsequent specific surveys in the future.

Conclusions

This report aimed at analysing existing historical and technical data on the Fuchs building and performing a condition assessment of its recent state for aiding in the plan of a restoration proposal.

The future restoration plan should be followed by an ordinary selection procedure to choose the new use and tenant. Regarding other similar cases (e.g. the City Market in Nicosia – another case study of this project) certain concerns are relevant regarding the community participation in the selection of the future use of the building. A way to preserve some aspects of the recent usage should be investigated and alternative approaches to the restoration should be considered.

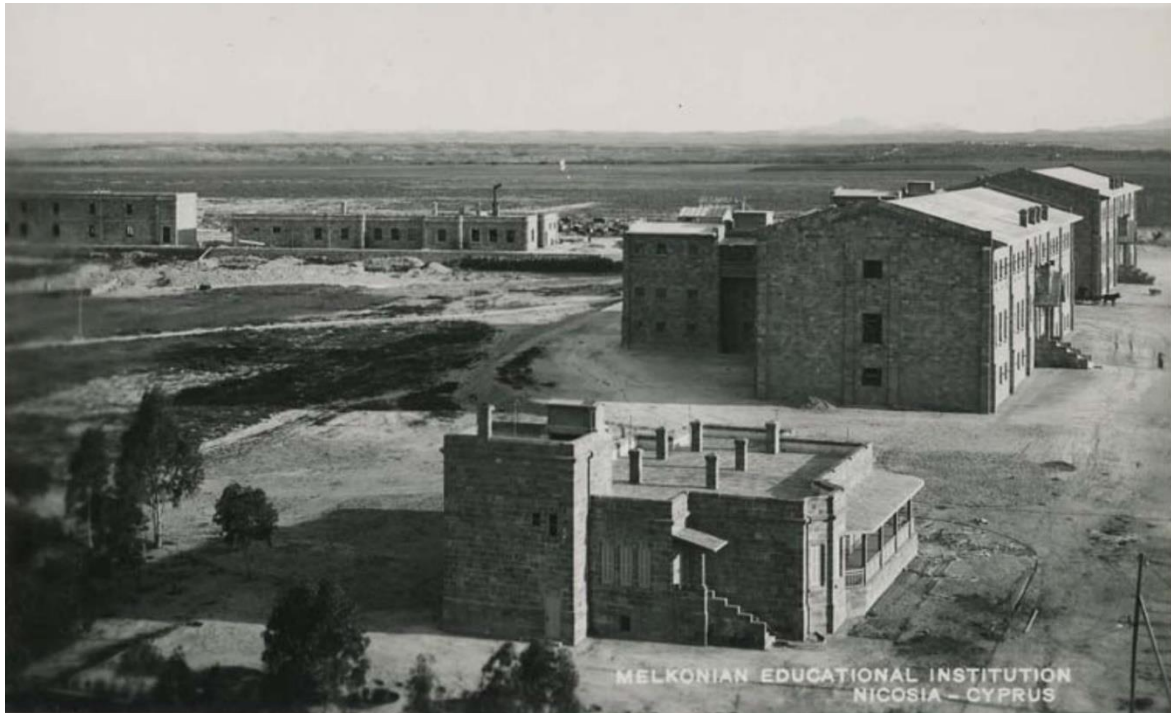
References

- [1] J. Javůrek, V. Thiele, and M. Nováková, “Studie využitelnosti objektu Fuchsovy kavárny č.p. 1125, Praha 7,” Prague, 2015.
- [2] J. Holeček, J. Jr. Holeček, and O. Němec, “Rešerše a vyhodnocení existujících podkladů a archivních materiálů,” Prague, 2015.

- [3] J. Starý, “Technická studie stavebně technických parametrů objektu Fuchsovy kavárny, Štvanice č.p. 1125, Praha 7,” 2015.
- [4] P. Přikryl, “Koncepce statického a stavebně technického řešení rekonstrukce,” Prague, 2015.
- [5] L. Dostál and Z. Potužák, “Zpráva o stavebně technickém průzkumu objektu Fuchsovy kavárny, ostrov Štvanice č.p. 1125, Praha 7- Holešovice,” 2015.
- [6] J. Holeček, “Restaurátorský průzkum, objektu č.p.1125, budova Fuchsovy kavárny na ostrově Štvanice, Praha 7- Holešovice,” Prague, 2015.
- [7] R. Švácha, *Od moderny k funkcionalismu*. Prague: Victoria Publishing, 1995.
- [8] J. Vybíral, R. Švácha, and M. Masák, *Veletržní palác v Praze*. Prague: Národní galerie, 1995.
- [9] A. Vondrová, “Český funkcionalismus 1920- 1940 (architektura).” the Museum of Applied Arts, Prague , 1978.
- [10] R. Švácha *et al.*, *Naprej!: Česká sportovní architektura 1567-2012*. Prague: Prostor - architektura, interi , 2012.
- [11] B. Scheuer, Structural Analysis of Historic Reinforced Concrete Building - Fuchs' Cafe in Prague, Master Thesis undertaken within the CONSECH20 project, CTU, Prague, 2020
- [12] Monument Diagnosis and Conservation System.
<https://mdcs.monumentenkenis.nl/> (retrieved on July 2020)

Report on In-Depth Case Study

The Melkonian Education Center (Nicosia, Cyprus, 1924 and 1926)



CONSECH20 – WP2 (iii)

In-Need of Restoration Case Study

Georgiou, A.

Hadjimichael, M.

Ioannou, I.

October 5, 2021

Introduction

Historical background & Description

The Melkonian Educational Institute was originally built by the Melkonian brothers to operate as an orphanage / boarding school for Armenian orphans, following the Armenian genocide [1]. The architect was the Armenian Garo Balian, a descendant of a renowned Armenian family of Ottoman court architects in the service of the Ottoman Empire during the 18th and 19th centuries [2]. Construction of the building took place between 1924 and 1926. During the first years, the Melkonian Educational Institute operated as an orphanage and an elementary school, whilst in 1934 a secondary school was also established in the premises. The endowment of Melkonian was transferred to the Armenian General Benevolent Union (AGBU) via a notarised act, dated 28 December 1925, with AGBU being obliged to equip and maintain the School for up to 500 students and provide a number of subsidies. In 1926, AGBU was granted the absolute ownership of the Melkonian [3]. Known as ‘an island within an island’, the Melkonian has a great social and cultural importance for the Armenian diaspora and came to be a world-known high-school [4]. It thus holds great importance, both culturally and socially, as well as in architectural terms. In 2005, the Armenian General Benevolent Union (AGBU) decided to close the school, a decision which was met with protests by the local Armenian community, which described the act as a ‘second Armenian Genocide’.

The Melkonian Educational Institute is located at the entrance of Nicosia, the capital city of Cyprus, in a heavily built area of Aglandjia Municipality. When originally built, however, back in 1926, the area was secluded and very much rural. The land upon which the Melkonian Educational Institute was built was a “*bone-dry and wind-swept land, full of foxes, for which later on large sums of money were spent to be cultivated*” [3]. The total area upon which Melkonian is built consists of 18,63 hectares, and includes 4,95 hectares bought by the government at the time for the purpose of squaring the area. According to the legend, the area was originally known as the ‘hill of snakes’, and was selected by the Melkonian brothers because no minaret was visible within a radius of 3 km, something which, in their opinion, would make the students feel safe [5]. Nevertheless, further studies of the Cyprus State Archives suggest otherwise. According to these studies, the Adana Archbishop Seropian and the Armenian Bishop of Cyprus, Bedros Saradjian, simply chose that area in Nicosia over an area in the Larnaca region [3]. In front of the Melkonian, arises the ‘Forest of Remembrance’, planted by the first orphan students of Melkonian, in memory of their loved ones killed during the Armenian Genocide. The land became known at the time as Ծաղկաբլուր (Flower Hill), a name given to it by Archbishop Seropian. Aerial photographs and digital maps from 1963 and today highlight the changing urban landscape surrounding the Melkonian Educational Institute (Figure 21). This suggests that the land upon which the Institute stands has increased in value and importance.



Figure 21. Aerial photo from 1963 (above) and 2020 (below) of the Melkonian Educational Institute (in the red rectangle) and the surrounding area [6].

The Melkonian Educational Institute complex comprises of two rectangular buildings, identical to each other, with simple repetitive window openings and arches supported on pilasters at each entrance, and what has come to be known as the Headmaster's mansion, which is the building this in-depth report will focus on (Figure 38). At the beginning, Melkonian also had its own power station, a printing press, a farm, a hospital and a 35-metre water tower [7]. The three buildings, as well as the 'Forest of Remembrance' in front of them, were listed in 2007 [8]. The current complex has also been included in the index of the 100 (most) important buildings, sites and neighbourhoods from Cyprus compiled by the National Register of Docomomo Cyprus, and it is thought to be the first building on the island built using the proprietary Hennebique system, allowing the construction of large floors and roof spans using a small number of internal columns. The load bearing walls of the building are built in local limestone, quarried from the nearby area.

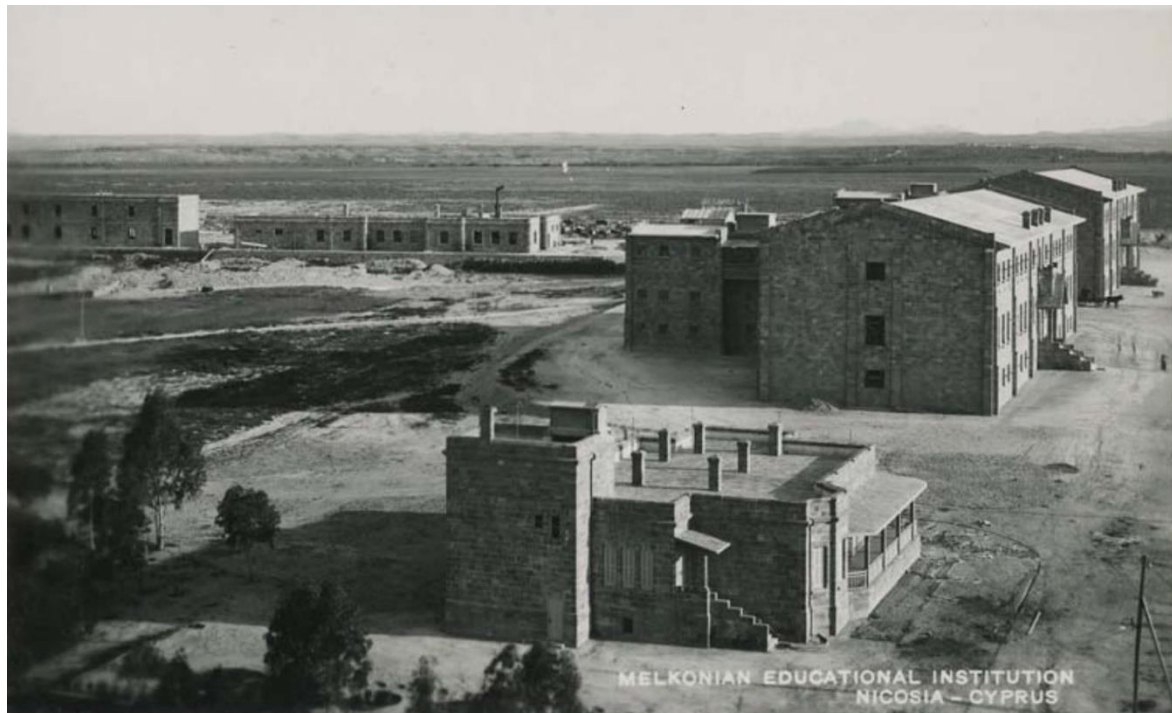


Figure 22. The Melkonian complex consisting of the two school buildings and the Headmaster's Mansion [9].



Figure 23. Aerial photo of the Melkonian Headmaster's Mansion

The Headmaster's mansion (Figure 39) was built at the same time as the main buildings and was completed in 1925. It was originally built with the purpose of being the private residence of the founder of the Institute, Garabed Melkonian (his brother passed away in 1920). Following his passing in 1934, and according to his own wish, the mansion functioned as the residence of the headmaster of the Institute, whilst it also hosted important guests, such as the Catholic Patriarch of Cilicia. Between 1989-1991, AGBU used the building as its office and a club, and up until 2004 it was rented out and used as

an office (for architectural firms). Personal testimonies from old students of Melkonian suggest that in the mansion there were unique antiques and paintings, the fate of which is not known since the rearrangement of the building towards the late 80s [10]. The mansion has been abandoned since 2004 and there have been suggestions to turn it into a library / archive for the Armenian community.

Characteristics of the Concrete Building and Structure

The residence was part of a complex of buildings consisting of two 3-floor structures, used as orphanage and school, and a single-story residence, all designed according to the Hennebique patented method, with a hybrid structure of reinforced concrete and load bearing masonry walls. The residence occupies approximately 380 m² and has an almost square plan of 22 m x 17 m (Figure 40), with a height of 4 m. A small proportion of the plan has a basement that continues up to a first floor, with a total height of 9 m. The building consists of load bearing masonry walls and reinforced concrete slabs, beams and columns.

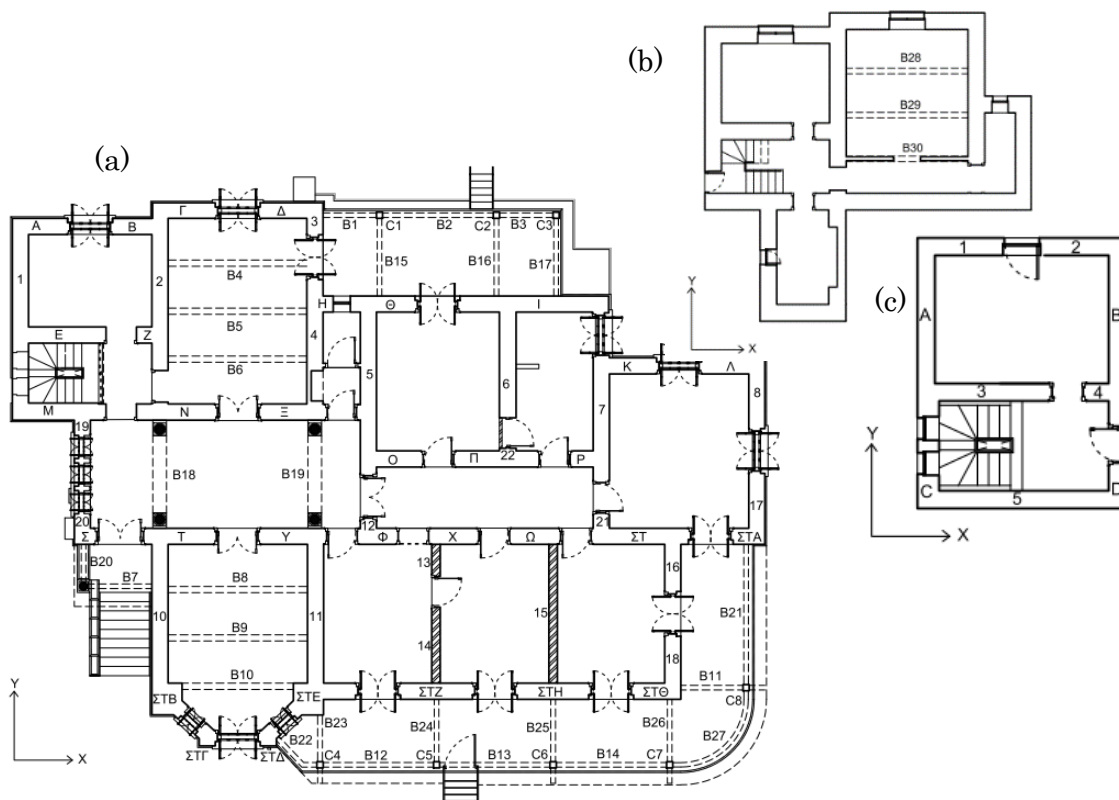


Figure 24. (a) Ground floor plan, (b) Basement plan and (c) 1st floor plan

Typical damages found in the Melkonian Headmaster's Mansion

The overall state of the building is rather good, despite its abandonment for many years. In general, there are no visible cracks on the reinforced concrete elements from either

service or seismic loads. The damages were recorded on section cuts of the building as shown in Figure 25.

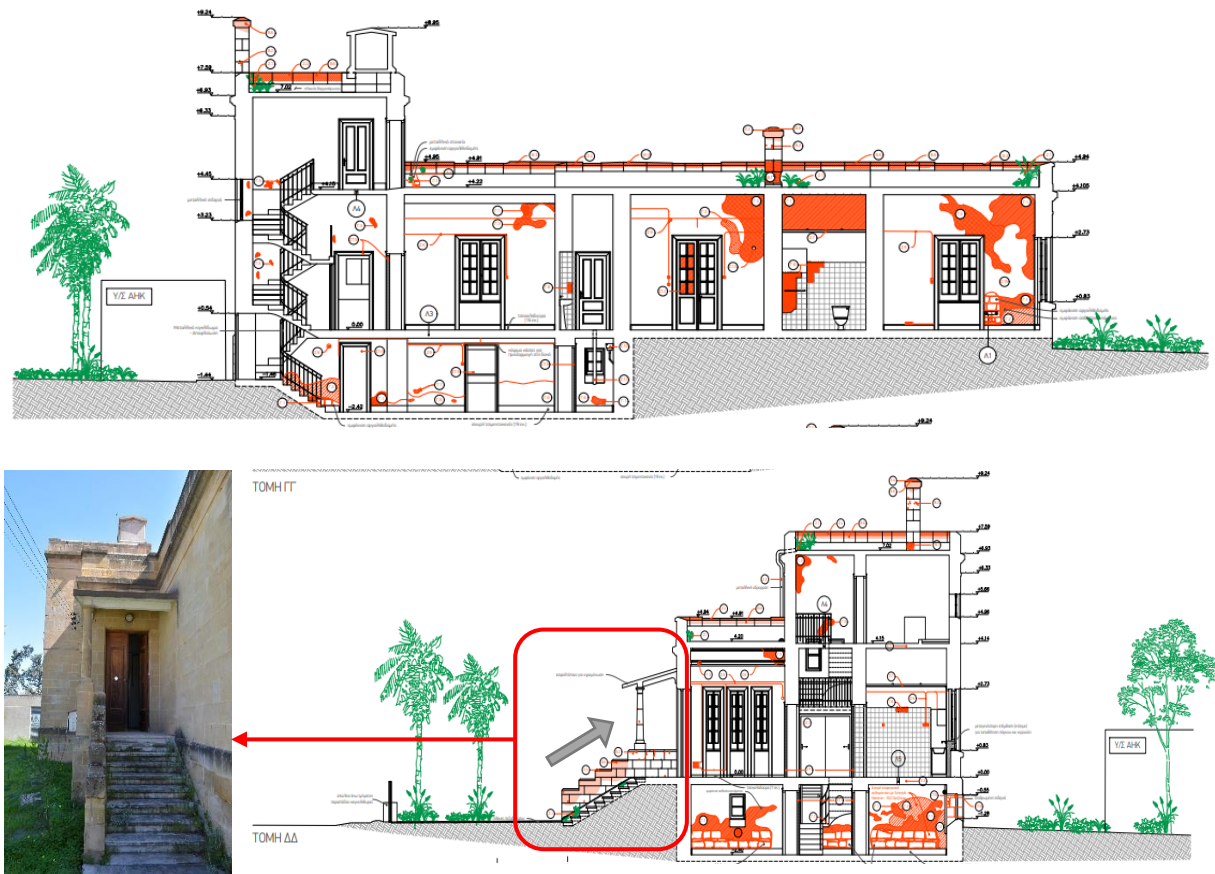


Figure 25. Recorded damages of the Melkonian Residence (2020).

Corrosion is evident in the beams and columns of the porches, where cover has spalled and the reinforcement is visible, in one of the beams of the basement top slab and in specific locations of the ground floor top slab, especially at the locations where the rain water is not properly directed away from the roof. The slabs at these locations have black stains and show cover delamination (Figure 26a). All deterioration in reinforced concrete elements is linked to moisture, carbonation and corrosion of the reinforcement.

Figure 26b depicts the damages of the masonry elements. At the stone masonry walls, mostly in the basement, the plaster is detached and the limestone walls are filled with voids due to salt crystallization, related to their high porosity which renders them prone to moisture-related damage. Also, in the basement, the masonry wall that is below the soil level, shows extensive deterioration of the mortar (Figure 26b). The same is also evident in some of the ground floor walls, mostly at the locations where the roof slab retains water. The masonry walls in the back north-east room further show some diagonal cracking that suggests minor settlement of the foundations; yet, with the use of crack measuring devices, this was found not to be active. Mosses and blemishes are extensively evident on the exterior surfaces of the masonry walls, while cracking of the masonry units is evident on the roof parapet.



Figure 26. (a) Damage in the reinforced concrete members and (b) Damage of the masonry members.

Investigation, Methods and Results

For the seismic assessment of the residence, EC8:3 [11] was used. The procedure of the seismic assessment consisted of:

- i. verification of the geometry of the structural elements and reinforcement detailing in regards to the original plans,
- ii. evaluation of the material properties through in situ non-destructive and laboratory destructive tests,
- iii. simulation of the building using the analysis program SAP2000 [12] and
- iv. assessment of its structure capacity following time-history analysis.

Survey and testing of materials

Extended survey was performed for the verification of the geometry and member sizes. For the detailing information, only some of the original construction drawings were found, consisting mainly of the slab reinforcements. In order to enrich this information, a rebar detector (PROCEQ) was used to verify the slab reinforcement in relation to the original drawings and to detect the steel bar reinforcement, the bar cover and diameter in the beams and columns (Figure 27).



Figure 27. Rebar detection and diameter/cover measurement.

The detection of the reinforcement position was also used to determine the locations for the non-destructive rebound tests (EN 12504-2) and the possible positions for core sampling of concrete (EN 12504-1). The number of core samples had to be limited, due to the fact that the building is listed. For this reason, core samples were taken only from four points of the load bearing masonry walls, one column, one location at the basement ceiling slab and one location at the ground floor roof slab (Figure 28). Additionally, some samples from the masonry wall mortars were also taken for analysis. Sample and test locations are recorded in Appendix A and list of samples in Appendix B.



Figure 28. Coring of stone and concrete samples from various locations.

Load bearing masonry walls

Tests on materials included, for stone: (a) measurement of dry mass, density and porosity (EN 1936 [13]), (b) water absorption coefficient by capillarity (EN1925 [14]), (c) uniaxial compression test (EN1926 [15]) and (d) XRD analysis and classification of the samples (EN 12670 [16]) (Figure 29). Additionally, fractionation and mineralogical analysis with the assistance of XRD analysis were performed on the mortar samples in order to define the binder:aggregate ratio and the mix components. XRD results may be found in Appendix C.

The natural stone may be described as bioclastic limestone, according to EN 12670 [16], with high calcite percentage. This stone belongs to the Nicosia Formation (Pliocene, 4Ma), and has an average apparent density of 1513 kg/m^3 and an open porosity of 38.6%, while the capillarity coefficient ranges between $3324\text{-}4150 \text{ g/m}^2/\text{s}^{0.5}$ (with a linear relation between the capillarity and open porosity). The compressive strength ranged between 1.67 and 3.13 MPa, with an average of 2.49 MPa, with higher strengths observed in the stone samples taken from the front porch's external masonry surface.

For the mortar, the binder:aggregate ratio ranged between 1:3.5-1:6; the binder consisted mostly of carbonate minerals (calcite and magnesite > 49%), while the aggregates were of ophiolitic origin. Hence, the composite may be classified as a lime-based mortar.



Figure 29. Tests on masonry materials: Specimens in vacuum vessel, Water absorption test by capillarity, Failure planes from stone compression, Stereomicroscopic view of sample S1 (16x)

Reinforced concrete

For the case of concrete, the following tests were carried out: (a) dry mass, density and porosity by vacuum assisted water absorption and (b) uniaxial compression (EN12390-3 [17]) (Figure 44).



Figure 30. Tests on concrete: Specimens in vacuum vessel, Testing apparatus for concrete in compression, Failure of concrete in compression.

The concrete samples showed low variability in the test results, even though concrete at the time the building was constructed was manually mixed in small batches. The average apparent density was found to be 2181 kg/m³, while the open porosity was 18.3%. The average compressive strength was 15.21 MPa, resulting from samples of 1:1 width to depth ratio, therefore characterized as mean cube strength, with the lower value of 13.92 MPa obtained from the roof slab, and 17.11 MPa obtained from the column sample of the external front porch. The maximum aggregate size from the samples tested was recorded as 52 mm; the aggregates may be characterized as uncrushed river material. Visually the mix design showed no apparent voids, even though at the time there were no mechanical means of compaction, without visible voids or cracks.

Rebound Number and compressive strength

The non-destructive Rebound test was deployed in order to assess the compressive strength variance among the different members of the structure, in combination with the compressive strength resulting from the core samples that were extracted. The Rebound number recorded at various elements is shown in Table 6, where the type of element, direction of testing, R value, R average and corresponding cube and cylinder strength, extracted from Figure 31 are recorded. The tests show a consistent overestimation of the compressive strength of concrete by the use of the Rebound test.

Table 2. Rebound measurements and compressive strength

| Element | Direction | R | R (ave) | Cube Comp. Strength (MPa) | Cylinder Comp. Strength (MPa) | Sample core strength comp., cube equivalent (MPa) |
|---------|-----------|----|---------|---------------------------|-------------------------------|---|
| Beam | Vertical | 39 | 33.7 | 24 | 19.2 | |
| | | 43 | | | | |
| | | 34 | | | | |
| | | 23 | | | | |
| | | 24 | | | | |
| | | 34 | | | | |
| | | 33 | | | | |
| | | 28 | | | | |
| | | 41 | | | | |
| | | 38 | | | | |
| Slab | Vertical | 38 | 36.5 | 28 | 22.4 | 14 |
| | | 44 | | | | |
| | | 39 | | | | |
| | | 39 | | | | |
| | | 29 | | | | |
| | | 41 | | | | |
| | | 33 | | | | |
| | | 31 | | | | |
| | | 40 | | | | |

| | | | | | | |
|--------|------------|----|------|----|------|----|
| | | 31 | | | | |
| Column | Horizontal | 28 | 27 | 20 | 16 | |
| | | 32 | | | | |
| | | 28 | | | | |
| | | 28 | | | | |
| | | 22 | | | | |
| | | 24 | | | | |
| | | 38 | | | | |
| | | 32 | | | | |
| | | 16 | | | | |
| | | 22 | | | | |
| Column | Horizontal | 37 | 37.1 | 36 | 28.8 | 16 |
| | | 37 | | | | |
| | | 30 | | | | |
| | | 45 | | | | |
| | | 45 | | | | |
| | | 35 | | | | |
| | | 33 | | | | |
| | | 36 | | | | |
| | | 33 | | | | |
| | | 40 | | | | |

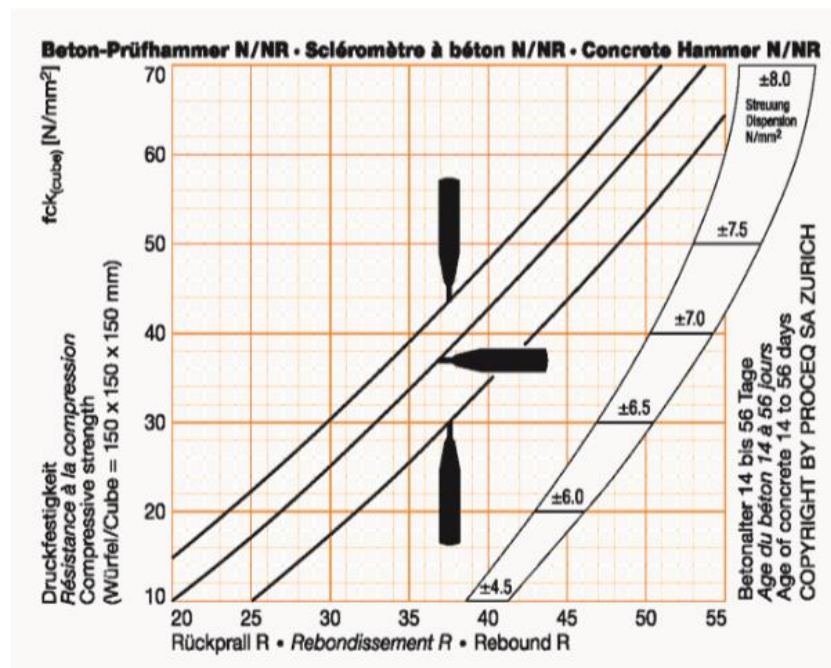


Figure 31. Rebound to compressive strength value for PROSEQ equipment

Concrete cover

The cover of the reinforcement was established both by the use of the PROSEQ rebar detector and also from one of the samples taken from the slab that cut through the steel bars (as well as from the columns that suffered from cover delamination and the reinforcement was thus visible). The concrete cover of the longitudinal bars was in the order of 20 mm.



Figure 32. Reinforcement in slab sample, Exposed reinforcement in column, Hennebique column tie of bars

Reinforcement layout and diameter

The reinforcement was in close agreement with the original detailing drawings. Exploratory excavations showed that the columns continued up to 2 m underground in order for the foundation to reach a solid ground. Some caves were found below the ground floor slabs. The columns at the foundation level were connected with beams with very sparse reinforcement. Many of the columns had drainage pipes embedded in them, something that is now forbidden by the Codes. Stirrups in beams were sparse, not suitable for ductile structures and the formation of plastic hinges at the edges of members. The lap splicing of the longitudinal reinforcement was also found to be less than what is required as per current seismic codes. Additionally, the reinforced concrete walls shown on the original drawings were connected only on beams at the foundation level, leading to the conclusion that they cannot attain flexure due to the lack of foundation system. Photo evidence of the above is shown in Figure 46.



Figure 46. Exploratory excavations and concrete cover removal during retrofit works

Assessment of seismic capacity of the structure

Simulation of the structure

Modelling of the structure was performed by a 3D model, to include any possible torsional effects. The assessment analysis performed was Time-History with the use of an inelastic model.

Elements, materials and other parameters

The structure was modelled in the commercial program SAP2000 [6] in order to assess its capacity under seismic conditions. The reinforced concrete beams and columns were simulated as 2-node frames. The mean average strengths were used for determining the properties of the various materials. For all the elements in the structure under study, modifiers were used to decrease the stiffness of the cross sections to the actual cracked stiffness, assessed by the actual Moment-curvature diagrams with the use of RESPONSE2000 [9], in order to take into consideration the stiffness degradation during the seismic event [10,11]. Diaphragmatic action was applied to all the nodes of the floor levels. The members were connected to the ground with linear links, according to the properties of the foundation system and the soil, while the walls in the basement under the soil level were assigned with springs that allow movement away from the soil, but prevent movement when in contact with it. All the floor slabs were assigned with the load combination of $G+0.3Q$, with additional load for the finishing of the floor surfaces. The live load was chosen based on the Cypriot Annex of Eurocode 1 [12]. This load combination was also used to derive the mass of the structure for the modal analysis. Some of the columns of the GF were assigned with hinges (zero moment), at their bottom node, due to the increased axial load ratio $\nu=N_{G+0.3Q}/(A_c f_c)$ (Figure). Note that those columns are subjected to a value of ν that is close to the limit of 0.4 that corresponds to balanced column failure, which identifies the limit of brittle response in the Axial – Load vs. Moment Interaction Diagram. This load ratio is estimated from service life loads only, without considering the additional axial load that the seismic overturning action will impose to the columns. On account of the high value of ν and the reported corrosion of reinforcement in the base of those columns, it is concluded that no moment can be resisted in their base; thus, a hinge was assigned in the model.

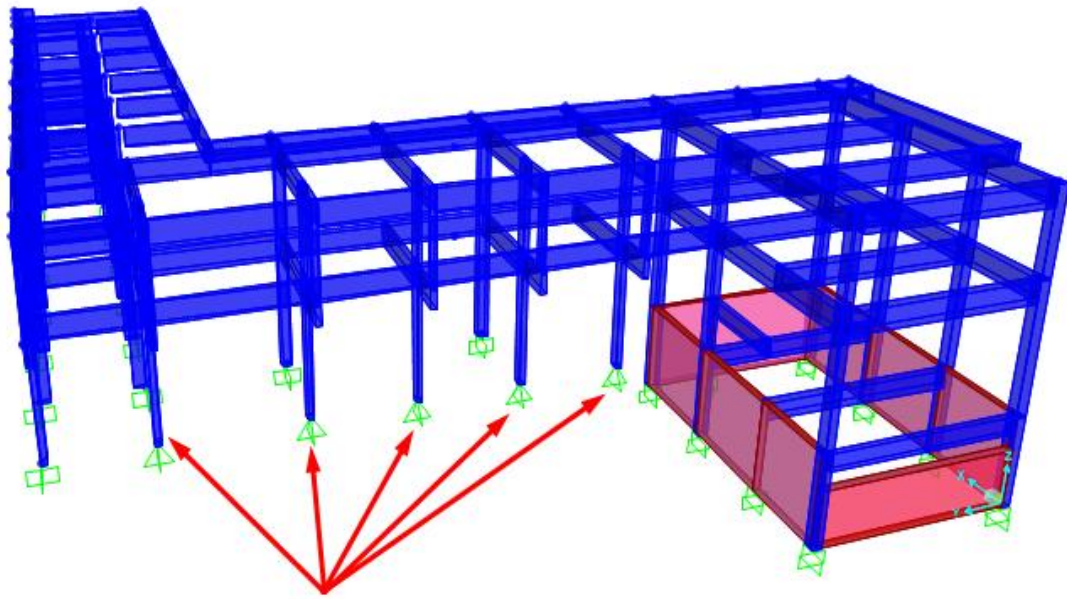


Figure 47. Simulation of the structure in SAP2000 and hinge assignment at the bottom of columns

Discussion

Assessment of the failure mechanism in reinforced concrete columns

The brittle failures that may incur to old substandard members, designed without any seismic provisions, are a crucial parameter for the assessment and retrofit of reinforced concrete structures [13]. The hierarchy between the individual failure mechanisms must be assessed in order to determine any prevailing brittle failure. The mechanisms of column failure, in terms of Shear Force, in the columns that were examined were the following (**Error! Reference source not found.**):

- Yielding of the flexural reinforcement and failure in flexure, (V_{flex})
- Shear failure, (V_v)
- Anchorage and Lap splice failure, (V_a / V_{lap})
- Joint shear failure, (V_j)
- Formation of plastic hinges in the adjacent beams (ductile behavior) V_{by}

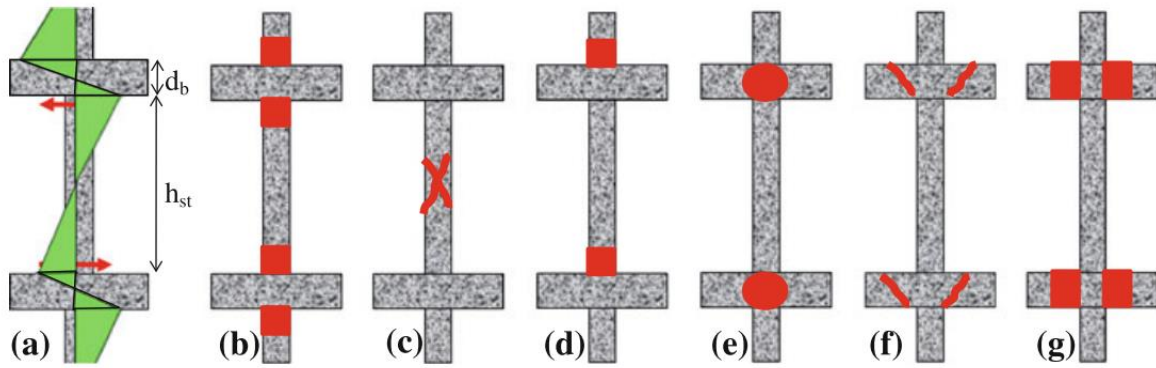
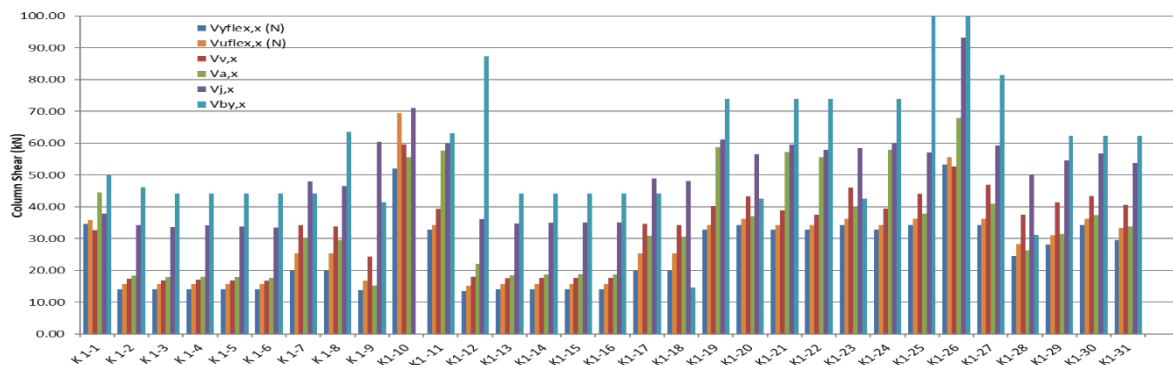


Figure 48. a Moment distribution and b–f possible failure modes of a reinforced concrete column: b flexural yielding, c shear failure, d bar anchorage/lap-splice failure, e joint shear failure, f connection punching failure, g column shear limited by plastic hinging in the beams \Rightarrow ductile frame behaviour [13].

The results from the analysis performed are shown for the X-direction in the charts of Figure 49. The first assumption to be made is that in almost all cases the failure of the columns will prevail yielding of the beams. This is attributed to the wrong type of design of RC members of the era that required “strong beams-weak columns”. The earthquakes that followed showed that, that kind of design was wrong, leading to collapse of the members, while modern seismic codes, through the capacity based design approach, have rectified the approach promoting a “strong column-weak beam” design.

Additionally, the results indicate that most of the columns in the ground floor will behave in a ductile manner with flexural failures, except for some columns with very high axial load that will show brittle failure of the compressive zone prior to yielding of reinforcement, and some cases of brittle shear failure for loads parallel to the weak axis of the members. On the contrary, most of the columns in the 1st floor will fail due to brittle shear failure, due to their short length, in combination with the very sparse stirrups, having a spacing of more than 300 mm.



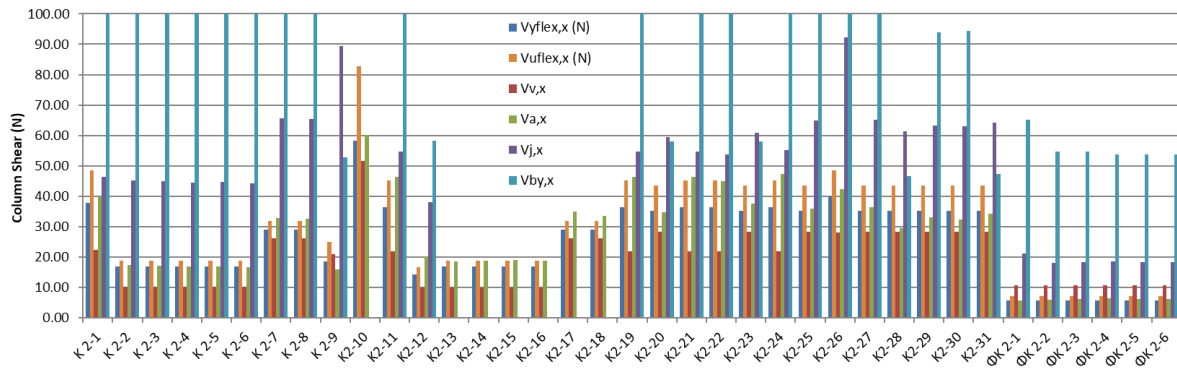


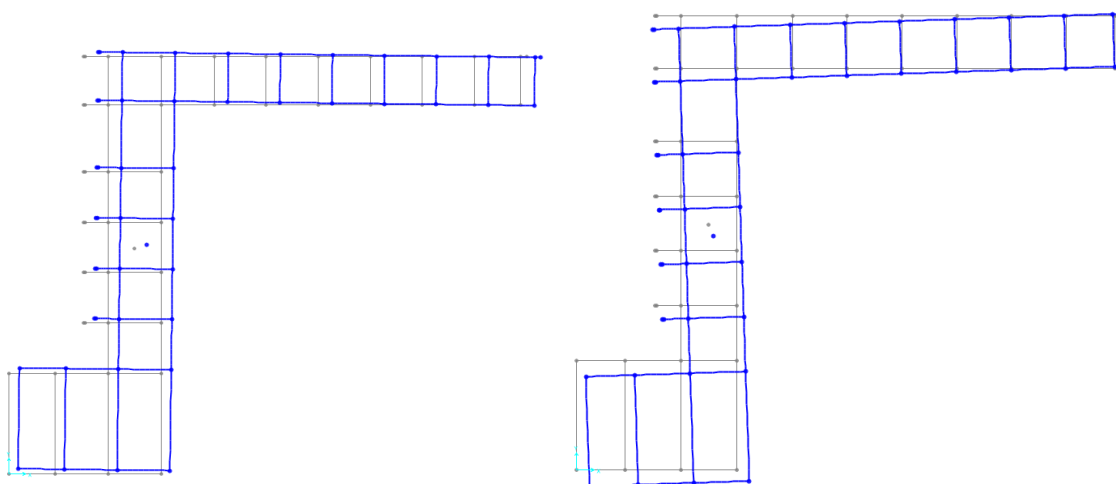
Figure 49. Shear force for different mechanisms of failure for the X-direction of seismic action, for the ground floor columns (top) and the 1st floor columns (bottom)

Modal characteristics of the structure

The first three modal shapes of the structure are depicted in Figure 50 and their characteristics are recorded in Table 7. While the first mode of the structure is primarily translational in the X-direction, with a very high period, compared to new structures designed as per the Eurocode, the second and third modes are combined translational to the Y-axis and rotational around the Z-axis. This is in agreement with the finding that the CM has high eccentricity to the CR in the X-direction.

Table 7. Results from modal analysis

| StepNum | Period | SumUX | SumUY | SumUZ | SumRX | SumRY | SumRZ |
|----------|--------------|----------|----------|----------|----------|----------|----------|
| Unitless | Sec | Unitless | Unitless | Unitless | Unitless | Unitless | Unitless |
| 1 | 0.995 | 0.826 | 0.045 | 0.000 | 0.00014 | 0.00584 | 0.05029 |
| 2 | 0.936 | 0.897 | 0.614 | 0.000 | 0.00218 | 0.00625 | 0.2555 |
| 3 | 0.459 | 0.897 | 0.892 | 0.000 | 0.00468 | 0.00626 | 0.87396 |



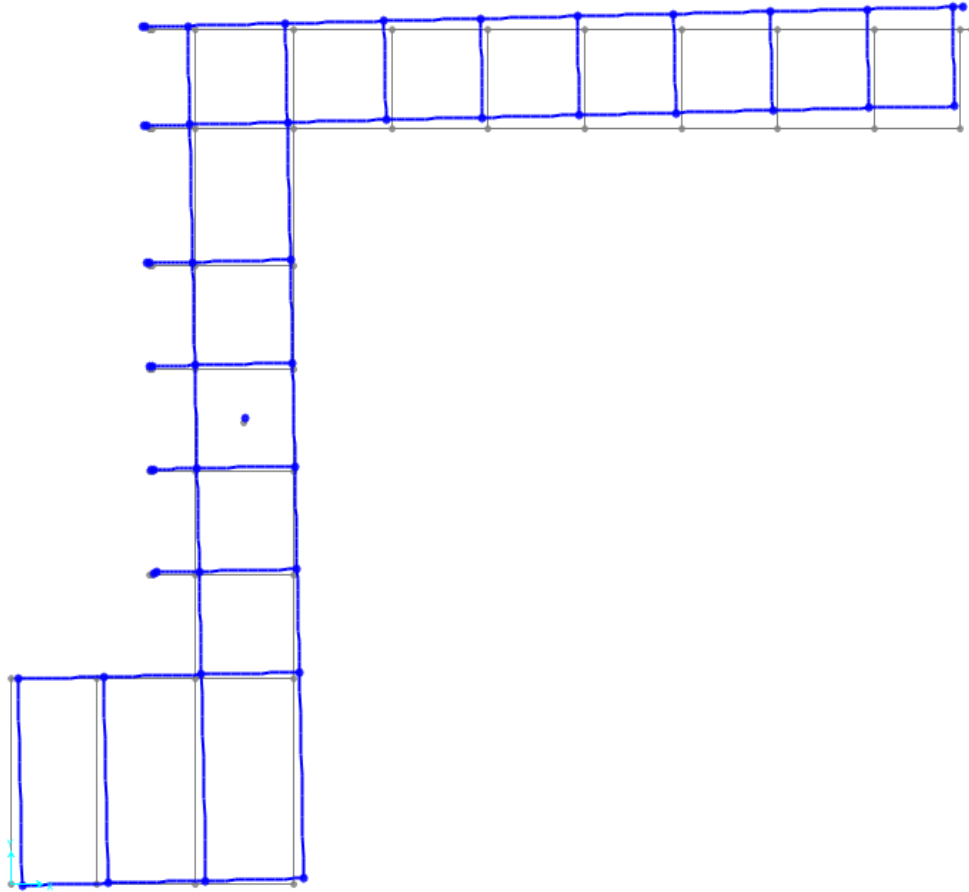


Figure 50. 1st mode $T=1.003$ sec, 2nd mode $T=0.95$ sec and 3rd mode $T=0.495$ sec.

Additionally, when the mode shapes are plotted heightwise in Figure 51, it is clear that the structure behaves as a pilotis, with a soft ground floor storey, indicating that during the seismic loading most of the displacement that will be induced in the structure due to the motion, will be undertaken by the ground floor columns, leading to increased levels of ductility demand.

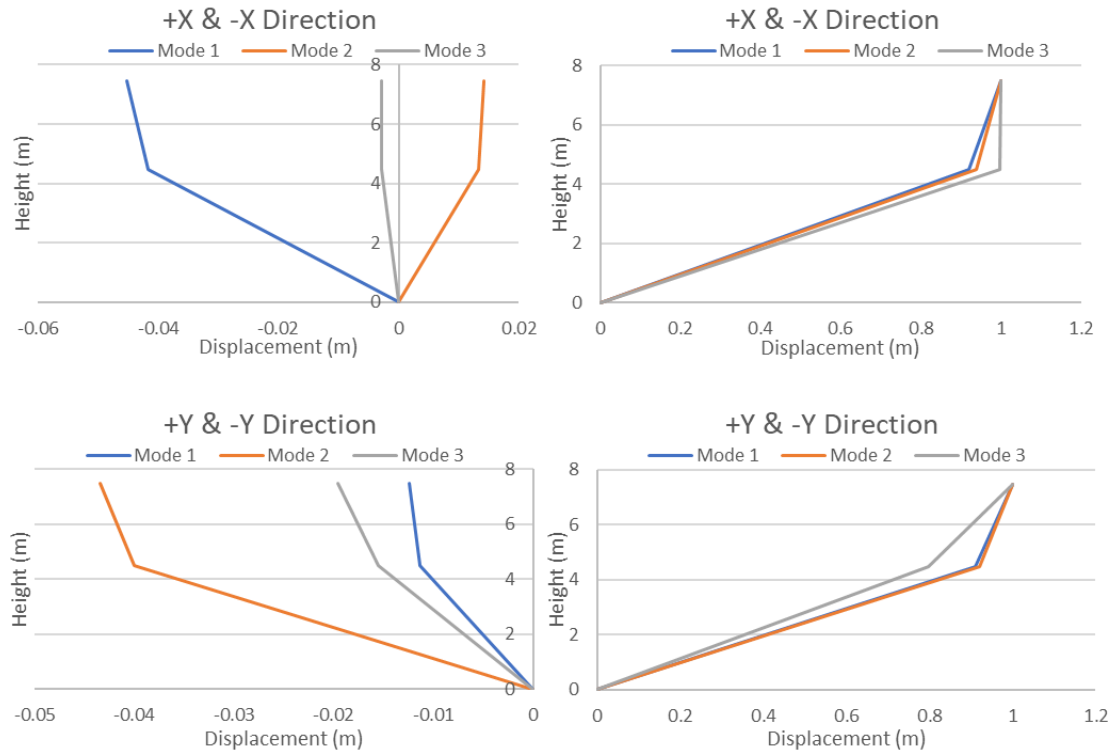


Figure 51. Displacements from modal analysis (left) and Mode shapes heightwise (right) at the CM

Time History Analysis

In order to determine the seismic displacement demand, Time History analysis was performed with a set of seven natural accelerograms that were selected based on the provisions of EC8:1 [14]. The accelerograms were selected to have similar geological conditions with the site soil (Type C), with magnitudes between 6.0-7.0 that correspond to the seismological context of Cyprus and with an epicentral distance range of 5-60 km. The average PGA from the accelerograms was the same as $\gamma_{rag}S$, while the average spectrum in the range of periods between $0.2T_1$ - $2T_1$, was above 90% of the response spectrum accelerations, in each direction of motion. Figure 52 (a) shows the ADRS for the selected accelerograms and the corresponding EC8 response spectrum. The accelerograms were placed in each direction simultaneously and in combination, while the average values from all load combinations were derived for the assessment.

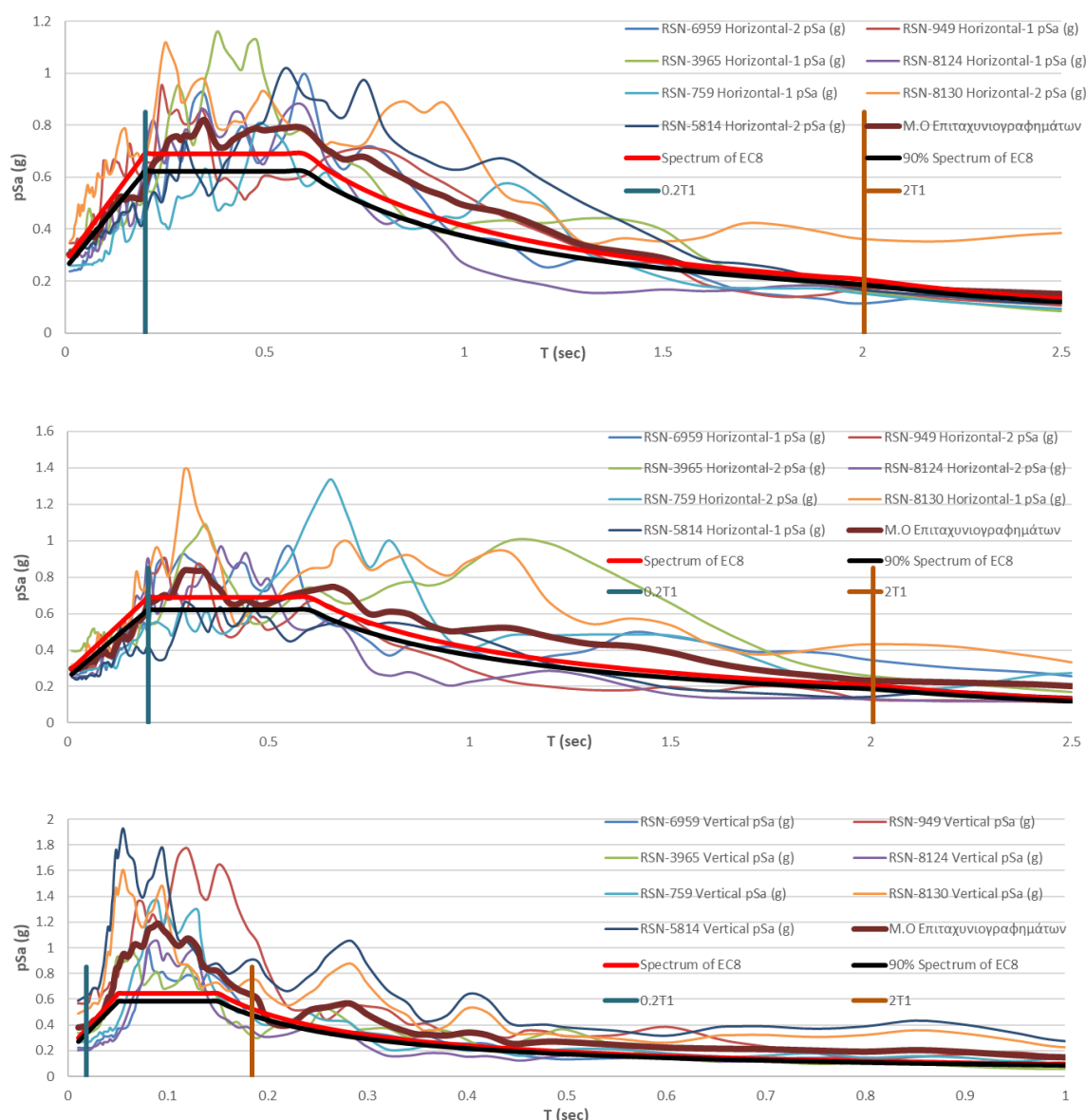


Figure 52. (a) Acceleration spectra for the selected accelerograms and the corresponding EC8 response spectrum in X, Y and Z direction.

Figure 53 depicts the drift demands along the height of the structure, from all load combinations, and the levels of damage of the members from the analysis. Even though the 1st floor columns undergo a very low level of drift in the order of 0.5% (related to the yielding of the flexural reinforcement), it is seen that most of them have failed and are in levels of damage not accepted by the assessment performance objectives. This is due to the previous conclusion that the 1st floor columns collapse in brittle shear failure prior to yielding of the flexural reinforcement. Additionally, the drift demands in the ground floor, in the order of 2-2.5%, require great drift ductility of the ground floor columns, in the order of 4, yet the members seem able to perform them, albeit in the level of significant damage, something that is accepted by the Performance objective.

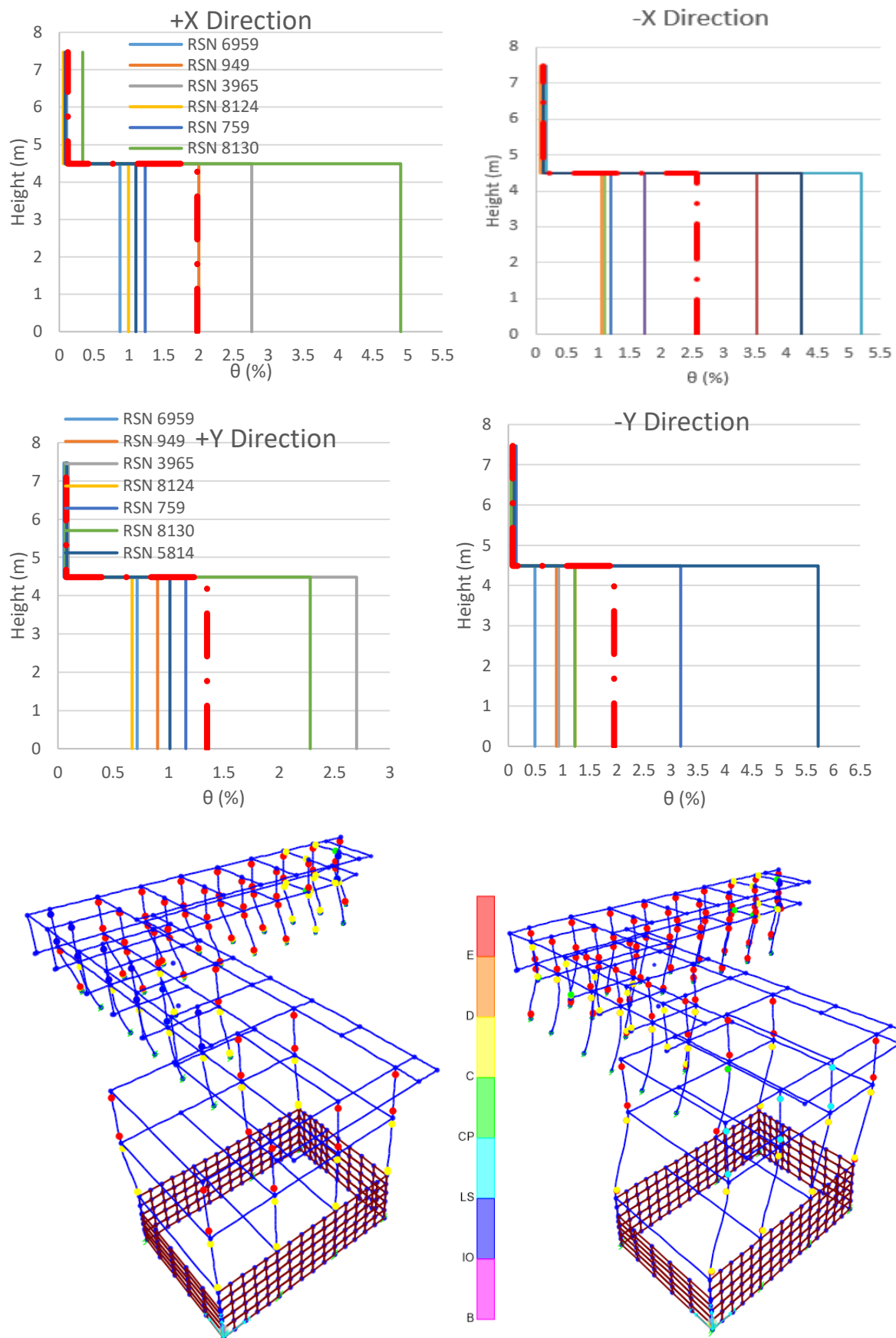


Figure 53. Drift demands from all accelerogram combinations and Damage level of the structure for combinations (RSN 759) and (RSN 8130)

Conclusions

The structural assessment of buildings requires good understanding of the various components of the structure, their interconnection and material mechanical properties, and finally the global behaviour under seismic excitation. In the local components level, the task of assessing the properties of members is becoming even more challenging in the case of historic structures. In such cases thorough member analysis has to be explicitly performed and all possible failure mechanisms must be taken under consideration. While the code specifically states that for the case of historic structures the assessment and retrofit “often requires different types of provisions and approaches”, there are no other guidelines that can be applied, which are at the same time legitimate for the practicing engineer to use. Therefore, what is prescribed in EC8:3 as assessment procedure, is often the only option available.

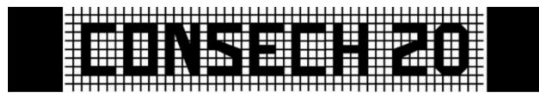
This case study explored a cultural heritage listed reinforced concrete-masonry structure, as an example for carrying out seismic assessment as per EC8:3. Non-linear Time History analysis was used. The results from the assessment procedures show the possibility of brittle shear failure in the 1st floor columns due to their intrinsic characteristics: sparse stirrups, low concrete strength. Additionally, the report shows that extensive repair is required for the overall structure due to carbonation, corrosion and other types of damages that have been effected by environmental conditions and the many years of lack of maintenance and abandonment of the building. Seismic strengthening of historic concrete structures is mandatory in areas prone to earthquakes, such as Cyprus, if the society does not want to let these types of buildings collapse and vanish in a future seismic event.

References

- [1] MINISTRY OF INTERIOR, Geoportal of the Department of Lands and Surveys, Repub. Cyprus. (n.d.). <https://portal.dls.moi.gov.cy/el-gr/FrontEndHelp/Pages/MapView.aspx>.
- [2] S. Michael, A., Constantinou, C., & Feraios, Learning from the Heritage of the Modern., 2009.
- [3] Listing Decree, Department of Town House and Planning, 2011. http://www.cylaw.org/KDP/data/2011_1_53.pdf.
- [4] Anon, Inaction at the Central Municipal Market of Nicosia., Newsp. 'Haravgi.' (n.d.) Page 1.
- [5] CEN. EN1998-3, Eurocode 8 : Design of structures for earthquake resistance — Part 3: Assessment and retrofitting of buildings. European Committee for Standardization, Bruxelles, 3 (2004). http://www.125books.com/inc/pt4321/pt4322/pt4323/pt4324/pt4325/data_all/books/B/BS EN 1998-1 2004 - Eurocode 8 - Design provisions for earth.pdf (accessed September 28, 2015).
- [6] CSI, SAP2000: Static and Dynamic Finite Element Analysis of Structures 14.0, (2009).
- [7] BS EN 12390-3:2009, Testing hardened concrete, Part 3: Compressive strength of test specimens (2009), Br. Stand. Inst. (2009).
- [8] L. Logothetis, Combination of three non-destructive methods for the determination of the strength of concrete, Athens University, 1979.
- [9] M.P.C. Evan C Bentz, RESPONSE2000 Reinforced Concrete Sectional Analysis using the Modified Compression Field Theory, (2000).
- [10] KANEPE, Greek Retrofitting Code, Greek Ministry for Environmental Planning and Public Works, Athens, Greece, 2017.
- [11] NZSEE, The Seismic Assesment of Existing Buildings, 1st ed., Ministry of Business, Innovation and Employment and the Earthquake Commission, New Zealand, 2017.
- [12] E. Standard, EUROPEAN STANDARD Eurocode 1 - Actions on structures Part 4 : Silos and tanks European Committee for Standardization, (2003) 1–110.
- [13] S.J. Pardalopoulos, G.E. Thermou, S.J. Pantazopoulou, Screening criteria to identify brittle R.C. structural failures in earthquakes, Bull. Earthq. Eng. 11 (2013) 607–636. <https://doi.org/10.1007/s10518-012-9390-7>.
- [14] P.E. Draft, NATIONAL ANNEX TO CYS EN 1998-1 : 2005 Eurocode 8 : Design of

structures for earthquake resistance Part1 : General rules , seismic actions and rules for buildings, (2007) 1–12.

Restored Cases



Report on In-Depth Case Study

Case Study: Timmerfabriek (Vlissingen)



Type: **Restored Case**

Partner Institution: TU Delft

Project: **CONSECH 20**

Working Package 2 – Task (iii)

Date: **October 15, 2021**

By:

Gabriel Pardo Redondo
Silvia Naldini
Barbara Lubelli

Introduction

The Timmerfabriek in Vlissingen is a reinforced-concrete building built between 1913 and 1915 (Figure 54). The 3-storey building was part of a larger shipyard; its main function was to manufacture the wood elements of the ships. In the decade of the 1990s, the building was abandoned. In 2010 a restoration campaign was performed to address the severe damage in the façades, consisting of concrete spalling and cracks.

In May 2021, 10 years after the repairs, TU Delft performed an in-depth assessment of the interventions and the overall condition of the concrete structure. At the time of the inspections, the building was under renovation to convert it into a hotel.

The investigation aimed to assess the condition of the repaired zones in 2010 as an indication of the quality of the repair and its durability after a period of 10 years. The investigation started off with an archival research to find out the characteristics of the intervention (materials, procedures, etc.), followed by a visual inspection to localize the areas where to run further testing. Lastly, a non-destructive testing campaign was performed to assess the condition of the repairs. The results of this investigation aims to provide information about what are the key parameters for successful patch repairs.



Figure 54. The Timmerfabriek (1914). Source: <https://architectenweb.nl/nieuws/artikel.aspx?ID=22688>

Characteristics of the Concrete Building and Structure

Materials

The existing reinforced concrete has an estimated compressive strength of 38.5 MPa (+/- 3.77) assessed with Schmidt Hammer (refer to Section 0). The reinforcement is plain round rebar and has a concrete cover in exterior columns between 20 to 25 mm; the cover in walls varies between 20 to less than 10 mm, as the thickness of the walls varies. The coarse aggregates of the concrete are natural and round, with maximum side dimension of 20 mm. The binder used in the concrete is unknown, but given the grey colour and the year of construction, it is very likely that is Portland cement (Figure 55).



Figure 55. Section of the wall cut during the 2021 renovation.

Type of structure

The building structure is a reinforced concrete frame with no interior shear walls. The frame has rectangular and square columns, girders running north-south, and secondary beams running east-west supporting one-way floor slabs (Figure 56). The foundations are likely piles, but this is not confirmed.

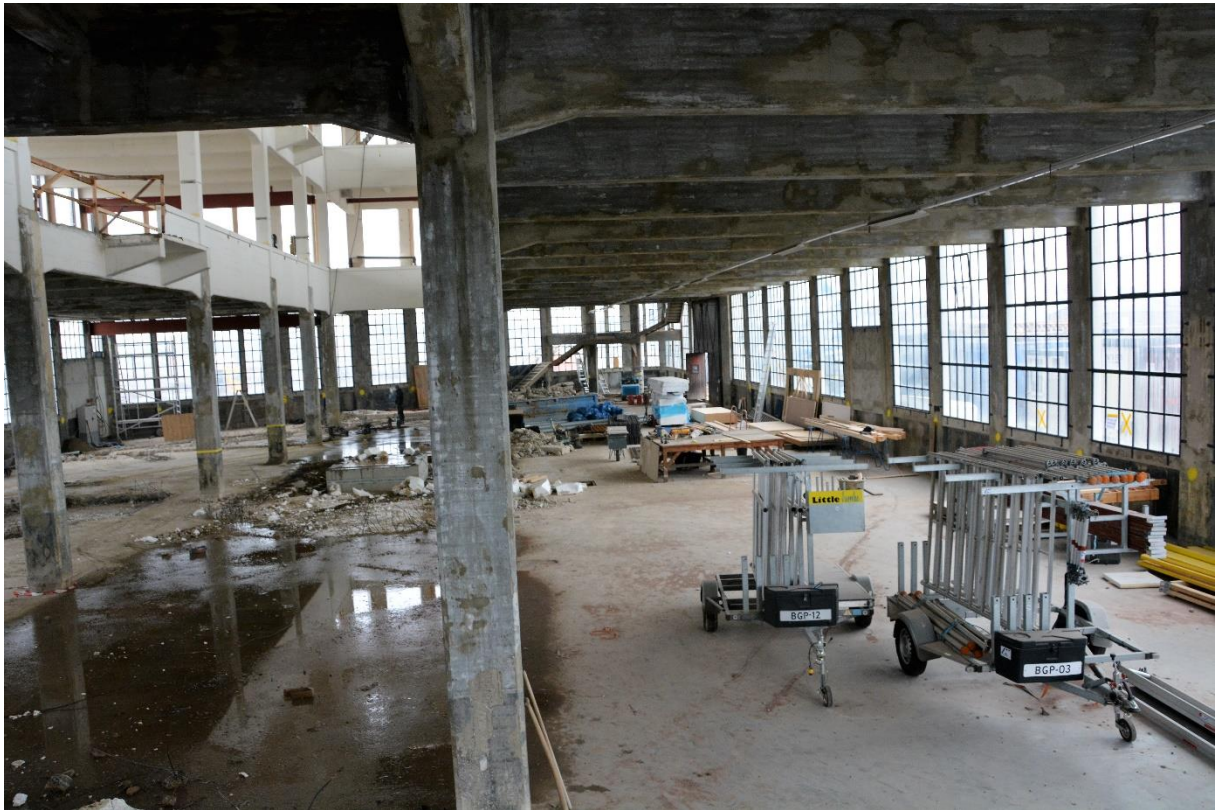


Figure 56. Inside of the building. Ground floor looking north.

Condition of the building

Damage types found in 2010

The damage found in 2010 were vertical individual cracks in walls under windows, and spalling in exterior columns and walls (refer to Figure 57 & Figure 58).

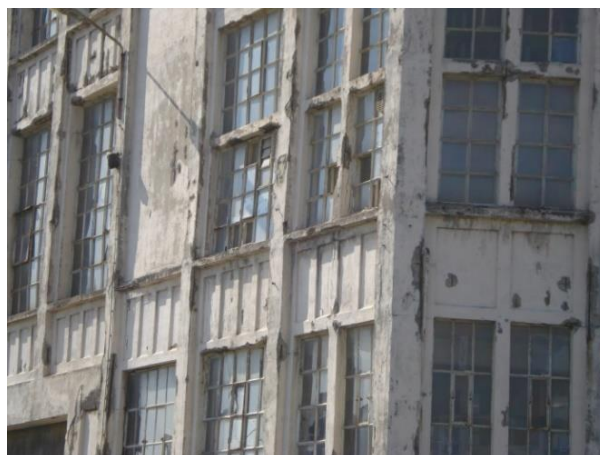


Figure 57. Damage in 2010. Source: TNO.



Figure 58. Condition of the building in 2010. Source: TNO.

Hypothesis on damage processes

Given the type of damage, and the testing performed in the building (refer to Sections 0 & 0), the likely cause of the damage is carbonation-induced corrosion. The visible cracks are aligned with the reinforcement, suggesting expansion forces due to corrosion. Spalling was localized in areas of reinforcement where the concrete cover is minimum. From the pictures obtained, pitting corrosion is not visible; neither is it mentioned in the documentation related to the intervention.

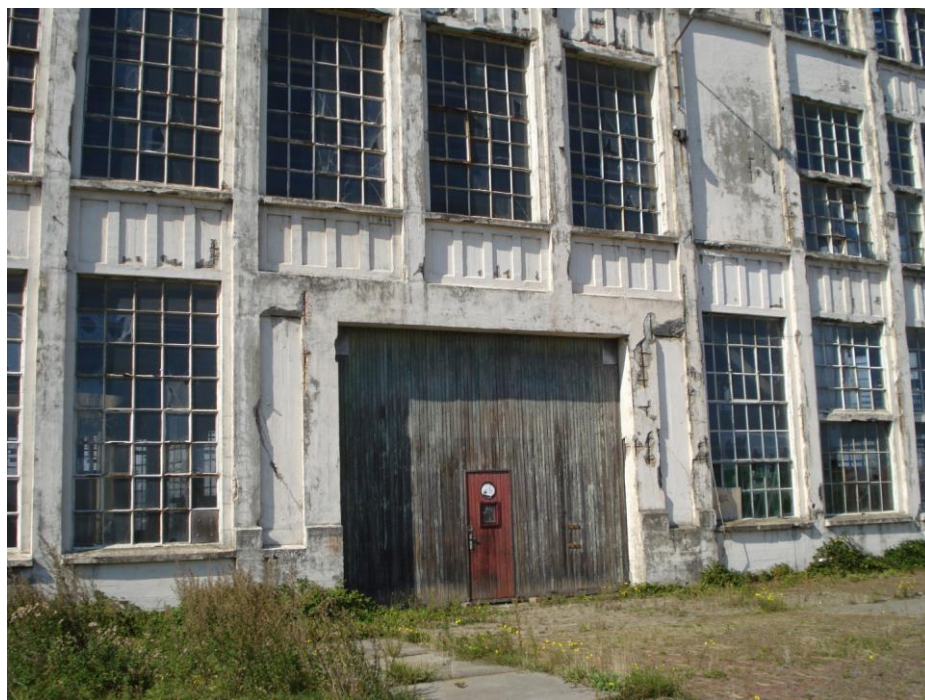


Figure 59. Condition of the building in 2010. Source: TNO.

Intervention in 2010

The architects Rothuizen, specialized in the restoration of young and historic monuments, carried the intervention project of 2010. For the assessment of the concrete

and the advice on the repairs. The specialized company SGS-Intron was hired to complete the damage assessment of the exterior facades. In elevation drawings and pictures, the damage types were annotated (Figure 60).

The architects also provided a catalogue with the different types of repairs depending on type and characteristics of the damage (Figure 61). With this catalogue, the subcontractor performing the repairs could apply the specific repair detail according to the damage.

According to the architect's specifications, the subcontractor in charge for the concrete repairs needed to have the accreditation BRL 3201. This accreditation ensures that the company has experience in concrete repairs and is aware of the different materials and procedures. This accreditation, however, it is not specifically suited for historic concrete.

The patch repairs were done according to the Dutch guidelines CUR Recommendations 53 "Sprayed Concrete" and CUR 54 "Concrete repair with polymer-modified repair mortars". It also followed the European norms EN-1504 that specify materials, surface preparation and installation of repair mortars. However, in the documentation, it was not found what specific part of this EN norm was used. The mortar repairs were selected to have higher compressive strength but similar stiffness to the existing concrete.

The overall process of the patch repairs was: (1) removal of loose concrete and carbonated concrete around the reinforcement, (2) surface preparation, (3) application of bonding agent, (4) repair mortar application, (5) pull-out testing, (6) water repellent, and (7) final coating.

The repair mortars used for patch repairs were polymer-based mortars from Silka, precisely Sika MonoTop 620 for thin layers, and MonoTop 613 for thicker layers. Prior to the application of the repair mortar, a bonding agent was applied on the surfaces of the existing concrete and exposed rebar, Sika MonoTop 610. Once the patch repairs were done, and the previous paint removed, a coating was applied on all the exposed concrete in the facades. The moisture of the concrete was measured for a proper application. According to the contractor's budget, a water repellent was applied before the finish coating. However, the only information found was the brand of the product, Funcosil. Regarding the finishing coating, the water-based polymer paint Alpha Topcoat Flex, from the brand Sikkens was used. This coating is especially suited for surfaces where a high flexibility is desired. It has a lifespan of 10 years according to the manufacturer. After the patch repairs, at least six pullout tests were performed to verify proper bonding.

Current condition (2021)

The concrete façade did not show signs of generalized damage (Figure 63). Scattered damage was found in a few locations. The damage consisted in small spalling and was located in the areas of the wall below the windows (Figure 64). The damage did not seem to correspond with previous patch repairs.



Figure 63. East facade condition in 2021.



Figure 64. Spalling and incipient spalling recorded in the thinner parts of the wall in 2021.

Aim of the investigation

Patch repair is the most common concrete repair in concrete but still its success and durability is a bone difficult to chew. According to the results of the project

CONREPNET [1], patch repairs have a limited life span. After surveying 247 repaired constructions the results were that 60% of the patch repairs failed in less than 10 years, and 90% within 25 years [1]. In the case of patch repairs in historic concrete, this rate might be even higher. The components of the concoction in early concrete buildings were often not standardized or even known. For instance, different compositions were used until the beginning of the 20th century, and their formulation and design were kept secret. That can lead to incompatibilities between the mortar repair and the parent concrete.

The aim of the investigation is to examine patch repairs in historic concrete that are performing well after 10 years. The investigation has two specific goals: (1) identify parameters that can contribute to increase the durability of patch repairs. (2) Evaluate NDT techniques to assess the performance of patch repairs. The investigation is performed in only one building, thus the results are exploratory.

The research questions are: **What are the key parameters for patch repairs in historic concrete to perform properly after 10 years? How can patch repairs be assessed using NDT?**

Methods

The methodology of the investigation was:

1. Assess the overall condition of the building.
2. Archival research.
3. Assess the patch repairs from 2010.
4. Evaluate different NDTs to assess the condition of patch repairs.

The tests were divided in two groups. One to determine the basic characteristics of the concrete, and the other to assess the patch repairs.

- Tests to assess the existing concrete
 - **Concrete cover** with Proceq Profoscope (three exterior columns).
 - **Carbonation depth**. Phenolphthalein sprayed over concrete powder from drills at 10 mm steps (three exterior columns).
 - **Compressive strength** with Schmidt Hammer (four exterior columns).
- Tests to assess the patch repairs:
 - **Hammer sounding** with rubber hammer to assess delamination or failure of patch repairs (19 patch repairs in exterior columns).

- **Thermal camera** to identify repairs and possible delamination or failure (11 patch repairs in exterior columns).
- **Ultra-pulse sound velocity (UPV)** (Pundit Lab+ of Proceq) for strength and delamination, applied on one side of 12 exterior columns (indirect reading).

The first step of the investigation was to obtain information of the building and the intervention done in 2010. The restoration company Bouwgroep Peters B.V provided a information about the products used for the repairs, the procedure and the location of the repairs.

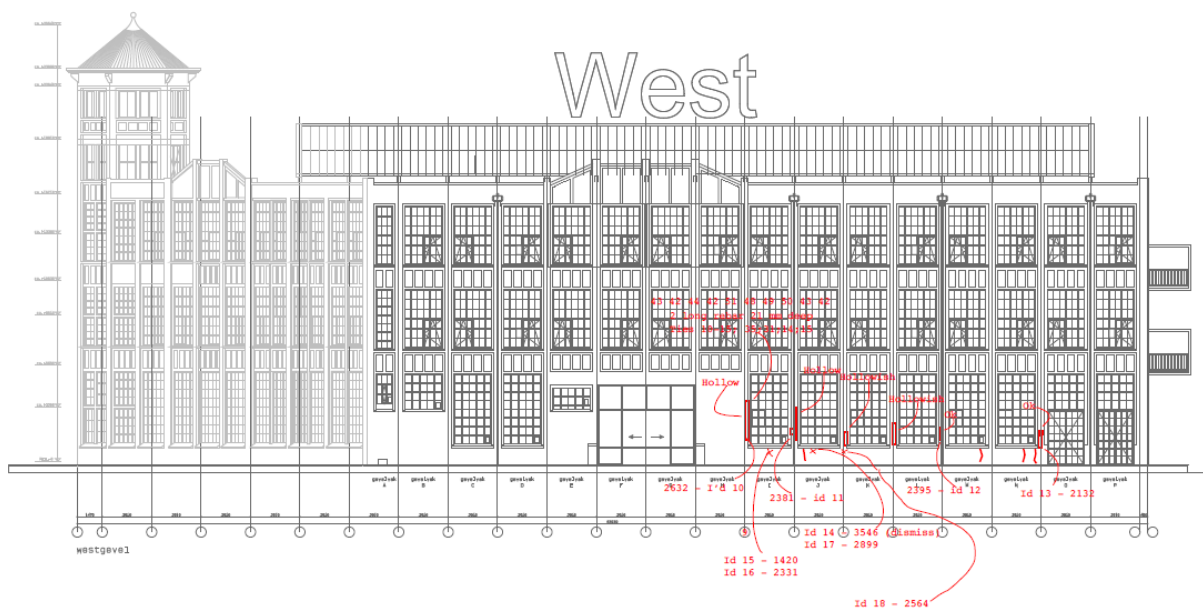


Figure 65. Annotations of the inspection and tests in the west facade.

Once the patch repairs were located, they were tested with the three techniques: first, with the rubber hammer to assess if debonding was noticed by a hollow sound (Figure 66_left); secondly with the thermal camera to corroborate if the unbound and bound conditions were noticeable (Figure 66_right); thirdly with UPV.

Results

The results of the testing are summarized in Table 8.

| Test | N | Results (Avg.) | Units | Comments |
|---------------------------------------|----|-------------------------|-------------------|--|
| Compressive strength | 4 | 38,25 ($\pm 3,77$) | N/mm ² | |
| Carbonation depth in columns | 2 | < 20 ($\pm 0,00$) | mm | |
| Carbonation depth in patch repairs | 1 | < 10 ($\pm 0,00$) | mm | |
| Concrete cover | 3 | 21,67 ($\pm 2,88$) | mm | |
| Hammer sounding (Hollow sound) | 19 | 42,11% - | - | Percentage of patches sounding hollow. |
| Thermal camera (Hollow-sound patches) | 6 | 50,00% - | - | Percentage of patches showing thermal differences with concrete. |
| Thermal camera (Solid-sound patches) | 5 | 20,00% - | - | Percentage of patches showing thermal differences with concrete. |
| UPV (Hollow-sound patches) | 5 | 2.357,6 ($\pm 248,3$) | m/s | Indirect reading. |
| UPV (Solid-sound patches) | 4 | 2.370,0 ($\pm 215,6$) | m/s | Indirect reading. |

Table 8. Results of the testing performed in the building.

The original concrete has a fair strength given its age (38.5 MPa), the carbonation depth is less than 20 mm, and the concrete cover is slightly over 20 mm over columns – although it can reach less than 10 mm in some sections of the walls.

The results of the tests on the patch repairs show a minimum carbonation depth, less than 10 mm; and no clear visual signs of patch failure, only 2 patches out of 19 had minor crazing. The results of the hammer sounding reveals that almost half of the patches sounded hollow (41%), suggesting the patch have some debonding. However, in general in other sound areas of the walls with no previous repairs did not sound solid. The thermal camera shows that the unbounded patches are more likely to be visible than the bounded patches, 50% of the hollow-sound patch repairs were visible using infrared camera (Figure 67), whereas only 20% of the solid-sound patches were visible. The results of the ultrasonic pulse velocity on surface show a similar wave velocity between hollow- and solid-sound patch repairs.

Discussion

Regarding the existing concrete

The compressive strength is relatively high for the age; the minimum required strength at the time was 8 MPa [2]. The **carbonation front** in the original concrete is not too deep for a building this age, 20 mm in 106 years; meaning a good compaction and lower permeability if compared to buildings of similar age and exposure [3,4].

The extensive damage visible in 2010 was likely due to carbonated induced (C-I) corrosion. The damage was present in the exposed sides of walls and columns. The cover of the columns is slightly larger than the carbonation front, therefore the reinforcement should have been protected by non-carbonated concrete. Still, scattered spalling in columns was visible. The spalling in columns may be due to a reduction of the cover during the construction process. If not properly tied and secured, the reinforcement may move while pouring the concrete. This can create localized areas with reduced concrete cover and thus C-I corrosion can appear earlier in localized spots. Regarding the spalling and cracks in the walls (Figure 68), the thinnest section of the walls have a minimum

concrete cover, less than 10 mm (Figure 68). Thus, the carbonation front reached earlier the reinforcement than in other areas with thicker covers.

Regarding the assessment of the patch repairs

Approximately half of the patches sounded hollow according to the rebound hammer. However, this is not supported by the other testing methods (visual inspection, thermal camera and UPV). In addition, other types of damage linked to debonding, e.g. cracking or delamination, were not visible. The sound hollow can have different causes, the most plausible one being related to the compactness of historic concrete. A lower density of concrete can lead to a non-solid sound regardless repaired or non-repaired concrete.

The carbonation front in the patch mortar is very low (<10mm), as expected due to the young age, so the reinforcement is still protected by the passivity layer provided by the repair mortar. Consequently, there was no signs of active corrosion in the repaired areas. The acrylic polymer based coating applied in 2010 would have contributed to block the CO₂ and water ingress into the concrete [5]. According to the research of Diamanti et al. [6], acrylic based coatings reduce chloride diffusion coefficient better than epoxy coating and chlorinated rubber. In addition, the addition of a water repellent, as it is in this case, considerably reduced carbonation and water content in exposed concrete [7]. In the building under investigation, the damage due to active corrosion was residual, suggesting the surface treatment has hindered the corrosion progress.

Regarding the evaluation of the NDT

The hammer sounding test did not give a good estimation of debonding. This technique has proven useful for other concrete structures [8] but it does not seem effective in historic concrete. All the columns tested sounded hollow regardless repaired or non-repaired concrete. The hollow sound is likely to be related to the low density of historic concrete compared to modern concrete. Historic concrete tend to have higher w/c ratios than allowed in current standards. When hammered it can create a sound that does not sound solid. Therefore, caution must be taken when used in historic concrete. In addition, this technique is also time consuming -not recommended in large areas- and the results cannot be precisely recorded.

The thermal camera showed modest results, detecting delamination in 50% of the presumably debonded patch repairs. The main shortcoming is that the inspectors need to have an idea where the patch repairs are located; otherwise, they are difficult to detect.. Pre-heating the surfaces would increase the thermal differences, which will improve the interpretation of the results.

Ultrasonic pulse velocity (UPV) showed non-reliable results. UPV has consistently been used to estimate compressive strength and detect voids and cracks in concrete [9]. However, when estimating the bonding of the repairs it has shown that there is not a substantial difference between the results of bound and presumably unbound repairs. Testing on one side only is not as accurate as testing in opposite sides, but the results

were expected to have given clearer results. The device has potential to detect it but investigation that is more experimental need to be conducted first.

Conclusions

The patch repairs performed in 2010 were done according to Dutch and European standards. The repairs were assessed, designed and executed by experienced professionals. After 10 years, the state of the concrete in the façade is in good condition; there is not visible signs of active damage in the patch repairs. The testing performed does not suggest failures in the patch repairs neither. There is no signs of active corrosion in the repaired areas, neither in the non-repaired areas. Suggesting that the surface treatment applied in 2010 has diminished the corrosion rate by blocking carbonation and water ingress into the concrete.

Hammer sounding has proved to be a non-reliable technique in this case due to the generalized hollow sound when tested throughout the structure. The hollow sound is thought to be related characteristics of historic concrete, which is typically less dense than modern concrete. The hammer sounding should be accompanied by other testing methods. Thermal camera assessment seems to have the potential to detect early states of debonding if the repair is previously located and the area is previously heated, but further research is needed to confirm this hypothesis. The ultrasonic pulse velocity (UPV) applied on one surface did not provide data to determine failure in existing patch repairs. Given the limited number of tests, further research is needed to clarify the true potential of UPV in detecting patch failure.

Bibliography

- [1] S. Matthews, CONREPNET: Performance-based approach to the remediation of reinforced concrete structures: Achieving durable repaired concrete structures, *J. Build. Apprais.* 3 (2007) 6–20. <https://doi.org/10.1057/palgrave.jba.2950063>.
- [2] Koninklijk Instituut van Ingenieurs, *Gewapend Beton Voorschriften 1912*, 1912.
- [3] W.C. Choi, M. Picornell, S. Hamoush, Performance of 90-year-old concrete in a historical structure, *Constr. Build. Mater.* 105 (2016). <https://doi.org/10.1016/j.conbuildmat.2015.12.158>.
- [4] I. Monteiro, F.A. Branco, J. De Brito, R. Neves, Statistical analysis of the

- carbonation coefficient in open air concrete structures, *Constr. Build. Mater.* 29 (2012) 263–269. <https://doi.org/10.1016/j.conbuildmat.2011.10.028>.
- [5] R. Amirtharajan, D. Jeyakumar, Repair, rehabilitation & retrofitting of RCC for sustainable development with case studies, *Int. J. Civ. Eng. Technol.* 9 (2018) 1593–1599. <https://doi.org/10.5121/civej.2016.3203>.
 - [6] M. V. Diamanti, A. Brenna, F. Bolzoni, M. Berra, T. Pastore, M. Ormellese, Effect of polymer modified cementitious coatings on water and chloride permeability in concrete, *Constr. Build. Mater.* 49 (2013) 720–728. <https://doi.org/10.1016/j.conbuildmat.2013.08.050>.
 - [7] P. Zhang, P. Li, H. Fan, H. Shang, S. Guo, T. Zhao, Carbonation of Water Repellent-Treated Concrete, *Adv. Mater. Sci. Eng.* 2017 (2017). <https://doi.org/10.1155/2017/1343947>.
 - [8] H.J. Parsaie, *Training and Reference Manual for Special Inspectors*, iUniverse, 2001.
 - [9] D. Breyse, J.P. Balayssac, S. Biondi, D. Corbett, A. Goncalves, M. Grantham, V.A.M. Luprano, A. Masi, A.V. Monteiro, Z.M. Sbartai, Recommendation of RILEM TC249-ISC on non destructive in situ strength assessment of concrete, *Mater. Struct. Constr.* 52 (2019). <https://doi.org/10.1617/s11527-019-1369-2>.

Photos by TU Delft - CONSECH20 project (if no other source indicated)

Report on In-Depth Case Study

Museum of the Treasury of San Lorenzo, Genoa



Type: Restored

Partner Institution: Unige

Project: CONSECH 20

Working Package 2 – Task (iii)

Date: 27/09/2021

By:

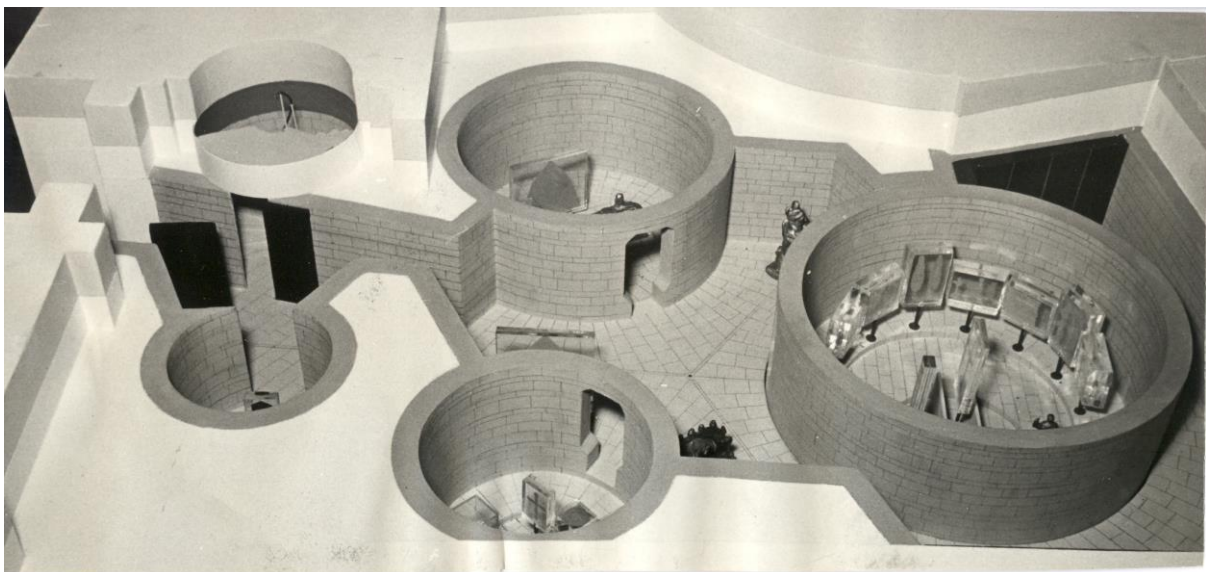
Author 1 Giovanna Franco

Author 2 Stefan F. Musso

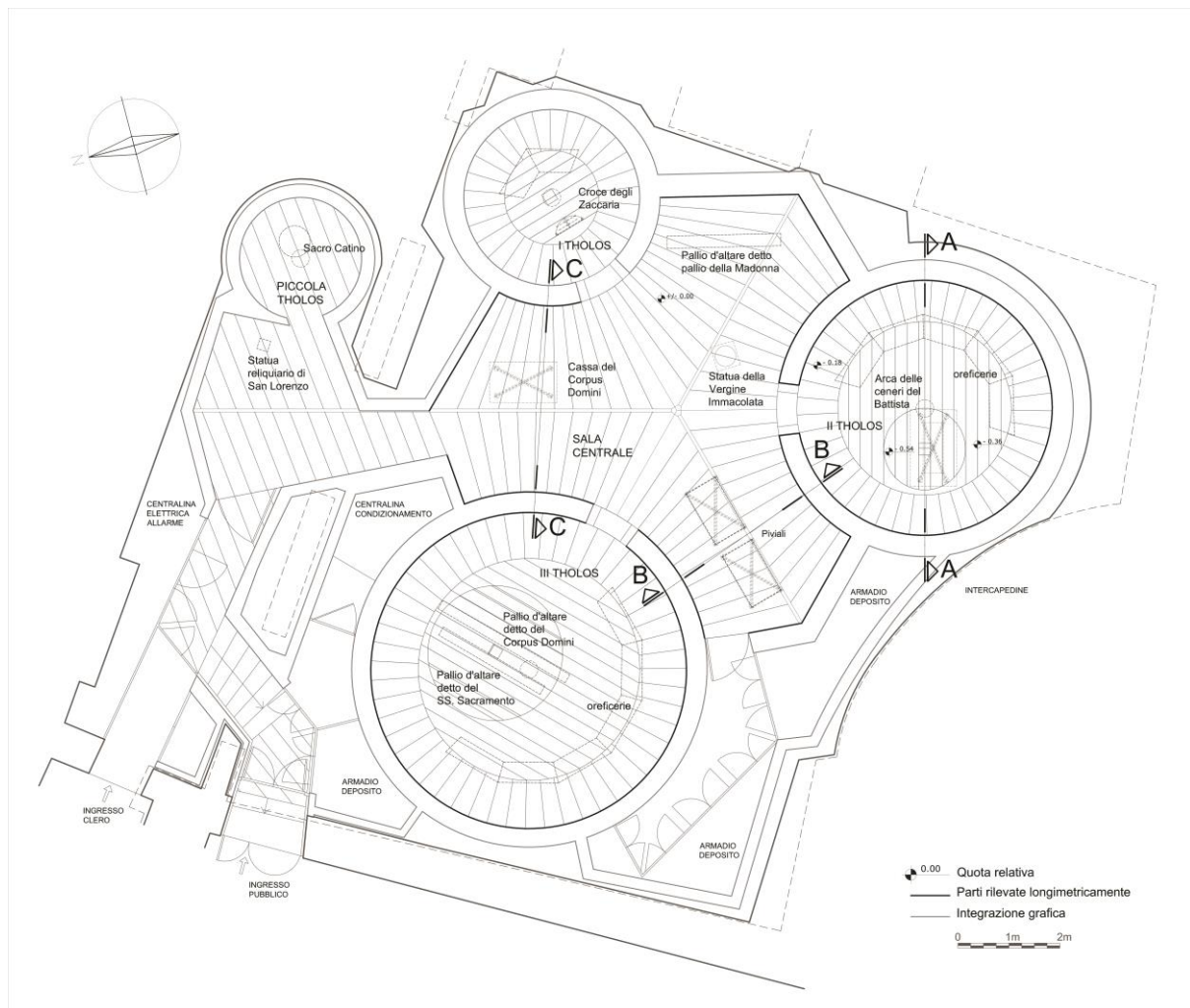
Introduction

The Museum of the Treasury of the Cathedral of San Lorenzo in Genoa was designed and built by Franco Albini in the years 1952-56. The very site upon which the structure ‘stands’

is itself unique: the museum is actually hidden from view because it is underground, a sort of hypogeum with no exterior as such, it is enclosed between the foundations of the Renaissance apse which Galezzo Alessi had built for the renovated high altar of the medieval cathedral and the foundations of the Archiepiscopal Palace. The Treasury is also unique because of the precious artefacts it contains; forming a collection that has been put together over centuries, the items here are in part the property of the Metropolitan Chapter of Genoa and in part the property of the city itself. This feature of the collection would itself have important consequences in determining the choices made by Franco Albini (choices in part inspired by Caterina Marcenaro, the then Director of Genoa City Museums who was the commissioning client, faithful custodian and irrepressible champion of the work); and those decisions still affect the management of museum. The conceptual idea was born and evolved from the idea of intersecting pure geometric forms: a regular hexagon and three circles of different radii (1.75 metres, 2.50 metres and 3.10 metres), the fampus 'Tholos' recalling the treasure of Atreus in Mycenae, whose centres coincide with the vertices of non-adjacent segments of the hexagon itself. To these are added an irregular space, connecting with the access staircase, as well as a further smaller circle (with a radius of 1.20 metres). In these spaces the treatment of the floor, the corrugated roof and the concavity and convexity of the perimeter walls contribute to reinforcing the idea of "interlocking organisms", where the objects on display find a natural setting. where the objects on display find a natural position, carefully studied on the basis of the generating axes of the basic geometries used. The Treasury Museum itself would from the start be considered a veritable 'work of art' (a genuine creation by a specific artist, it was assumed, therefore, that it had been conserved in its original state). Astonished scholars and architects had immediately expressed admiration for the expressive power and novelty of the project when seen within the rich context of Italian museum design at the time, which often involved work within the stratified framework of already-existing architectural structures. One feature that had been of fundamental importance for Franco Albini and Caterina Marcenaro was light: evocative and mysterious, it is throughout the design used in a refined manner to create the interplay of bright illumination, deep shadows and surprising reflections. The Museum is listed by Italian Ministry of Culture.



Maquette of the Museum, Franco Albini. Courtesy Piero Boccardo, Direzione Musei di Strada Nuova



Plan of the Museum, survey by Architecture and Design Department (S.F. Musso, G. Franco)

Characteristics of the Concrete Building and Structure

Materials

As the Museum is located underground in the courtyard, the maximum depth of the excavation, from the highest point of the floor, is 5.50 m; the existing foundations had to be consolidated. Along the excavation the retaining structure was grafted onto a continuous foundation, consisting of a concrete retaining wall cast directly in contact with the terrain. For straight sections longer than 2 metres, a rib was cast in the terrain; for the curved sections, it was not necessary to stiffen the wall because the very curvature of the wall increased its resistance. For the lower half of the wall the thickness is 30 cm and is reduced to 15 cm in the upper half. For the entire area within the perimeter of the foundations a lean concrete slab was cast to form the crawl space.

In order to protect the interior from possible water infiltration, a waterproofing layer was laid vertically along the whole of the counter wall and horizontally along the whole of the under-floor cavity slab. On the inside of the counter-reinforcement wall, always resting on

the continuous foundations, a 15 cm thick brick wall was built, all visible parts of which were covered with chiselled promontory stone (4/6 cm thick) up to a height of 2.30 m.

The prevalent materials used in the Treasury Museum are therefore:

Foundation: reinforced concrete

Structural walls: solid bricks

Roof structure: reinforced concrete

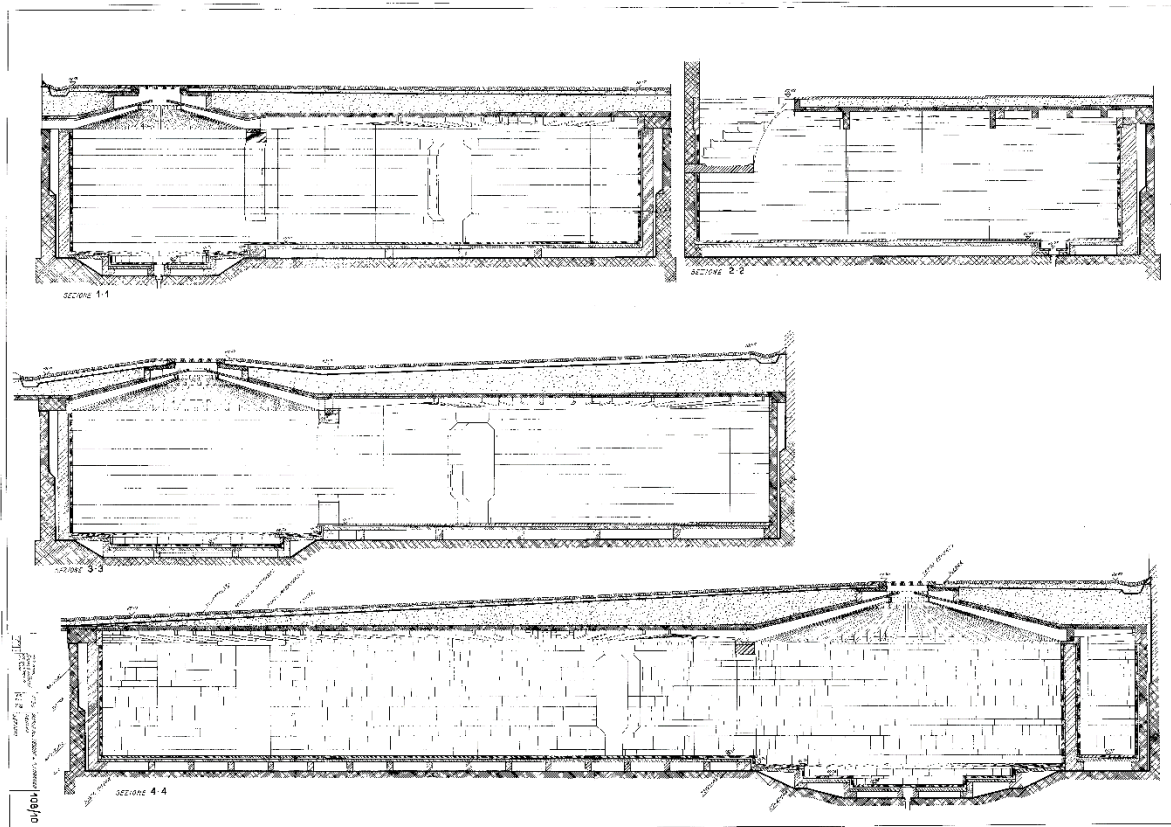
Internal finishing (pavement and walls) slabs of *Promontorio* stones

External roof covering: mosaic in black and white stones (*Risseau*), insertion of three cement discs with block glass (at the top of the three 'false domes').

As far as concerns the reinforced concrete works, archive research has shown that:

- The bottom of the crawl space was made of: concrete kg 150 hydraulic lime/cubic metre - cubic metre 0.800 gravel and cubic metre 0.400 sand
- The foundations and the counterfloor wall were made of reinforced concrete kg 300 cement 500/mc - mc 0,800 washed live gravel and mc 0,400 live sand
- On the perimeter of the building and on the circular rooms, a reinforced concrete wall was built (300 kg cement 500/mc - 0.800 m³ gravel and 0.400 m³ sand).
- The false dome roof structure is made of T-joists cast on site with planed formworks, surface of the casting in view reinforced concrete kg 300 cement 500/mc - mc 0,800 gravel and mc 0,400 sand. - m³ 0.800 gravel and m³ 0.400 sand
- A reinforced concrete distribution slab with wire mesh weighing 1.5 kg/sq.m. was cast over the joists.
- The distribution slab was filled with pumice concrete above the distribution slab to form the courtyard slopes
- The courtyard floor is made of cobblestones on a sand foundation and a band of stone curbs

Three concrete discs and glass diffusers close the false cupolas at the top and provide interior lighting. These are made of glass-cement panels: diffusers diameter 14.5, h. 8.4, Iperfan type, Fidenza Vetraria, later better described.



Design sections, Franco Albini. Courtesy Piero Boccardo, Direzione Musei di Strada Nuova

Type of structure

The architectural and structural solutions adopted for the underground space of the Museum are clearly explained in the project reports (1953), and described in greater detail in the final assessments.

Over the concrete foundation were posed a series of brick walls of the honeycomb foundation beneath the flooring are of different heights, and – as photographs of the original work show – perforated at their base to allow for drainage. These walls are protected by lead sheeting bent vertically at its edges and support prefabricated slabs of concrete, upon which is laid the flooring in *pietra di Promontorio* (a grey local marly limestone).

The elevation structures of the museum, the curved walls that constitute the cylinders of the 'tholos', were designed and built with solid bricks, separated from the perimetral wall by a cavity of varying thickness (from 5 to 20 cm) and equipped with arches in correspondence to the openings for access to the tholos themselves. Great importance was immediately given to the stone covering the horizontal and vertical internal surfaces, made from blocks of dark grey *Promontorio* stone worked on the external face with a chisel and squared to obtain perfectly matching sides. To this aim, Albini scrupulously designed, on several occasions, the dimensions of the individual pieces needed for their facing, which were made up of alternating repeated modules of varying thickness. The stones were then laid with filling mortar and "cadmium iron" clamps.

Works were done in the following phases.

Once the excavation and substructure had been completed (the subject of the first lot of work), a slab of lean concrete was poured and a series of 12 cm thick brick walls were built on top, "arranged concentrically or parallel to each other according to the needs of the floor plan". The initial idea, which was only partially modified on site as far as the height of the walls was concerned, was to create a 20 cm high crawl space to separate the floor structure from the ground below. More information can be found in the final report of 1956. "A layer of gravel and concrete was placed at the bottom of the excavation, with a slope for the outflow of the remaining water infiltration towards the drainage sumps. This concrete shell, which with the floor and walls of the Museum forms a continuous, aerated cavity, was also waterproofed with asphalt. From the photographs of the early stages of construction, the contours of the cavity and the brick and concrete slab crawl spaces for the stone floor are clearly visible. Each foundation element of the floor and wall structures was also insulated with lead sheets. As in the case of the roofing structures, the presence of lead as a waterproofing material seems to be the result of a choice made during the works, because in the report of the second lot there is no trace of this item, neither as a supply of material nor as labour necessary for its installation. In addition, compared to the project drawings, the level on which the under-floor cavity is set is all at the same depth, and its thickness seems to increase in the highest parts of the floor (the central hexagonal area and the outer rings of the tholos) rather than being variable, following a stepped profile, as indicated in the project sections.

Lastly, as opposed to the initial plan to use brick slabs to support the walls, preformed concrete slabs were used to build the floor, as can be deduced both from the site photos and from reading the accounting documents. On this surface, after the casting of a special slab, the floor was then laid in slabs of promontory stone, 6c thick and, therefore, thicker than in the project.



Building site, foundations and drainage system. Courtesy Piero Boccardo, Direzione Musei di Strada Nuova

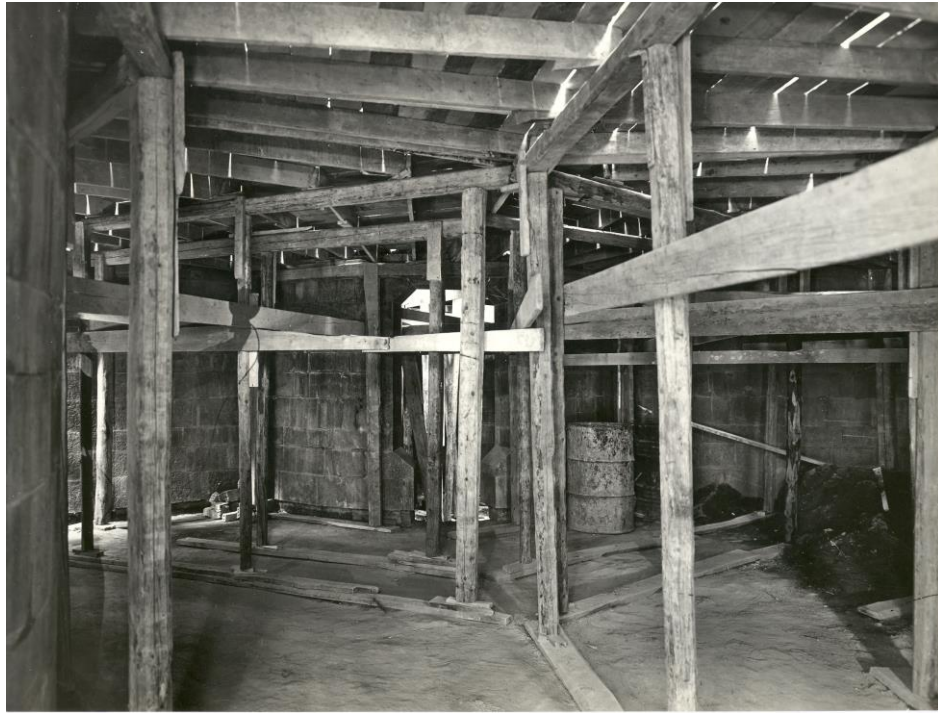


Building site, elevation of brick circular walls and stone cladding. Courtesy Piero Boccardo, Direzione Musei di Strada Nuova

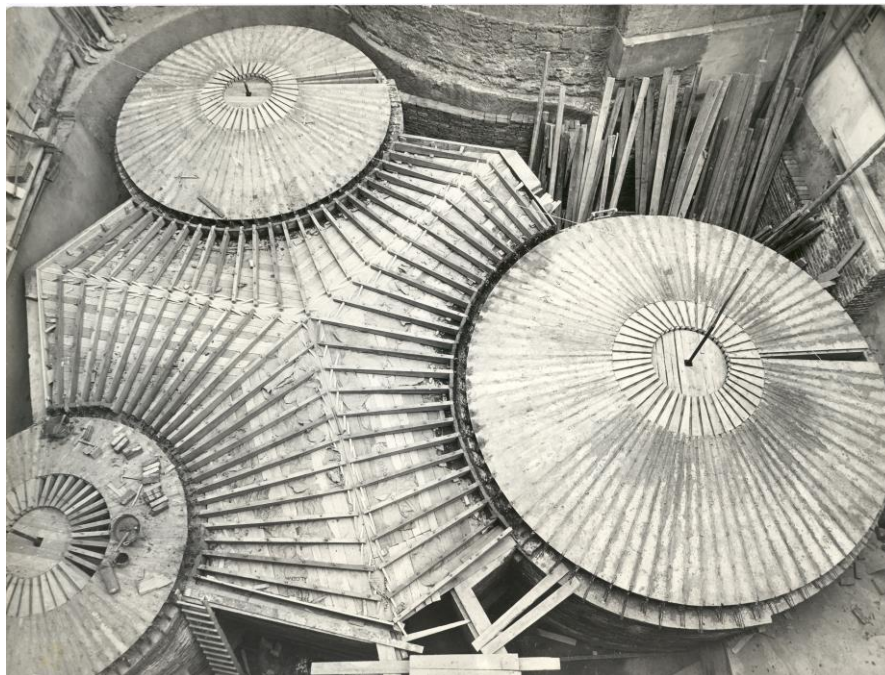
One of the most evocative elements of the Museum is certainly the roof, made up - in the various tholos - of concave ceilings (in the form of a false dome) that are very low and - in the central hexagon - of a flat ceiling corrugated by a dense series of T-joists in reinforced concrete of variable section, arranged in such a way as to emphasise the generating geometries of the design. The T-joists are cast in place and then arranged radially around the centres of the three cylindrical rooms. A distribution slab, reinforced with wire mesh, is cast on the joists. The body of the rafters has a constant thickness of 6 cm and a variable height from 8 to 25 cm according to a constant inclination; the wing of the rafters has a constant thickness of 4 cm and a variable width from 8 to 40 cm. The joists must not be plastered and therefore planed formwork must be used. These rafters are corbelled, resting on the internal walls or embedded in the external walls, and connected by a reinforced concrete *correa*. A distribution slab, reinforced with wire mesh, is cast on the joists. For the interior walls, in the area where the joists are laid, there is a covering of hand-blasted bricks, laid flat. For the external walls, the rafters are 65 cm wide, so as to tie the internal wall to the retaining wall, fixing the waterproof covering and closing the air space.

The rafters that form the ribs of the roof behave statically as double brackets set radially on the cylindrical walls of the Tholos; the variable length was obtained by inserting mobile diaphragms in the wooden formworks smoothed in plaster for the off-site construction. The same expedient was adopted for the construction of the circular sector slabs that are superimposed on the joists, in order to adapt them to the different radii of the three Tholos. For the central compartment, on the other hand, the completion of the intrados of the roof

was obtained by means of a sand and plaster formwork, compacting it between the joists and the lower wooden scaffolding, spreading it with plaster and then casting the distribution slab directly; once it had set, the sand and plaster formwork was dismantled and it came apart by itself. On top of the roof, the cross-weave load distribution reinforcement was prepared, forming a homogeneous cast with the annular beams running above the three cylinders and forming the three central rings of the skylights".



Building site, scaffolding for the roof structure and reinforced concrete rafters Courtesy Piero Boccardo, Direzione Musei di Strada Nuova





Building site, the steel net before the concrete mould and a view from above, the pavement of the courtyard over the false domes. Courtesy Piero Boccardo, Direzione Musei di Strada Nuova

Once the beams and preformed slabs of reinforced concrete had been laid, the so-called "distribution slab" was laid and properly anchored to the irons protruding from the beams and slabs (as visible in the site photos). The slab was made of cement concrete, reinforced with a metal mesh and resting on the perimeter wall and on the cylindrical walls of the tholos, and ended, at the centre of each cylinder, with reinforced concrete rings to house the planned skylights at the top. This last structural and construction layer was then covered with lead sheets welded and turned up on the sides (of which, however, no trace can be found in the project reports, nor in the final summary calculation, nor in the works report for the second lot), with an overlying protective caulking, (of which, however, there is no trace in the project reports, nor in the final summary calculation, nor in the expert's report on the second lot), with an overlying protective caulking, designed to prevent lead

perforations, made with cement mortar (and not hydraulic lime, as foreseen by Albini), and the further laying of a final layer of asphalt to connect the plaster to the lapels, in correspondence with the perimeter walls. Finally, a sloping layer was made, lightened with pumice stone, which also functioned as thermal and acoustic insulation, and on this last layer were then laid both the black and white cobblestones of the Archbishop's Palace courtyard, following the sunburst design of the underlying structure, and the glass cement "disks" of the skylights of the internal tholos. Lastly, the ventilation shafts and four grid openings, cut into the outer perimeter walls and raised above the ground level to provide fresh air to the underground rooms, were housed in the thickness of the roofing layer.



View from inside, 1957 (Photo Silverstone). Courtesy Piero Boccardo, Direzione Musei di Strada Nuova

Briefly, the work that was carried out for the roof structure and covering involved:

- the installation of prefabricated reinforced concrete beams of rectangular section (constant in width but increasing in height) which were to either irradiate from the centre of the cupola over the three main 'tholos' or, in the part located beneath the portico of the Archiepiscopal Palace, run parallel;
- the installation of prefabricated reinforced concrete slabs, above the beams;
- the construction of a ceiling in reinforced cement, resting on the surrounding walls or the walls of the individual 'tholos';
- the creation of ring-shaped string-courses at the centre of each cupola, and the insertion therein of discs of block glass;
- the installation on the ceiling of welded lead sheeting upturned at the edges and the laying of mortar under the paving to protect it, with a layer of asphalt to bond the plastering with the upturned edges of the lead sheeting around the walls;

- the installation of a layer of pumice stone of variable thickness, with street surfacing for vehicles then laid over it;
- the installation within the roofing of channels for ventilation and four grilled openings in the outside walls, raised above the traffic level;
- laying of a pavement in black and white cobbles in the courtyard above the museum, corresponding with the ceilings of the 'tholos' beneath.

Other relevant characteristics

Particularly innovative was the lighting system designed by Franco Albini with the help of Franca Helg, characterised by criteria of flexibility, maintainability and modifiability that are still valid today. The larger objects displayed in the open space were lit by a series of spotlights powered by electric cables running in a circular cavity at the base of the display cases (protected by a flat iron) and at the top of the internal walls, in special recesses cut out at the top of the cladding slabs, hidden by a bakelite plate.



View of the lighting system (photo G. Franco)

Condition of the building

The Museum of the Treasury, with its "robust" character, as defined several times in the official documents accompanying its construction, has survived almost intact for more than fifty years thanks to the properties of its constituent materials, which are durable and solid, and to its underground location, protected - except for the skylights at the top of the internal ceilings - from the aggression of external agents. Despite this, the building has been affected, like any other architecture, by changes in conditions of use, the obsolescence of the technological systems, and wear and tear (at the most fragile points), requiring maintenance, improvement and enhancement since its inauguration.

Immediately after the inauguration, and in the years that followed, a number of problems arose regarding the safety of visitors, who risked falling on the steps inside the too narrow space of the tholos containing the Ark of the Ashes of Saint John the Baptist, as Monsignor Storace, Provost of the Metropolitan Chapter of San Lorenzo, wrote to the Director Caterina Marcenaro and as she pointed out to Albini, requesting the insertion of platforms to connect the different levels. The lighting system was also considered not entirely safe, especially at the entrance staircase, which was poorly lit except by a single wall spotlight that projected a light beam of modest amplitude. More or less accidental damage, if not outright theft, has repeatedly occurred to some of the exhibits, which are unprotected, in particular the Ark of the Baptist, which was recently protected by a glass case, and the processional case of Corpus Christi, for which Monsignor Storace had already proposed the installation of a special protective glass in October 1956.

The sacred vestments, which were placed on supports of an unsuitable size and shape for the proper conservation of the fabrics, also required careful restoration and a rethink in terms of display methods. The suggestive lighting system for the objects on display, which was modified several times with the replacement of light fittings, did not fully enhance the preciousness of some of the jewellery, which was also dulled by the patina of time. In addition to this, there were renewed needs for study and conservation, which led the Director of the Strada Nuova Museums, on which the Treasury also depends, to think about a new exhibition arrangement. Not to mention the infiltrations that penetrated into the museum from the skylights at the top of the domes of the circular rooms and that required urgent and more substantial interventions than mere routine maintenance.

Although minimal in nature, the new requirements, which were the expression of a cultural context different from the one in which the Museum had its genesis, motivated above all by the better conservation and enhancement of the works on display, inevitably clashed with the need for "absolute" conservation and rigorous protection that the extraordinary nature of this architecture (which marked one of the most innovative and mature examples in the field of Italian museography) could/should require.

Balancing between these two instances (new requirements and the most "integral" preservation of Albini's museum), in search of an (im)possible mediation, the working group coordinated by the authors has made a journey back through the recent history of the Tesoro, within the elegance and power of an abstract form whose value is certainly enhanced by the technical refinement of Franco Albini's design choices and the executive methods of his concepts on site.

Damage types

Infiltration of the roofing system, which Director Marcenaro had already complained about when the work was not yet completed (but the museum had already been inaugurated), following a violent downpour and probably due to the way the flooring in the Archbishop's Palace courtyard had been constructed, reappeared and occurred several times over time, especially in the area of the glass-cement skylights in the tholos below. On the intrados of the ceiling, in fact, the reinforcement rods of the concrete were visible, already oxidised and corroded and no longer protected by the layer of concrete cover, which probably triggered carbonation of the concrete (2011, before the intervention).



View of the deterioration (photo G. Franco)

Hypothesis on damage processes

The deterioration of these elements was probably related to thermal stress and certainly to mechanical stress induced by the incongruous use of the Archbishopric courtyard as a parking space for cars and motorbikes. In order to temporarily repair the most serious cracks, some of the glass diffusers of the skylights had already been covered with a layer of mortar or sealed with silicone to stop the infiltration of rainwater into the tholos, thus compromising their readability from inside the museum.

In spite of these precautionary measures, water infiltration occurred repeatedly in the intervening years, with visible results especially in the tholos where the Zacharias Cross is displayed.





Temporary reparations (photo G. Franco)

Aim of the investigation

Archival analysis, completely new and specially conducted for this work (in the Archive of Municipality of Genova, Public works and in the Direction of Museums of Strada Nuova) made it possible to reconstruct the history of construction. This was why archive sources were carefully studied, with some new documents making it possible to chart the structure's history in greater detail, providing information of some micro-transformations whose very occurrence had been forgotten.

The reading and complete transcription of all the technical documents, from the first design reports to the final one, allowed us to know in detail the construction history of

the Museum, starting from the characteristics of the materials and the structural solutions adopted.

Direct observation of the few phenomena of deterioration, mainly on reinforced concrete exposed to atmospheric agents, was supplemented by chemical analyses to assess the process of carbonation underway.

Analysis of the causes and agents of damage and decay – as well as an evaluation of their impact upon the structural features, display fittings and exhibits – led the authors, together with the Scientific Committee, to draw up plans first of all for certain work that was strictly conservational in character. For example, work began on cleaning the surfaces of the architectural structure and the display apparatus in order to remove surface deposits, stains and the more substantial and adherent deposits on the display units themselves; at the same time, specialist restorers worked on the artefacts exhibited without special protection and on those within display cases. However, these measures were not sufficient to resolve all the problems that had emerged. As a result, it was necessary to plan and implement certain measures that did involve an element of modification, even if the maximum possible level of conservation remained the primary objective of all work.

The more consistent intervention on the covering is described in the following paragraph.

Methods and intervention

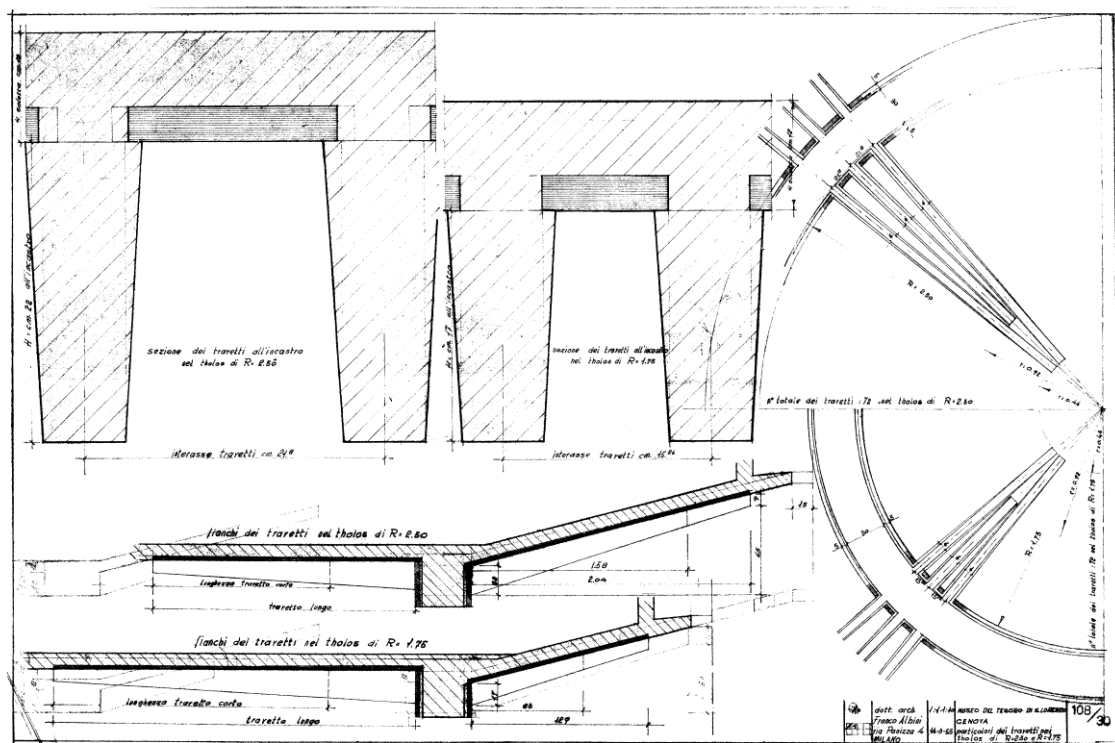
Sometimes it is necessary to make changes in order to truly conserve. Conservation itself presupposes on-going change (or controlled transformation) which, for example, makes it possible to pass from the dirty to the clean, the fragile to the reinforced, the divided to the re-composed, etc. The real problem lies in deciding how and within what limits - using what forms and materials – these 'modifications' can be carried out so as to be acceptable. Should one intervene continually, thus having resort to a sort of reproduction and imitation? Or is it preferable to intervene by changing forms and materials whilst operating in full respect for what already exists (primarily in the design of features that were previously not even present). A significant example of this issue was the repair of the block-glass skylight and their light diffusers (many of which were broken and some blocked up altogether).

The most significant intervention was the repair of the block-glass skylight and their light diffusers (many of which were broken and some blocked up altogether). To prevent the leaking that became apparent during the study phase from becoming worse, the three existing discs in block glass were replaced with similar but newly manufactured discs.

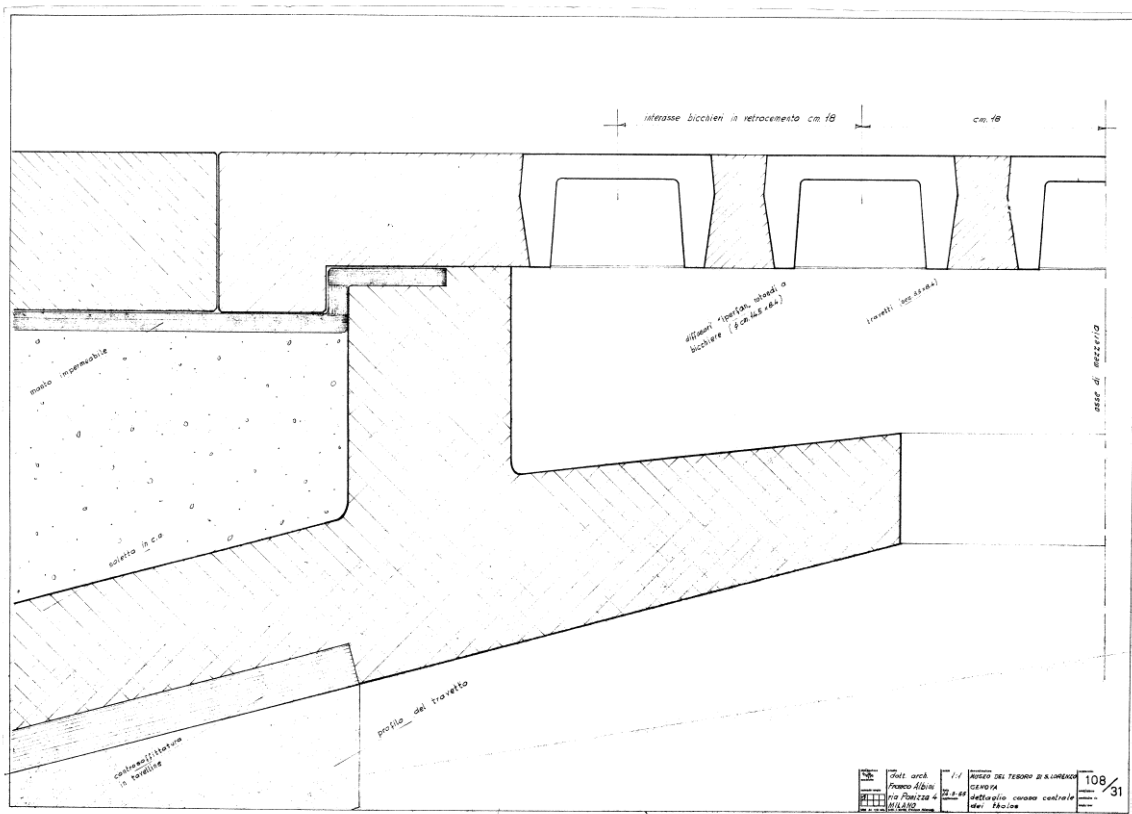
Since the "useful life cycle" of the glass-cement panels was inevitably considered to be over, they had to be replaced in their entirety, and the problem of the unavailability of the original glass diffusers had to be addressed. The company merged with the company Seves Glass Block, based in Florence, which continues to produce glass "cups" with a cylindrical base, but smaller than those used in the museum, with a production diameter of 11.7 cm. However, given the small number of pieces (less than 60), it was possible to find some pieces belonging to the same batch, stored in some of the warehouse funds of the firm that had taken over the stocks of the original supplier, which has now disappeared. They were of the same size and had the same surface finish (concentric stripes) as those in place but were irreparably damaged and unrecoverable. They could therefore be inserted into new

reinforced concrete panels (discs) of similar size and shape to the existing discs but now inefficient (133 cm diameter, 5.5 cm thick). Given the delicate nature of the work, it was recommended that, in order to prevent possible future damage to the relocated glass diffusers, the transit and parking of cars and motorbikes in the courtyard of the Archbishop's Palace should be limited as much as possible, especially near the skylights. In short, the work involved the following:

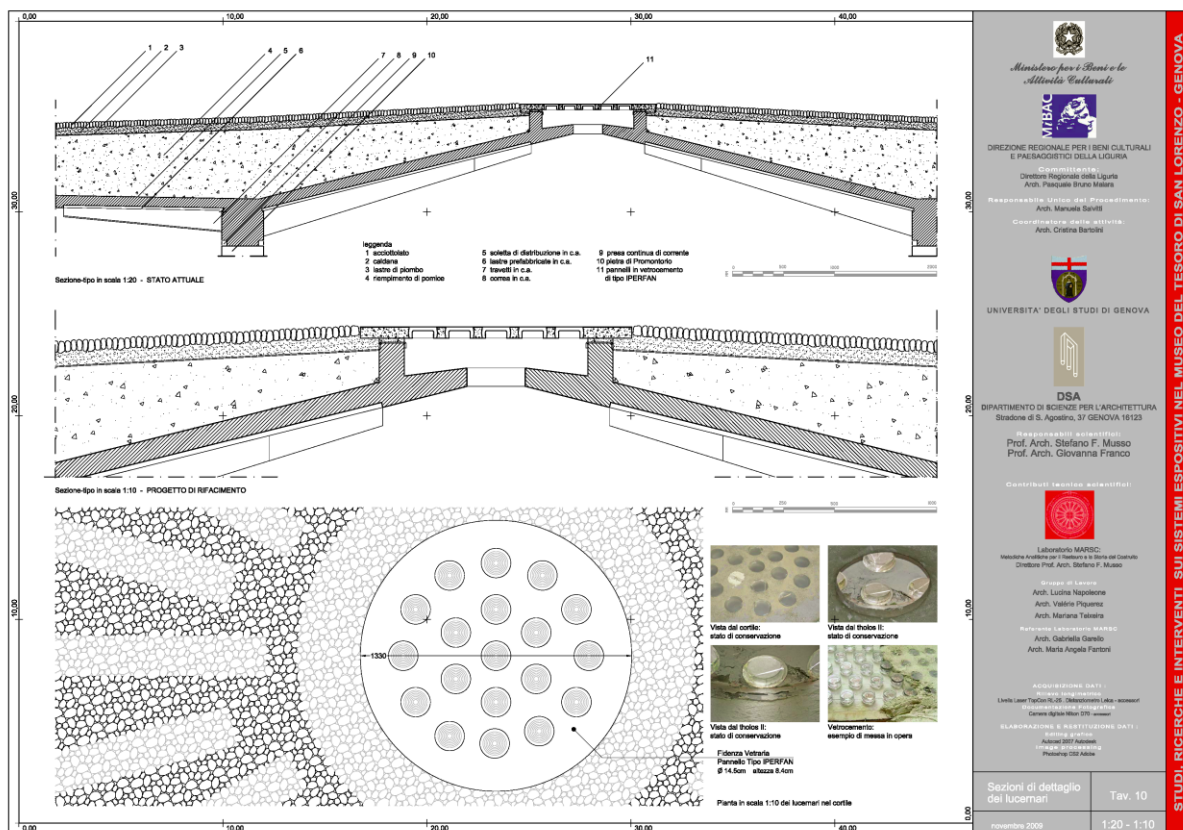
- removal of the original discs (lifted out mechanically, after breaking through a few of the diffusers);
- breaking up the first ring of cobble stones in the courtyard paving immediately around the discs;
- removal of the related backing and the lead-sheet waterproofing;
- installation of the new prefabricated discs (these were completely flat and not shaped at the edges – a feature that appears on the original designs); re-laying of the backing and new lead-sheet waterproofing and levelling of the ground around the ring supporting the slab
- re-laying the cobbles around the new disc.



Detailed drawings of the roofing structure, Franco Albini. Courtesy Piero Boccardo, Direzione Musei di Strada Nuova



Detailed drawings of the skylight, Franco Albini. Courtesy Piero Boccardo, Direzione Musei di Strada Nuova



Detailed drawing of the intervention on the glass-concrete discs (Architecture and Design Department, the authors)

Results

The Department of Architectural Sciences (actually Architecture and Design Department) at University of Genoa was responsible for carrying out the studies and tests within the museum, then coordinating the work that went into drafting the restoration project and the measures for putting it into effect.

Each of the bodies involved had its own legitimate concerns and goals, which might be shared by others but could also become the cause of conflict. Specially set up by the Regional Cultural Heritage and Activities Department, the Scientific Committee for the project made it possible for all to voice and debate those concerns to the full. The intervention of conservation, maintenance, repair and - in few parts - modification, represented an occasion to look at the clashes – sometimes, the outright contradictions – that arose between the notions of ‘origin’ and ‘originality’, ‘authentic’ and ‘authorial’, ‘modern’ and ‘contemporary’, which underlie all reflection upon restoration, especially those concerning Modern Architecture.

Discussion

Sometimes it is necessary to make changes in order to truly conserve. Conservation itself presupposes on-going change (or controlled transformation) which, for example, makes it possible to pass from the dirty to the clean, the fragile to the reinforced, the divided to the re-composed, etc. The real problem lies in deciding how and within what limits - using what forms and materials – these 'modifications' can be carried out so as to be acceptable. Should one intervene continually, thus having resort to a sort of reproduction and imitation? Or is it preferable to intervene by changing forms and materials whilst operating in full respect for what already exists (primarily in the design of features that were previously not even present)?

The first question that the Committee set itself was 'Which Treasury are we dealing with?'. The clear response to that had to be the Treasury as it existed at that precise moment, and in that precise state. The answer might seem obvious but it is certainly not without consequences for anyone who wishes to work in full respect of the past and present. In fact, thanks to source material that made it possible to reconstruct some of the genesis and implementation of Albini's ideas, we could see that there were some differences between the project designs and what was actually built. Furthermore, there was the obvious truth that many things had changed in the museum over the years, the means and outcomes of those changes being only partially documented. Numerous 'micro-transformations' had occurred in silence, almost the only trace they had left behind being a faint echo of them in varied documentary sources. Thus we had to decide whether the differences they had produced were to be considered as now forming part of the genuine original work.

Analysis of published material did not fully resolve the issue; while it made it possible to reconstruct the history of critical appreciations of the work, it did not cast full light upon everything that had happened after the project was completed. This was why further archive sources were studied, with some new documents making it possible to chart the structure's history in greater detail, providing information of some micro-transformations whose very occurrence had been forgotten.

Conclusions

In examining the museum and its history, we had to respond to a crucial question that remains partially unresolved: how much of the design and actual structure of the museum was Franco Albini's work and how much was due to Caterina Marcenaro? Another equally important question concerned how much of the Treasury was built as designed and how much was simply accepted once it had been built.

These two issues clearly influenced any attempt to clarify the limits of the oft-mentioned 'originality' of Albini's work, the question of his intangible presence as its 'author'. Often, in fact, the conservation of a work of architecture is predicated upon reference to the basis of its value as bearing authentic witness to the original work of an architect, or as the expression of a particular moment in the history of architecture. Here, however, one also had to look at the necessity/legitimacy of conserving possible 'errors' and 'chance' results in the planning and building of the museum, together with features that might be the fruit of what had happened to it during the course of its existence.

Bibliography

- Marginalia – New Museums*, in *The Architectural Review*, London, 1956
- A Buried Treasury* in *Architectural Forum* n. 4, 1957
- “Musées – Muséographie” – monograph issue of *Techniques et Architecture*, n. 326, 1979
- Albini, F. 1956. *Le Musée du Trésor de la cathédral de Saint Laurent de Gênes*, in *Museums*, vol IX, n.2. UNESCO, Paris
- Albini, F. 1958. *Museo del Tesoro di San Lorenzo* in *Goya-Revista de arte*, n. 22. Madrid.
- Argan, G. C. 1956. *Museo del Tesoro a Genova, architetto Franco Albini*, in *L'Architettura*, cronache e storia, n. 14.
- De Seta, C. 1980. “Franco Albini architetto, fra razionalismo e tecnologia”, in *Franco Albini Architettura e design 1930-1970*. Centro Di, Florence.
- Franco, G, Musso, S.F. *Franco Albini et le Musée du Trésor de la Cathédral San Lorenzo à Gênes. Problèmes de conception, construction et conservation*, in “Cahiers Thématiques. Technologie et bâtiments: un patrimoine silencieux” n° 19, pp. 57-68, ÉCOLE NATIONALE SUPÉRIEURE D'ARCHITECTURE ET DE PAYSAGE DE LILLE, Éditions de la Maison des sciences de l'homme, 2021.
- Labò, M. 1956. *Il Museo del Tesoro*, in *Casabella - Continuità*, n. 213.
- Marcenaro, C. 1969. *Il Museo del tesoro della Cattedrale a Genova*. Cassa di Risparmio di Genova e Imperia, Genoa.
- Musso, S.F., Franco, G. 2015. *The Conservation of the “Modern”: Franco Albini and the Museum of the Treasury of San Lorenzo, Genoa* in *Journal of Architectural Conservation*, vol 21, issue 1 2015, pp. 30-50, Taylor & Francis Group, London.
- Salvitti, M., Musso, S.F., Franco, G., Napoleone, L., *Conservare il Moderno: Franco Albini e il Museo del Tesoro di San Lorenzo, a Genova*, Quaderni di ANANKE, n. 5, 2015.
- Russoli, F. 1960. *Pour une muséographie efficace*, in *L'Oeil*, n. 61. Paris.
- Tafuri, M. 1982. *Storia dell'architettura italiana, 1944-1985*. Einaudi, Turin.
- Van Ravestein, S. 1963. *De modernisairung der Italiaanse Muse ana de corlog*, in “Bouwkundig weekblad”. The Hague.
- Zevi, B. 1956. *Un tesoro in quattro cilindri*, in *L'Espresso*, 10 June.

Report on In-Depth Case Study

Alexandros Dimitrou Tower (Nicosia, Cyprus, 1966)



CONSECH20 – WP2 (iii)

Restored Case Study

Georgiou, A.

Hadjimichael, M.

Ioannou, I.

October 5, 2021

Introduction

Historical background

The Alexandros Demetriou Tower is one of the most important buildings of the international style modernism in Cyprus, featuring in a publication (in the Greek journal 'Architecture') dating back to 1966 [1]. The building was listed, following a Decree issued by the Minister of Interior, in 2006 (Κ.Δ.Π. 342/2006). It has also been included in the index of the 100 (most) important buildings, sites and neighbourhoods from Cyprus, compiled by the National Register of Docomomo Cyprus [2].

The building was originally commissioned by Alexandros Demetriou & Sons, as an investment. The owners, who were merchants and importers of tractors and agricultural equipment, wanted a large building to host the offices, an exhibition area and storage spaces for the equipment of their company, as well as a number of apartments for sale. The famous Cypriot architect Neoptolemos Michaelides thus designed an eight-storey tower block above a basement and a semi-basement, measuring 34.50 m in height. The building comprises of an exposed reinforced concrete structural frame with visible frames on the two narrow facades (NW and SE), in line with the norm of the era. The plan view was left open to allow for future changes in the interior of the building [1]. A panoramic view of the building at the early stages of its life cycle in the 1960s, can be seen in Figure 69.



Figure 69. Panoramic view of 'Alexandros Demetriou Tower' in the early 1960s [3]

Other attributes of the building include passive systems for climate improvement, a characteristic feature of the environmental sensitivities of the architect. According to the description provided by the architect himself in the journal 'Architecture' in 1966, the basement, semi-basement and ground floor hosted the owners' storages, offices and exhibition spaces for the agricultural equipment. The semi-basement was also partly used for parking. Additionally, there was one 1-bedroom apartment and two 3-bedroom apartments on each floor (from the 1st to the 7th floor). The 8th floor comprised of a covered roof. The circular external staircase was pre-fabricated, and it is similar to the staircase at the entrance of the building, which leads to the raised ground-floor show room (Figure 70).



Figure 70. Circular prefabricated staircase (left) and entrance staircase (right)

At the time of its construction, the Alexandros Demetriou Tower was one of the tallest buildings in the capital of Cyprus, Nicosia, just outside the southern part of the Venetian walls of the old city, and one of the few efforts of the period to design a high-rise building. The interior space design of the building, as well as the open and semi-open spaces, created opportunities for understanding societal perceptions (of a certain class) regarding accommodation, at a time of shift towards modernity. For example, the original lack of view towards the Venetian Walls suggests that the Old City of Nicosia was not considered worthy of a view at the time. Indeed, in the 1950s, the Old City of Nicosia (within the context of modernism) was considered to be the one that we need to leave behind [4].

The building was successfully restored by Vasilis Ierides and Aimilios Michael in 2008. The architects described the refurbishment process as the building's 'second youth' in the proposal submitted to the Town Planning and Housing Department [5]. According to Michael et al. (2012) [6], they based the methodology of the restoration work on a detailed analysis of the building's functional, morphological, structural, and bioclimatic aspects, and on extensive discussions with the owners and the competent authorities, whilst showing respect to the importance of the building in terms of contemporary architectural heritage, as well as to the local society. Some of these changes aimed towards enhancing the bioclimatic features of the initial design, in order to improve thermal and visual comfort conditions, as well as to reduce the consumption of conventional energy for heating, cooling and lighting.

Additionally, the few changes made to the design of the building were indicative of the shift in societal and architectural standpoints, such as for example the opening of

windows towards the old city and the enlargement of the apartments (Fig. 3). Regarding the former change, this was also feasible in terms of bioclimatic design, as the new windows are facing south west, rather than south, as originally perceived by the architect.



Figure 71. South-west side: original construction with bricks (left) and large glass windows after restoration (right).

As for the enlargement of the apartments, the three original separate apartments (2 apartments and 1 studio) located on each floor were unified during the restoration of the building into a single apartment, thus creating 7 floor-size apartments, one on each floor. The covered terrace of the 8th floor was also converted into a housing unit, a feature that was actually included in the original design but was never realised. The historic timeline of the building is graphically summarized in Figure 72.

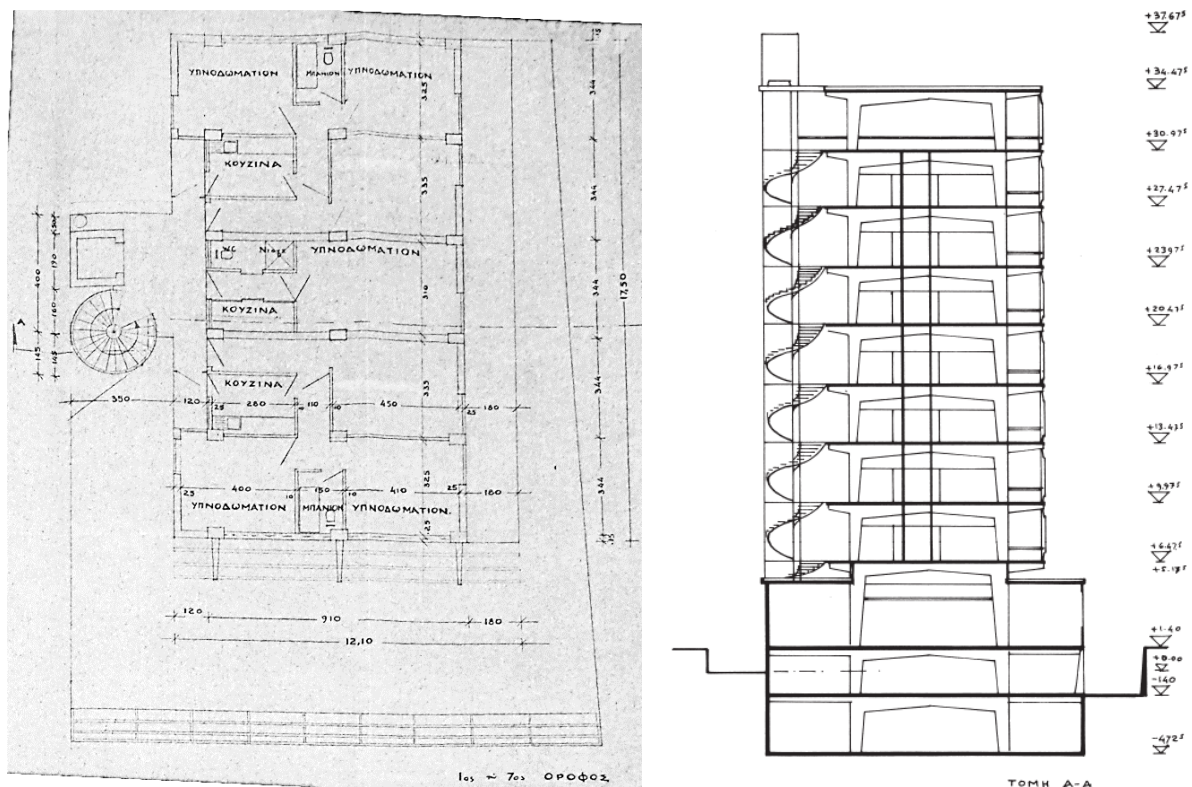


Figure 72. Timeline of important events in Alexandros Demetriou Building

Characteristics of the Concrete Building and Structure

For the structural verification of the building, the original plans that were submitted in 1954 for the building permit were obtained from the Nicosia Municipality. The original design of the building included a basement level, a semi-basement level and eight upper floor levels. The typical floors had a height of 3.5 m, whilst the ground floor had a height of 5.3 m. In Figure 73, the original typical architectural floor plan and section may be seen.

In the original submission, there was only one drawing showing the reinforcement plans of the four different floor slabs (semi-basement, ground, mezzanine, and typical floor levels); this included the columns and beams schedules. The original structural assessment of the building was also found (a hand-calculation set of 10 pages); this provided insightful information on the type of loads and assumptions made during the design stage of the project. As it was expected, the structure was designed to withstand only gravity loads, with no calculations carried out to consider horizontal dynamic loading (i.e. seismic or wind loads).



Based on the information collected, the main structure of each typical floor level is formed by six parallel reinforced concrete frames. These concrete frames have a total length of 9.1 m and are repeated every 3.4 m. According to the structural drawing, the frames are connected to each other with secondary beams that are smaller in size, when compared to the main beams of the frames. Each floor is formed by Zöllner one-way concrete slabs of 150 mm thickness. This type of concrete slabs was extensively used till the late 1970s in Cyprus, and basically comprises of ribbed slabs with masonry bricks as infill material, as shown in Figure 74. Amongst the main advantages of this type of slab is the reduced self-weight and the cost saving achieved by reducing the need for concrete and steel reinforcement.

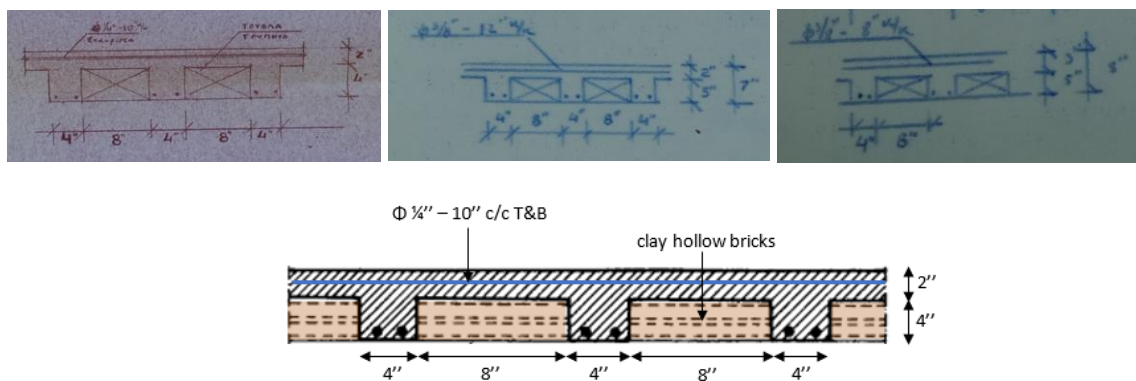


Figure 74. Zöllner slab detail, as specified by the original structural design

Based on the original drawings (Figure 75), the slabs depth varied between each floor, or within the same floor, based on the vertical loads and on the dimensions of the slab, ranging between 6" (152.4 mm) to 8" (203.2 mm).

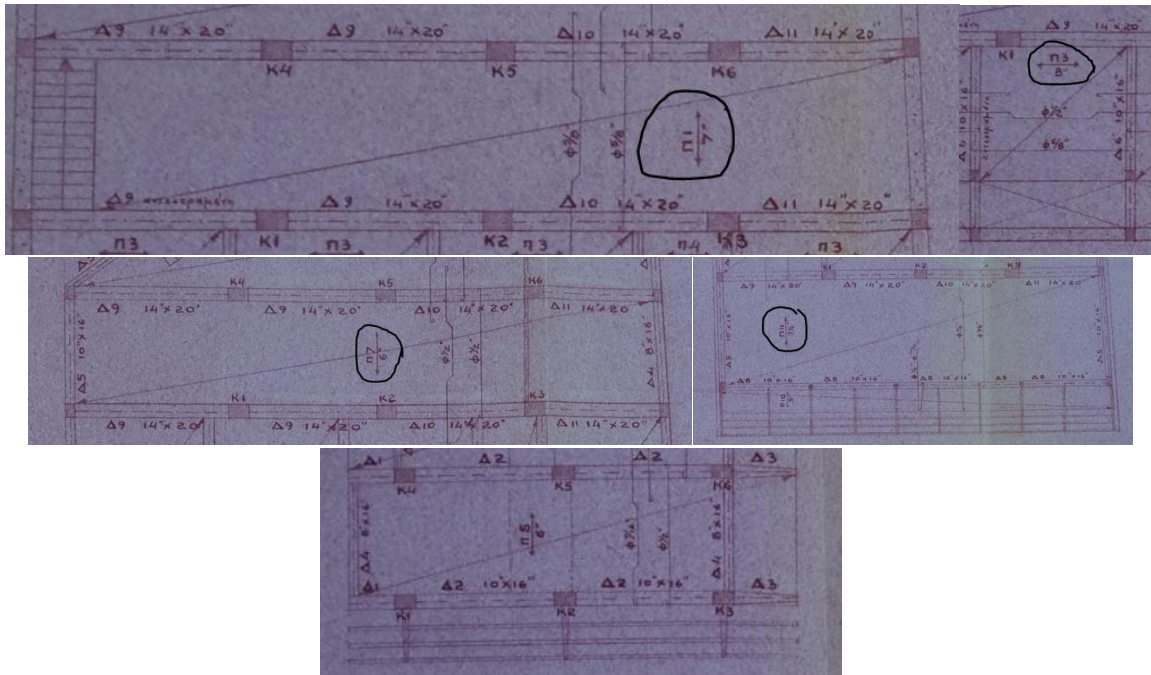


Figure 75. Slab depth based on original drawings: (a) over 2nd basement, (b) under ground floor, (c) above ground, (d) typical floor

When comparing the original set of drawings to the recent survey drawings created for the restoration of the building in 2008, some important discrepancies of the structural system were found. The original drawings showed a series of columns located in the middle of the main frames from the ground level up to the roof level; this row of columns was not found during the recent surveys, as illustrated in Figure 76. The absence of these columns was confirmed during the site inspections that followed.

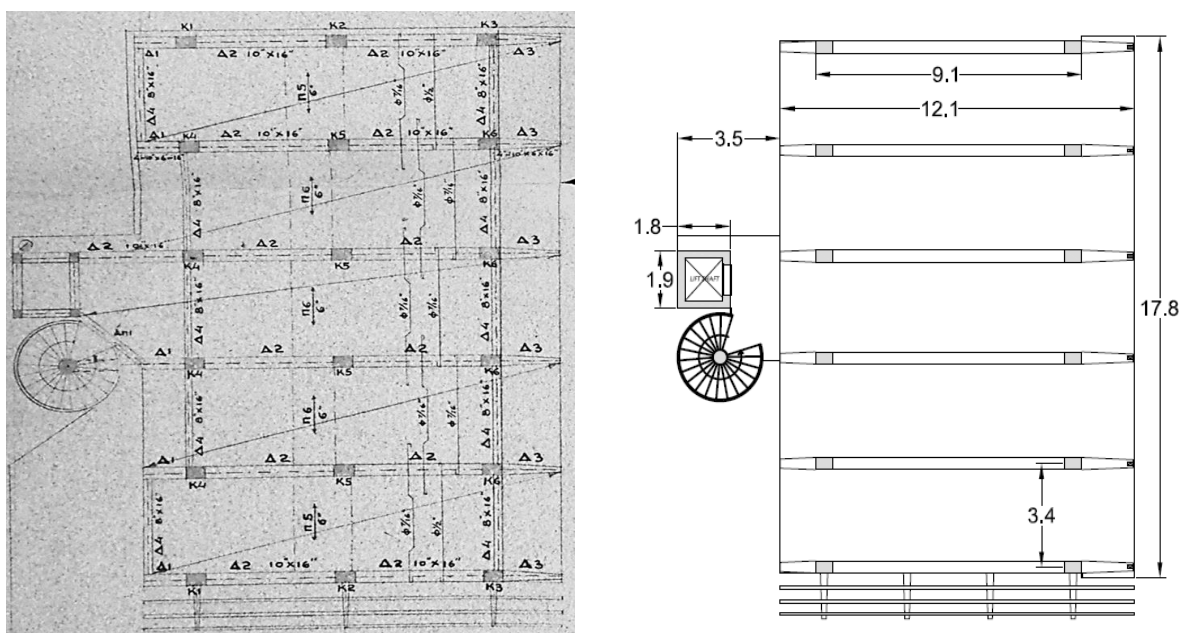


Figure 76. Typical floor plan as per: the original design (left) [7] and the survey plan (right)

Description of the Retrofit Design and Works

The information on the structural aspects of retrofit works carried out were collected from the calculation set and structural report of the retrofit design, and through an interview with the Structural Engineer of the project. According to these sources, 26 columns at the two basement levels were strengthened with the RC jacketing technique, as per the detail shown in Figure 77, while the rest of the columns at the upper floor levels (121 in total) were retrofitted with 2 layers of carbon FRP. Prior to applying the FRP, all damages related to the corrosion of reinforcing steel were rectified. No strengthening works were carried out at the foundation level, or on the beams and slabs of the building [7].

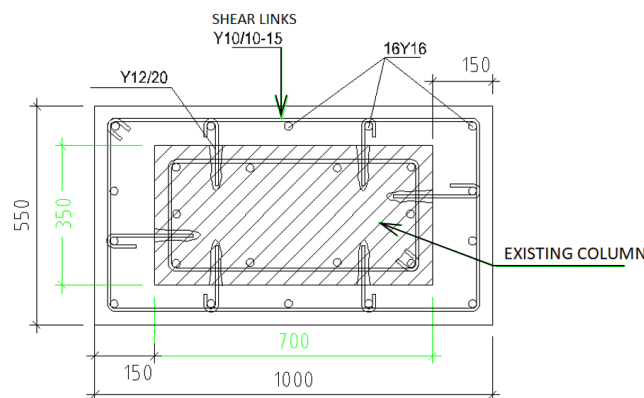


Figure 77. Reinforced Concrete jacketing detail [7]

Typical damages found in the structure prior and after the retrofit

It is highlighted that visual inspections contribute towards the identification of damage caused by weathering or previous seismic actions. Furthermore, it is noted that the full occupancy of the case study building imposed a major limitation on the extent of testing carried out during the site investigation stage. The visual inspections took place on multiple occasions between 2019-2021 and the overall status of the structure, in terms of damaging, was characterised as good. This is of course related to the recent retrofit works, during which many defects were identified and rectified. For completeness purposes, the three major defects identified prior to the retrofit works are presented below (Figure 78) [7]:

- The laboratory test results on concrete core specimens extracted from various locations, showed significantly reduced compressive strength, ranging between 15-17 N/mm².
- Steel reinforcement corrosion on the structural elements of the 8th floor, owing to continuous exposure to open weather conditions.
- Peeling/flaking of external plasterwork and painting in numerous locations, owing to the lack of regular maintenance and inadequate waterproofing of the building.



Figure 78. Defects identified prior to the retrofit works

The damages identified during the visual inspection (post-retrofit inspection) were not severe and were mainly related to moisture ingress, causing peeling/flaking of external plasterwork and painting (Figure 79). The other type of damage found was microcracking at the junction points of beams-columns and horizontal cracking of the wall finishes (Figure 80). The most severe defect found was related to steel reinforcement corrosion and the corrosion of other embedded metal elements in concrete, that led to local concrete spalling (Figure 81). Inside the building, no significant defects were identified, although the majority of the concrete elements were not visible because of the addition of false ceilings and drywall partitions.



Figure 79. Minor defects related to moisture ingress causing plaster and paint flaking





Figure 80. Micro-cracks on concrete elements and wall finishes

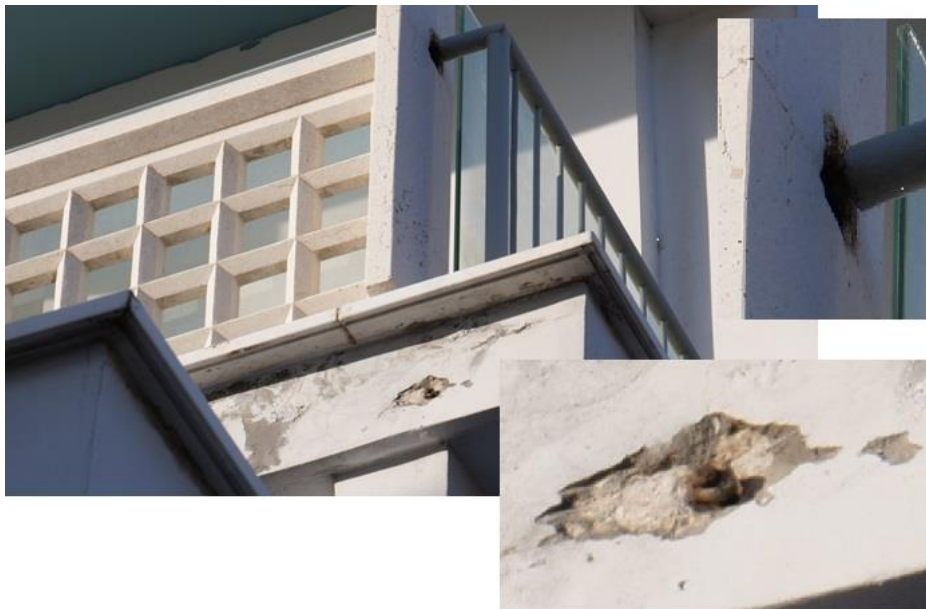


Figure 81. Reinforcement and other embedded metal corrosion causing local concrete spalling

Investigation, Methods and Results

For the seismic assessment of the residence, EC8:3 [8] was used. The methodology adopted is shown below:

- v. verification of the geometry of the structural elements and reinforcement detailing with regards to the original plans provided by the municipality,
- vi. evaluation of the material properties through in situ non-destructive tests,
- vii. assessment of local brittle failure possible damages
- viii. simulation of a typical frame with non-linear characteristics
- ix. assessment of a typical frame capacity under Pushover analysis.

Survey and testing of materials

A survey was performed for the verification of the geometry and size of the various elements. The original construction drawings showed great variation compared to the as-built investigation. In order to increase the detailing information, a rebar detector was used to detect the steel bar reinforcement, the bar cover and diameter, both in the beams and columns (Figure 82). The steel used in that era was mild S220 without ribs.



Figure 82. Rebar detection and diameter/cover measurement

Concrete mix and compressive strength

At the time of the construction of the case-study building, there were no batching plants in Cyprus and concrete was thus prepared on site, in small quantities ca. 2 tn at a time. This led to great variability in the quality of concrete in the various parts of a structure, even from the bottom to the top of a column, as there was also no equipment for vibration and thus proper compaction and consolidation. The original concrete mix design (Figure 83) was either 1:1:2 by volume (cement:sand:coarse aggregates) for columns (as described on one drawing) or 1:2:4 by volume for all beams, slabs and columns (as described in the technical specifications). For the case of 1:2:4 analogies, which were the most commonly used in Cyprus, based on oral communication, 1 part of water was used if the aggregates were wet, while 1.5-2 parts of water were used if the aggregates were dry.

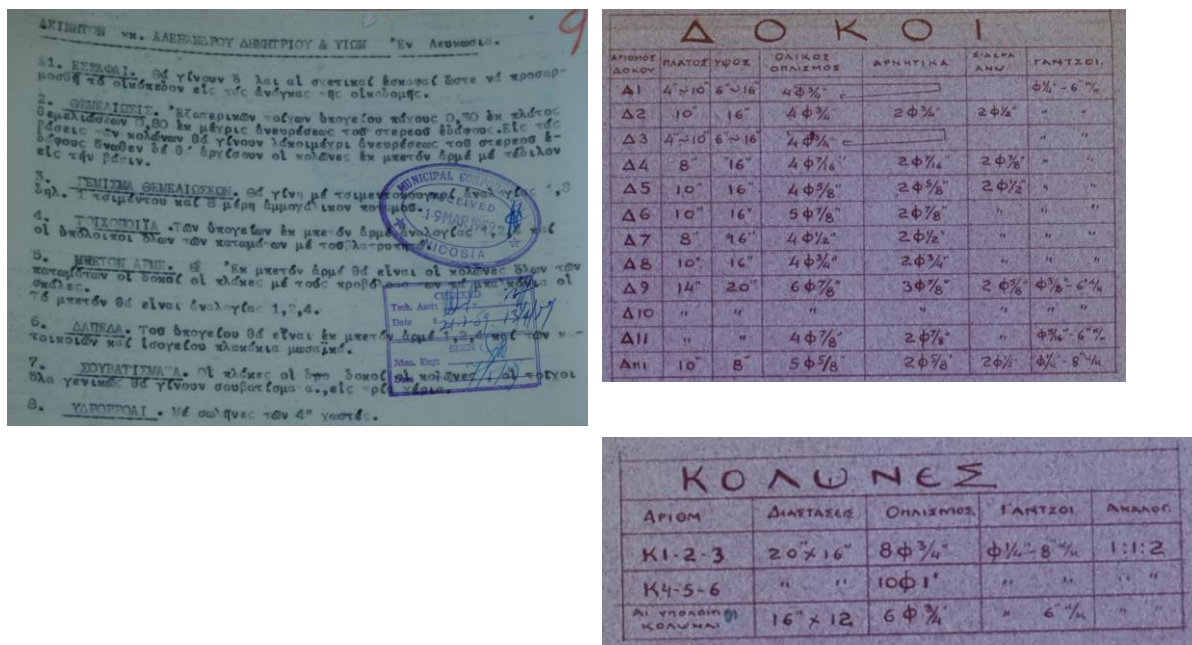


Figure 83. Concrete mix design as per specifications (left) and instructions on drawings (right).

Some uniaxial compression (EN12390-3 [9]) tests were performed in 2008 on a number of cores extracted from various members of the structure; yet it was not possible to acquire the results. The only available information was an average compressive strength of 19.5 MPa (cube) for the columns, provided by the Engineer in charge of the project. According to the same person, the samples extracted in March 2008 led to the assumption that the concrete used at the time of the construction of the building was C16/20. Nevertheless, some of the columns (nr. 4) had lower compressive strengths (12-15 MPa). The average cube compressive strength of the beams was 17 MPa, albeit again with 4 cases with strength lower than 15 MPa. Yet, the number of core samples was not available in order to assume that these were enough to determine the Knowledge Level of the strength of materials as extensive, KL3, as required for nonlinear assessment, based on EC8 Part 3 [8]. Table 1 summarises the information available regarding the original concrete compressive strength.

Table 9. Compressive strength of concrete

| Member | Average compressive strength from tests (N/mm ²) - cube | For assessment |
|---------------|---|----------------|
| Columns | 19 (4 cores under 12-15) | C16/20 |
| Beams + Slabs | 17 (4 cores under 15) | C12/16 |

Concrete cover, Rebar Diameter and Member detailing

The cover to the reinforcement was established through the use of the rebar detector, while the same procedure was used to determine the rebar diameter and detailing of the

rebars. The detailing of the columns and beams, as recorded in the original drawings, is shown in Table 9 and Table 10.

Table 10. Member detailing as per original drawings

| Columns | Original drawings | | | From measurements | | |
|--------------------------------|-------------------|----------|--------------------|--------------------|----------------------------|-----------------|
| Number | Dimensions (mm) | Long. | Trans. | Dimensions (mm) | Long. | Trans. |
| K1-2-3 (EXT) | 508x406.4 | 8Φ19 | Φ6.35/203.2 | 400x600 to 400x900 | 8Φ19 | Φ6/150 |
| K4-5-6 (INT) | 508x406.4 | 10Φ25.4 | Φ6.35/203.2 | 400x600 to 400x900 | 8Φ25 | Φ6/200 |
| ALL OTHER | 406.4x304.8 | 6Φ19 | Φ6.35/152.4 | | | |
| Beams | | | | | | |
| Number | B | H | Long. total | Negative | Upper reinforcement | Stirrups |
| Δ2 (main frame beam detailing) | 254 | 406.4 | 4Φ19.05 | 2Φ19.05 | 2Φ12.7 | Φ6.35/152.4 |
| | | | | | | |
| Δ4 | 203.02 | 406.4 | 4Φ11.11 | 2Φ11.11 | 2Φ9.53 | Φ6.35/152.4 |

The reinforcement layout and diameter were measured with the rebar detector on two columns and one main frame beam at the 3rd floor level, which was the only floor accessible. The first problem encountered was the difference between the dimensions of the beams and columns between the original drawings and the as-built findings. As per the original drawings, the columns and beams should be of constant rectangular shape, while in reality they were built as tapered. Additionally, measuring the reinforcement was difficult, especially of the corner rebars, because of the use of metallic corners during the retrofit of the building. Yet, the rebar diameters were in close approximation to the ones mentioned in the original plans, as the columns during that time served only to transfer vertical loads to the foundation. The measured values are depicted in Figure . The main issue encountered during the measurements was the absence of reinforcement -both longitudinal and transverse- within the joint between the columns and the beams, which was also of a wider area than normal, due to the tapered geometry of the members.

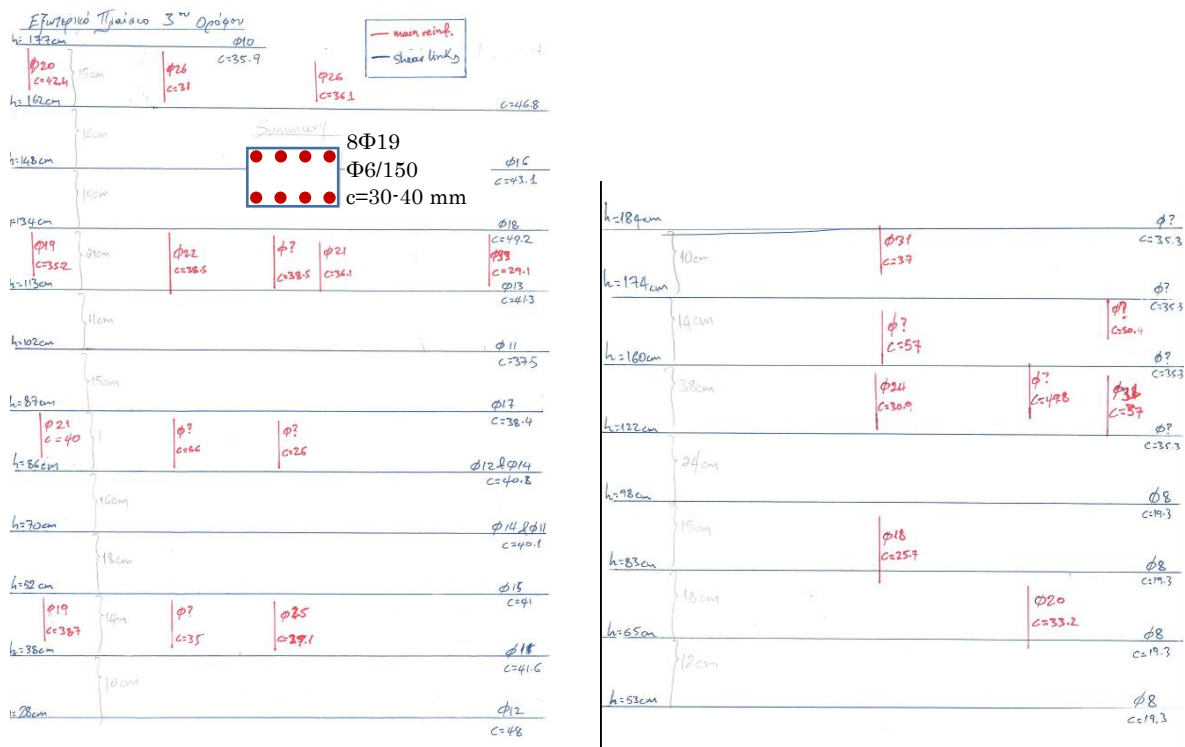


Figure 84. Reinforcement measurements on 3rd floor columns; external frame (left) and internal frame (right)

Assessment of the seismic capacity of the structure

Simulation of the structure

Figure shows the typical floor plan with the columns numbering and dimensions at their base. Modelling was performed only for two typical frames in the X-direction, as per the on-site measurements of the 3rd floor. The geometry and detailing of the external frame K14-K16 and the internal frame K21-K23 are depicted in Figure 86. The frames were loaded with the distributed load of the slab, on the beam, based on the G+0.3Q combination, while the vertical load of the floors above was also added to the columns.

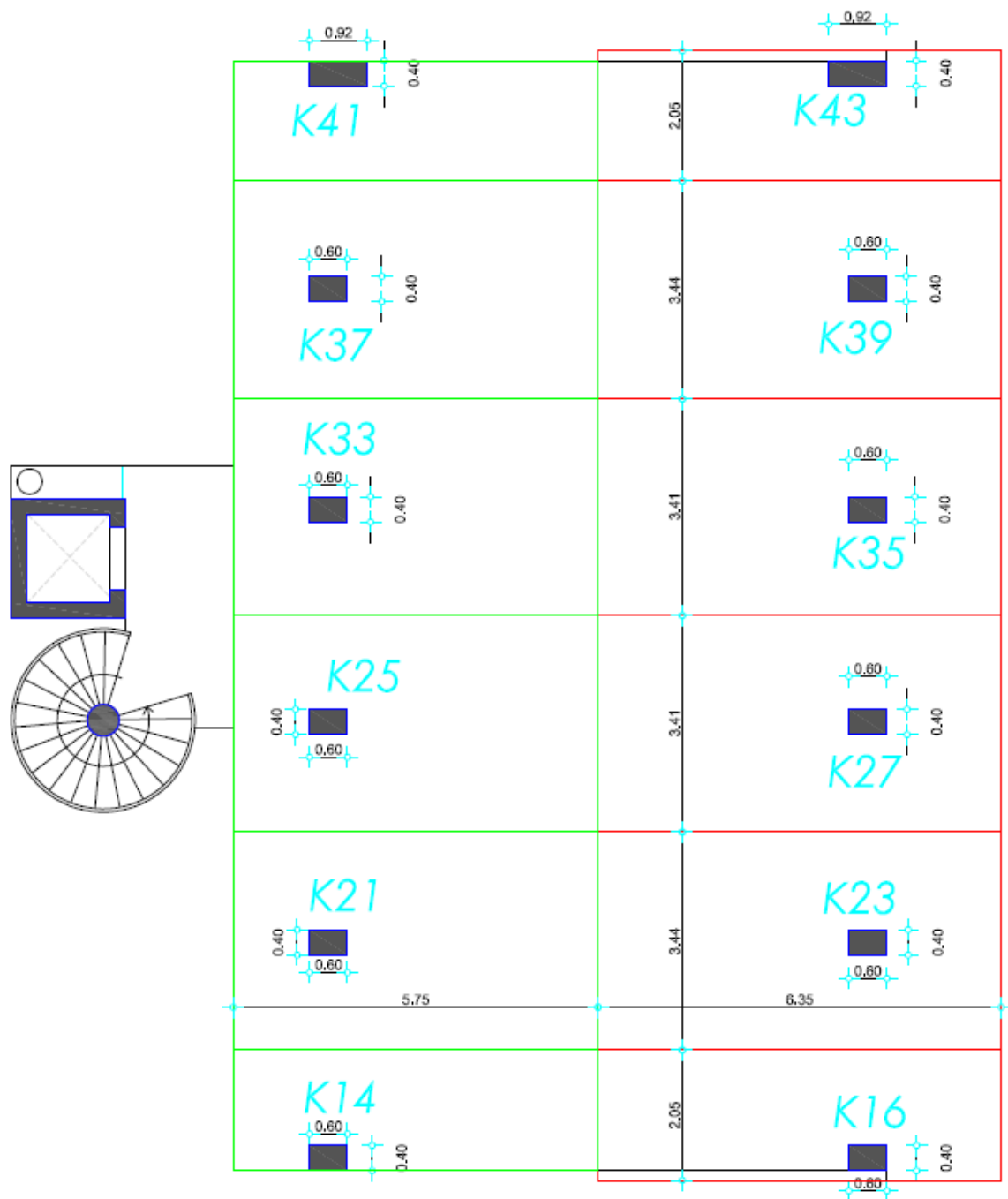


Figure 85. Typical floor plan with the columns numbering and dimensions at their base

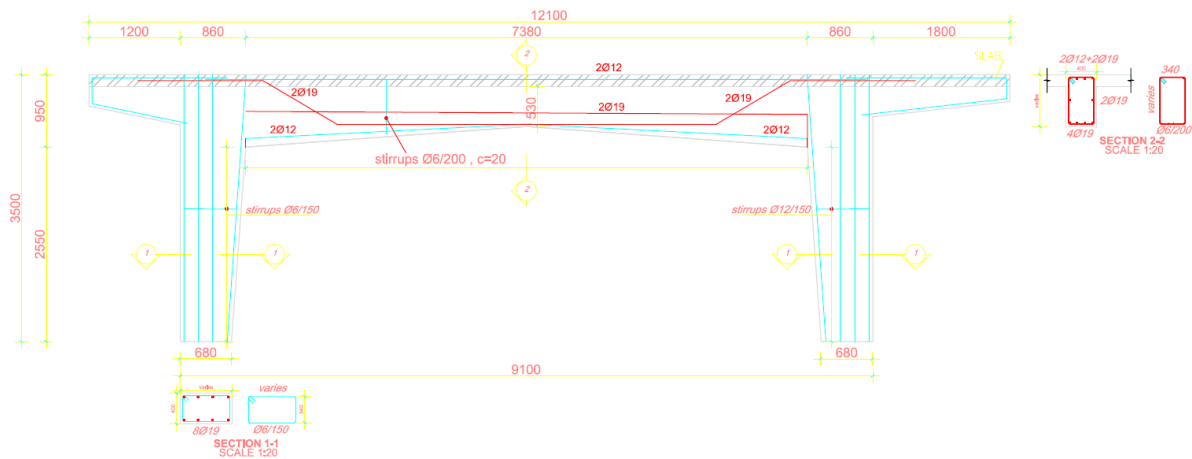


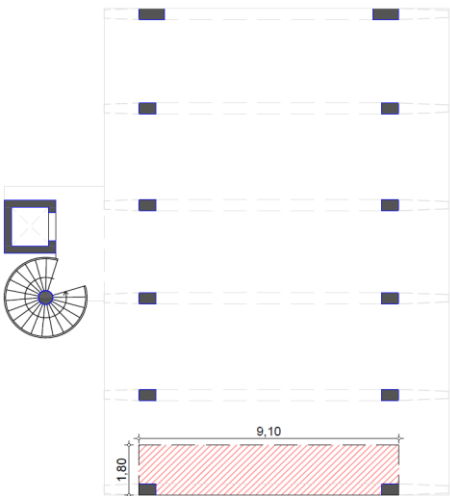
Figure 86. Geometry and detailing of 3rd floor external frame

As far as the vertical loads ‘G+0.3Q’ of the 3rd floor’s external frame are considered (Table 11):

- North side column (close to staircase): 650.66 kN
- South side column (next to balcony): 697.43 kN
- Beam: 10.08 kN/m

The axial load imposed on the columns will be the one calculated as per Annex B 4th floor column load, since the 3rd floor’s slab’s weight contribution will be the distributed load on the beam.

Table 11. Loading of the external 3rd floor frame

| LOADING | |
|---|-------|
|  | |
| Slab self weight [kN/m ²] | 3.80 |
| S _{imposed} permanent load [kN/m ²] | 1.20 |
| Live floor load [kN/m ²] | 2.00 |
| G+0.3Q [kN/m ²] | 5.6 |
| Length [m] | 9.1 |
| Width of slab [m] | 1.8 |
| Beam Load [kN/m] | 10.08 |

Assessment of the failure mechanism in reinforced concrete columns

The brittle failures that may incur to old substandard members, designed without any seismic provisions, are a crucial parameter for the assessment and retrofit of historic reinforced concrete structures [10]. The hierarchy between the individual failure mechanisms must be assessed in order to determine any prevailing brittle failure. The mechanisms of column failure, in terms of Shear Force, in the columns of the external frame of the 3rd floor, were:

- Yielding of the flexural reinforcement and failure in flexure, (V_y , V_{flex})
- Shear failure, (V_v by stirrups and V_{strut} by shear strut)
- Lap splice failure, (V_{lap})
- Joint shear failure, (V_j)
- Formation of plastic hinges in the adjacent beams (ductile behavior) V_{by}

Flexural yielding and failure

For the columns under study, the moment and curvature at yielding and flexural failure were assessed by the actual Moment-Curvature diagrams with the use of RESPONSE2000 [11], and are shown in Figure 87. Due to the higher static depth of the reinforcement of the top cross section, the moment that develops is more than 100 kNm greater than the moment in the bottom cross section.

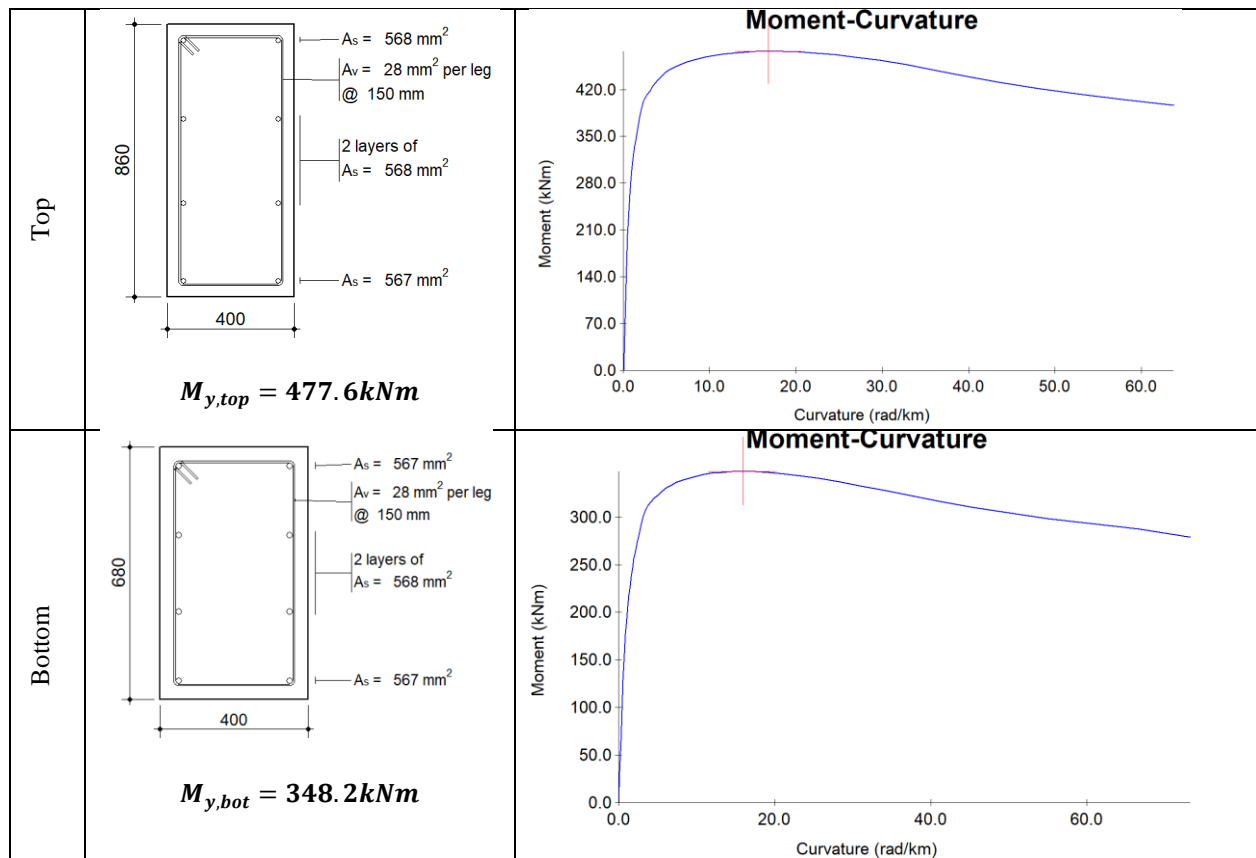


Figure 87. Moment – Curvature diagrams for external 3rd floor columns, top and bottom.

The shear corresponding to flexural failure is therefore obtained as:

$$V_{flex} = \frac{My, top + My, bot}{Ls, top + Ls, bot} = \frac{477.6 + 348.2}{2.487} = 332.046 \text{ kN}$$

$$Ls, top = 1.44 \text{ m and } Ls, bot = 1.05 \text{ m}$$

Shear failure

In order to establish the Shear load at the columns for shear failure, the Ls/h ratio is determined as <2 for both cases, top and bottom of the column. Therefore:

$$V_R = \frac{1}{\gamma_{el}} \left[\frac{h-x}{2L_v} \min(N; 0.55A_c f_c) + \left(1 - 0.05 \min(5; \mu_{\Delta}^{pl})\right) \cdot \left[0.16 \max(0.5; \rho_{tot}) \left(1 - 0.16 \min\left(5; \frac{L_v}{h}\right)\right) \sqrt{f_c} A_c + V_w \right] \right]$$

$$\text{Column bottom} \rightarrow V_R = 315 \text{ kN and } V_{Rmax} = 454 \text{ kN}$$

$$\text{Column top} \rightarrow V_R = 486 \text{ kN and } V_{Rmax} = 516 \text{ kN}$$

Joint failure

The column-beam joints in this specific case do not have any shear reinforcement and are therefore prone to failure. Another parameter that limits their structural capacity is their distance from the slab and the perpendicular frame beams; this limits the beneficial action of confinement usually provided by the aforementioned structural elements.

$$V_{j,x} = \gamma_j \cdot 0.5 \cdot \sqrt{f_{c,b}} \cdot \sqrt{1 + \frac{v_j \cdot f_{c,b}}{0.5 \cdot \sqrt{f_{c,b}}} \cdot \frac{b_j \cdot d \cdot d_{beam}}{H_{col}}}$$

Where $\gamma_j=1$ for external unconfined joints.

$$V_{j,x} = 1 \cdot 0.5 \cdot \sqrt{16} \cdot \sqrt{\left(1 + \frac{0.20 \cdot 16}{0.5 \cdot \sqrt{16}}\right) \cdot \frac{400 \cdot 800 \cdot 900}{2500}} = \mathbf{284 \text{ kN}}$$

Lap splice failure

The lap splice of the longitudinal reinforcement in the column's bottom was also calculated for the analysis. In this specific case, the limited confinement and insufficient length of the lapping of the steel bars may lead to pullout failure due to cracking of the concrete cover around the steel bars. Another parameter that limits the lapping length capacity is the lack of ribs and the low strength of concrete. The column's shear load at lap splice failure is derived as per [12]:

$$V_{lap}$$

$$= \frac{\left[\min \left\{ \left(\mu_{fr} \cdot L_{lap} \cdot \left[\frac{A_{tr}}{s} \cdot f_{st} + \alpha_b \cdot (b - N_b \cdot D_b) \cdot f_t \right] + \right) ; N_b \cdot A_b \cdot f_y \right\} \cdot d \cdot (1 - 0.4 \cdot \xi) + \right. \\ \left. + v \cdot b \cdot d^2 \cdot f_c \cdot (0.5 \cdot h/d - 0.4 \cdot \xi) \right]}{h_{col}/2}$$

$$V_{lap} = 64 \text{ kN}$$

Prevailing mode of failure

The above analysis shows that the prevailing mode of failure of the main frames of the structure will be brittle lap splice failure. Especially for the external frames, the failure load will be 64 kN per column, or 128 kN per frame.

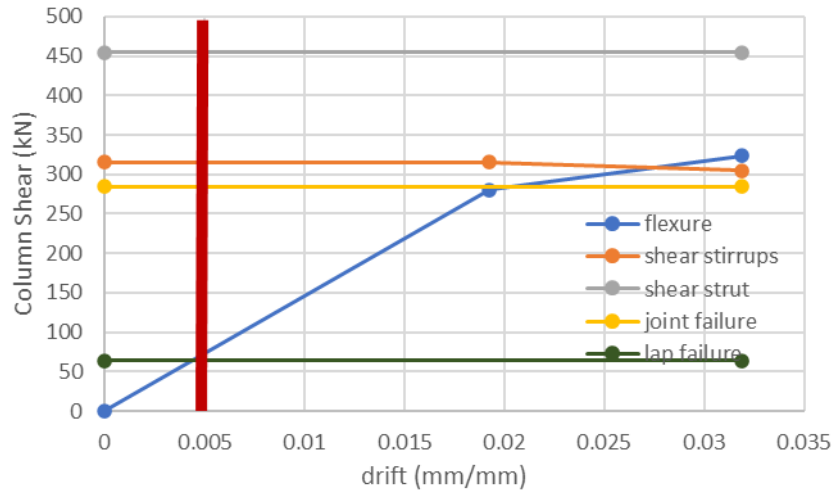


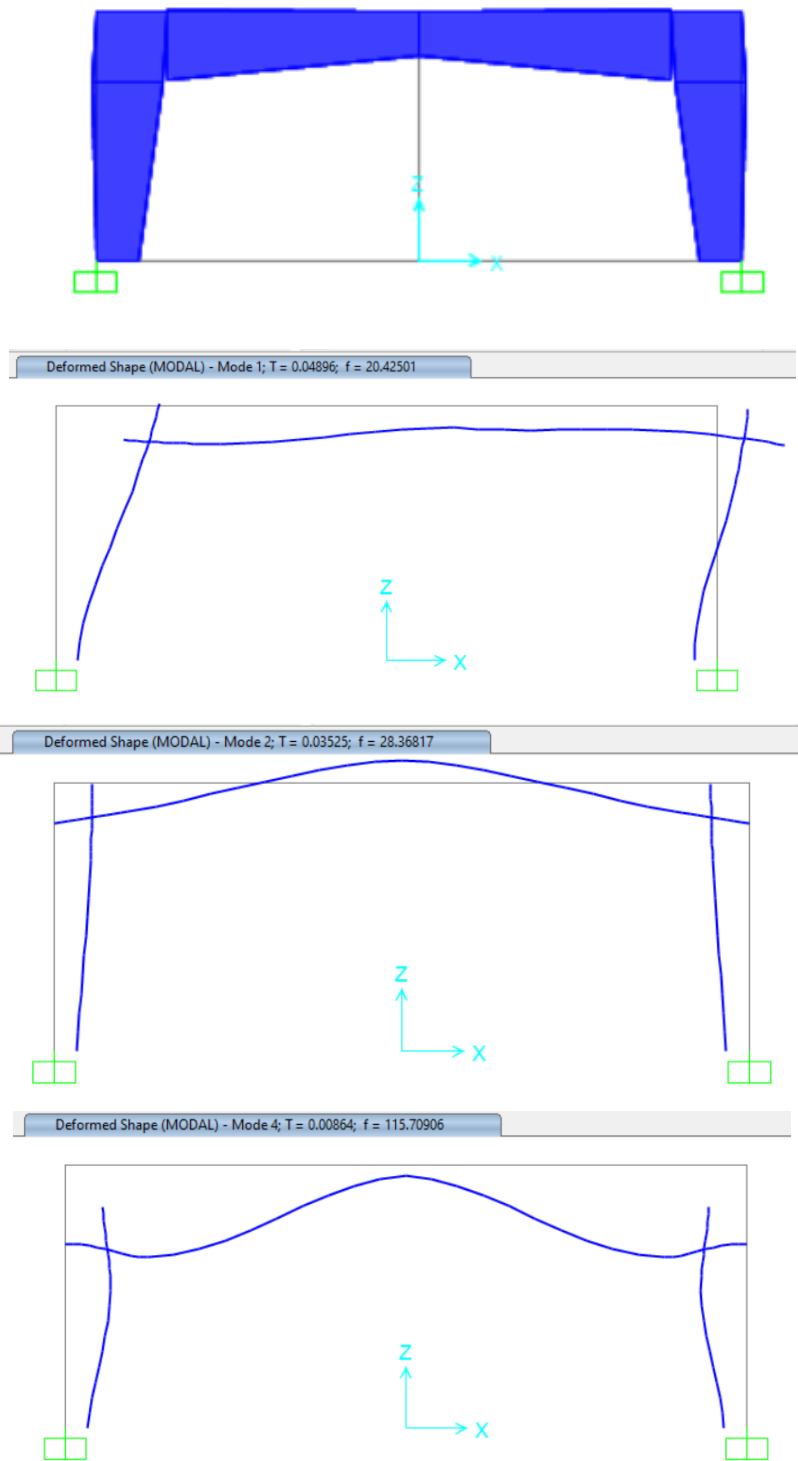
Figure 88. Comparison of different failure mechanisms in the bottom of the column

Simulation of a single frame in SAP2000

The structure was modelled in the commercial program SAP2000 [13] in order to assess its capacity under seismic conditions. The reinforced concrete beams and columns were simulated as 2-node frames. The mean average strengths were used for determining the properties of the various materials. Diaphragmatic action was applied to all the nodes of the floor level. The columns were supported on rigid joints. All the floor slabs were assigned with the load combination of $G+0.3Q$. The live load was chosen based on the Cypriot Annex of Eurocode 1 [14]. This load combination was also used as the mass of the frame for the modal analysis.

Modal characteristics of the structure

The modal analysis results are depicted in Figure 89, with the first mode to be translational in the X-direction, with a mass participation factor of 0.98.



| OutputCase | StepType Text | StepNum Unitless | Period Sec | UX Unitless | UY Unitless | UZ Unitless |
|------------|------------------|---------------------|---------------|----------------|----------------|----------------|
| MODAL | Mode | 1 | 0.04896 | 0.98186 | 0 | 0 |
| MODAL | Mode | 2 | 0.035251 | 0 | 0 | 0.30126000... |
| MODAL | Mode | 3 | 0.008868 | 2.563E-06 | 0 | 0 |
| MODAL | Mode | 4 | 0.008642 | 0 | 0 | 0.61293 |

Figure 89. Simulation of the frame with tapered members in SAP2000 and modal shapes

Pushover analysis

Two types of hinges were used in the two types of analysis performed. The first scenario was the use of ductile hinges at the column's ends, that do not take into account the brittle shear failure. The second type of hinge was only brittle shear failure, with the corresponding maximum shear strength resulting from the aforementioned analysis to be incorporated in the hinge's properties, as shown in Figure 90.

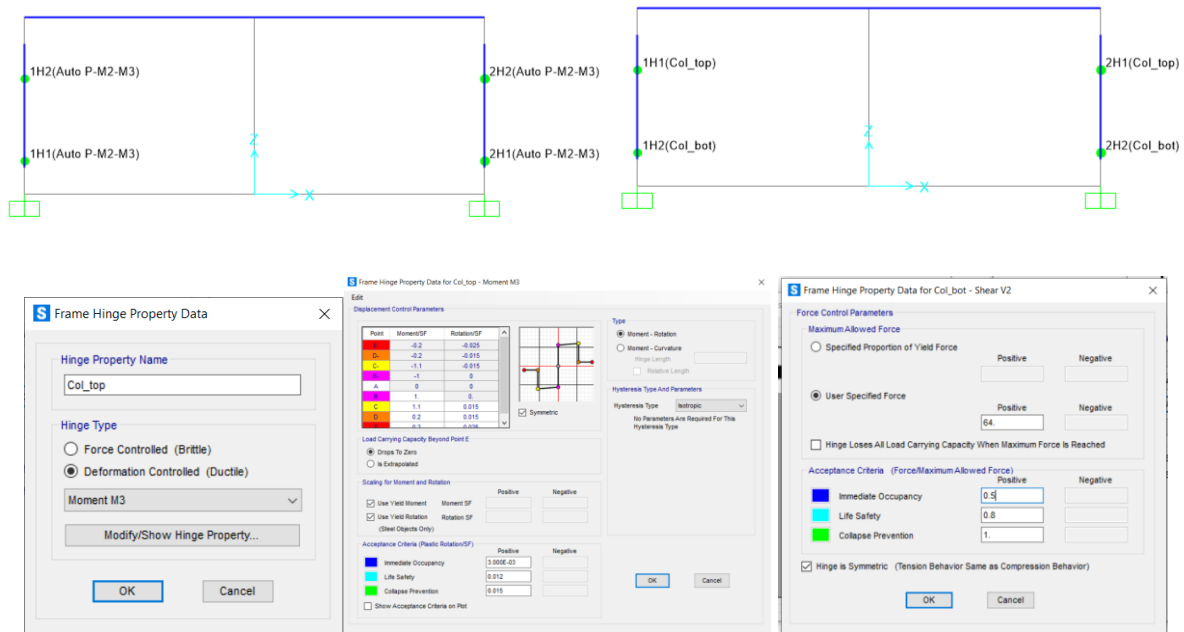


Figure 90. Hinges properties in SAP2000

The pushover curve in the case of the ductile hinges is shown in Figure 91 (top). The frame behaves elastically up to a load of 720 kN, corresponding to yielding of the flexural reinforcement in the columns, while after that a plateau appears, suggesting a great amount of ductility for the frame up to the failure of the hinges. The actual behavior of the frame is depicted in the bottom part of the same figure, where the brittle lap splice failure was incorporated in the properties of the hinges. In this case, the frame was not able to reach its yield load as before, since the columns failed at a Base Shear of 120 kN, and after that the frame's capacity to transfer loads dropped to zero.

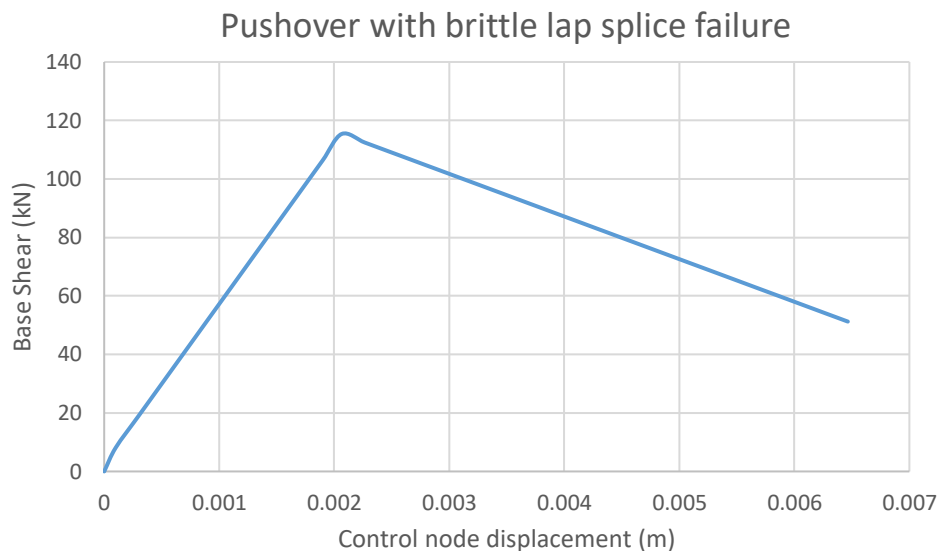
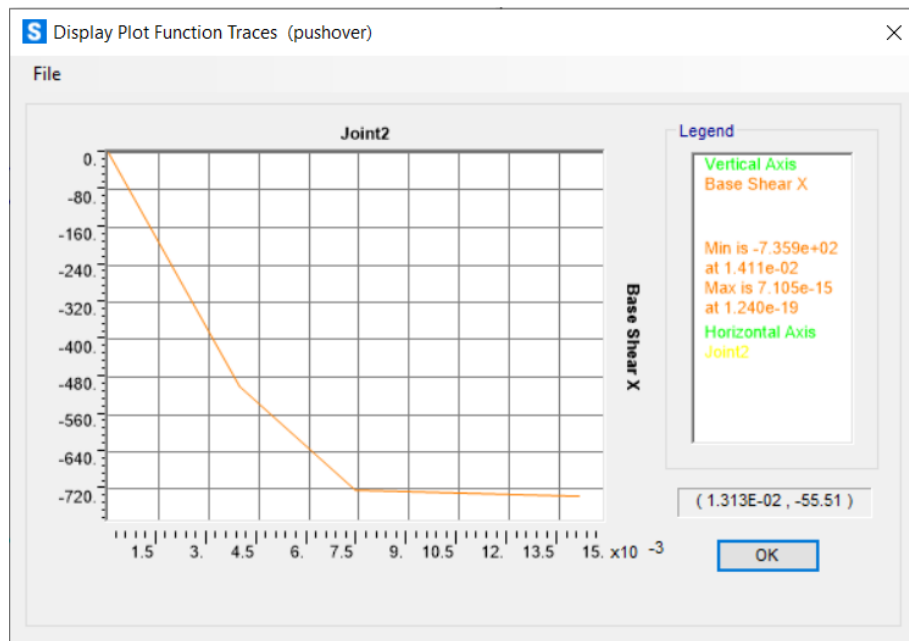


Figure 91. Pushover curve with ductile hinges (top) and brittle hinges (bottom)

Conclusions

The structural assessment of buildings requires good understanding of the various components of the structure, their interconnection and material mechanical properties, and of the global behaviour under seismic excitation. In the local components level, the task of assessing the properties of members is becoming even more challenging in the case of historic structures. In such cases, thorough member analysis has to be explicitly performed and all possible failure mechanisms must be taken under consideration.

This case study explored a cultural heritage listed reinforced concrete structure that underwent some strengthening. Non-linear pushover analysis was used for assessing the capacity of one external frame. The results from the assessment procedures show the brittle lap splice failure in the columns due to their intrinsic characteristics: sparse

stirrups, low concrete strength, no ribs. The report highlights that this type of failure must be incorporated in the analysis in order to assess the actual behavior of the structure and the brittle failures.

References

- [1] Architektoniki_issue_55_on_Cyprus.pdf n.d.
- [2] Docomomo Cyprus. Cyprus 100 [most] Important Buildings, Sites and Neighbourhoods. Nicosia: 2014.
- [3] Αιμίλιος Μιχαήλ. Ιστορική αναδρομή στο μοντερνισμό – Το μοντέρνο στην Κύπρο. Συνθέσεις 2013:86–9.
- [4] Michael, A. 18th January 2021. Personal Communication. n.d.
- [5] Ierides V, Michael E, Christophilopoulou S. Modernism second youth reserves: The example of Alexandros Demetriou Tower. Cyprus Archit Assoc Vol 6 2009:78.
- [6] Michael A, Christofilopoulou S, Ierides V. Conservation and Modern Architecture Reserves: The Alexander Demetriou Building Case, Nicosia, Cyprus. 12th Int. Docomomo Conf. Surviv. Mod. from Coffee Cup to Gen. Plan, Espoo, Finland: 2012.
- [7] Nicosia Municipality. Building Permit File of “Alexandros Demetriou Tower” 2012.
- [8] CEN. EN1998-3. Eurocode 8 : Design of structures for earthquake resistance — Part 3: Assessment and retrofitting of buildings. European Committee for Standardization, Bruxelles 2004;3.
- [9] BS EN 12390-3:2009. Testing hardened concrete, Part 3: Compressive strength of test specimens (2009). Br Stand Inst 2009.
- [10] Pardalopoulos SJ, Thermou GE, Pantazopoulou SJ. Screening criteria to identify brittle R.C. structural failures in earthquakes. Bull Earthq Eng 2013;11:607–36. <https://doi.org/10.1007/s10518-012-9390-7>.
- [11] Evan C Bentz MPC. RESPONSE2000 Reinforced Concrete Sectional Analysis using the Modified Compression Field Theory 2000.
- [12] Syntzirma D V., Pardalopoulos SI, Pantazopoulou SJ. Experimental evaluation of strength assessment procedures for R.C. elements with sub-standard details. Eng Struct 2020;224. <https://doi.org/10.1016/j.engstruct.2020.111191>.
- [13] CSI. SAP2000: Static and Dynamic Finite Element Analysis of Structures 14.0 2009.
- [14] Standard E. EUROPEAN STANDARD Eurocode 1 - Actions on structures Part 4 : Silos and tanks European Committee for Standardization 2003:1–110.

Discussion and Conclusions

Historic concrete structures are resilient at many levels. Even abandoned structures constructed over 115 years ago, like the Hennebique Silos, are still capable to perform structurally. Of course, there are damages and local failures that have to be addressed, but even in a marine environment, which is proven to be one of the worst environments for concrete, most of the structure is still salvable.

The research has shown that, in terms of structural damage, a main issue from which the historic concrete buildings can suffer are the forces derived from seismic events. As seen in the cases of Cyprus, the issues derive from the poor detailing of the reinforcement, insufficient lap splice in the joints between components and lack of shear reinforcement. Also, the strength of concrete is in some cases insufficient. Interventions, aiming at increasing its strength and ductility of the structure, are often done, when a new function is planned for the buildings.

The reports show that the quality of the reinforced concrete slightly differs among the countries, in terms of detailing and composition. The difference can be explained on the basis of the experimental character of the historic concrete, the fabrication entrusted to handicraft, and the fact that the norms on concrete fabrication and use changed in time with the acquisition of more knowledge on the new material. It should be also noticed that not always were the norms followed, as it is clearly stated by the research on the Fruit and Vegetable market in Genoa.

Two of the three buildings selected in Cyprus are an example of a late use of reinforced concrete (later than 1960); however, also on these buildings still detailing mistakes were made, which in other countries with longer concrete tradition were already resolved.

Carbonation induced corrosion of the reinforcement leading to spalling of the concrete cover and superficial damage due to moisture are the most common damage types found across the case studies. This is in agreement with the literature on the conservation of historic concrete. Besides, interventions done in the course of time may have introduced damage or have failed.

A lack of proper detailing is also commonly found in building pre-1930s like the Fenix II in Rotterdam and the market and silos of Genoa. Although this is not particularly worrisome if the building in question is not located in a seismic area.

Regarding the restored buildings, most relevant aspects for a successfully restoration seem to be the co-operation of experts, the selection of building contractors guaranteeing good quality work and a well-planned intervention. Engaging contractors, architects and engineers specialized in concrete restoration contributes to obtaining a good result, i.e. interventions technically, historically and aesthetically compatible. A precise damage mapping and detailing for each damage according to current norms, as found in the Timber factory in Vlissingen, guarantees a proper quality of the intervention and makes monitoring possible.

Specific guidelines are needed to direct the development of a consistent plan of conservation and also transformation of buildings in historic concrete in view of the (re)use. Due to their experimental character each of these buildings should be considered as a unique case, and the guidelines should be flexible enough to be applicable to different situations, though providing the basis for an integral and homogeneous approach.

The slab reinforcement was in the order of 8 mm diameter and in consistency with the original plans that were found. Based on the slab cored specimen (Figure 32), the re-bar was in a good state without any visible corrosion. The longitudinal reinforcement of the columns, based on the exposed element (Figure 32) and on a series of measurements with the rebar detector was determined to be in the order of 5/8" (15.875 mm), since inches were used at that time for bar sizing, while no stirrups were used to confine the longitudinal bars (only some thin wires to hold them in place during casting). This is in agreement with detailing plans found in the bibliography (Figure 32).

Assessment of the seismic capacity of the structure

Simulation of the structure

Modelling of the structure was performed using a 3D model, to include any possible torsional effects. The structural assessment was carried out using dynamic modal time-history analysis with the use of an elastic model. The advantage of 3D modal analysis is the improved representation of the higher modes of vibration (compared to static analysis), while its drawbacks are the sometimes unrealistic estimates of member stiffness, the doubtful validity of the results from modal combinations, the underestimation of drifts in lower stories and the non-consideration of the alteration of stiffness due to the axial force variation caused by the seismic axial load [18].

Elements, materials and other parameters

The structure was modelled in the commercial program SAP2000 [12] in order to assess its capacity under seismic conditions. The masonry units were simulated as 4-node thick shells to account for shear deformations, the concrete slabs as 4-node thin shells and the reinforced concrete beams and columns as 2-node frames. The mean average strengths were used for determining the properties of the various materials. A summary of the properties used in the model is listed in Table 9. The masonry walls had a thickness of 0.6 m in the basement and 0.5 m in the rest of the structure, except for Type C masonry that was 0.275 m thick. The concrete slabs varied between 0.08 – 0.12 m. Columns were square with edge dimensions 0.2 m and slab beams measured 0.2 m x 0.35 m.

Table 2. Member material properties used in the 3D model

| Element | f_k (MPa) | E (GPa) | ν | ρ (kg/m ³) |
|----------------|-------------|---------|-------|-----------------------------|
| Type A masonry | 1.09 | 1.255 | 0.398 | 1512.7 |
| Type B masonry | 1.1658 | 1.32 | 0.396 | 1512.7 |
| Type C masonry | 2.40 | 1.26 | 0.394 | 1800.0 |
| Concrete | 12.17 | 21.85 | 0.2 | 2500.0 |

For all the elements in structure under study, modifiers were used to decrease the stiffness of the cross sections to half that of the uncracked sections, in order to take into consideration the stiffness degradation during the seismic event [19,20]. The existence of concrete slabs leads to the conclusion that diaphragmatic action can be applied to all the nodes of the floor levels [21]. The two Type C walls were found not to be rigidly connected with the perpendicular walls, therefore their connection was performed with the use of 2-node gap link elements that work only when compression is applied. The members were rigidly connected to the ground (Figure 33), while the walls in the basement under the soil level, were assigned with springs that allow movement away from the soil, but prevent movement when in contact with it. All the floor slabs were assigned with the load combination of $G+0.3Q$, with an additional $G=2.6 \text{ kN/m}^2$ to account for the finishing of the floor surfaces. The live load was chosen as C1 category, based on the Cypriot Annex of Eurocode 1 [22]. This load combination was also used to derive the mass of the structure for the modal analysis.

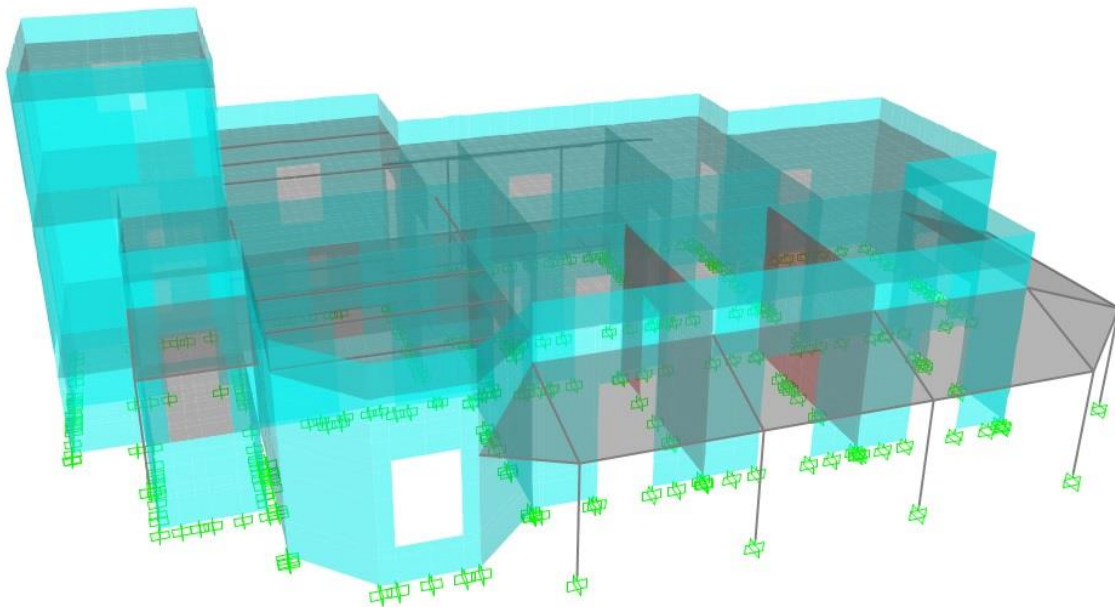


Figure 33. Model of the structure in SAP2000 and rigid restrains

Discussion

Assessment of the capacity of the Hennebique reinforced concrete columns

In older type construction, shear reinforcement was used only for supporting the longitudinal reinforcement against buckling, to resist a small fraction of the design shear force due to vertical loads and torsion [23]. Especially in the case of the early Hennebique system, and as can be seen in the Melkonian residence, the longitudinal bars were connected with thin wire instead of stirrups (Figure 32). While the moment-

curvature analysis would imply a ductile performance of the members, the actual amount of displacement capacity is a matter of the failure prevailing mechanism between flexure, shear, lap-splice, buckling, beam-column joint failure [23–25]. The curvatures ϕ , drifts θ and displacements Δ of the Melkonian column members at yield and ultimate load, were derived in order to assess the deformation capacities, ductility and local damage of the reinforced concrete components. The results were used to assess the hierarchy of damage on the column members of the structure and assist in guiding the repair and retrofit strategy.

Error! Reference source not found.a depicts the Moment-Axial Load interaction diagram and the columns' Moment capacities, approximately 20 kNm for the G+0.3Q load combination (compression positive), and between -45 kNm to +45 kNm for the seismic combination. **Error! Reference source not found.**b depicts the Moment-Curvature diagrams of the Hennebique columns for the minimum and maximum axial loads from all combinations. The drift rotation at yield and at ultimate load were determined as per Annex A, EC8:3 [11]. Yet, it is of crucial importance to also determine the cyclic shear resistance V_R of the columns, since the lack of transverse reinforcement is more probable to result in brittle shear failure, even prior to yielding. The shear capacity (V_R), as per Annex A, EC8:3 [11], is equal to $V_R=6.66$ kN, thus less than the shear equivalent of yielding of the longitudinal reinforcement, $V_y=11.42$ kN; therefore, the Hennebique columns will have premature shear failure in a future seismic event, at a drift of 0.6%.

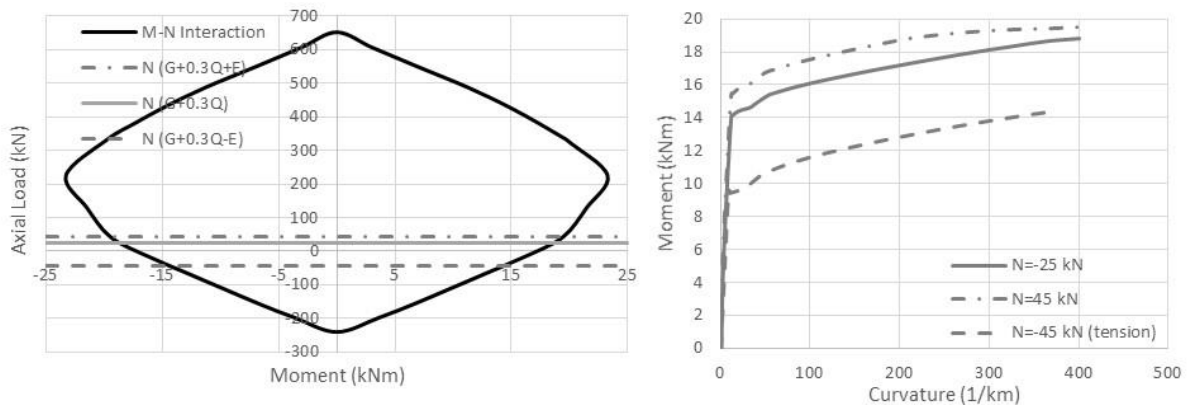


Figure 34. (a) Moment-Axial Load Interaction for Hennebique columns and (b) Moment-Curvature diagrams for various axial loads.

1.1 Elastic Time History Analysis

In order to determine the seismic displacement demand, Time History analysis was performed with a set of three natural accelerograms that were selected based on the provisions of EC8:1 [26]. The three accelerograms were selected to have similar geological conditions with the Melkonian site Type B soil, with magnitudes between 6.5–7.5 that correspond to the seismological context of Cyprus, and with an epicentral distance range of 5–60 km. The average PGA from the three accelerograms was the same as $\gamma_I \cdot a_g \cdot S$, while the average spectrum in the range of periods was between $0.2T_1$ – $2T_1$, i.e. above the 90% of the response spectrum accelerations. Figure 52a shows the ADRS for the three selected accelerograms and the corresponding EC8 response spectrum. The three accelerograms (A, B, C) were placed with load combinations, one in each direction,

while the maximum values from all load combinations were derived for the assessment. Figure 35b depicts the maximum and minimum displacements of the masonry walls, along the height of the structure, from all load combinations.

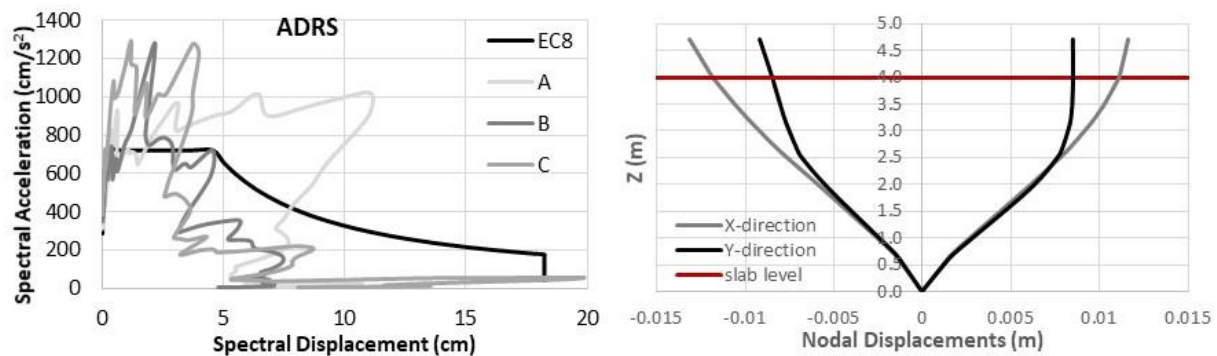


Figure 35. (a) ADRS for the three selected accelerograms and the corresponding EC8 response spectrum and (b) Max and min displacements of Time History analysis over the masonry height in X and Y direction.

The Moment and Shear envelope exhibited by one of the porch columns in the Time History analysis is depicted in Figure 36. Both the shear force and the drift demand suggest that the reinforced Hennebique columns will result in premature shear failure due to the seismic excitation. The low strength of the concrete, the low axial force, as well as the lack of stirrups will all contribute to this brittle type of failure during the design seismic demand.

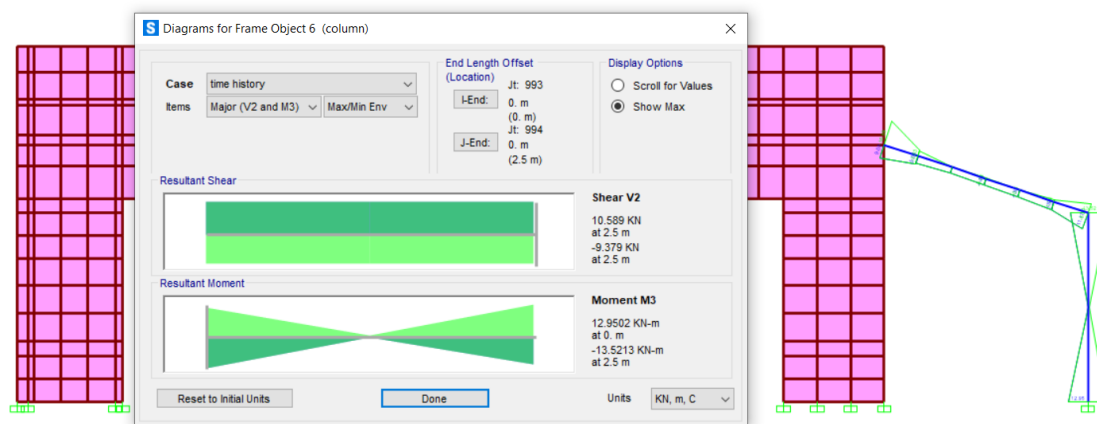


Figure 36. Moment and Shear envelope of Time History analysis of an external column.

2 Conclusions

The structural assessment of buildings requires good understanding of the various components of the structure and of their interconnection, as well as of the material mechanical properties, and finally of the global behaviour under seismic excitation. In the local components level, the task of assessing the properties of members is becoming even more challenging in the case of historic structures, especially those of 100-year old patented designs, such as the Hennebique system. In such cases, thorough member

analysis has to be explicitly performed and all possible failure mechanisms must be taken under consideration. While EC8:3 specifically states that for the case of historic structures the assessment and retrofit “often requires different types of provisions and approaches”, there are no other guidelines that can be applied, bearing in mind that these need to be legitimate for the practicing engineer to use. Therefore, what is prescribed in EC8:3 as assessment procedure is often the only option available.

This research investigated a cultural heritage listed hybrid reinforced concrete-masonry structure, as an example for applying seismic structural assessment according to EC8:3. The analysis used was the linear Time History analysis. The results from the assessment procedures show the definite possibility of brittle shear failure that will be exhibited in the Hennebique columns due to their intrinsic characteristics: i.e., no stirrups, low concrete strength.

Other than this problem of the reinforced concrete Hennebique columns, the report shows that extensive repair is required for the overall structure, due to carbonation, corrosion and other types of damages that have emerged due to the environmental conditions and the many years of abandonment of the structure.

References

- [1] A.M. Chatzilyras, The armenians of Cyprus, Kalatzian Foundation, n.d.
- [2] No Title, (n.d.). <https://alchetron.com/Balyan-family>.
- [3] No Title, (n.d.). http://mei1970.org/history_Of_MEI.
- [4] M.A. Hadjilyras, Armenians of Cyprus, Press and Information Office, Republic of Cyprus, 2013.
- [5] No Title, (n.d.). https://phivosnicolaides.blogspot.com/2009/08/blog-post_09.html.
- [6] MINISTRY OF INTERIOR, Geoportal of the Department of Lands and Surveys, Repub. Cyprus. (n.d.). <https://portal.dls.moi.gov.cy/el-gr/FrontEndHelp/Pages/MapView.aspx>.
- [7] No Title, (n.d.). <http://nonument.org/nonuments/melkonian-educational-institute/#>.
- [8] Listing Decree, n.d. http://www.cylaw.org/KDP/data/2007_1_99.pdf.
- [9] Melkonian Postcard, (n.d.). <https://picclick.com/Cyprus-Postcard-Armenian-Melkonian-Educational-Institute-Nicosia-144073123560.html#&gid=1&pid=1>.
- [10] S. Hadjipanteli, The Melkonian Educational Institute Headmaster’s Mansion, University of Cyprus, 2020.
- [11] CEN. EN1998-3, Eurocode 8 : Design of structures for earthquake resistance —

- Part 3: Assessment and retrofitting of buildings. European Committee for Standardization, Bruxelles, 3 (2004).
http://www.125books.com/inc/pt4321/pt4322/pt4323/pt4324/pt4325/data_all/books/B/BS EN 1998-1 2004 - Eurocode 8 - Design provisions for earth.pdf (accessed September 28, 2015).
- [12] CSI, SAP2000: Static and Dynamic Finite Element Analysis of Structures 14.0, (2009).
 - [13] CEN, Natural stone test methods - Determination of real density and apparent density, and of total and open porosity, European Committee for Standardization, 2006.
 - [14] CEN, Natural stone test methods - Determination of water absorption coefficient by capillarity, European Committee for Standardization, 1999.
 - [15] CEN, Natural stone test methods - Determination of uniaxial compressive strength, European Committee for Standardization, 2006.
 - [16] CEN, Natural stone. Terminology., European Committee for Standardization, 2019.
 - [17] BS EN 12390-3:2009, Testing hardened concrete, Part 3: Compressive strength of test specimens (2009), Br. Stand. Inst. (2009).
 - [18] M.J.N. Priestley, Myths and Fallacies in Earthquake Engineering, Revisited, Rose School, Pavia Italy, 2003.
 - [19] KANEPE, Greek Retrofitting Code, Greek Ministry for Environmental Planning and Public Works, Athens, Greece, 2017.
 - [20] NZSEE, The Seismic Assessment of Existing Buildings, 1st ed., Ministry of Business, Innovation and Employment and the Earthquake Commission, New Zealand, 2017.
 - [21] ΔΟΜΗΤΙΚΕΣ ΕΠΙΕΜΒΑΣΕΙΣ ΤΟΙΧΟΠΟΙΙΑΣ (ΚΑΔΕΤ), (n.d.).
 - [22] E. Standard, EUROPEAN STANDARD Eurocode 1 - Actions on structures Part 4 : Silos and tanks European Committee for Standardization, (2003) 1–110.
 - [23] fib Bulletin No. 24, Seismic Assessment and retrofit of reinforced concrete buildings, International Federation for Structural Concrete (fib), Lausanne, Switzerland, 2003.
 - [24] S.J. Pardalopoulos, G.E. Thermou, S.J. Pantazopoulou, Simple Criteria for Seismic Assessment of Reinforced Concrete Buildings, Bull. Earthq. Eng. 11 (2013) 607–636. <https://doi.org/10.1007/s10518-012-9390-7>.
 - [25] D.V. Syntzirma, S.J. Pantazopoulou, Deformation capacity of r.c. members with

brittle details under cyclic loads, ACI Spec. Publ. 236. ACI-ASCE C (2007).

- [26] P.E. Draft, NATIONAL ANNEX TO CYS EN 1998-1 : 2005 Eurocode 8 : Design of structures for earthquake resistance Part1 : General rules , seismic actions and rules for buildings, (2007) 1–12.

Report on In-Depth Case Study

Old municipal market (Nicosia, Cyprus, 1965)



CONSECH20 – WP2 (iii)

In-Need of Restoration Case Study

Georgiou, A.

Hadjimichael, M.

Ioannou, I.

October 5, 2021

Introduction

Historical background

The modernist building of the ‘Old Municipal Market’ in Nicosia, the capital city of the Republic of Cyprus, is located within the walls of the old city, in the area controlled by the Republic of Cyprus. The construction of Nicosia’s Old Municipal Market began in 1965 and the building opened for business on 18 September 1967. The architect was Stavros Economou, though the design was a collaboration with some other important architects of that period, namely the Zembyla Brothers, D.Kythreoti and C. Vafeadi.

The Market was built in the area where the old Nicosia Town Hall was located (Figure 37), and cost approximately 70,000 CYP. At the time of its design and construction, it aimed to be a modern retail market, an example of its kind in the Middle East, with 70 branches for vegetable sellers, 21 butcheries and 3 fish sellers, as well as a few grocers. The Old Municipal Market was an attempt of the Nicosia Municipality to revive the within the walls city of Nicosia, which was in a recession following the bi-communal clashes which divided the old city of Nicosia in 1963. It thus somehow marks a new era for the old city of Nicosia. In this new era, everyday life and socialisation was no longer bicommunal.

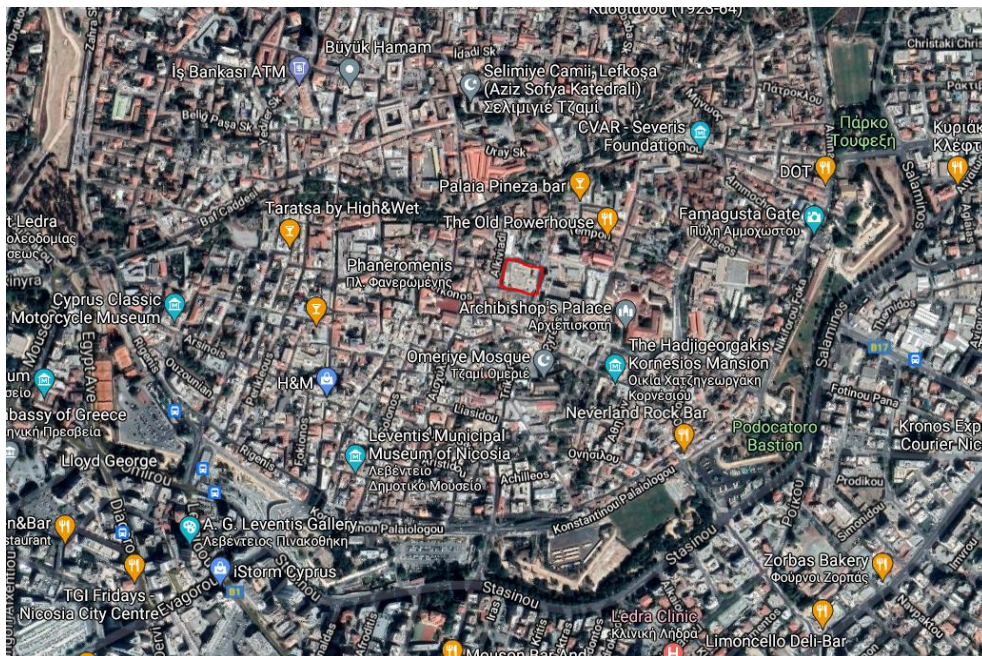


Figure 37. Aerial photo of the Old Municipality Market (in the red rectangle) and the surrounding area [1].

The building has been included in the index of the 100 (most) important buildings, sites and neighbourhoods from Cyprus, compiled by the National Register of Docomomo Cyprus, and is considered to be an excellent example of modernist architecture, also described as ‘mature modernism’; it is characterised by the ‘structural expression of the

grid on the façade', as well as the materials of fair-faced concrete and non-plastered red fired clay bricks [2]. It was listed in 2011, with the decree K.Δ.Π. 53/2011 [3].

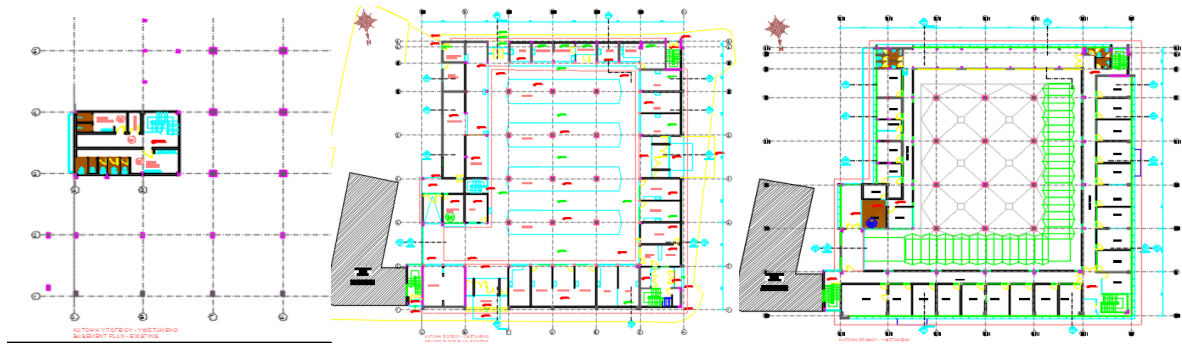


Figure 38. Plans of basement, ground floor and mezzanine, as recorded by Nicosia Municipality

The building is currently in good condition. It comprises of three levels; lavatories in the basement, the retail market on the ground floor, and offices in the mezzanine (Figure 38). The offices were used up until 2020 by the Nicosia Municipality. The retail market is deployed in one large high-roof space on the ground floor, where the vegetable market was taking place (Figure 39). At the perimeter of the ground floor, there are small orthogonal shops (whose entrance is connected with the main central space), which were individually leased to butchers, fish mongers, as well as grocers (Figure 39).



Figure 39. Photos from the Market (2019): Internal views at ground floor (top), roof and mezzanine level (bottom).

According to press cuts of the time [4], retailers active at the market were not particularly happy with the building. They considered the separate branches to be too small and cramped, particularly in combination with the high rent, and it was not

possible to display or store all their products. Sellers in the Municipal Market have also been complaining regarding the lack of ventilation and proper lighting, as well as overcrowding, which led to a suffocating atmosphere.

In 1986, besides the permanent retail sellers in the market, the Nicosia Municipality decided, in another attempt to revive the area, to move the Saturday outdoor Market from Ayios Antonios to the square of the Old Municipal Market. Nevertheless, primarily due to the lack of parking spaces, retailers asked for the outdoor market to move at the bastion near the OCHI square, where it is still taking place.

Putting things into perspective, it is important to remember that such markets have been spaces of socialisation for communities across time and space, and looking into their history/ies one can gather useful information regarding urban and societal shifts.

Though between the 1980s and the early 2000 the Market was an important element, keeping Nicosia within the walls 'alive', it was slowly abandoned, with only 3 sellers remaining in the market by 2017. Between July 2018 and July 2019, the building became home to the 'Agora Project', a project where a group of young social entrepreneurs, artists and activists were given the freedom to run the space and decide upon its functions and ambitions. The 'Agora Project' brought a 'new life' to the space, and though it also gave it a new contemporary meaning, it kept its social value for which markets are known. It was inclusive and multicultural, welcoming people from different backgrounds and ages. It hosted upcycling and ecological initiatives, as well as initiatives of rather more social justice nature. It attracted a number of youth, who got to experience the old town beyond its cafes and shops. Nevertheless, the 'Agora Project' was merely a short metamorphosis of the space, as the Municipality had already promised and offered the building to a newly established Centre of Excellence, known as RISE - Research Centre on Interactive Media, Smart Systems and Emerging Technologies -, to host its activities. This decision by the Municipality falls within its wider plans to turn the area in an entrepreneurship area. New architectural plans have been approved by the Town Planning and Housing Department and restoration works have commenced in Spring 2021. This shift in use of the building will inevitably change the original (social) character of the space and its surrounding area.

Characteristics of the Concrete Building and Structure

The building is of Reinforced Concrete cast on site and consists of four statically independent parts, separated with construction joints (3-5 cm). One part has a basement, but the rest of the structure has two floors above ground. Only the East-South part (green frame) of the structure was selected for analysis in this report, as shown in Figure 40, while some preliminary seismic assessment was also performed for the West part (red frame). The four individual parts consist of R/C slabs, beams, columns and walls; the latter, according to exploratory excavations, are supported on connecting beams without footings. Most frames in the perimeter of the building have brick infill walls that do not extend to the full column height, thus creating captive columns.

Additionally, there is a great irregularity of the structure in terms of stiffness height wise, due to the different height of the floors, great variation of mass distribution and increased masonry infill percentage in the 1st floor.

The west side of the structure consists of R/C frame beams and columns, while in plan it has an irregular L-shape, indicating that the center of rotation will be offset from the center of mass. Most of the columns continue with the same dimensions in the 1st floor, while the reinforcement remains the same or is slightly reduced. Some of the 1st floor columns are supported on beams and are not continued to the ground floor. The cross-sectional width of the beams varies from 0.200 m to 0.515 m, while the beam height is 0.7 m. The ground floor has a height of 4.45 m, while the height of the first floor is 3.10 m. The floor slabs are 0.2 m deep.



Figure 40. Floor plan showing the structure that was assessed in this report (in green)

Note that the Republic of Cyprus, which was only established in 1960, had no universities or research centres until about 25 years ago, and no regulations for the design of concrete structures existed in the past. Cypriot engineers who studied in various countries abroad were designing according to the regulations of those countries. There was no knowledge of the design practices against seismic excitations and no measurements of the local intensities of earthquakes, and therefore buildings were designed only for gravity loads. At that time, it is also important to note that there were no batching plants in Cyprus either, and concrete was thus prepared on site in small quantities ca. 2 tn at a time. This led to great variability in the quality of concrete in the

various parts of a structure, even from the bottom to the top of a column, as there was also no equipment for vibration and proper compaction and consolidation.

Typical damages found in the Old Municipal Market

Typical damages were recorded and are shown in Figure 25. Cracks are visible in most of the beams of the structure. Drainage from the roof passes through some of the external columns of the building, increasing moisture in the columns and inducing potential corrosion to the reinforcement. The base of the columns with drainage systems, in fact, shows extensive concrete cracking, probably due to the corrosion of the reinforcement. The overall state of the building is rather good, despite its abandonment and lack of maintenance for many years. In general, there are no visible cracks from seismic loads on the reinforced concrete elements.

Corrosion is evident in some of the slabs of the 1st floor, especially at the locations where the rain water is not properly removed from the roof and in the columns of the ground floor, where cover has spalled and the reinforcement is exposed. The slabs at these locations have black stains and show cover delamination. All deterioration in reinforced concrete is connected with moisture, carbonation and corrosion of the reinforcement. The walls in one of the shops also have some diagonal cracking, that suggests minor settlement of the foundations. Mosses and blemishes were recorded to be extensive in the exterior surfaces of reinforced concrete.



(a) Rust stains



(b) Rust stains



(g) Poor cover – exposure of reinforcement



(h) Poor cover – exposure of reinforcement –

extensive erosion



(c) Cover delamination and rebar corrosion



(d) Cover delamination and rebar corrosion



(e) Water drainage passing through columns with extensive stains and cracking



(f) Mold, stains, efflorescence internally under slab



(i) Deformations in the cantilever slab



(j) Horizontal cracks at the connections of the infill walls with the structural system



(k) Deflection cracks on beams



(l) Short columns due to partial infill walls

Figure 41. Recorded damages in the Old Municipal Market (2019-2020).

Investigation, Methods and Results

For the seismic assessment of the residence, EC8:3 [5] was used. The procedure adopted is shown below:

- x. verification of the geometry of the structural elements and reinforcement detailing with regards to the original plans provided by the municipality,
- xi. evaluation of the material properties through in situ non-destructive and destructive tests (results provided by the municipality),
- xii. simulation of the building in the analysis program SAP2000 [6] and
- xiii. assessment of its capacity under Time-History analysis.

Survey and testing of materials

Extended survey was performed for the verification of the geometry and member sizes. Only some of the original construction drawings were found, that showed great variation with the as-built investigation. In order to increase the detailing information, a rebar detector was used to detect the steel bar reinforcement, the bar cover and diameter, in the beams and columns (Figure 42). Steel was mild S220 without ribs. Based on the old drawings of the structure, the column concrete cover was specified at 2-5 cm, while the lap splices were $40d_b$ long.

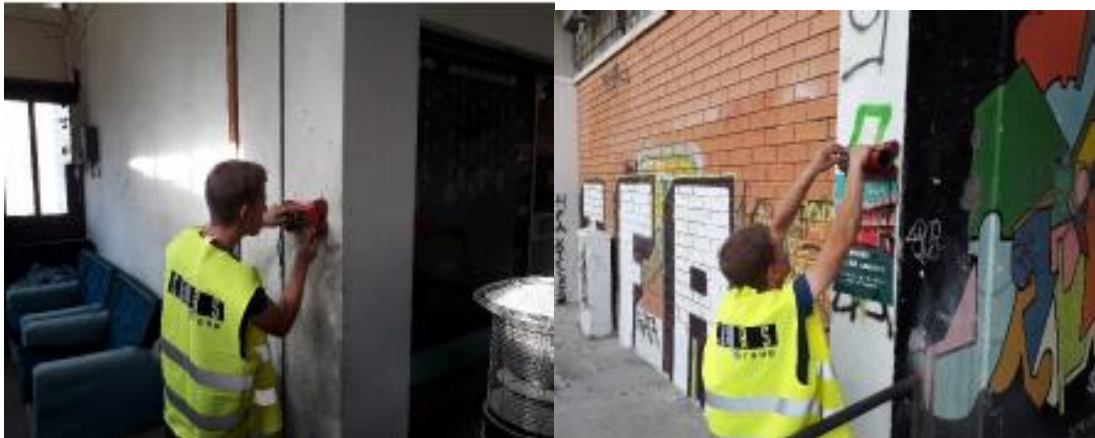


Figure 42. Rebar detection and diameter/cover measurement (CEARS Cyprus)

The detection of the reinforcement position was also used to determine the locations for non-destructive rebound tests (EN 12504-2) and the possible positions for core sampling of concrete (EN 12504-1). The core samples were enough to determine the Knowledge Level of the strength of materials as extensive, KL3, as required for nonlinear assessment based on EC8 Part 3 [5]. Core samples were also used to determine the carbonation depth, the aggregate size and the chloride content of concrete. All the tests were performed by the Laboratories CERS Cyprus and Geoinvest Ltd, and the results were kindly provided for this report by Nicosia Municipality. Exact locations of the tests are recorded in Appendix A.

Carbonation depth

Figure 43 depicts the tests for the determination of carbonation depth on the structural members after core extraction and on the cores themselves, using phenolphthalein (EN 14630). The uncarbonated concrete shows in purple colour. The carbonation depth at each test location is registered in Table 3. The results indicate that, in most cases, carbonation depth was less than the cover of the reinforcement, with only limited members (highlighted) exhibiting values up to the cover depth.



Figure 43. Coring of concrete samples and carbonation depth test.

Table 3. Carbonation Depth, GF: Ground floor, 1F: 1st floor, BF: Basement

| Geoinvest | Member | Carbonation depth (cm) | Member | Carbonation depth (cm) |
|----------------|--------|------------------------|--------|------------------------|
| | K1 GF | 1.0-1.5 | K5 1F | 0.5-1.0 |
| | K2 GF | 2.5-3.0 | K6 1F | 4.5-5.0 |
| | K3 GF | 1.0-1.5 | Δ1 1F | 1.0-1.5 |
| | K4 GF | 0.5-1.0 | Δ2 1F | 1.5-2.0 |
| | K5 GF | 4.5-5.0 | Δ3 1F | 2.0-2.5 |
| | K6 GF | 1.0-1.5 | Δ4 1F | 1.0-1.5 |
| | Δ1 GF | 2.0-2.5 | Δ5 1F | 2.5-3.0 |
| | Δ2 GF | 0.5-1.0 | Δ6 1F | 3.5-4.0 |
| | Δ3 GF | 0.5-1.0 | Π1 1F | 0.0 |
| | Δ4 GF | 0.5-1.0 | Π2 1F | 0.0 |
| | Δ5 GF | 1.0-1.5 | Π3 1F | 0.0 |
| | Δ6 GF | 1.0-1.5 | Σ1 BF | 1.5-2.0 |
| | Π1 GF | 0.0 | Σ2 BF | 2.0-2.5 |
| | Π2 GF | 0.0 | Σ3 BF | 2.0-2.5 |
| | Π3 GF | 0.0 | K1 BF | 0.0 |
| | K1 1F | 0.5-1.0 | K2 BF | 0.0 |
| | K2 1F | 1.5-2.0 | Δ1 BF | 1.0-1.5 |
| | K3 1F | 1.5-2.0 | Δ2 BF | 1.0-1.5 |
| | K4 1F | 1.5-2.0 | | |
| CERS Cyprus | Zone | Level | Member | Carbonation depth (cm) |
| | Π1 | GF | K9 | 0.8 |
| | Π2 | GF | K9 | 1.5 |

Chloride content in concrete

The results of the laboratory testing for chloride content are recorded in Table 4. The maximum accepted quantity as per BS 8110 is 0.4% by weight of cement, while in CYS 300:2008 that is 0.2%. The laboratory carrying out the tests assumed the percent of cement in the specimens tested to be in the order of 15%.

Table 4. Chloride content in concrete (Geoinvest)

| Member | By weight of sample Cl ⁻ % | By weight of cement Cl ⁻ % |
|--------|---------------------------------------|---------------------------------------|
| K2 GF | 0.012 | 0.08 |
| K6 GF | 0.003 | 0.02 |
| K2 1F | 0.033 | 0.22 |
| K6 1F | 0.037 | 0.25 |
| Δ3 GF | 0.003 | 0.02 |
| Δ2 GF | 0.027 | 0.18 |
| Δ1 1F | 0.001 | 0.01 |
| Δ5 1F | 0.051 | 0.34 |

Concrete mix and compressive strength

At the time of the construction of the case-study building, there were no batching plants in Cyprus and concrete was thus prepared on site in small quantities ca. 2 tn at a time. This led to great variability in the quality of concrete in the various parts of a structure, even from the bottom to the top of a column, as there was also no equipment for vibration and proper compaction and consolidation. The concrete mix design, as described on the old drawings that were found, was 1:1.5:3 by volume (cement:sand:coarse aggregates) for columns and 1:2:4 by volume for beams and slabs. For the case of 1:2:4 analogies, based on oral communication, 1 part of water was used if the aggregates were wet, while 1.5-2 parts of water were used if the aggregates were dry. For the concrete mix, crushed diabase coarse aggregates and natural sand were used. From the concrete cores, aggregate with diameter >20 mm can be observed. The compaction of the concrete was deemed average to good, while the pore diameters are small (0.5-3.0 mm).

Uniaxial compression (EN12390-3 [7]) tests were performed on a number of cores extracted from the members of the structure (Figure 44). The results are listed in Table 9. An average of 17.77 MPa was found from the compression tests (EN 12504-1) on the ground floor columns at higher levels, with a standard deviation of 3.48 MPa, while when the tests were performed in the lower parts of the columns, the results reached only 10.6 MPa. The mean compressive strength of the columns on the first floor was 12.77 MPa. Beams and floor slabs had higher compressive strengths.

Table 5. Compressive strength of concrete

| Member | Average compressive strength from tests (N/mm ²) | SD |
|----------------------------|--|------|
| Columns GF | 17.77 (10.60 at lower parts) | 3.48 |
| Columns 1 st 1F | 12.77 | 4 |
| Beams GF | 17.74 | 2.6 |
| Beams 1 st 1F | 16.51 | 6.7 |



Figure 44. Concrete cylindrical specimens extracted from the structure.

Rebound Number and compressive strength

The non-destructive Rebound test was deployed in order to assess the compressive strength variance among the different members of the structure, in combination with the compressive strength resulting from the core samples that were extracted (see also section 2.1.3). The compressive strength assessed from the Rebound test is recorded in Table 6, for different types of elements and floor levels. The corresponding strengths based on measurements from Ultrasonic Pulse Velocity tests, calculated from Eq.1 [8], are also shown and average values of strength are derived.

$$f_{v,cm} = 14.143 \cdot V^2 - 98.044 \cdot V + 179.57 \quad (1)$$

Where $3.5 \leq V \leq 5.5$ the velocity of pulse in km/sec.

Table 6. Rebound and Ultrasonic Pulse Velocity measurements - Non-destructive testing CERS Cyprus

| Non-destructive testing CERS Cyprus | | | |
|-------------------------------------|------------------|---------------------|--|
| | Rebound test | Pulse velocity test | |
| | $f_{Q,cm}$ (MPa) | $f_{v,cm}$ (MPa) | $f_{m,is}$ (MPa)=($f_{Q,cm}$ + $f_{v,cm}$)/2 |
| K9 1 st Floor | 29.6 | 9.7 | 19.65 |
| Δ64 GF beam | 39.8 | 9.7 | 24.75 |
| Δ68 GF beam | 15.6 | 9.7 | 12.65 |
| Δ79 GF beam | 22.8 | 9.7 | 16.25 |
| Δ79 GF beam | 23.7 | 9.7 | 16.7 |
| | | Mean | 17.59 |
| | | SD | 5.11 |
| Δ84 1F beams | 29.3 | 12.2 | 20.75 |
| Δ84 1F beams | 23.2 | 9.7 | 16.45 |
| Δ64 1F beams | 37.8 | 9.7 | 23.75 |

| | | | |
|--------------|------|------|-------|
| Δ68 1F beams | 31.0 | 12.1 | 21.55 |
| | | Mean | 20.63 |
| | | SD | 3.06 |

Concrete cover and Rebar Diameter

The cover to the reinforcement was established both by the use of the rebar detector and also from exploratory removal of the cover, while the same procedure was used to determine the rebar diameter (Figure 45). The concrete cover to the longitudinal bars was in the order of 20-50 mm.



Figure 45. Verification of bar diameter in RC members (CEARS Cyprus)

Reinforcement layout and diameter with rebar detector

The reinforcement was in close agreement with the original detailing drawings. Exploratory excavations showed that the columns continued up to 2 m underground in order for the foundation to reach a solid ground. Some caves were found below the ground floor slabs. The columns at the foundation level were connected with beams with very sparse reinforcement. Many of the columns had drainage pipes embedded in them, something that is now forbidden by the Codes. Stirrups in beams were sparse, not suitable for ductile structures and the formation of plastic hinges at the edges of members. The lap splicing of the longitudinal reinforcement was also found to be less than what is required as per current seismic codes. Additionally, the reinforced concrete walls shown on the original drawings were connected only on beams at the foundation level, leading to the conclusion that they cannot attain flexure due to the lack of foundation system. Photo evidence of the above is shown in Figure 46.



Figure 46. Exploratory excavations and concrete cover removal during retrofit works

Assessment of seismic capacity of the structure

Simulation of the structure

Modelling of the structure was performed by a 3D model, to include any possible torsional effects. The assessment analysis performed was Time-History with the use of an inelastic model.

Elements, materials and other parameters

The structure was modelled in the commercial program SAP2000 [6] in order to assess its capacity under seismic conditions. The reinforced concrete beams and columns were simulated as 2-node frames. The mean average strengths were used for determining the properties of the various materials. For all the elements in the structure under study, modifiers were used to decrease the stiffness of the cross sections to the actual cracked stiffness, assessed by the actual Moment-curvature diagrams with the use of RESPONSE2000 [9], in order to take into consideration the stiffness degradation during the seismic event [10,11]. Diaphragmatic action was applied to all the nodes of the floor levels. The members were connected to the ground with linear links, according to the properties of the foundation system and the soil, while the walls in the basement under the soil level were assigned with springs that allow movement away from the soil, but prevent movement when in contact with it. All the floor slabs were assigned with the load combination of $G+0.3Q$, with additional load for the finishing of the floor surfaces. The live load was chosen based on the Cypriot Annex of Eurocode 1 [12]. This load combination was also used to derive the mass of the structure for the modal analysis. Some of the columns of the GF were assigned with hinges (zero moment), at their bottom node, due to the increased axial load ratio $\nu = N_{G+0.3Q} / (A_c f_c)$ (Figure). Note that those columns are subjected to a value of ν that is close to the limit of 0.4 that corresponds to balanced column failure, which identifies the limit of brittle response in the Axial – Load vs. Moment Interaction Diagram. This load ratio is estimated from service life loads only, without considering the additional axial load that the seismic overturning action will impose to the columns. On account of the high value of ν and the reported corrosion of reinforcement in the base of those columns, it is concluded that no moment can be resisted in their base; thus, a hinge was assigned in the model.

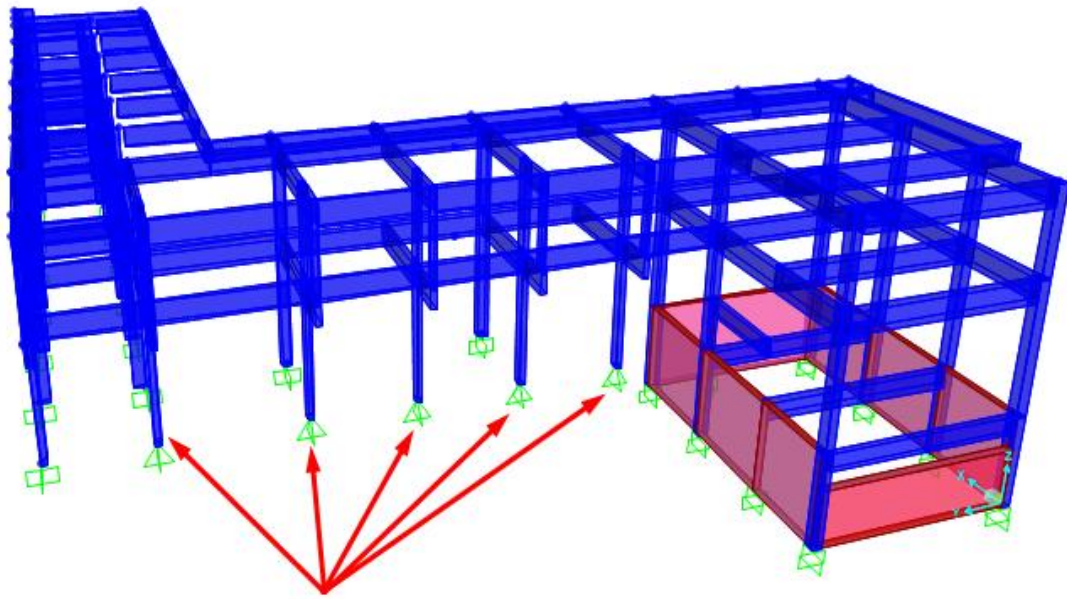


Figure 47. Simulation of the structure in SAP2000 and hinge assignment at the bottom of columns

Discussion

Assessment of the failure mechanism in reinforced concrete columns

The brittle failures that may incur to old substandard members, designed without any seismic provisions, are a crucial parameter for the assessment and retrofit of reinforced concrete structures [13]. The hierarchy between the individual failure mechanisms must be assessed in order to determine any prevailing brittle failure. The mechanisms of column failure, in terms of Shear Force, in the columns that were examined were the following (**Error! Reference source not found.**):

- Yielding of the flexural reinforcement and failure in flexure, (V_{flex})
- Shear failure, (V_v)
- Anchorage and Lap splice failure, (V_a / V_{lap})
- Joint shear failure, (V_j)
- Formation of plastic hinges in the adjacent beams (ductile behavior) V_{by}

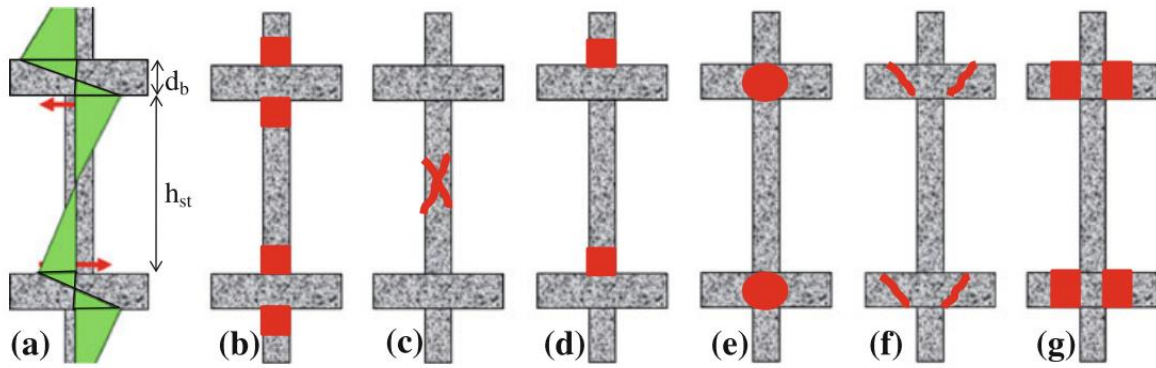
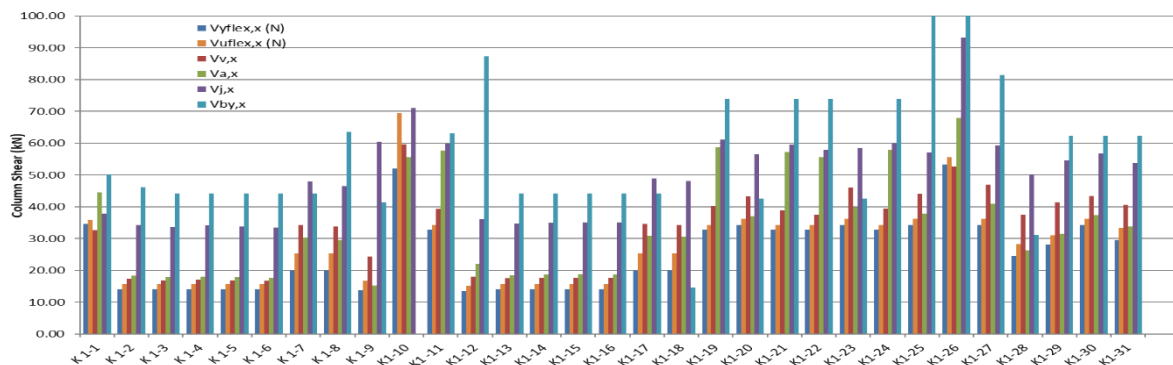


Figure 48. a Moment distribution and b–f possible failure modes of a reinforced concrete column: b flexural yielding, c shear failure, d bar anchorage/lap-splice failure, e joint shear failure, f connection punching failure, g column shear limited by plastic hinging in the beams \Rightarrow ductile frame behaviour [13].

The results from the analysis performed are shown for the X-direction in the charts of Figure 49. The first assumption to be made is that in almost all cases the failure of the columns will prevail yielding of the beams. This is attributed to the wrong type of design of RC members of the era that required “strong beams-weak columns”. The earthquakes that followed showed that, that kind of design was wrong, leading to collapse of the members, while modern seismic codes, through the capacity based design approach, have rectified the approach promoting a “strong column-weak beam” design.

Additionally, the results indicate that most of the columns in the ground floor will behave in a ductile manner with flexural failures, except for some columns with very high axial load that will show brittle failure of the compressive zone prior to yielding of reinforcement, and some cases of brittle shear failure for loads parallel to the weak axis of the members. On the contrary, most of the columns in the 1st floor will fail due to brittle shear failure, due to their short length, in combination with the very sparse stirrups, having a spacing of more than 300 mm.



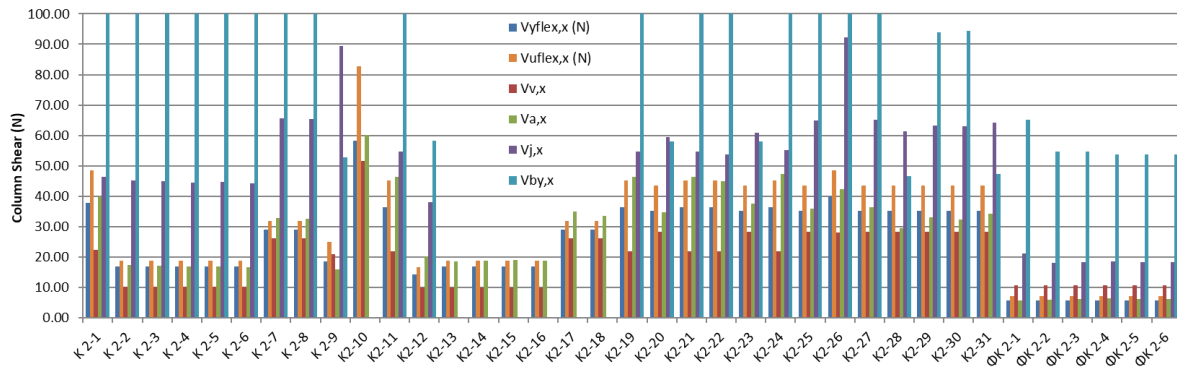


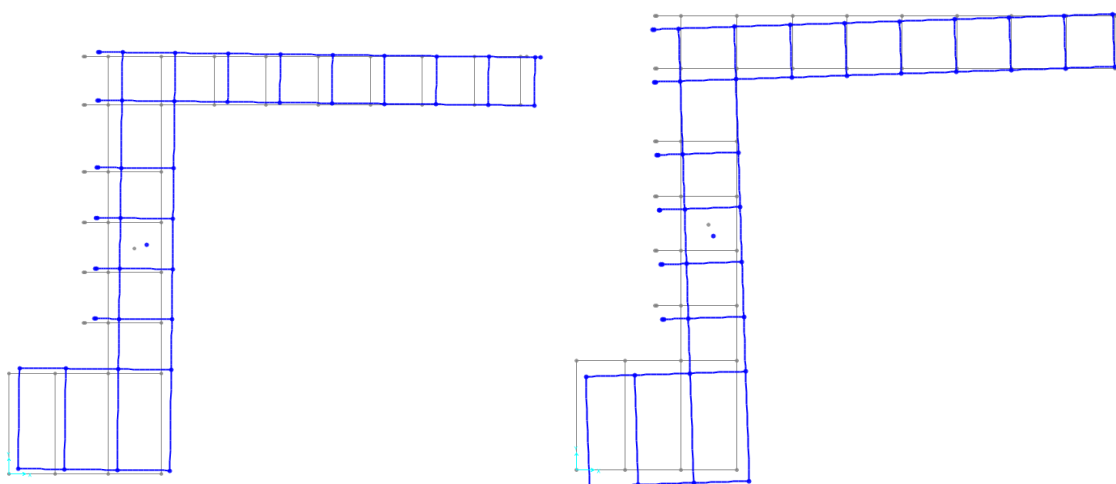
Figure 49. Shear force for different mechanisms of failure for the X-direction of seismic action, for the ground floor columns (top) and the 1st floor columns (bottom)

Modal characteristics of the structure

The first three modal shapes of the structure are depicted in Figure 50 and their characteristics are recorded in Table 7. While the first mode of the structure is primarily translational in the X-direction, with a very high period, compared to new structures designed as per the Eurocode, the second and third modes are combined translational to the Y-axis and rotational around the Z-axis. This is in agreement with the finding that the CM has high eccentricity to the CR in the X-direction.

Table 7. Results from modal analysis

| StepNum | Period | SumUX | SumUY | SumUZ | SumRX | SumRY | SumRZ |
|----------|--------------|----------|----------|----------|----------|----------|----------|
| Unitless | Sec | Unitless | Unitless | Unitless | Unitless | Unitless | Unitless |
| 1 | 0.995 | 0.826 | 0.045 | 0.000 | 0.00014 | 0.00584 | 0.05029 |
| 2 | 0.936 | 0.897 | 0.614 | 0.000 | 0.00218 | 0.00625 | 0.2555 |
| 3 | 0.459 | 0.897 | 0.892 | 0.000 | 0.00468 | 0.00626 | 0.87396 |



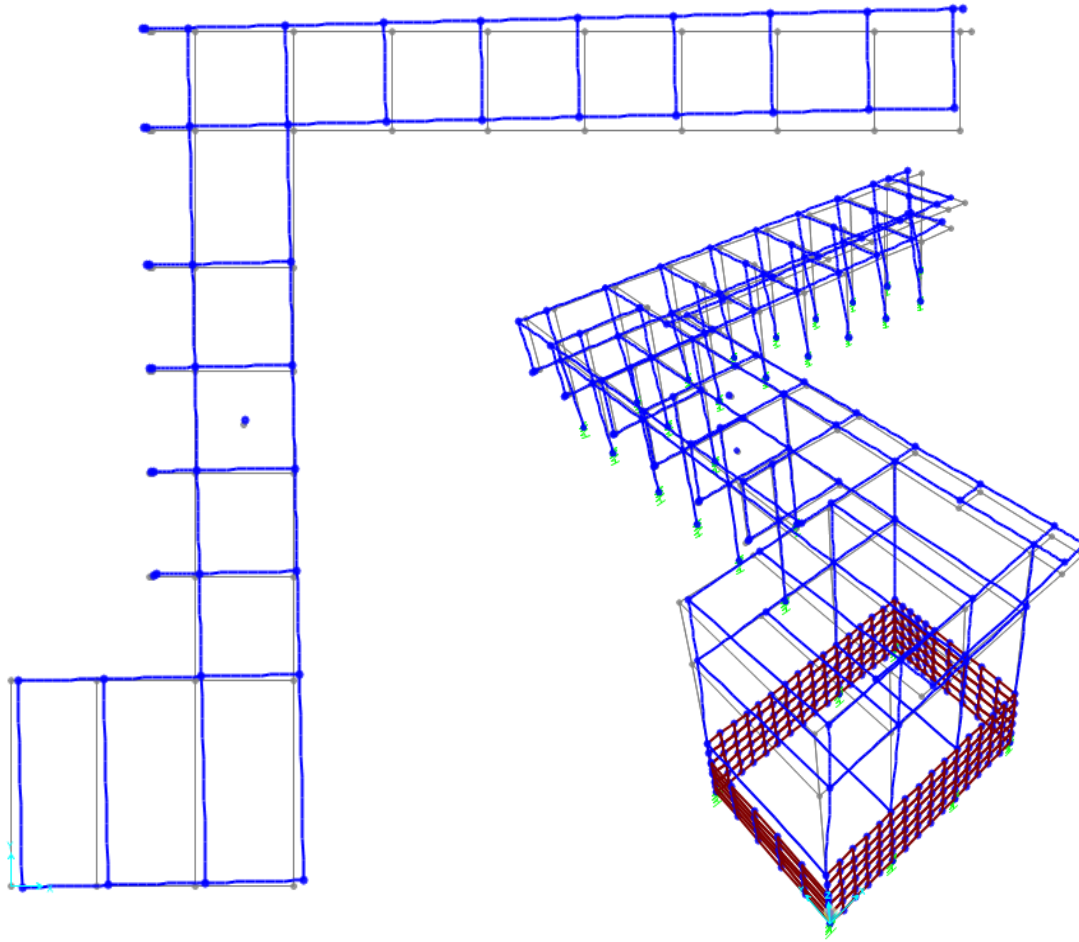


Figure 50. 1st mode $T=1.003$ sec, 2nd mode $T=0.95$ sec and 3rd mode $T=0.495$ sec.

Additionally, when the mode shapes are plotted heightwise in Figure 51, it is clear that the structure behaves as a pilotis, with a soft ground floor storey, indicating that during the seismic loading most of the displacement that will be induced in the structure due to the motion, will be undertaken by the ground floor columns, leading to increased levels of ductility demand.

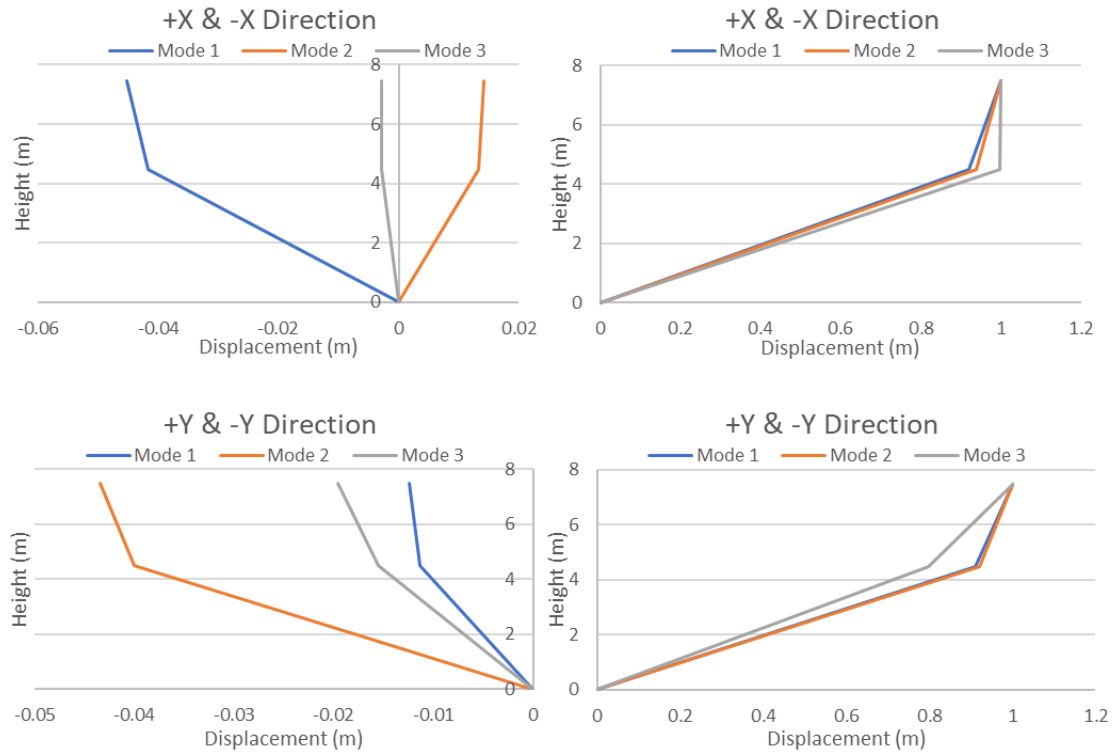


Figure 51. Displacements from modal analysis (left) and Mode shapes heightwise (right) at the CM

Time History Analysis

In order to determine the seismic displacement demand, Time History analysis was performed with a set of seven natural accelerograms that were selected based on the provisions of EC8:1 [14]. The accelerograms were selected to have similar geological conditions with the site soil (Type C), with magnitudes between 6.0-7.0 that correspond to the seismological context of Cyprus and with an epicentral distance range of 5-60 km. The average PGA from the accelerograms was the same as $\gamma_{rag}S$, while the average spectrum in the range of periods between $0.2T_1$ - $2T_1$, was above 90% of the response spectrum accelerations, in each direction of motion. Figure 52 (a) shows the ADRS for the selected accelerograms and the corresponding EC8 response spectrum. The accelerograms were placed in each direction simultaneously and in combination, while the average values from all load combinations were derived for the assessment.

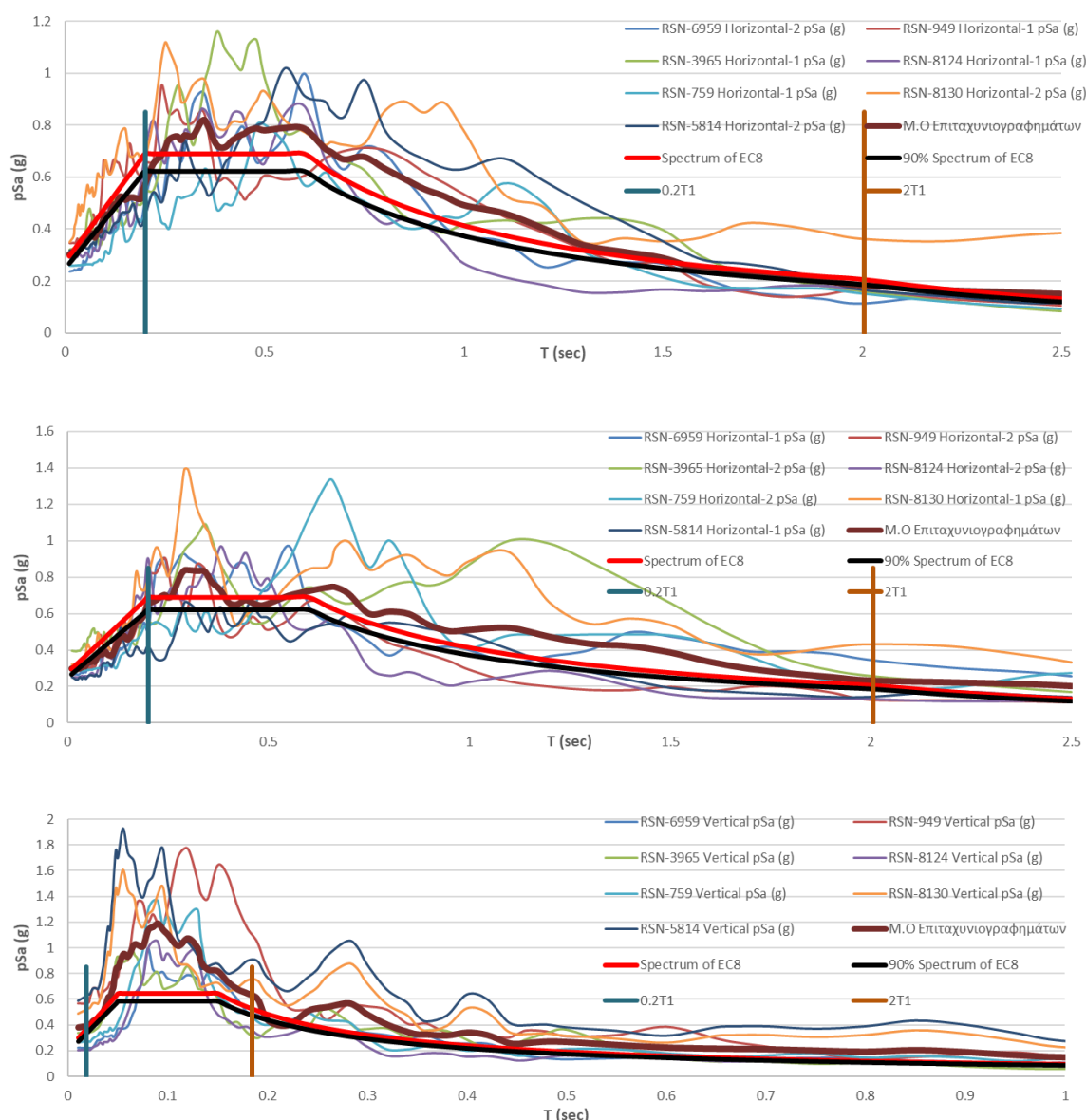


Figure 52. (a) Acceleration spectra for the selected accelerograms and the corresponding EC8 response spectrum in X, Y and Z direction.

Figure 53 depicts the drift demands along the height of the structure, from all load combinations, and the levels of damage of the members from the analysis. Even though the 1st floor columns undergo a very low level of drift in the order of 0.5% (related to the yielding of the flexural reinforcement), it is seen that most of them have failed and are in levels of damage not accepted by the assessment performance objectives. This is due to the previous conclusion that the 1st floor columns collapse in brittle shear failure prior to yielding of the flexural reinforcement. Additionally, the drift demands in the ground floor, in the order of 2-2.5%, require great drift ductility of the ground floor columns, in the order of 4, yet the members seem able to perform them, albeit in the level of significant damage, something that is accepted by the Performance objective.

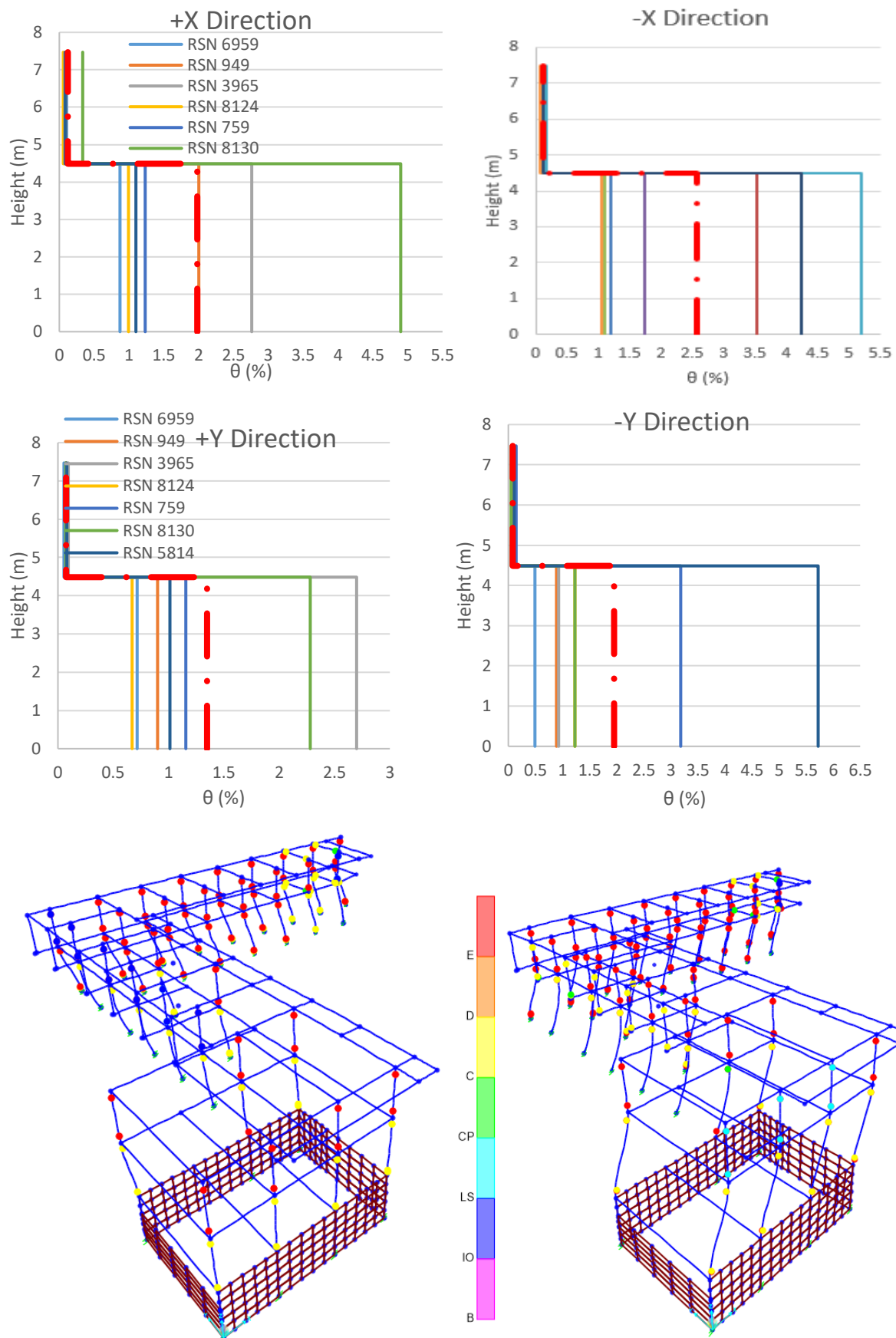


Figure 53. Drift demands from all accelerogram combinations and Damage level of the structure for combinations (RSN 759) and (RSN 8130)

Conclusions

The structural assessment of buildings requires good understanding of the various components of the structure, their interconnection and material mechanical properties, and finally the global behaviour under seismic excitation. In the local components level, the task of assessing the properties of members is becoming even more challenging in the case of historic structures. In such cases thorough member analysis has to be explicitly performed and all possible failure mechanisms must be taken under consideration. While the code specifically states that for the case of historic structures the assessment and retrofit “often requires different types of provisions and approaches”, there are no other guidelines that can be applied, which are at the same time legitimate for the practicing engineer to use. Therefore, what is prescribed in EC8:3 as assessment procedure, is often the only option available.

This case study explored a cultural heritage listed reinforced concrete-masonry structure, as an example for carrying out seismic assessment as per EC8:3. Non-linear Time History analysis was used. The results from the assessment procedures show the possibility of brittle shear failure in the 1st floor columns due to their intrinsic characteristics: sparse stirrups, low concrete strength. Additionally, the report shows that extensive repair is required for the overall structure due to carbonation, corrosion and other types of damages that have been effected by environmental conditions and the many years of lack of maintenance and abandonment of the building. Seismic strengthening of historic concrete structures is mandatory in areas prone to earthquakes, such as Cyprus, if the society does not want to let these types of buildings collapse and vanish in a future seismic event.

References

- [1] MINISTRY OF INTERIOR, Geoportal of the Department of Lands and Surveys, Repub. Cyprus. (n.d.). <https://portal.dls.moi.gov.cy/el-gr/FrontEndHelp/Pages/MapView.aspx>.
- [2] S. Michael, A., Constantinou, C., & Feraios, Learning from the Heritage of the Modern., 2009.
- [3] Listing Decree, Department of Town House and Planning, 2011. http://www.cylaw.org/KDP/data/2011_1_53.pdf.
- [4] Anon, Inaction at the Central Municipal Market of Nicosia., Newsp. 'Haravgi.' (n.d.) Page 1.
- [5] CEN. EN1998-3, Eurocode 8 : Design of structures for earthquake resistance — Part 3: Assessment and retrofitting of buildings. European Committee for Standardization, Bruxelles, 3 (2004). http://www.125books.com/inc/pt4321/pt4322/pt4323/pt4324/pt4325/data_all/books/B/BS EN 1998-1 2004 - Eurocode 8 - Design provisions for earth.pdf (accessed September 28, 2015).
- [6] CSI, SAP2000: Static and Dynamic Finite Element Analysis of Structures 14.0, (2009).
- [7] BS EN 12390-3:2009, Testing hardened concrete, Part 3: Compressive strength of test specimens (2009), Br. Stand. Inst. (2009).
- [8] L. Logothetis, Combination of three non-destructive methods for the determination of the strength of concrete, Athens University, 1979.
- [9] M.P.C. Evan C Bentz, RESPONSE2000 Reinforced Concrete Sectional Analysis using the Modified Compression Field Theory, (2000).
- [10] KANEPE, Greek Retrofitting Code, Greek Ministry for Environmental Planning and Public Works, Athens, Greece, 2017.
- [11] NZSEE, The Seismic Assesment of Existing Buildings, 1st ed., Ministry of Business, Innovation and Employment and the Earthquake Commission, New Zealand, 2017.
- [12] E. Standard, EUROPEAN STANDARD Eurocode 1 - Actions on structures Part 4 : Silos and tanks European Committee for Standardization, (2003) 1–110.
- [13] S.J. Pardalopoulos, G.E. Thermou, S.J. Pantazopoulou, Screening criteria to identify brittle R.C. structural failures in earthquakes, Bull. Earthq. Eng. 11 (2013) 607–636. <https://doi.org/10.1007/s10518-012-9390-7>.
- [14] P.E. Draft, NATIONAL ANNEX TO CYS EN 1998-1 : 2005 Eurocode 8 : Design of

structures for earthquake resistance Part1 : General rules , seismic actions and rules for buildings, (2007) 1–12.

Restored Cases

Report on In-Depth Case Study

Case Study: Timmerfabriek (Vlissingen)



Type: **Restored Case**

Partner Institution: TU Delft

Project: **CONSECH 20**

Working Package 2 – Task (iii)

Date: **October 15, 2021**

By:

Gabriel Pardo Redondo
Silvia Naldini
Barbara Lubelli

Introduction

The Timmerfabriek in Vlissingen is a reinforced-concrete building built between 1913 and 1915 (Figure 54). The 3-storey building was part of a larger shipyard; its main function was to manufacture the wood elements of the ships. In the decade of the 1990s, the building was abandoned. In 2010 a restoration campaign was performed to address the severe damage in the façades, consisting of concrete spalling and cracks.

In May 2021, 10 years after the repairs, TU Delft performed an in-depth assessment of the interventions and the overall condition of the concrete structure. At the time of the inspections, the building was under renovation to convert it into a hotel.

The investigation aimed to assess the condition of the repaired zones in 2010 as an indication of the quality of the repair and its durability after a period of 10 years. The investigation started off with an archival research to find out the characteristics of the intervention (materials, procedures, etc.), followed by a visual inspection to localize the areas where to run further testing. Lastly, a non-destructive testing campaign was performed to assess the condition of the repairs. The results of this investigation aims to provide information about what are the key parameters for successful patch repairs.



Figure 54. The Timmerfabriek (1914). Source: <https://architectenweb.nl/nieuws/artikel.aspx?ID=22688>

Characteristics of the Concrete Building and Structure

Materials

The existing reinforced concrete has an estimated compressive strength of 38.5 MPa (+/- 3.77) assessed with Schmidt Hammer (refer to Section 0). The reinforcement is plain round rebar and has a concrete cover in exterior columns between 20 to 25 mm; the cover in walls varies between 20 to less than 10 mm, as the thickness of the walls varies. The coarse aggregates of the concrete are natural and round, with maximum side dimension of 20 mm. The binder used in the concrete is unknown, but given the grey colour and the year of construction, it is very likely that is Portland cement (Figure 55).



Figure 55. Section of the wall cut during the 2021 renovation.

Type of structure

The building structure is a reinforced concrete frame with no interior shear walls. The frame has rectangular and square columns, girders running north-south, and secondary beams running east-west supporting one-way floor slabs (Figure 56). The foundations are likely piles, but this is not confirmed.

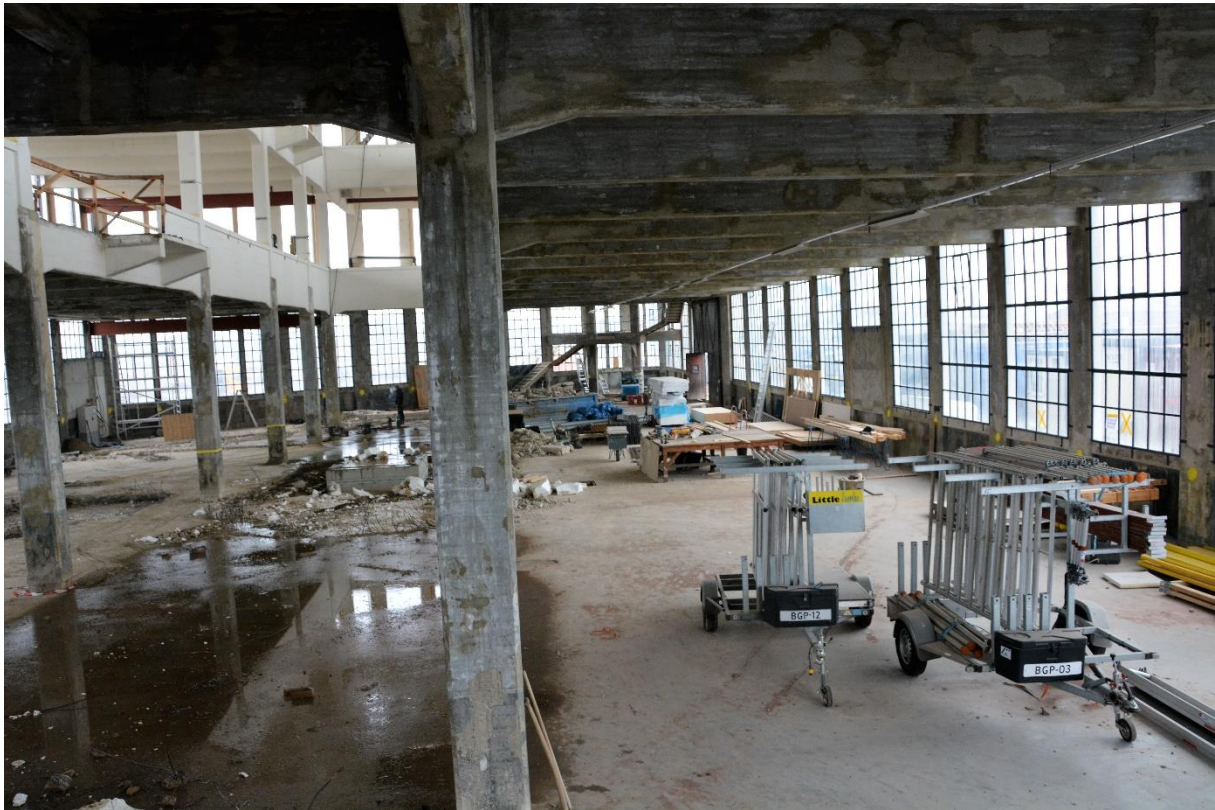


Figure 56. Inside of the building. Ground floor looking north.

Condition of the building

Damage types found in 2010

The damage found in 2010 were vertical individual cracks in walls under windows, and spalling in exterior columns and walls (refer to Figure 57 & Figure 58)².

² By examining the pictures and assessment reports provided by the company Bouwgroep Peters B.V. and TNO.



Figure 57. Damage in 2010. Source: TNO.



Figure 58. Condition of the building in 2010. Source: TNO.

Hypothesis on damage processes

Given the type of damage, and the testing performed in the building (refer to Sections 0 & 0), the likely cause of the damage is carbonation-induced corrosion. The visible cracks are aligned with the reinforcement, suggesting expansion forces due to corrosion. Spalling was localized in areas of reinforcement where the concrete cover is minimum. From the pictures obtained, pitting corrosion is not visible; neither is it mentioned in the documentation related to the intervention³.

³ Work specifications and Concrete reconstruction document by Roothuizen van Doorn't Hooft Architecten – Stedenbouwkundigen 2009



Figure 59. Condition of the building in 2010. Source: TNO.

Intervention in 2010

The architects Rothuizen, specialized in the restoration of young and historic monuments, carried the intervention project of 2010. For the assessment of the concrete and the advice on the repairs. The specialized company SGS-Intron was hired to complete the damage assessment of the exterior facades. In elevation drawings and pictures, the damage types were annotated (Figure 60).

The architects also provided a catalogue with the different types of repairs depending on type and characteristics of the damage (Figure 61). With this catalogue, the subcontractor performing the repairs could apply the specific repair detail according to the damage.

According to the architect's specifications, the subcontractor in

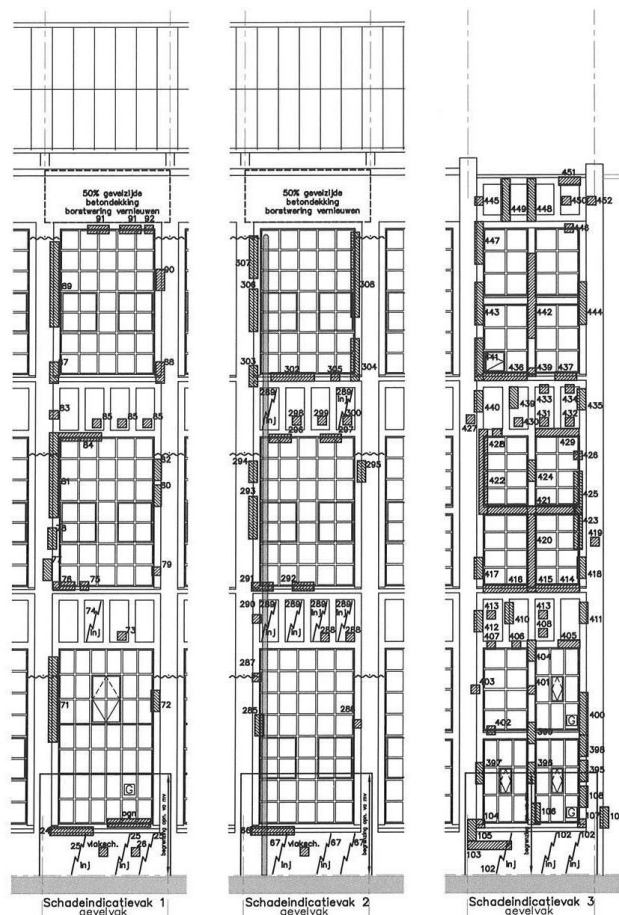


Figure 60. Partial elevation drawing with damage mapping from the company Rothuizen Architecten. Source: Rothuizen.

charge for the concrete repairs needed to have the accreditation BRL 3201. This accreditation ensures that the company has experience in concrete repairs and is aware of the different materials and procedures. This accreditation, however, it is not specifically suited for historic concrete.

The patch repairs were done according to the Dutch guidelines CUR Recommendations 53 “Sprayed Concrete” and CUR 54 “Concrete repair with polymer-modified repair mortars”⁴. It also followed the European norms EN-1504 that specify materials, surface preparation and installation of repair mortars. However, in the documentation, it was not found what specific part of this EN norm was used. The mortar repairs were selected to have higher compressive strength but similar stiffness to the existing concrete.

The overall process of the patch repairs was: (1) removal of loose concrete and carbonated concrete around the reinforcement, (2) surface preparation, (3) application of bonding agent, (4) repair mortar application, (5) pull-out testing, (6) water repellent, and (7) final coating.

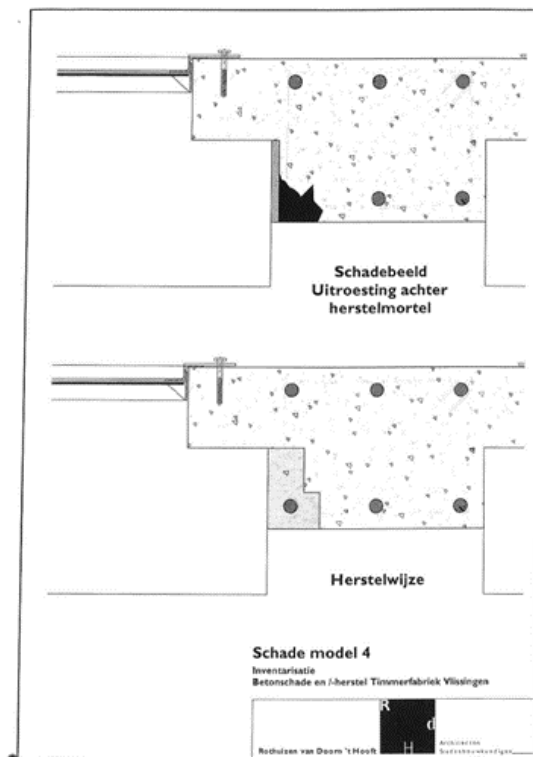


Figure 61. Sample of the specific detail for a patch repair in the corner of a column. Source: Rothuizen.

The repair mortars used for patch repairs were polymer-based mortars from Silka, precisely Sika MonoTop 620 for thin layers, and MonoTop 613 for thicker layers. Prior to the application of the repair mortar, a bonding agent was applied on the surfaces of the existing concrete and exposed rebar, Sika MonoTop 610. Once the patch repairs were done, and the previous paint removed, a coating was applied on all the exposed concrete in the facades. The moisture of the concrete was measured for a proper application. According to the contractor’s budget, a water repellent was applied before the finish coating. However, the only information found was the brand of the product, Funcosil. Regarding the finishing coating, the water-based polymer paint Alpha Topcoat Flex, from the brand Sikkens was used. This coating is especially suited for surfaces where a high flexibility is desired. It has a lifespan of 10 years according to the manufacturer⁵. After the patch repairs, at least six pullout tests were performed to verify proper bonding.

⁴ Per the project specifications provided by the company Bouwgroep Peters B.V.

⁵https://prdakzodecodocumentssa.blob.core.windows.net/public/tds/si/nl/nl/sikkens_alpha_topcoat_flex.pdf

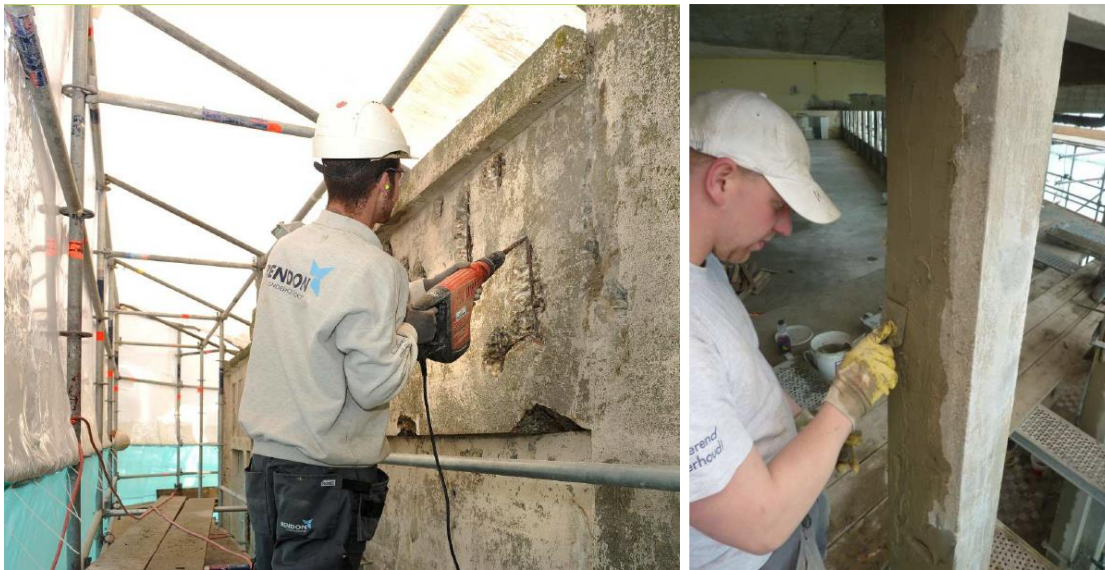


Figure 62. Repair works in 2010. Removing loose concrete (left) and applying mortar repair (right). Source: Bouwgroep Peters B.V.

Current condition (2021)

The concrete façade did not show signs of generalized damage (Figure 63). Scattered damage was found in a few locations. The damage consisted in small spalling and was located in the areas of the wall below the windows (Figure 64). The damage did not seem to correspond with previous patch repairs.



Figure 63. East facade condition in 2021.



Figure 64. Spalling and incipient spalling recorded in the thinner parts of the wall in 2021.

Aim of the investigation

Patch repair is the most common concrete repair in concrete but still its success and durability is a bone difficult to chew. According to the results of the project CONREPNET [1], patch repairs have a limited life span. After surveying 247 repaired constructions the results were that 60% of the patch repairs failed in less than 10 years, and 90% within 25 years [1]. In the case of patch repairs in historic concrete, this rate might be even higher. The components of the concoction in early concrete buildings were often not standardized or even known. For instance, different compositions were used until the beginning of the 20th century, and their formulation and design were kept secret. That can lead to incompatibilities between the mortar repair and the parent concrete.

The aim of the investigation is to examine patch repairs in historic concrete that are performing well after 10 years. The investigation has two specific goals: (1) identify parameters that can contribute to increase the durability of patch repairs.(2) Evaluate NDT techniques to assess the performance of patch repairs. The investigation is performed in only one building, thus the results are exploratory.

The research questions are: **What are the key parameters for patch repairs in historic concrete to perform properly after 10 years? How can patch repairs be assessed using NDT?**

Methods

The methodology of the investigation was:

5. Assess the overall condition of the building.
6. Archival research.
7. Assess the patch repairs from 2010.
8. Evaluate different NDTs to assess the condition of patch repairs.

The tests were divided in two groups. One to determine the basic characteristics of the concrete, and the other to assess the patch repairs.

- Tests to assess the existing concrete
 - **Concrete cover** with Proceq Profoscope (three exterior columns).
 - **Carbonation depth.** Phenolphthalein sprayed over concrete powder from drills at 10 mm steps (three exterior columns).
 - **Compressive strength** with Schmidt Hammer (four exterior columns).
- Tests to assess the patch repairs:
 - **Hammer sounding** with rubber hammer to assess delamination or failure of patch repairs (19 patch repairs in exterior columns).
 - **Thermal camera** to identify repairs and possible delamination or failure (11 patch repairs in exterior columns).
 - **Ultra-pulse sound velocity (UPV)** (Pundit Lab+ of Proceq) for strength and delamination, applied on one side of 12 exterior columns (indirect reading).

The first step of the investigation was to obtain information of the building and the intervention done in 2010. The restoration company Bouwgroep Peters B.V provided a information about the products used for the repairs, the procedure and the location of the repairs.



Figure 65. Annotations of the inspection and tests in the west facade.

Once the patch repairs were located, they were tested with the three techniques: first, with the rubber hammer to assess if debonding was noticed by a hollow sound (Figure 66_left); secondly with the thermal camera to corroborate if the unbound and bound conditions were noticeable (Figure 66_right); thirdly with UPV.

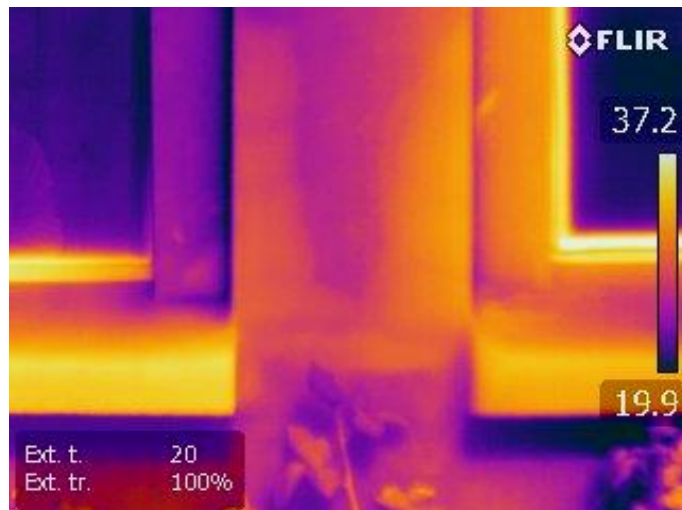


Figure 66. Hammer sounding (left) and thermal picture in a columns with patch repairs (right).

Results

The results of the testing are summarized in Table 8.

| Test | N | Results (Avg.) | Units | Comments |
|---------------------------------------|----|-------------------------|-------------------|--|
| Compressive strength | 4 | 38,25 ($\pm 3,77$) | N/mm ² | |
| Carbonation depth in columns | 2 | < 20 ($\pm 0,00$) | mm | |
| Carbonation depth in patch repairs | 1 | < 10 ($\pm 0,00$) | mm | |
| Concrete cover | 3 | 21,67 ($\pm 2,88$) | mm | |
| Hammer sounding (Hollow sound) | 19 | 42,11% - | - | Percentage of patches sounding hollow. |
| Thermal camera (Hollow-sound patches) | 6 | 50,00% - | - | Percentage of patches showing thermal differences with concrete. |
| Thermal camera (Solid-sound patches) | 5 | 20,00% - | - | Percentage of patches showing thermal differences with concrete. |
| UPV (Hollow-sound patches) | 5 | 2.357,6 ($\pm 248,3$) | m/s | Indirect reading. |
| UPV (Solid-sound patches) | 4 | 2.370,0 ($\pm 215,6$) | m/s | Indirect reading. |

Table 8. Results of the testing performed in the building.

The original concrete has a fair strength given its age (38.5 MPa), the carbonation depth is less than 20 mm, and the concrete cover is slightly over 20 mm over columns – although it can reach less than 10 mm in some sections of the walls.

The results of the tests on the patch repairs show a minimum carbonation depth, less than 10 mm; and no clear visual signs of patch failure, only 2 patches out of 19 had minor crazing. The results of the hammer sounding reveals that almost half of the patches sounded hollow (41%), suggesting the patch have some debonding. However, in general in other sound areas of the walls with no previous repairs did not sound solid. The thermal camera shows that the unbounded patches are more likely to be visible than the bounded patches, 50% of the hollow-sound patch repairs were visible using infrared camera (Figure 67), whereas only 20% of the solid-sound patches were visible. The results of the ultrasonic pulse velocity on surface show a similar wave velocity between hollow- and solid-sound patch repairs.

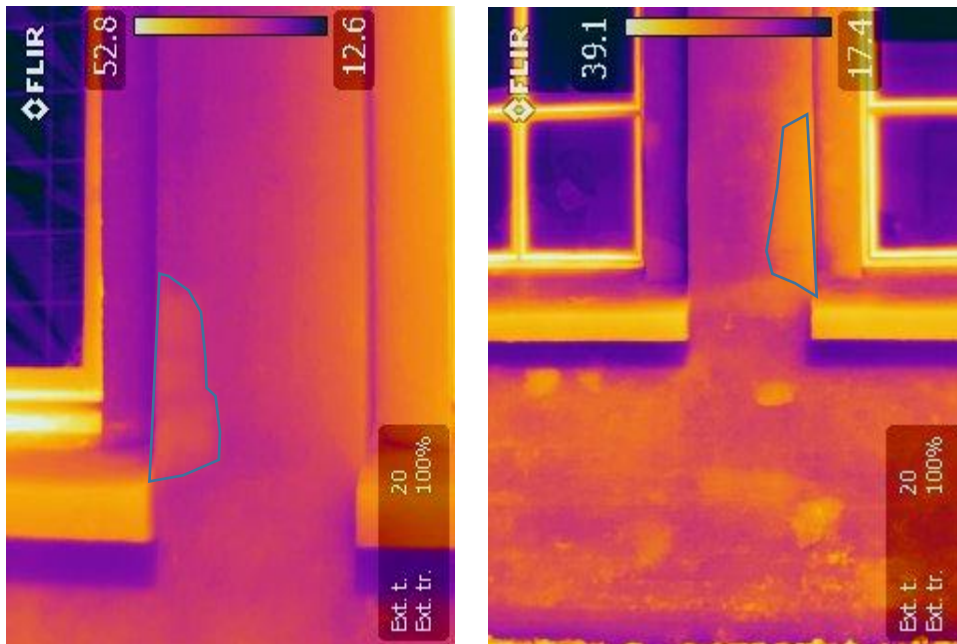


Figure 67. Thermal pictures of hollow-sound patch repairs showing thermal differences. The contour of the patches performed in 2010 are drawn.

Discussion

Regarding the existing concrete

The compressive strength is relatively high for the age; the minimum required strength at the time was 8 MPa [2]. The **carbonation front** in the original concrete is not too deep for a building this age, 20 mm in 106 years; meaning a good compaction and lower permeability if compared to buildings of similar age and exposure [3,4].

The extensive damage visible in 2010 was likely due to carbonated induced (C-I) corrosion. The damage was present in the exposed sides of walls and columns. The cover of the columns is slightly larger than the carbonation front, therefore the reinforcement should have been protected by non-carbonated concrete. Still, scattered spalling in columns was visible. The spalling in columns may be due to a reduction of the cover during the construction process. If not properly tied and secured, the reinforcement may move while pouring the concrete. This can create localized areas with reduced concrete cover and thus C-I corrosion can appear earlier in localized spots. Regarding the spalling and cracks in the walls (Figure 68), the thinnest section of the walls have a minimum concrete cover, less than 10 mm (Figure 68). Thus, the carbonation front reached earlier the reinforcement than in other areas with thicker covers.

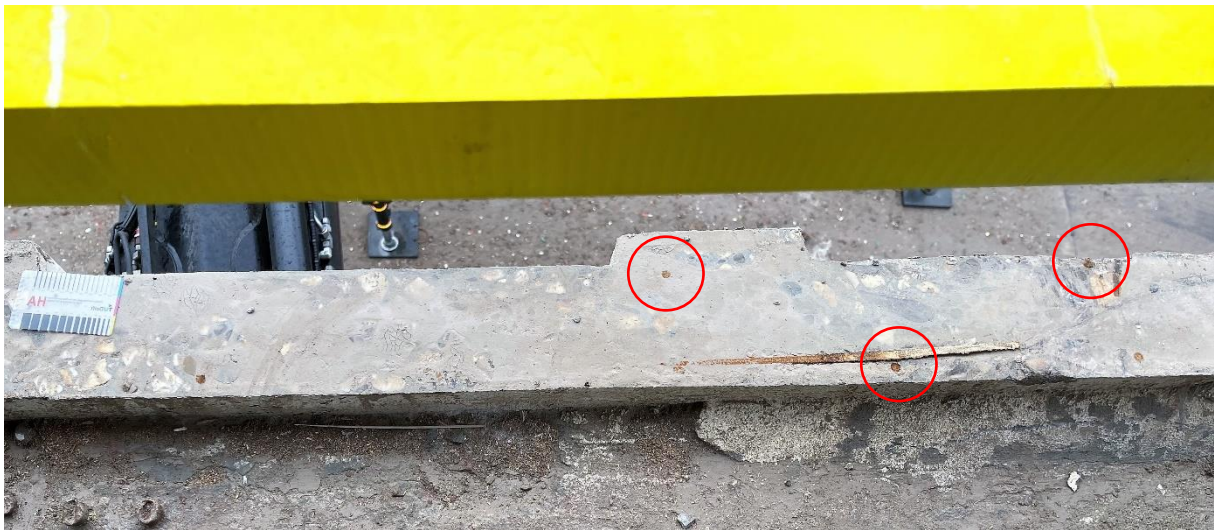


Figure 68. Location of vertical reinforcement in existing exterior walls (circled). Note the difference of concrete cover between the most left rebar and the most right rebar.

Regarding the assessment of the patch repairs

Approximately half of the patches sounded hollow according to the rebound hammer. However, this is not supported by the other testing methods (visual inspection, thermal camera and UPV). In addition, other types of damage linked to debonding, e.g. cracking or delamination, were not visible. The sound hollow can have different causes, the most plausible one being related to the compactness of historic concrete. A lower density of concrete can lead to a non-solid sound regardless repaired or non-repaired concrete.

The carbonation front in the patch mortar is very low ($<10\text{mm}$), as expected due to the young age, so the reinforcement is still protected by the passivity layer provided by the repair mortar. Consequently, there was no signs of active corrosion in the repaired areas. The acrylic polymer based coating applied in 2010 would have contributed to block the CO_2 and water ingress into the concrete [5]. According to the research of Diamanti et al. [6], acrylic based coatings reduce chloride diffusion coefficient better than epoxy coating and chlorinated rubber. In addition, the addition of a water repellent, as it is in this case, considerably reduced carbonation and water content in exposed concrete [7]. In the building under investigation, the damage due to active corrosion was residual, suggesting the surface treatment has hindered the corrosion progress.

Regarding the evaluation of the NDT

The hammer sounding test did not give a good estimation of debonding. This technique has proven useful for other concrete structures [8] but it does not seem effective in historic concrete. All the columns tested sounded hollow regardless repaired or non-repaired concrete. The hollow sound is likely to be related to the low density of historic concrete compared to modern concrete. Historic concrete tend to have higher w/c ratios than allowed in current standards. When hammered it can create a sound that does not sound solid. Therefore, caution must be taken when used in historic concrete. In

addition, this technique is also time consuming -not recommended in large areas- and the results cannot be precisely recorded.

The thermal camera showed modest results, detecting delamination in 50% of the presumably debonded patch repairs. The main shortcoming is that the inspectors need to have an idea where the patch repairs are located; otherwise, they are difficult to detect.. Pre-heating the surfaces would increase the thermal differences, which will improve the interpretation of the results.

Ultrasonic pulse velocity (UPV) showed non-reliable results. UPV has consistently been used to estimate compressive strength and detect voids and cracks in concrete [9]. However, when estimating the bonding of the repairs it has shown that there is not a substantial difference between the results of bound and presumably unbound repairs. Testing on one side only is not as accurate as testing in opposite sides, but the results were expected to have given clearer results. The device has potential to detect it but investigation that is more experimental need to be conducted first.

Conclusions

The patch repairs performed in 2010 were done according to Dutch and European standards. The repairs were assessed, designed and executed by experienced professionals. After 10 years, the state of the concrete in the façade is in good condition; there is not visible signs of active damage in the patch repairs. The testing performed does not suggest failures in the patch repairs neither. There is no signs of active corrosion in the repaired areas, neither in the non-repaired areas. Suggesting that the surface treatment applied in 2010 has diminished the corrosion rate by blocking carbonation and water ingress into the concrete.

Hammer sounding has proved to be a non-reliable technique in this case due to the generalized hollow sound when tested throughout the structure. The hollow sound is thought to be related characteristics of historic concrete, which is typically less dense than modern concrete. The hammer sounding should be accompanied by other testing methods. Thermal camera assessment seems to have the potential to detect early states of debonding if the repair is previously located and the area is previously heated, but further research is needed to confirm this hypothesis. The ultrasonic pulse velocity (UPV) applied on one surface did not provide data to determine failure in existing patch repairs. Given the limited number of tests, further research is needed to clarify the true potential of UPV in detecting patch failure.

Bibliography

- [1] S. Matthews, CONREPNET: Performance-based approach to the remediation of reinforced concrete structures: Achieving durable repaired concrete structures, *J. Build. Apprais.* 3 (2007) 6–20. <https://doi.org/10.1057/palgrave.jba.2950063>.
- [2] Koninklijk Instituut van Ingenieurs, *Gewapend Beton Voorschriften 1912*, 1912.
- [3] W.C. Choi, M. Picornell, S. Hamoush, Performance of 90-year-old concrete in a historical structure, *Constr. Build. Mater.* 105 (2016). <https://doi.org/10.1016/j.conbuildmat.2015.12.158>.
- [4] I. Monteiro, F.A. Branco, J. De Brito, R. Neves, Statistical analysis of the carbonation coefficient in open air concrete structures, *Constr. Build. Mater.* 29 (2012) 263–269. <https://doi.org/10.1016/j.conbuildmat.2011.10.028>.
- [5] R. Amirtharajan, D. Jeyakumar, Repair, rehabilitation & retrofitting of RCC for sustainable development with case studies, *Int. J. Civ. Eng. Technol.* 9 (2018) 1593–1599. <https://doi.org/10.5121/civej.2016.3203>.
- [6] M. V. Diamanti, A. Brenna, F. Bolzoni, M. Berra, T. Pastore, M. Ormellese, Effect of polymer modified cementitious coatings on water and chloride permeability in concrete, *Constr. Build. Mater.* 49 (2013) 720–728. <https://doi.org/10.1016/j.conbuildmat.2013.08.050>.
- [7] P. Zhang, P. Li, H. Fan, H. Shang, S. Guo, T. Zhao, Carbonation of Water Repellent-Treated Concrete, *Adv. Mater. Sci. Eng.* 2017 (2017). <https://doi.org/10.1155/2017/1343947>.
- [8] H.J. Parsaie, *Training and Reference Manual for Special Inspectors*, iUniverse, 2001.
- [9] D. Breyse, J.P. Balayssac, S. Biondi, D. Corbett, A. Goncalves, M. Grantham, V.A.M. Luprano, A. Masi, A.V. Monteiro, Z.M. Sbartaï, Recommendation of RILEM TC249-ISC on non destructive in situ strength assessment of concrete, *Mater. Struct. Constr.* 52 (2019). <https://doi.org/10.1617/s11527-019-1369-2>.

Photos by TU Delft - CONSECH20 project (if no other source indicated)

Report on In-Depth Case Study

Museum of the Treasury of San Lorenzo, Genoa



Type: Restored

Partner Institution: Unige

Project: **CONSECH 20**

Working Package 2 – Task (iii)

Date: 27/09/2021

By:

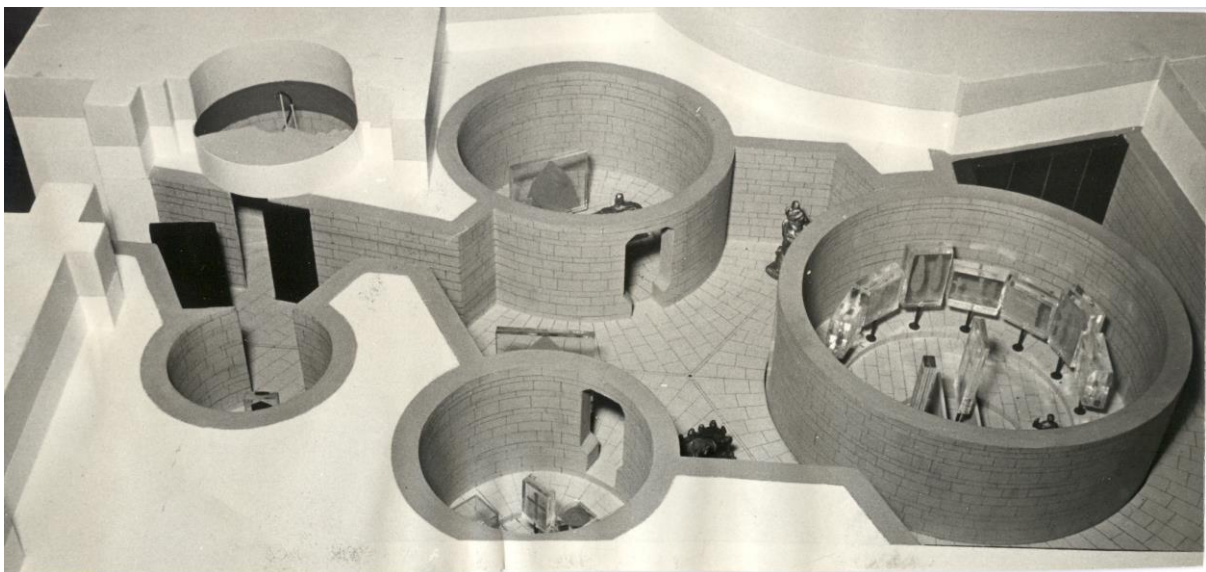
Author 1 Giovanna Franco

Author 2 Stefan F. Musso

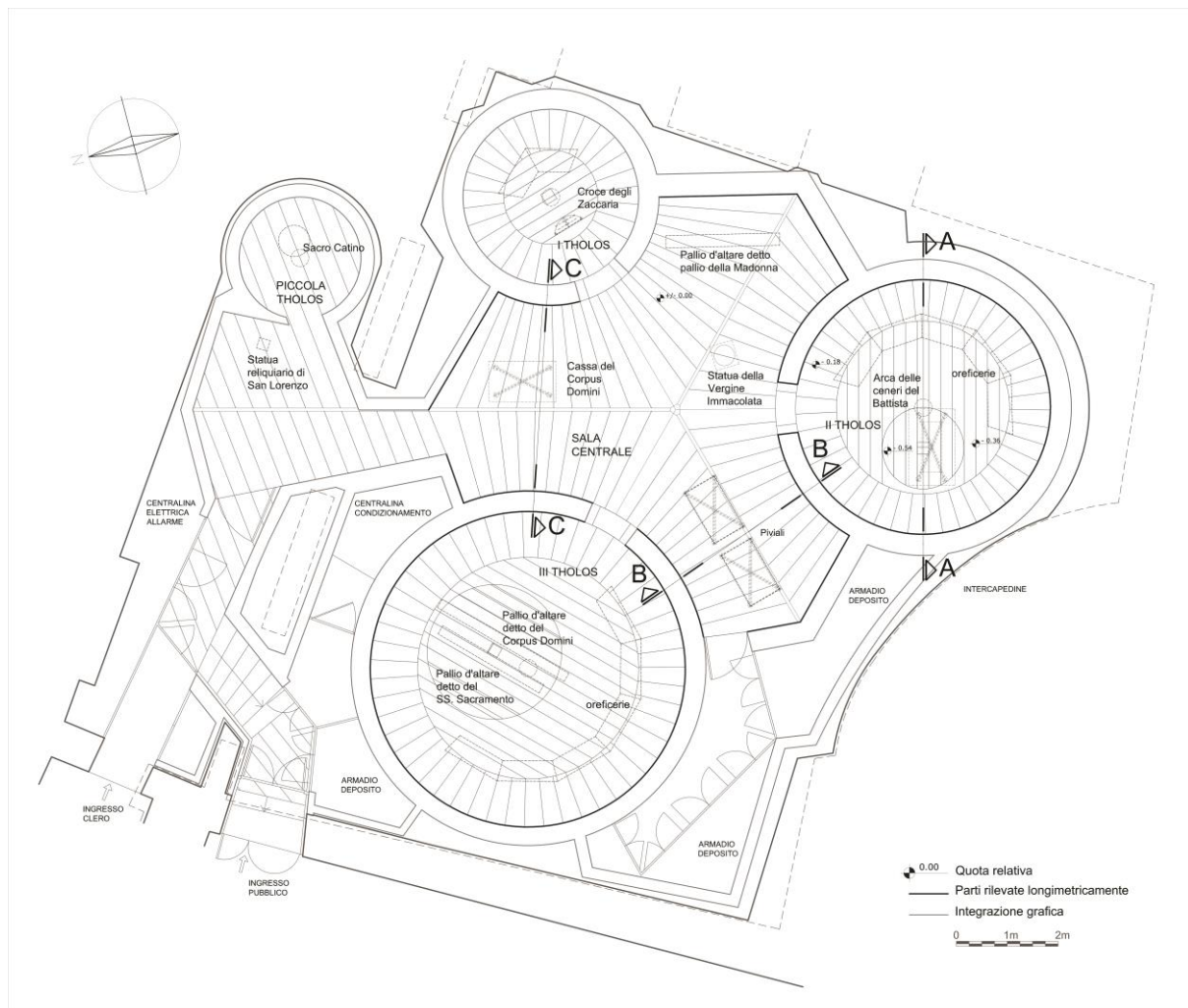
Introduction

The Museum of the Treasury of the Cathedral of San Lorenzo in Genoa was designed and built by Franco Albini in the years 1952-56. The very site upon which the structure ‘stands’

is itself unique: the museum is actually hidden from view because it is underground, a sort of hypogeum with no exterior as such, it is enclosed between the foundations of the Renaissance apse which Galezzo Alessi had built for the renovated high altar of the medieval cathedral and the foundations of the Archiepiscopal Palace. The Treasury is also unique because of the precious artefacts it contains; forming a collection that has been put together over centuries, the items here are in part the property of the Metropolitan Chapter of Genoa and in part the property of the city itself. This feature of the collection would itself have important consequences in determining the choices made by Franco Albini (choices in part inspired by Caterina Marcenaro, the then Director of Genoa City Museums who was the commissioning client, faithful custodian and irrepressible champion of the work); and those decisions still affect the management of museum. The conceptual idea was born and evolved from the idea of intersecting pure geometric forms: a regular hexagon and three circles of different radii (1.75 metres, 2.50 metres and 3.10 metres), the fampus 'Tholos' recalling the treasure of Atreus in Mycenae, whose centres coincide with the vertices of non-adjacent segments of the hexagon itself. To these are added an irregular space, connecting with the access staircase, as well as a further smaller circle (with a radius of 1.20 metres). In these spaces the treatment of the floor, the corrugated roof and the concavity and convexity of the perimeter walls contribute to reinforcing the idea of "interlocking organisms", where the objects on display find a natural setting. where the objects on display find a natural position, carefully studied on the basis of the generating axes of the basic geometries used. The Treasury Museum itself would from the start be considered a veritable 'work of art' (a genuine creation by a specific artist, it was assumed, therefore, that it had been conserved in its original state). Astonished scholars and architects had immediately expressed admiration for the expressive power and novelty of the project when seen within the rich context of Italian museum design at the time, which often involved work within the stratified framework of already-existing architectural structures. One feature that had been of fundamental importance for Franco Albini and Caterina Marcenaro was light: evocative and mysterious, it is throughout the design used in a refined manner to create the interplay of bright illumination, deep shadows and surprising reflections. The Museum is listed by Italian Ministry of Culture.



Maquette of the Museum, Franco Albini. Courtesy Piero Boccardo, Direzione Musei di Strada Nuova



Plan of the Museum, survey by Architecture and Design Department (S.F. Musso, G. Franco)

Characteristics of the Concrete Building and Structure

Materials

As the Museum is located underground in the courtyard, the maximum depth of the excavation, from the highest point of the floor, is 5.50 m; the existing foundations had to be consolidated. Along the excavation the retaining structure was grafted onto a continuous foundation, consisting of a concrete retaining wall cast directly in contact with the terrain. For straight sections longer than 2 metres, a rib was cast in the terrain; for the curved sections, it was not necessary to stiffen the wall because the very curvature of the wall increased its resistance. For the lower half of the wall the thickness is 30 cm and is reduced to 15 cm in the upper half. For the entire area within the perimeter of the foundations a lean concrete slab was cast to form the crawl space.

In order to protect the interior from possible water infiltration, a waterproofing layer was laid vertically along the whole of the counter wall and horizontally along the whole of the under-floor cavity slab. On the inside of the counter-reinforcement wall, always resting on

the continuous foundations, a 15 cm thick brick wall was built, all visible parts of which were covered with chiselled promontory stone (4/6 cm thick) up to a height of 2.30 m.

The prevalent materials used in the Treasury Museum are therefore:

Foundation: reinforced concrete

Structural walls: solid bricks

Roof structure: reinforced concrete

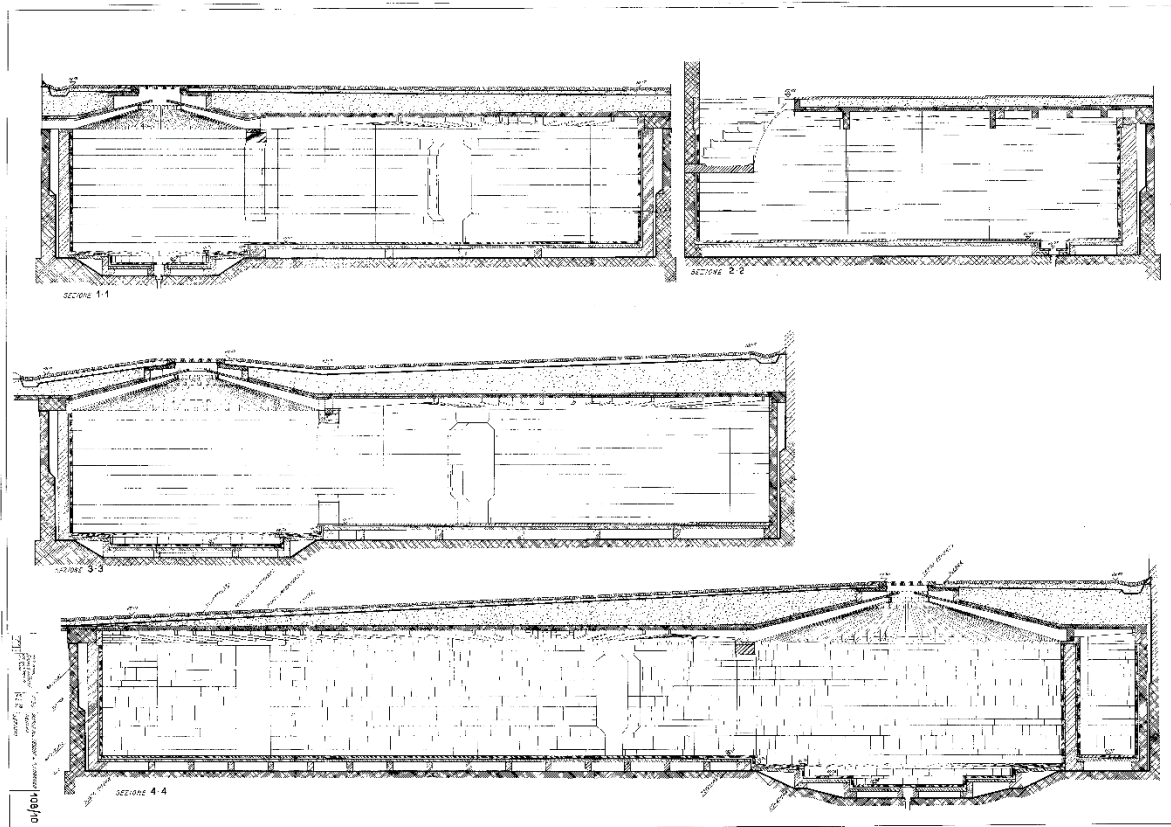
Internal finishing (pavement and walls) slabs of *Promontorio* stones

External roof covering: mosaic in black and white stones (*Risseau*), insertion of three cement discs with block glass (at the top of the three 'false domes').

As far as concerns the reinforced concrete works, archive research has shown that:

- The bottom of the crawl space was made of: concrete kg 150 hydraulic lime/cubic metre - cubic metre 0.800 gravel and cubic metre 0.400 sand
- The foundations and the counterfloor wall were made of reinforced concrete kg 300 cement 500/mc - mc 0,800 washed live gravel and mc 0,400 live sand
- On the perimeter of the building and on the circular rooms, a reinforced concrete wall was built (300 kg cement 500/mc - 0.800 m³ gravel and 0.400 m³ sand).
- The false dome roof structure is made of T-joists cast on site with planed formworks, surface of the casting in view reinforced concrete kg 300 cement 500/mc - mc 0,800 gravel and mc 0,400 sand. - m³ 0.800 gravel and m³ 0.400 sand
- A reinforced concrete distribution slab with wire mesh weighing 1.5 kg/sq.m. was cast over the joists.
- The distribution slab was filled with pumice concrete above the distribution slab to form the courtyard slopes
- The courtyard floor is made of cobblestones on a sand foundation and a band of stone curbs

Three concrete discs and glass diffusers close the false cupolas at the top and provide interior lighting. These are made of glass-cement panels: diffusers diameter 14.5, h. 8.4, Iperfan type, Fidenza Vetraria, later better described.



Design sections, Franco Albini. Courtesy Piero Boccardo, Direzione Musei di Strada Nuova

Type of structure

The architectural and structural solutions adopted for the underground space of the Museum are clearly explained in the project reports (1953), and described in greater detail in the final assessments.

Over the concrete foundation were posed a series of brick walls of the honeycomb foundation beneath the flooring are of different heights, and – as photographs of the original work show – perforated at their base to allow for drainage. These walls are protected by lead sheeting bent vertically at its edges and support prefabricated slabs of concrete, upon which is laid the flooring in *pietra di Promontorio* (a grey local marly limestone).

The elevation structures of the museum, the curved walls that constitute the cylinders of the 'tholos', were designed and built with solid bricks, separated from the perimetral wall by a cavity of varying thickness (from 5 to 20 cm) and equipped with arches in correspondence to the openings for access to the tholos themselves. Great importance was immediately given to the stone covering the horizontal and vertical internal surfaces, made from blocks of dark grey *Promontorio* stone worked on the external face with a chisel and squared to obtain perfectly matching sides. To this aim, Albini scrupulously designed, on several occasions, the dimensions of the individual pieces needed for their facing, which were made up of alternating repeated modules of varying thickness. The stones were then laid with filling mortar and "cadmium iron" clamps.

Works were done in the following phases.

Once the excavation and substructure had been completed (the subject of the first lot of work), a slab of lean concrete was poured and a series of 12 cm thick brick walls were built on top, "arranged concentrically or parallel to each other according to the needs of the floor plan". The initial idea, which was only partially modified on site as far as the height of the walls was concerned, was to create a 20 cm high crawl space to separate the floor structure from the ground below. More information can be found in the final report of 1956. "A layer of gravel and concrete was placed at the bottom of the excavation, with a slope for the outflow of the remaining water infiltration towards the drainage sumps. This concrete shell, which with the floor and walls of the Museum forms a continuous, aerated cavity, was also waterproofed with asphalt. From the photographs of the early stages of construction, the contours of the cavity and the brick and concrete slab crawl spaces for the stone floor are clearly visible. Each foundation element of the floor and wall structures was also insulated with lead sheets. As in the case of the roofing structures, the presence of lead as a waterproofing material seems to be the result of a choice made during the works, because in the report of the second lot there is no trace of this item, neither as a supply of material nor as labour necessary for its installation. In addition, compared to the project drawings, the level on which the under-floor cavity is set is all at the same depth, and its thickness seems to increase in the highest parts of the floor (the central hexagonal area and the outer rings of the tholos) rather than being variable, following a stepped profile, as indicated in the project sections.

Lastly, as opposed to the initial plan to use brick slabs to support the walls, preformed concrete slabs were used to build the floor, as can be deduced both from the site photos and from reading the accounting documents. On this surface, after the casting of a special slab, the floor was then laid in slabs of promontory stone, 6c thick and, therefore, thicker than in the project.



Building site, foundations and drainage system. Courtesy Piero Boccardo, Direzione Musei di Strada Nuova



Building site, elevation of brick circular walls and stone cladding. Courtesy Piero Boccardo, Direzione Musei di Strada Nuova

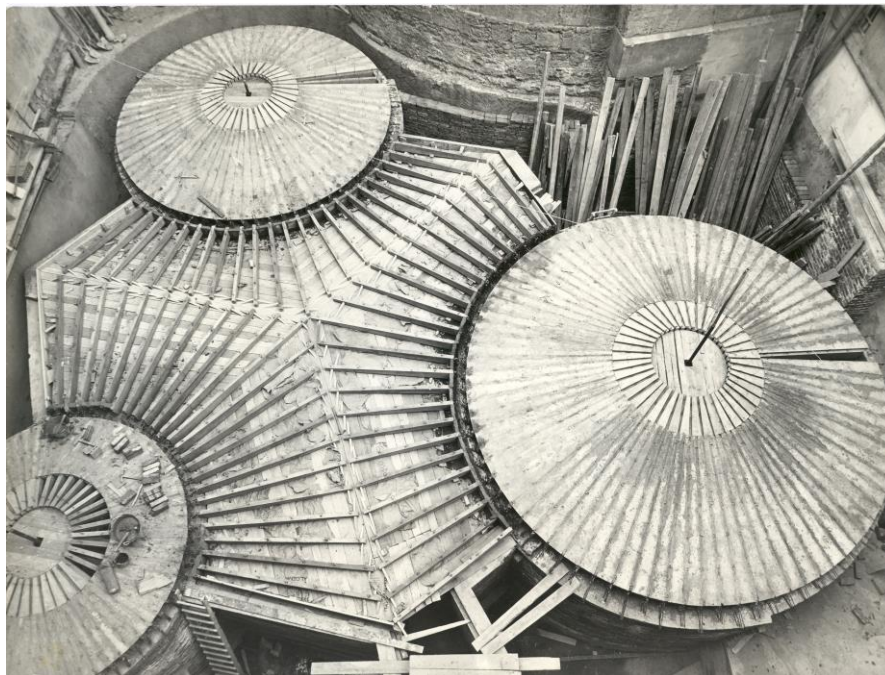
One of the most evocative elements of the Museum is certainly the roof, made up - in the various tholos - of concave ceilings (in the form of a false dome) that are very low and - in the central hexagon - of a flat ceiling corrugated by a dense series of T-joists in reinforced concrete of variable section, arranged in such a way as to emphasise the generating geometries of the design. The T-joists are cast in place and then arranged radially around the centres of the three cylindrical rooms. A distribution slab, reinforced with wire mesh, is cast on the joists. The body of the rafters has a constant thickness of 6 cm and a variable height from 8 to 25 cm according to a constant inclination; the wing of the rafters has a constant thickness of 4 cm and a variable width from 8 to 40 cm. The joists must not be plastered and therefore planed formwork must be used. These rafters are corbelled, resting on the internal walls or embedded in the external walls, and connected by a reinforced concrete *correa*. A distribution slab, reinforced with wire mesh, is cast on the joists. For the interior walls, in the area where the joists are laid, there is a covering of hand-blasted bricks, laid flat. For the external walls, the rafters are 65 cm wide, so as to tie the internal wall to the retaining wall, fixing the waterproof covering and closing the air space.

The rafters that form the ribs of the roof behave statically as double brackets set radially on the cylindrical walls of the Tholos; the variable length was obtained by inserting mobile diaphragms in the wooden formworks smoothed in plaster for the off-site construction. The same expedient was adopted for the construction of the circular sector slabs that are superimposed on the joists, in order to adapt them to the different radii of the three Tholos. For the central compartment, on the other hand, the completion of the intrados of the roof

was obtained by means of a sand and plaster formwork, compacting it between the joists and the lower wooden scaffolding, spreading it with plaster and then casting the distribution slab directly; once it had set, the sand and plaster formwork was dismantled and it came apart by itself. On top of the roof, the cross-weave load distribution reinforcement was prepared, forming a homogeneous cast with the annular beams running above the three cylinders and forming the three central rings of the skylights".



Building site, scaffolding for the roof structure and reinforced concrete rafters Courtesy Piero Boccardo, Direzione Musei di Strada Nuova

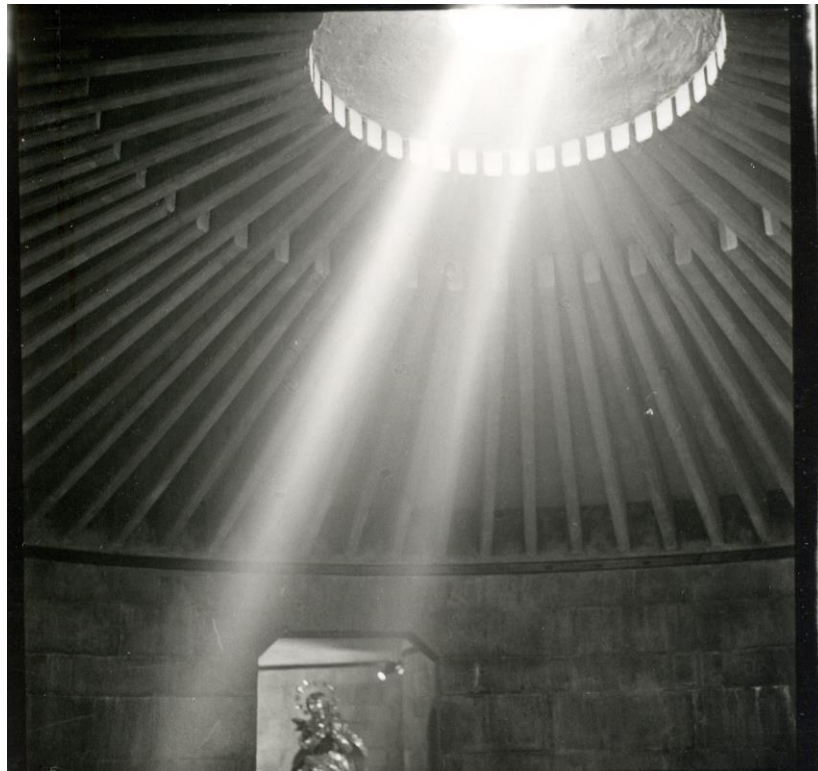




Building site, the steel net before the concrete mould and a view from above, the pavement of the courtyard over the false domes. Courtesy Piero Boccardo, Direzione Musei di Strada Nuova

Once the beams and preformed slabs of reinforced concrete had been laid, the so-called "distribution slab" was laid and properly anchored to the irons protruding from the beams and slabs (as visible in the site photos). The slab was made of cement concrete, reinforced with a metal mesh and resting on the perimeter wall and on the cylindrical walls of the tholos, and ended, at the centre of each cylinder, with reinforced concrete rings to house the planned skylights at the top. This last structural and construction layer was then covered with lead sheets welded and turned up on the sides (of which, however, no trace can be found in the project reports, nor in the final summary calculation, nor in the works report for the second lot), with an overlying protective caulking, (of which, however, there is no trace in the project reports, nor in the final summary calculation, nor in the expert's report on the second lot), with an overlying protective caulking, designed to prevent lead perforations, made with cement mortar (and not hydraulic lime, as foreseen by Albini),

and the further laying of a final layer of asphalt to connect the plaster to the lapels, in correspondence with the perimeter walls. Finally, a sloping layer was made, lightened with pumice stone, which also functioned as thermal and acoustic insulation, and on this last layer were then laid both the black and white cobblestones of the Archbishop's Palace courtyard, following the sunburst design of the underlying structure, and the glass cement "disks" of the skylights of the internal tholos. Lastly, the ventilation shafts and four grid openings, cut into the outer perimeter walls and raised above the ground level to provide fresh air to the underground rooms, were housed in the thickness of the roofing layer.



View from inside, 1957 (Photo Silverstone). Courtesy Piero Boccardo, Direzione Musei di Strada Nuova

Briefly, the work that was carried out for the roof structure and covering involved:

- the installation of prefabricated reinforced concrete beams of rectangular section (constant in width but increasing in height) which were to either irradiate from the centre of the cupola over the three main 'tholos' or, in the part located beneath the portico of the Archiepiscopal Palace, run parallel;
- the installation of prefabricated reinforced concrete slabs, above the beams;
- the construction of a ceiling in reinforced cement, resting on the surrounding walls or the walls of the individual 'tholos';
- the creation of ring-shaped string-courses at the centre of each cupola, and the insertion therein of discs of block glass;
- the installation on the ceiling of welded lead sheeting upturned at the edges and the laying of mortar under the paving to protect it, with a layer of asphalt to bond the plastering with the upturned edges of the lead sheeting around the walls;

- the installation of a layer of pumice stone of variable thickness, with street surfacing for vehicles then laid over it;
- the installation within the roofing of channels for ventilation and four grilled openings in the outside walls, raised above the traffic level;
- laying of a pavement in black and white cobbles in the courtyard above the museum, corresponding with the ceilings of the 'tholos' beneath.

Other relevant characteristics

Particularly innovative was the lighting system designed by Franco Albini with the help of Franca Helg, characterised by criteria of flexibility, maintainability and modifiability that are still valid today. The larger objects displayed in the open space were lit by a series of spotlights powered by electric cables running in a circular cavity at the base of the display cases (protected by a flat iron) and at the top of the internal walls, in special recesses cut out at the top of the cladding slabs, hidden by a bakelite plate.



View of the lighting system (photo G. Franco)

Condition of the building

The Museum of the Treasury, with its "robust" character, as defined several times in the official documents accompanying its construction, has survived almost intact for more than fifty years thanks to the properties of its constituent materials, which are durable and solid, and to its underground location, protected - except for the skylights at the top of the internal ceilings - from the aggression of external agents. Despite this, the building has been affected, like any other architecture, by changes in conditions of use, the obsolescence of the technological systems, and wear and tear (at the most fragile points), requiring maintenance, improvement and enhancement since its inauguration.

Immediately after the inauguration, and in the years that followed, a number of problems arose regarding the safety of visitors, who risked falling on the steps inside the too narrow space of the tholos containing the Ark of the Ashes of Saint John the Baptist, as Monsignor Storace, Provost of the Metropolitan Chapter of San Lorenzo, wrote to the Director Caterina Marcenaro and as she pointed out to Albini, requesting the insertion of platforms to connect the different levels. The lighting system was also considered not entirely safe, especially at the entrance staircase, which was poorly lit except by a single wall spotlight that projected a light beam of modest amplitude. More or less accidental damage, if not outright theft, has repeatedly occurred to some of the exhibits, which are unprotected, in particular the Ark of the Baptist, which was recently protected by a glass case, and the processional case of Corpus Christi, for which Monsignor Storace had already proposed the installation of a special protective glass in October 1956.

The sacred vestments, which were placed on supports of an unsuitable size and shape for the proper conservation of the fabrics, also required careful restoration and a rethink in terms of display methods. The suggestive lighting system for the objects on display, which was modified several times with the replacement of light fittings, did not fully enhance the preciousness of some of the jewellery, which was also dulled by the patina of time. In addition to this, there were renewed needs for study and conservation, which led the Director of the Strada Nuova Museums, on which the Treasury also depends, to think about a new exhibition arrangement. Not to mention the infiltrations that penetrated into the museum from the skylights at the top of the domes of the circular rooms and that required urgent and more substantial interventions than mere routine maintenance.

Although minimal in nature, the new requirements, which were the expression of a cultural context different from the one in which the Museum had its genesis, motivated above all by the better conservation and enhancement of the works on display, inevitably clashed with the need for "absolute" conservation and rigorous protection that the extraordinary nature of this architecture (which marked one of the most innovative and mature examples in the field of Italian museography) could/should require.

Balancing between these two instances (new requirements and the most "integral" preservation of Albini's museum), in search of an (im)possible mediation, the working group coordinated by the authors has made a journey back through the recent history of the Tesoro, within the elegance and power of an abstract form whose value is certainly enhanced by the technical refinement of Franco Albini's design choices and the executive methods of his concepts on site.

Damage types

Infiltration of the roofing system, which Director Marcenaro had already complained about when the work was not yet completed (but the museum had already been inaugurated), following a violent downpour and probably due to the way the flooring in the Archbishop's Palace courtyard had been constructed, reappeared and occurred several times over time, especially in the area of the glass-cement skylights in the tholos below. On the intrados of the ceiling, in fact, the reinforcement rods of the concrete were visible, already oxidised and corroded and no longer protected by the layer of concrete cover, which probably triggered carbonation of the concrete (2011, before the intervention).



View of the deterioration (photo G. Franco)

Hypothesis on damage processes

The deterioration of these elements was probably related to thermal stress and certainly to mechanical stress induced by the incongruous use of the Archbishopric courtyard as a parking space for cars and motorbikes. In order to temporarily repair the most serious cracks, some of the glass diffusers of the skylights had already been covered with a layer of mortar or sealed with silicone to stop the infiltration of rainwater into the tholos, thus compromising their readability from inside the museum.

In spite of these precautionary measures, water infiltration occurred repeatedly in the intervening years, with visible results especially in the tholos where the Zacharias Cross is displayed.





Temporary reparations (photo G. Franco)

Aim of the investigation

Archival analysis, completely new and specially conducted for this work (in the Archive of Municipality of Genova, Public works and in the Direction of Museums of Strada Nuova) made it possible to reconstruct the history of construction. This was why archive sources were carefully studied, with some new documents making it possible to chart the structure's history in greater detail, providing information of some micro-transformations whose very occurrence had been forgotten.

The reading and complete transcription of all the technical documents, from the first design reports to the final one, allowed us to know in detail the construction history of

the Museum, starting from the characteristics of the materials and the structural solutions adopted.

Direct observation of the few phenomena of deterioration, mainly on reinforced concrete exposed to atmospheric agents, was supplemented by chemical analyses to assess the process of carbonation underway.

Analysis of the causes and agents of damage and decay – as well as an evaluation of their impact upon the structural features, display fittings and exhibits – led the authors, together with the Scientific Committee, to draw up plans first of all for certain work that was strictly conservational in character. For example, work began on cleaning the surfaces of the architectural structure and the display apparatus in order to remove surface deposits, stains and the more substantial and adherent deposits on the display units themselves; at the same time, specialist restorers worked on the artefacts exhibited without special protection and on those within display cases. However, these measures were not sufficient to resolve all the problems that had emerged. As a result, it was necessary to plan and implement certain measures that did involve an element of modification, even if the maximum possible level of conservation remained the primary objective of all work.

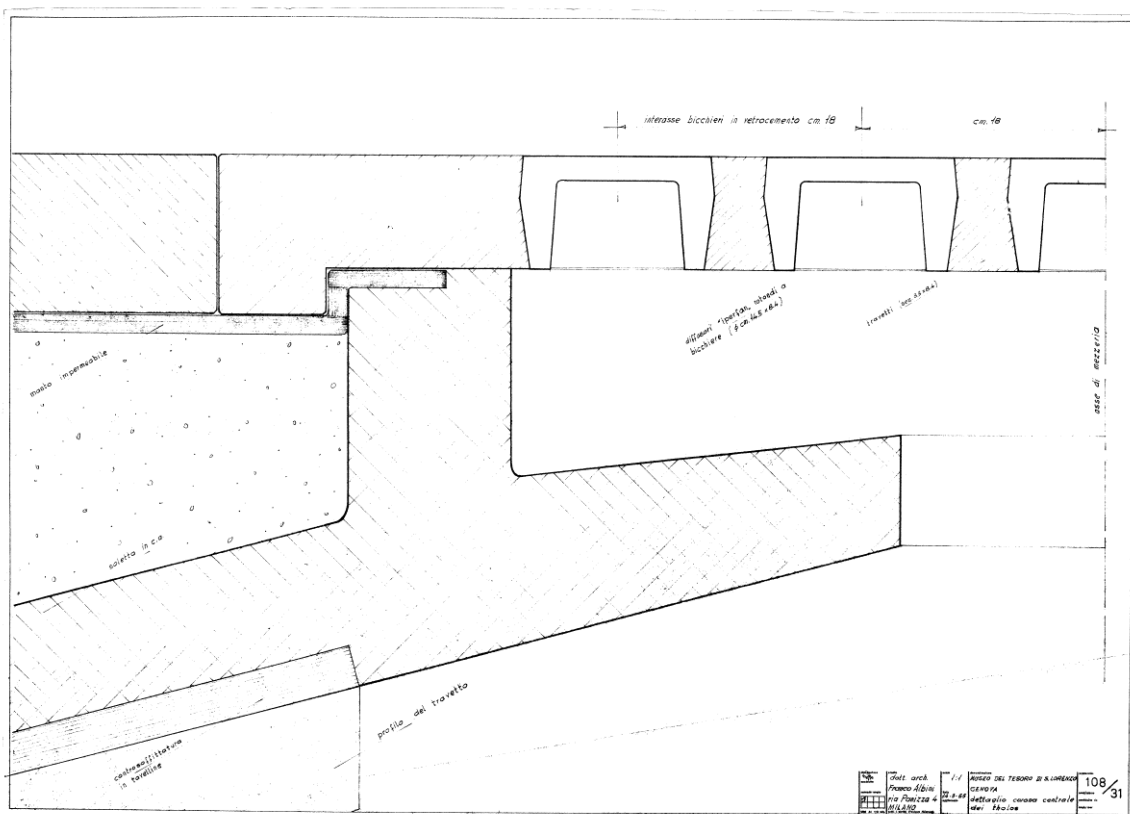
The more consistent intervention on the covering is described in the following paragraph.

Methods and intervention

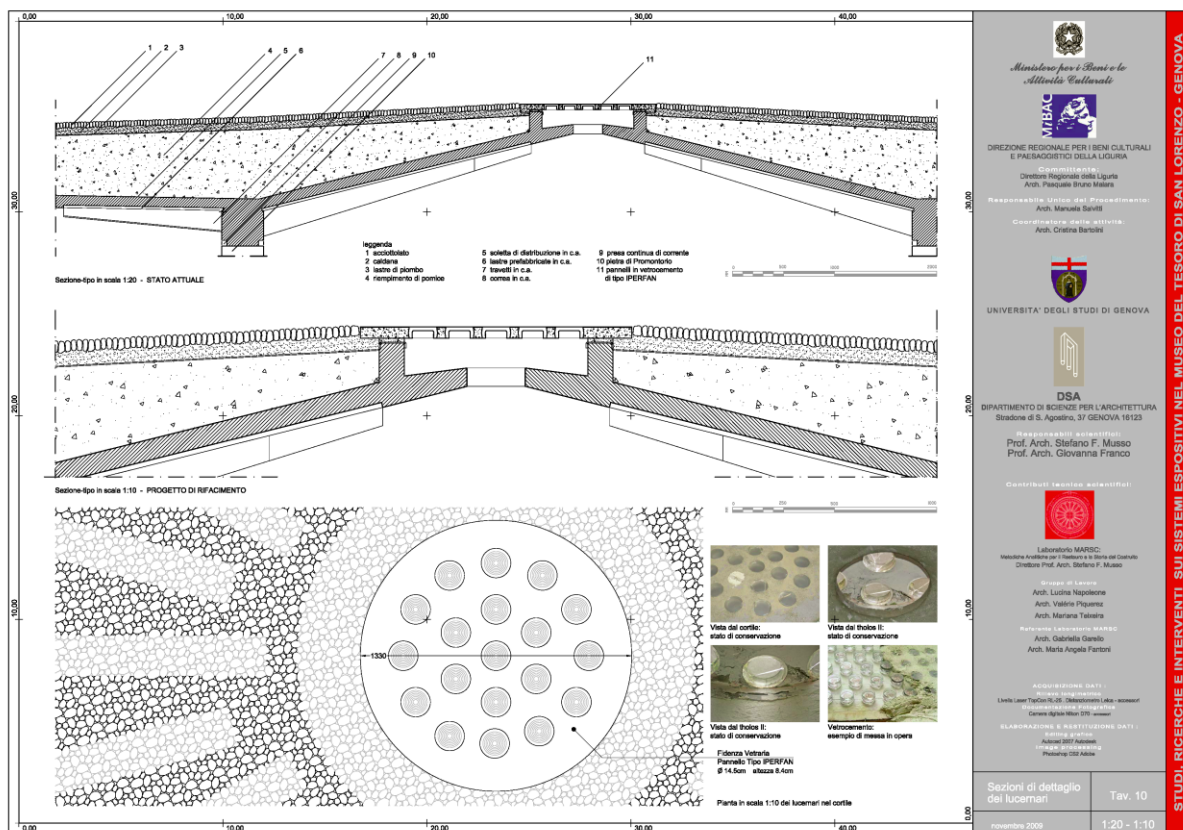
Sometimes it is necessary to make changes in order to truly conserve. Conservation itself presupposes on-going change (or controlled transformation) which, for example, makes it possible to pass from the dirty to the clean, the fragile to the reinforced, the divided to the re-composed, etc. The real problem lies in deciding how and within what limits - using what forms and materials – these 'modifications' can be carried out so as to be acceptable. Should one intervene continually, thus having resort to a sort of reproduction and imitation? Or is it preferable to intervene by changing forms and materials whilst operating in full respect for what already exists (primarily in the design of features that were previously not even present). A significant example of this issue was the repair of the block-glass skylight and their light diffusers (many of which were broken and some blocked up altogether).

The most significant intervention was the repair of the block-glass skylight and their light diffusers (many of which were broken and some blocked up altogether). To prevent the leaking that became apparent during the study phase from becoming worse, the three existing discs in block glass were replaced with similar but newly manufactured discs.

Since the "useful life cycle" of the glass-cement panels was inevitably considered to be over, they had to be replaced in their entirety, and the problem of the unavailability of the original glass diffusers had to be addressed. The company merged with the company Seves Glass Block, based in Florence, which continues to produce glass "cups" with a cylindrical base, but smaller than those used in the museum, with a production diameter of 11.7 cm. However, given the small number of pieces (less than 60), it was possible to find some pieces belonging to the same batch, stored in some of the warehouse funds of the firm that had taken over the stocks of the original supplier, which has now disappeared. They were of the same size and had the same surface finish (concentric stripes) as those in place but were irreparably damaged and unrecoverable. They could therefore be inserted into new



Detailed drawings of the skylight, Franco Albini. Courtesy Piero Boccardo, Direzione Musei di Strada Nuova



Discussion

Sometimes it is necessary to make changes in order to truly conserve. Conservation itself presupposes on-going change (or controlled transformation) which, for example, makes it possible to pass from the dirty to the clean, the fragile to the reinforced, the divided to the re-composed, etc. The real problem lies in deciding how and within what limits - using what forms and materials - these 'modifications' can be carried out so as to be acceptable. Should one intervene continually, thus having resort to a sort of reproduction and imitation? Or is it preferable to intervene by changing forms and materials whilst operating in full respect for what already exists (primarily in the design of features that were previously not even present)?

The first question that the Committee set itself was 'Which Treasury are we dealing with?'. The clear response to that had to be the Treasury as it existed at that precise moment, and in that precise state. The answer might seem obvious but it is certainly not without consequences for anyone who wishes to work in full respect of the past and present. In fact, thanks to source material that made it possible to reconstruct some of the genesis and implementation of Albini's ideas, we could see that there were some differences between the project designs and what was actually built. Furthermore, there was the obvious truth that many things had changed in the museum over the years, the means and outcomes of those changes being only partially documented. Numerous 'micro-transformations' had occurred in silence, almost the only trace they had left behind being a faint echo of them in varied documentary sources. Thus we had to decide whether the differences they had produced were to be considered as now forming part of the genuine original work.

Analysis of published material did not fully resolve the issue; while it made it possible to reconstruct the history of critical appreciations of the work, it did not cast full light upon everything that had happened after the project was completed. This was why further archive sources were studied, with some new documents making it possible to chart the structure's history in greater detail, providing information of some micro-transformations whose very occurrence had been forgotten.

Conclusions

In examining the museum and its history, we had to respond to a crucial question that remains partially unresolved: how much of the design and actual structure of the museum was Franco Albini's work and how much was due to Caterina Marcenaro? Another equally important question concerned how much of the Treasury was built as designed and how much was simply accepted once it had been built.

These two issues clearly influenced any attempt to clarify the limits of the oft-mentioned 'originality' of Albini's work, the question of his intangible presence as its 'author'. Often, in fact, the conservation of a work of architecture is predicated upon reference to the basis of its value as bearing authentic witness to the original work of an architect, or as the expression of a particular moment in the history of architecture. Here, however, one also had to look at the necessity/legitimacy of conserving possible 'errors' and 'chance' results in the planning and building of the museum, together with features that might be the fruit of what had happened to it during the course of its existence.

Bibliography

- Marginalia – New Museums*, in *The Architectural Review*, London, 1956
- A Buried Treasury* in *Architectural Forum* n. 4, 1957
- “Musées – Muséographie” – monograph issue of *Techniques et Architecture*, n. 326, 1979
- Albini, F. 1956. *Le Musée du Trésor de la cathédral de Saint Laurent de Gênes*, in *Museums*, vol IX, n.2. UNESCO, Paris
- Albini, F. 1958. *Museo del Tesoro di San Lorenzo* in *Goya-Revista de arte*, n. 22. Madrid.
- Argan, G. C. 1956. *Museo del Tesoro a Genova, architetto Franco Albini*, in *L'Architettura*, cronache e storia, n. 14.
- De Seta, C. 1980. “Franco Albini architetto, fra razionalismo e tecnologia”, in *Franco Albini Architettura e design 1930-1970*. Centro Di, Florence.
- Franco, G, Musso, S.F. *Franco Albini et le Musée du Trésor de la Cathédral San Lorenzo à Gênes. Problèmes de conception, construction et conservation*, in “Cahiers Thématiques. Technologie et bâtiments: un patrimoine silencieux” n° 19, pp. 57-68, ÉCOLE NATIONALE SUPÉRIEURE D'ARCHITECTURE ET DE PAYSAGE DE LILLE, Éditions de la Maison des sciences de l'homme, 2021.
- Labò, M. 1956. *Il Museo del Tesoro*, in *Casabella - Continuità*, n. 213.
- Marcenaro, C. 1969. *Il Museo del tesoro della Cattedrale a Genova*. Cassa di Risparmio di Genova e Imperia, Genoa.
- Musso, S.F., Franco, G. 2015. *The Conservation of the “Modern”: Franco Albini and the Museum of the Treasury of San Lorenzo, Genoa* in *Journal of Architectural Conservation*, vol 21, issue 1 2015, pp. 30-50, Taylor & Francis Group, London.
- Salvitti, M., Musso, S.F., Franco, G., Napoleone, L., *Conservare il Moderno: Franco Albini e il Museo del Tesoro di San Lorenzo, a Genova*, Quaderni di ANANKE, n. 5, 2015.
- Russoli, F. 1960. *Pour une muséographie efficace*, in *L'Oeil*, n. 61. Paris.
- Tafuri, M. 1982. *Storia dell'architettura italiana, 1944-1985*. Einaudi, Turin.
- Van Ravestein, S. 1963. *De modernisairung der Italiaanse Muse ana de corlog*, in “Bouwkundig weekblad”. The Hague.
- Zevi, B. 1956. *Un tesoro in quattro cilindri*, in *L'Espresso*, 10 June.

Report on In-Depth Case Study

Alexandros Dimitrou Tower (Nicosia, Cyprus, 1966)



CONSECH20 – WP2 (iii)

Restored Case Study

Georgiou, A.

Hadjimichael, M.

Ioannou, I.

October 5, 2021

Introduction

Historical background

The Alexandros Demetriou Tower is one of the most important buildings of the international style modernism in Cyprus, featuring in a publication (in the Greek journal 'Architecture') dating back to 1966 [1]. The building was listed, following a Decree issued by the Minister of Interior, in 2006 (Κ.Δ.Π. 342/2006). It has also been included in the index of the 100 (most) important buildings, sites and neighbourhoods from Cyprus, compiled by the National Register of Docomomo Cyprus [2].

The building was originally commissioned by Alexandros Demetriou & Sons, as an investment. The owners, who were merchants and importers of tractors and agricultural equipment, wanted a large building to host the offices, an exhibition area and storage spaces for the equipment of their company, as well as a number of apartments for sale. The famous Cypriot architect Neoptolemos Michaelides thus designed an eight-storey tower block above a basement and a semi-basement, measuring 34.50 m in height. The building comprises of an exposed reinforced concrete structural frame with visible frames on the two narrow facades (NW and SE), in line with the norm of the era. The plan view was left open to allow for future changes in the interior of the building [1]. A panoramic view of the building at the early stages of its life cycle in the 1960s, can be seen in Figure 69.



Figure 69. Panoramic view of 'Alexandros Demetriou Tower' in the early 1960s [3]

Other attributes of the building include passive systems for climate improvement, a characteristic feature of the environmental sensitivities of the architect. According to the description provided by the architect himself in the journal 'Architecture' in 1966, the basement, semi-basement and ground floor hosted the owners' storages, offices and exhibition spaces for the agricultural equipment. The semi-basement was also partly used for parking. Additionally, there was one 1-bedroom apartment and two 3-bedroom apartments on each floor (from the 1st to the 7th floor). The 8th floor comprised of a covered roof. The circular external staircase was pre-fabricated, and it is similar to the staircase at the entrance of the building, which leads to the raised ground-floor show room (Figure 70).



Figure 70. Circular prefabricated staircase (left) and entrance staircase (right)

At the time of its construction, the Alexandros Demetriou Tower was one of the tallest buildings in the capital of Cyprus, Nicosia, just outside the southern part of the Venetian walls of the old city, and one of the few efforts of the period to design a high-rise building. The interior space design of the building, as well as the open and semi-open spaces, created opportunities for understanding societal perceptions (of a certain class) regarding accommodation, at a time of shift towards modernity. For example, the original lack of view towards the Venetian Walls suggests that the Old City of Nicosia was not considered worthy of a view at the time. Indeed, in the 1950s, the Old City of Nicosia (within the context of modernism) was considered to be the one that we need to leave behind [4].

The building was successfully restored by Vasilis Ierides and Aimilios Michael in 2008. The architects described the refurbishment process as the building's 'second youth' in the proposal submitted to the Town Planning and Housing Department [5]. According to Michael et al. (2012) [6], they based the methodology of the restoration work on a detailed analysis of the building's functional, morphological, structural, and bioclimatic aspects, and on extensive discussions with the owners and the competent authorities, whilst showing respect to the importance of the building in terms of contemporary architectural heritage, as well as to the local society. Some of these changes aimed towards enhancing the bioclimatic features of the initial design, in order to improve thermal and visual comfort conditions, as well as to reduce the consumption of conventional energy for heating, cooling and lighting.

Additionally, the few changes made to the design of the building were indicative of the shift in societal and architectural standpoints, such as for example the opening of

windows towards the old city and the enlargement of the apartments (Fig. 3). Regarding the former change, this was also feasible in terms of bioclimatic design, as the new windows are facing south west, rather than south, as originally perceived by the architect.



Figure 71. South-west side: original construction with bricks (left) and large glass windows after restoration (right).

As for the enlargement of the apartments, the three original separate apartments (2 apartments and 1 studio) located on each floor were unified during the restoration of the building into a single apartment, thus creating 7 floor-size apartments, one on each floor. The covered terrace of the 8th floor was also converted into a housing unit, a feature that was actually included in the original design but was never realised. The historic timeline of the building is graphically summarized in Figure 72.

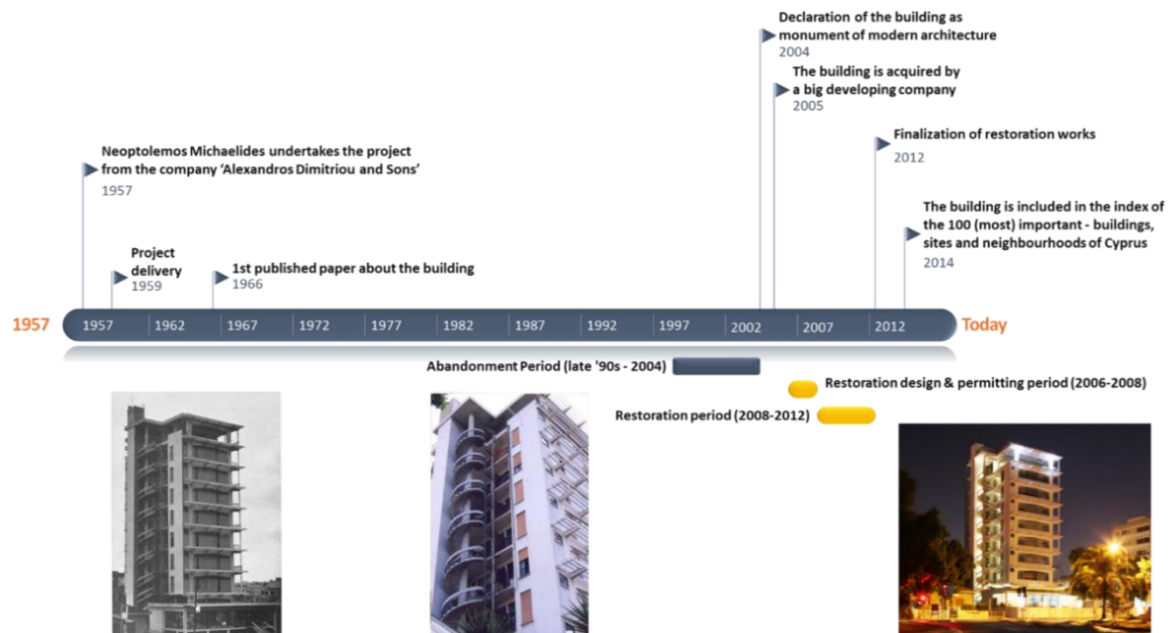


Figure 72. Timeline of important events in Alexandros Demetriou Building

Characteristics of the Concrete Building and Structure

For the structural verification of the building, the original plans that were submitted in 1954 for the building permit were obtained from the Nicosia Municipality. The original design of the building included a basement level, a semi-basement level and eight upper floor levels. The typical floors had a height of 3.5 m, whilst the ground floor had a height of 5.3 m. In Figure 73, the original typical architectural floor plan and section may be seen.

In the original submission, there was only one drawing showing the reinforcement plans of the four different floor slabs (semi-basement, ground, mezzanine, and typical floor levels); this included the columns and beams schedules. The original structural assessment of the building was also found (a hand-calculation set of 10 pages); this provided insightful information on the type of loads and assumptions made during the design stage of the project. As it was expected, the structure was designed to withstand only gravity loads, with no calculations carried out to consider horizontal dynamic loading (i.e. seismic or wind loads).

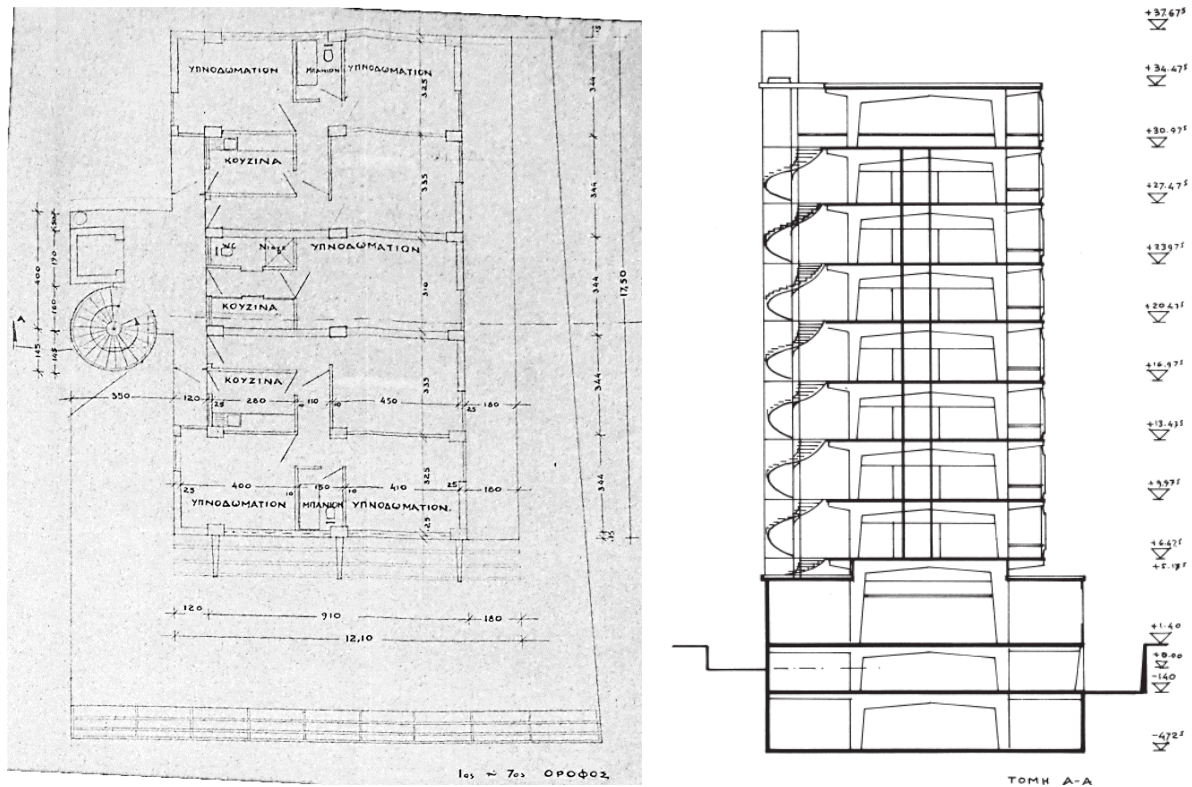


Figure 73. Original typical floor plan layout (left) and section view of the building (right) [7]

Based on the information collected, the main structure of each typical floor level is formed by six parallel reinforced concrete frames. These concrete frames have a total length of 9.1 m and are repeated every 3.4 m. According to the structural drawing, the frames are connected to each other with secondary beams that are smaller in size, when compared to the main beams of the frames. Each floor is formed by Zöllner one-way concrete slabs of 150 mm thickness. This type of concrete slabs was extensively used till the late 1970s in Cyprus, and basically comprises of ribbed slabs with masonry bricks as infill material, as shown in Figure 74. Amongst the main advantages of this type of slab is the reduced self-weight and the cost saving achieved by reducing the need for concrete and steel reinforcement.

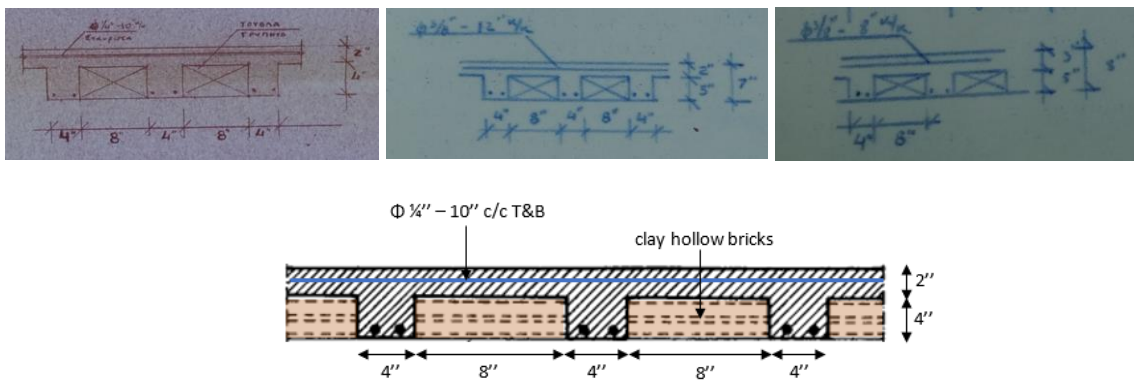


Figure 74. Zöllner slab detail, as specified by the original structural design

Based on the original drawings (Figure 75), the slabs depth varied between each floor, or within the same floor, based on the vertical loads and on the dimensions of the slab, ranging between 6" (152.4 mm) to 8" (203.2 mm).

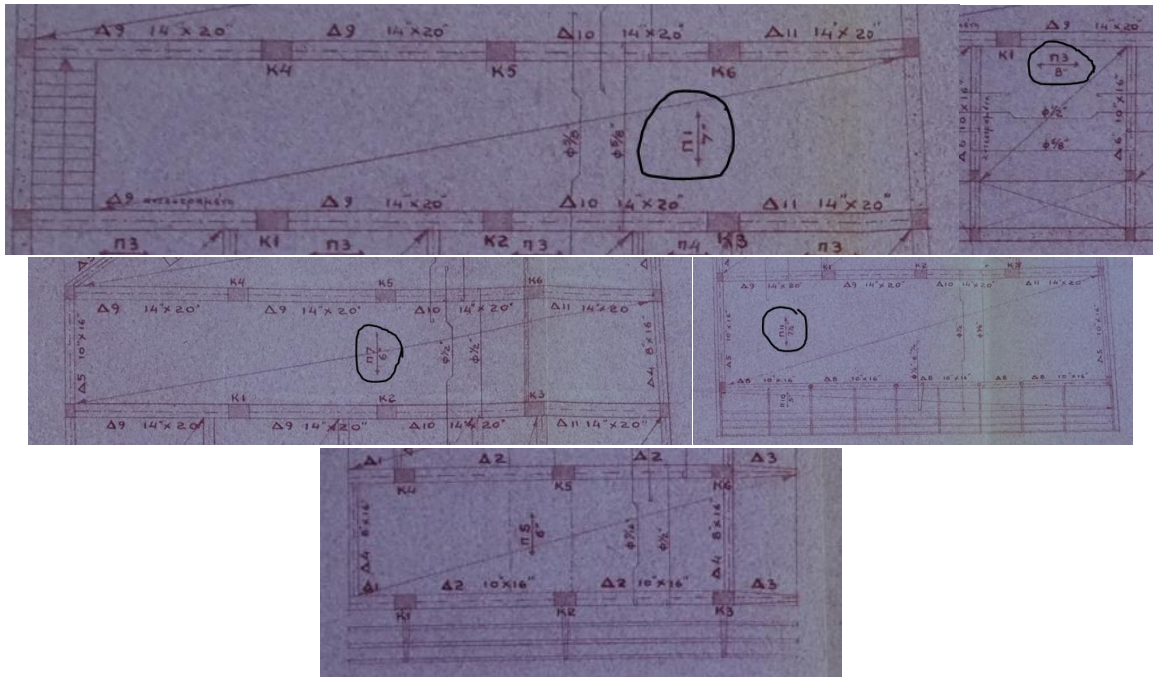


Figure 75. Slab depth based on original drawings: (a) over 2nd basement, (b) under ground floor, (c) above ground, (d) typical floor

When comparing the original set of drawings to the recent survey drawings created for the restoration of the building in 2008, some important discrepancies of the structural system were found. The original drawings showed a series of columns located in the middle of the main frames from the ground level up to the roof level; this row of columns was not found during the recent surveys, as illustrated in Figure 76. The absence of these columns was confirmed during the site inspections that followed.

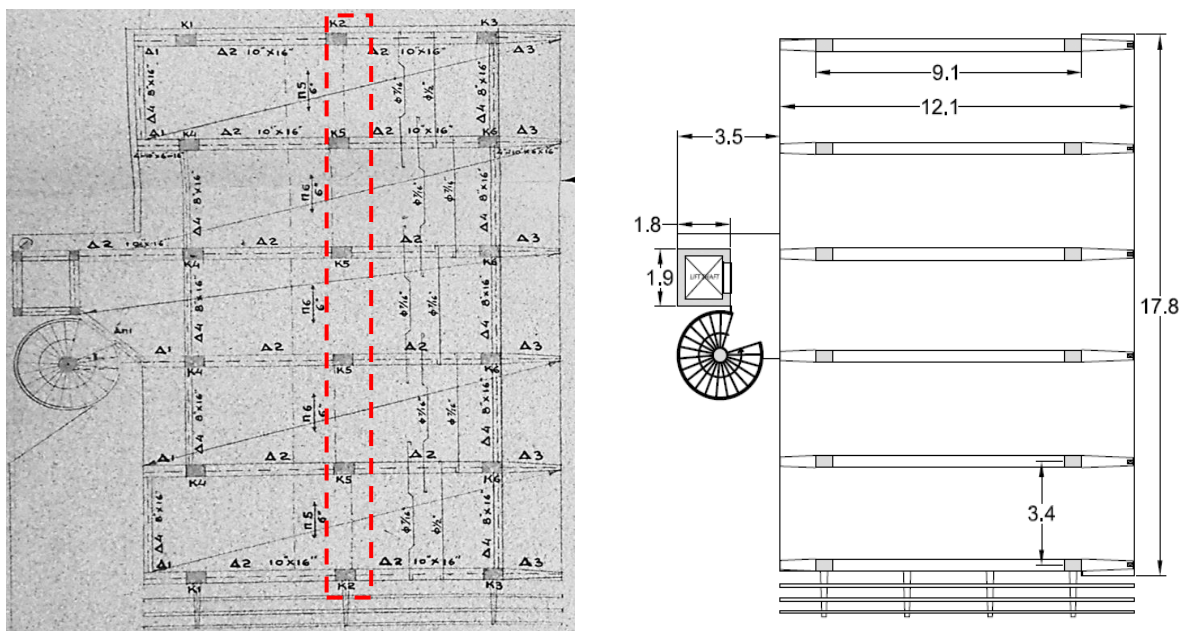


Figure 76. Typical floor plan as per: the original design (left) [7] and the survey plan (right)

Description of the Retrofit Design and Works

The information on the structural aspects of retrofit works carried out were collected from the calculation set and structural report of the retrofit design, and through an interview with the Structural Engineer of the project. According to these sources, 26 columns at the two basement levels were strengthened with the RC jacketing technique, as per the detail shown in Figure 77, while the rest of the columns at the upper floor levels (121 in total) were retrofitted with 2 layers of carbon FRP. Prior to applying the FRP, all damages related to the corrosion of reinforcing steel were rectified. No strengthening works were carried out at the foundation level, or on the beams and slabs of the building [7].

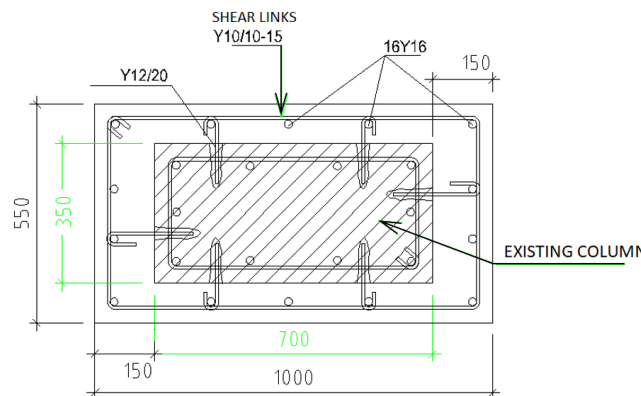


Figure 77. Reinforced Concrete jacketing detail [7]

Typical damages found in the structure prior and after the retrofit

It is highlighted that visual inspections contribute towards the identification of damage caused by weathering or previous seismic actions. Furthermore, it is noted that the full occupancy of the case study building imposed a major limitation on the extent of testing carried out during the site investigation stage. The visual inspections took place on multiple occasions between 2019-2021 and the overall status of the structure, in terms of damaging, was characterised as good. This is of course related to the recent retrofit works, during which many defects were identified and rectified. For completeness purposes, the three major defects identified prior to the retrofit works are presented below (Figure 78) [7]:

- The laboratory test results on concrete core specimens extracted from various locations, showed significantly reduced compressive strength, ranging between 15-17 N/mm².
- Steel reinforcement corrosion on the structural elements of the 8th floor, owing to continuous exposure to open weather conditions.
- Peeling/flaking of external plasterwork and painting in numerous locations, owing to the lack of regular maintenance and inadequate waterproofing of the building.



Figure 78. Defects identified prior to the retrofit works

The damages identified during the visual inspection (post-retrofit inspection) were not severe and were mainly related to moisture ingress, causing peeling/flaking of external plasterwork and painting (Figure 79). The other type of damage found was microcracking at the junction points of beams-columns and horizontal cracking of the wall finishes (Figure 80). The most severe defect found was related to steel reinforcement corrosion and the corrosion of other embedded metal elements in concrete, that led to local concrete spalling (Figure 81). Inside the building, no significant defects were identified, although the majority of the concrete elements were not visible because of the addition of false ceilings and drywall partitions.

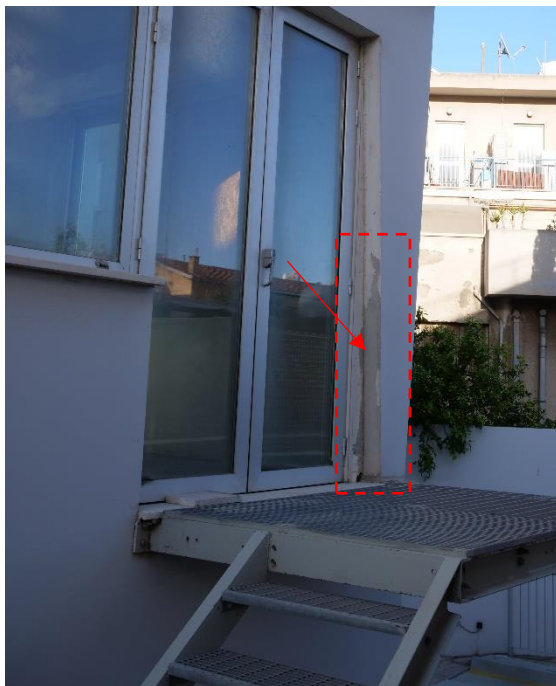
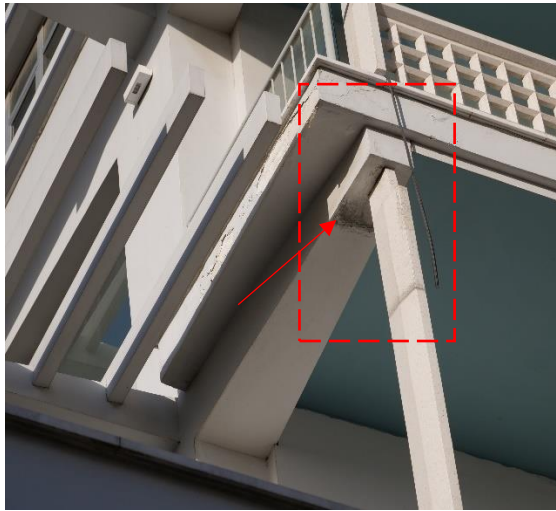


Figure 79. Minor defects related to moisture ingress causing plaster and paint flaking





Figure 80. Micro-cracks on concrete elements and wall finishes



Figure 81. Reinforcement and other embedded metal corrosion causing local concrete spalling

Investigation, Methods and Results

For the seismic assessment of the residence, EC8:3 [8] was used. The methodology adopted is shown below:

- xiv. verification of the geometry of the structural elements and reinforcement detailing with regards to the original plans provided by the municipality,
- xv. evaluation of the material properties through in situ non-destructive tests,
- xvi. assessment of local brittle failure possible damages
- xvii. simulation of a typical frame with non-linear characteristics
- xviii. assessment of a typical frame capacity under Pushover analysis.

Survey and testing of materials

A survey was performed for the verification of the geometry and size of the various elements. The original construction drawings showed great variation compared to the as-built investigation. In order to increase the detailing information, a rebar detector was used to detect the steel bar reinforcement, the bar cover and diameter, both in the beams and columns (Figure 82). The steel used in that era was mild S220 without ribs.



Figure 82. Rebar detection and diameter/cover measurement

Concrete mix and compressive strength

At the time of the construction of the case-study building, there were no batching plants in Cyprus and concrete was thus prepared on site, in small quantities ca. 2 tn at a time. This led to great variability in the quality of concrete in the various parts of a structure, even from the bottom to the top of a column, as there was also no equipment for vibration and thus proper compaction and consolidation. The original concrete mix design (Figure 83) was either 1:1:2 by volume (cement:sand:coarse aggregates) for columns (as described on one drawing) or 1:2:4 by volume for all beams, slabs and columns (as described in the technical specifications). For the case of 1:2:4 analogies, which were the most commonly used in Cyprus, based on oral communication, 1 part of water was used if the aggregates were wet, while 1.5-2 parts of water were used if the aggregates were dry.

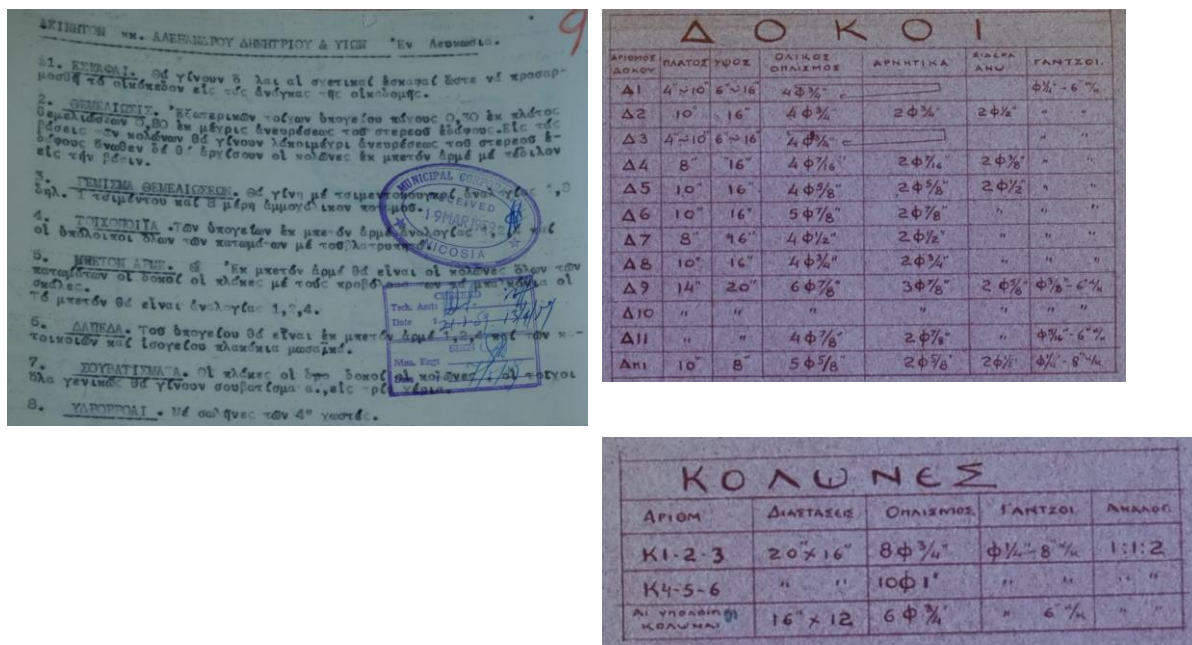


Figure 83. Concrete mix design as per specifications (left) and instructions on drawings (right).

Some uniaxial compression (EN12390-3 [9]) tests were performed in 2008 on a number of cores extracted from various members of the structure; yet it was not possible to acquire the results. The only available information was an average compressive strength of 19.5 MPa (cube) for the columns, provided by the Engineer in charge of the project. According to the same person, the samples extracted in March 2008 led to the assumption that the concrete used at the time of the construction of the building was C16/20. Nevertheless, some of the columns (nr. 4) had lower compressive strengths (12-15 MPa). The average cube compressive strength of the beams was 17 MPa, albeit again with 4 cases with strength lower than 15 MPa. Yet, the number of core samples was not available in order to assume that these were enough to determine the Knowledge Level of the strength of materials as extensive, KL3, as required for nonlinear assessment, based on EC8 Part 3 [8]. Table 1 summarises the information available regarding the original concrete compressive strength.

Table 9. Compressive strength of concrete

| Member | Average compressive strength from tests (N/mm ²) - cube | For assessment |
|---------------|---|----------------|
| Columns | 19 (4 cores under 12-15) | C16/20 |
| Beams + Slabs | 17 (4 cores under 15) | C12/16 |

Concrete cover, Rebar Diameter and Member detailing

The cover to the reinforcement was established through the use of the rebar detector, while the same procedure was used to determine the rebar diameter and detailing of the

rebars. The detailing of the columns and beams, as recorded in the original drawings, is shown in Table 9 and Table 10.

Table 10. Member detailing as per original drawings

| Columns | Original drawings | | | From measurements | | |
|--------------------------------|-------------------|----------|--------------------|--------------------|----------------------------|-----------------|
| Number | Dimensions (mm) | Long. | Trans. | Dimensions (mm) | Long. | Trans. |
| K1-2-3 (EXT) | 508x406.4 | 8Φ19 | Φ6.35/203.2 | 400x600 to 400x900 | 8Φ19 | Φ6/150 |
| K4-5-6 (INT) | 508x406.4 | 10Φ25.4 | Φ6.35/203.2 | 400x600 to 400x900 | 8Φ25 | Φ6/200 |
| ALL OTHER | 406.4x304.8 | 6Φ19 | Φ6.35/152.4 | | | |
| Beams | | | | | | |
| Number | B | H | Long. total | Negative | Upper reinforcement | Stirrups |
| Δ2 (main frame beam detailing) | 254 | 406.4 | 4Φ19.05 | 2Φ19.05 | 2Φ12.7 | Φ6.35/152.4 |
| | | | | | | |
| Δ4 | 203.02 | 406.4 | 4Φ11.11 | 2Φ11.11 | 2Φ9.53 | Φ6.35/152.4 |

The reinforcement layout and diameter were measured with the rebar detector on two columns and one main frame beam at the 3rd floor level, which was the only floor accessible. The first problem encountered was the difference between the dimensions of the beams and columns between the original drawings and the as-built findings. As per the original drawings, the columns and beams should be of constant rectangular shape, while in reality they were built as tapered. Additionally, measuring the reinforcement was difficult, especially of the corner rebars, because of the use of metallic corners during the retrofit of the building. Yet, the rebar diameters were in close approximation to the ones mentioned in the original plans, as the columns during that time served only to transfer vertical loads to the foundation. The measured values are depicted in Figure . The main issue encountered during the measurements was the absence of reinforcement -both longitudinal and transverse- within the joint between the columns and the beams, which was also of a wider area than normal, due to the tapered geometry of the members.

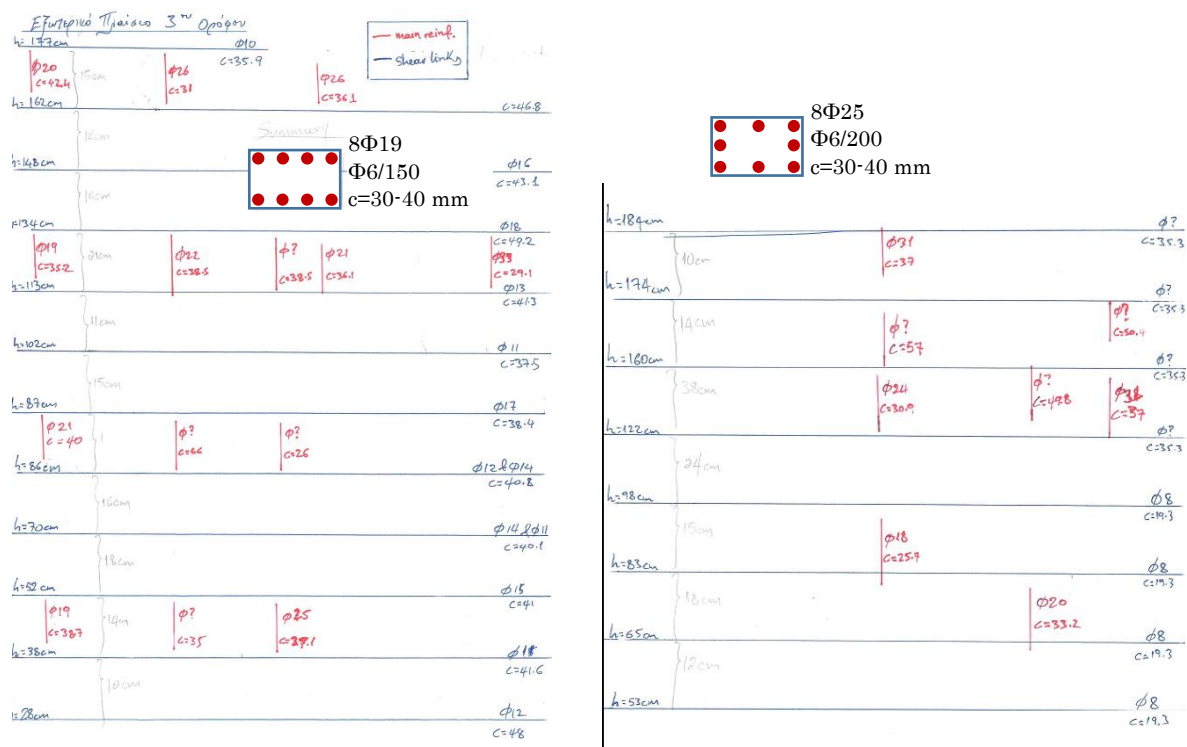


Figure 84. Reinforcement measurements on 3rd floor columns; external frame (left) and internal frame (right)

Assessment of the seismic capacity of the structure

Simulation of the structure

Figure shows the typical floor plan with the columns numbering and dimensions at their base. Modelling was performed only for two typical frames in the X-direction, as per the on-site measurements of the 3rd floor. The geometry and detailing of the external frame K14-K16 and the internal frame K21-K23 are depicted in Figure 86. The frames were loaded with the distributed load of the slab, on the beam, based on the G+0.3Q combination, while the vertical load of the floors above was also added to the columns.

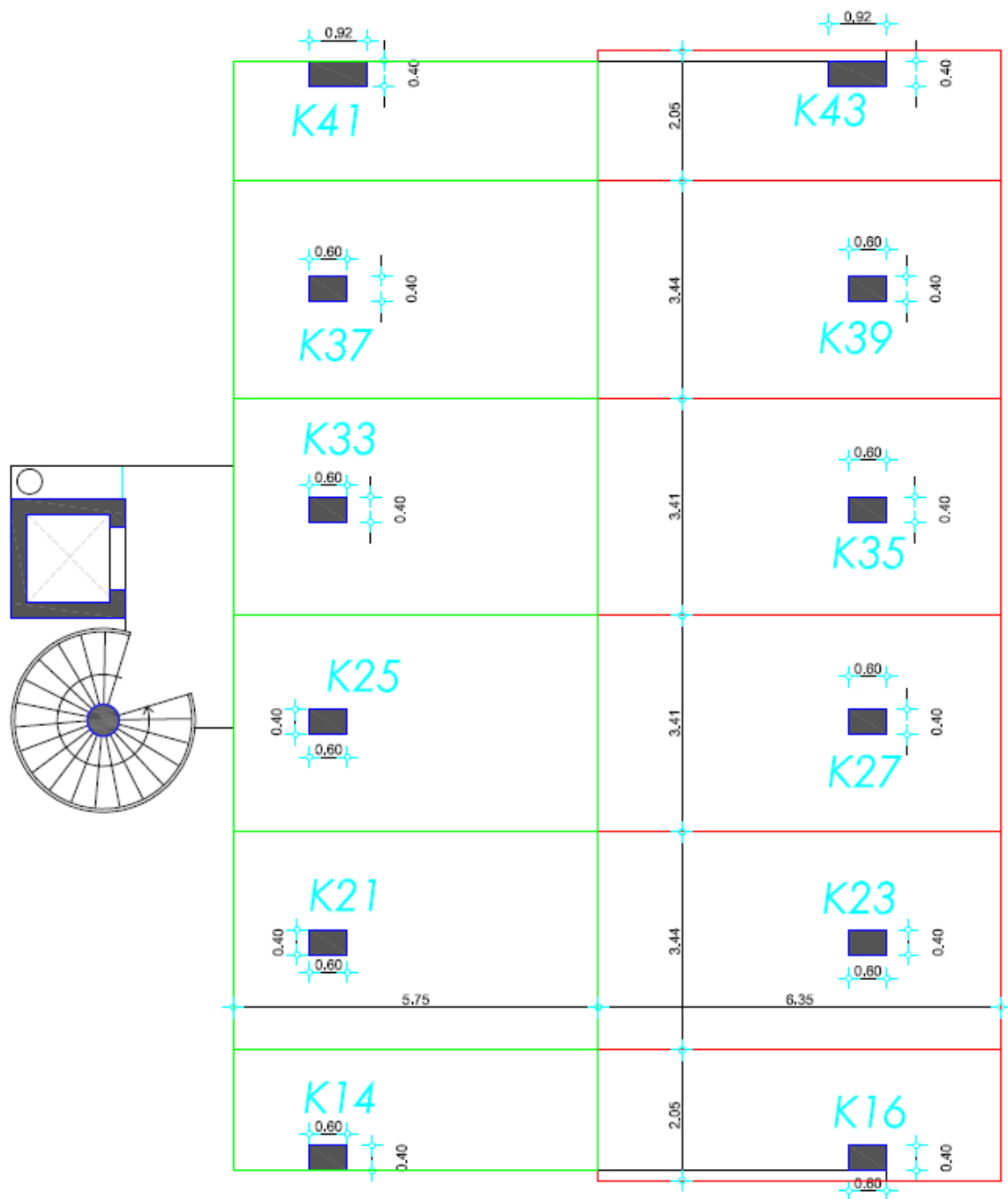


Figure 85. Typical floor plan with the columns numbering and dimensions at their base

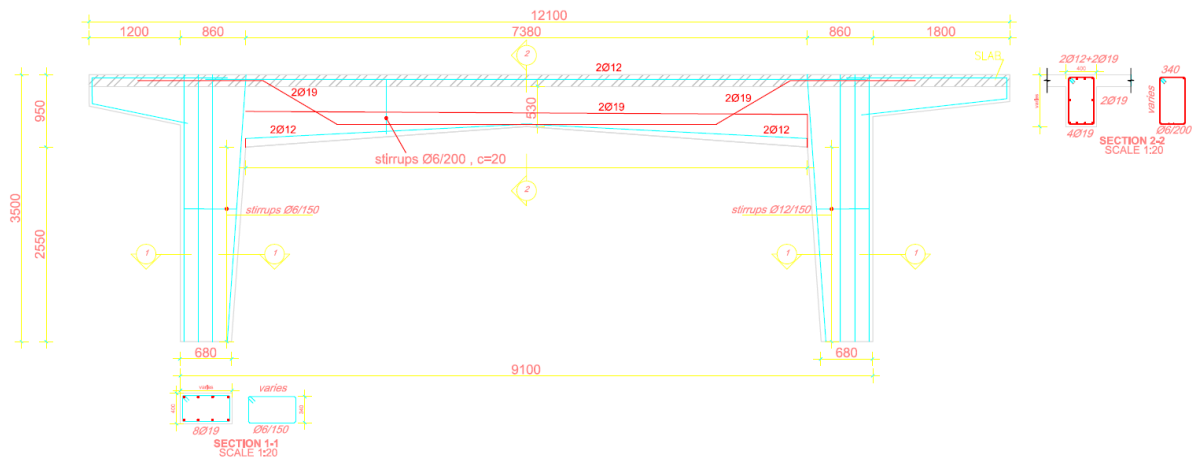


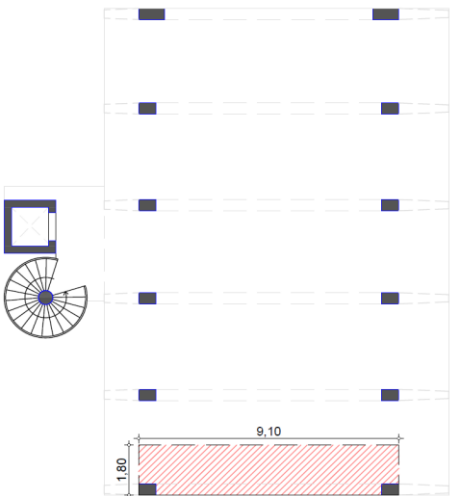
Figure 86. Geometry and detailing of 3rd floor external frame

As far as the vertical loads 'G+0.3Q' of the 3rd floor's external frame are considered (Table 11):

- North side column (close to staircase): 650.66 kN
- South side column (next to balcony): 697.43 kN
- Beam: 10.08 kN/m

The axial load imposed on the columns will be the one calculated as per Annex B 4th floor column load, since the 3rd floor's slab's weight contribution will be the distributed load on the beam.

Table 11. Loading of the external 3rd floor frame

| LOADING | |
|---|-------|
|  | |
| Slab self weight [kN/m ²] | 3.80 |
| S _{imposed} permanent load [kN/m ²] | 1.20 |
| Live floor load [kN/m ²] | 2.00 |
| G+0.3Q [kN/m ²] | 5.6 |
| Length [m] | 9.1 |
| Width of slab [m] | 1.8 |
| Beam Load [kN/m] | 10.08 |

Assessment of the failure mechanism in reinforced concrete columns

The brittle failures that may incur to old substandard members, designed without any seismic provisions, are a crucial parameter for the assessment and retrofit of historic reinforced concrete structures [10]. The hierarchy between the individual failure mechanisms must be assessed in order to determine any prevailing brittle failure. The mechanisms of column failure, in terms of Shear Force, in the columns of the external frame of the 3rd floor, were:

- Yielding of the flexural reinforcement and failure in flexure, (V_y , V_{flex})
- Shear failure, (V_v by stirrups and V_{strut} by shear strut)
- Lap splice failure, (V_{lap})
- Joint shear failure, (V_j)
- Formation of plastic hinges in the adjacent beams (ductile behavior) V_{by}

Flexural yielding and failure

For the columns under study, the moment and curvature at yielding and flexural failure were assessed by the actual Moment-Curvature diagrams with the use of RESPONSE2000 [11], and are shown in Figure 87. Due to the higher static depth of the reinforcement of the top cross section, the moment that develops is more than 100 kNm greater than the moment in the bottom cross section.

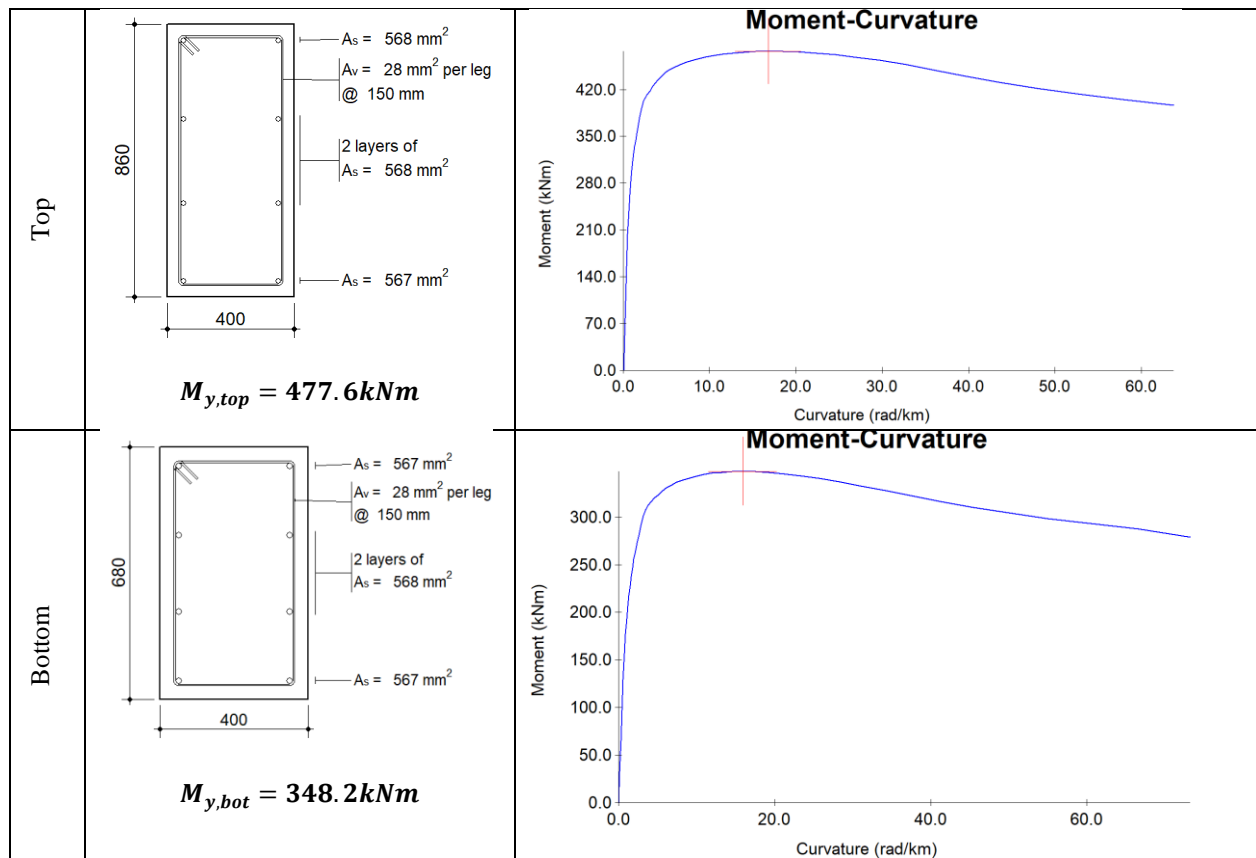


Figure 87. Moment – Curvature diagrams for external 3rd floor columns, top and bottom.

The shear corresponding to flexural failure is therefore obtained as:

$$V_{flex} = \frac{My, top + My, bot}{Ls, top + Ls, bot} = \frac{477.6 + 348.2}{2.487} = 332.046 \text{ kN}$$

$$Ls, top = 1.44 \text{ m and } Ls, bot = 1.05 \text{ m}$$

Shear failure

In order to establish the Shear load at the columns for shear failure, the Ls/h ratio is determined as <2 for both cases, top and bottom of the column. Therefore:

$$V_R = \frac{1}{\gamma_{el}} \left[\frac{h-x}{2L_v} \min(N; 0.55A_c f_c) + \left(1 - 0.05 \min\left(5; \mu_{\Delta}^{pl}\right)\right) \cdot \left[0.16 \max(0.5; \rho_{tot}) \left(1 - 0.16 \min\left(5; \frac{L_v}{h}\right)\right) \sqrt{f_c} A_c + V_w \right] \right]$$

$$\text{Column bottom} \rightarrow V_R = 315 \text{ kN and } V_{Rmax} = 454 \text{ kN}$$

$$\text{Column top} \rightarrow V_R = 486 \text{ kN and } V_{Rmax} = 516 \text{ kN}$$

Joint failure

The column-beam joints in this specific case do not have any shear reinforcement and are therefore prone to failure. Another parameter that limits their structural capacity is their distance from the slab and the perpendicular frame beams; this limits the beneficial action of confinement usually provided by the aforementioned structural elements.

$$V_{j,x} = \gamma_j \cdot 0.5 \cdot \sqrt{f_{c,b}} \cdot \sqrt{1 + \frac{v_j \cdot f_{c,b}}{0.5 \cdot \sqrt{f_{c,b}}} \cdot \frac{b_j \cdot d \cdot d_{beam}}{H_{col}}}$$

Where $\gamma_j=1$ for external unconfined joints.

$$V_{j,x} = 1 \cdot 0.5 \cdot \sqrt{16} \cdot \sqrt{\left(1 + \frac{0.20 \cdot 16}{0.5 \cdot \sqrt{16}}\right) \cdot \frac{400 \cdot 800 \cdot 900}{2500}} = \mathbf{284 \text{ kN}}$$

Lap splice failure

The lap splice of the longitudinal reinforcement in the column's bottom was also calculated for the analysis. In this specific case, the limited confinement and insufficient length of the lapping of the steel bars may lead to pullout failure due to cracking of the concrete cover around the steel bars. Another parameter that limits the lapping length capacity is the lack of ribs and the low strength of concrete. The column's shear load at lap splice failure is derived as per [12]:

$$V_{lap}$$

$$= \frac{\left[\min \left\{ \left(\mu_{fr} \cdot L_{lap} \cdot \left[\frac{A_{tr}}{s} \cdot f_{st} + \alpha_b \cdot (b - N_b \cdot D_b) \cdot f_t \right] + \right) ; N_b \cdot A_b \cdot f_y \right\} \cdot d \cdot (1 - 0.4 \cdot \xi) + \right. \\ \left. + v \cdot b \cdot d^2 \cdot f_c \cdot (0.5 \cdot h/d - 0.4 \cdot \xi) \right]}{h_{col}/2}$$

$$V_{lap} = 64 \text{ kN}$$

Prevailing mode of failure

The above analysis shows that the prevailing mode of failure of the main frames of the structure will be brittle lap splice failure. Especially for the external frames, the failure load will be 64 kN per column, or 128 kN per frame.

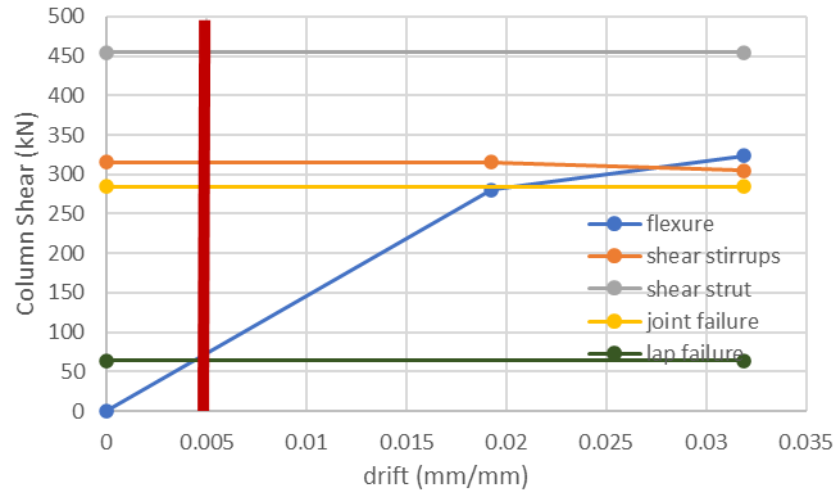


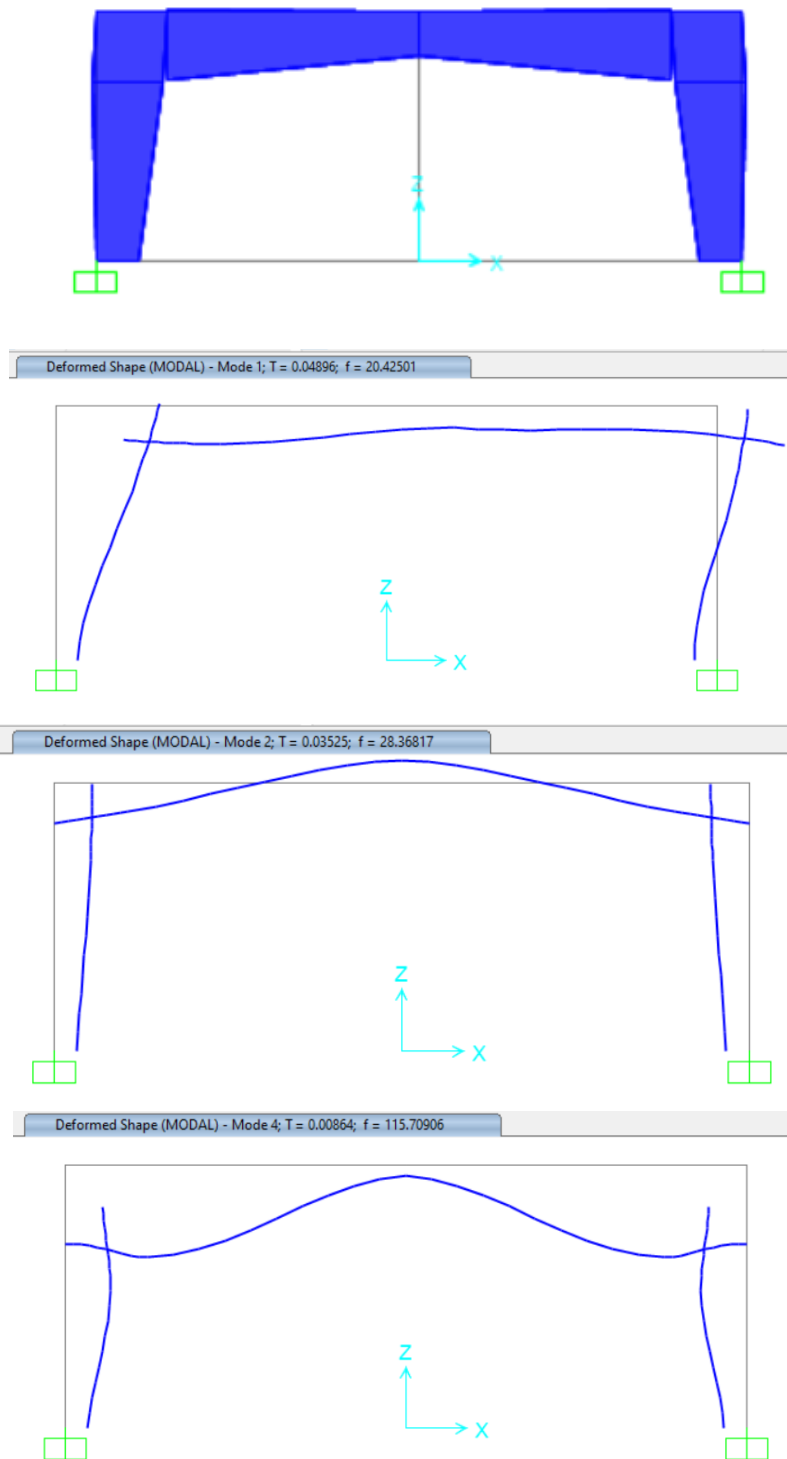
Figure 88. Comparison of different failure mechanisms in the bottom of the column

Simulation of a single frame in SAP2000

The structure was modelled in the commercial program SAP2000 [13] in order to assess its capacity under seismic conditions. The reinforced concrete beams and columns were simulated as 2-node frames. The mean average strengths were used for determining the properties of the various materials. Diaphragmatic action was applied to all the nodes of the floor level. The columns were supported on rigid joints. All the floor slabs were assigned with the load combination of $G+0.3Q$. The live load was chosen based on the Cypriot Annex of Eurocode 1 [14]. This load combination was also used as the mass of the frame for the modal analysis.

Modal characteristics of the structure

The modal analysis results are depicted in Figure 89, with the first mode to be translational in the X-direction, with a mass participation factor of 0.98.



| OutputCase | StepType Text | StepNum Unitless | Period Sec | UX Unitless | UY Unitless | UZ Unitless |
|------------|------------------|---------------------|---------------|----------------|----------------|----------------|
| MODAL | Mode | 1 | 0.04896 | 0.98186 | 0 | 0 |
| MODAL | Mode | 2 | 0.035251 | 0 | 0 | 0.30126000... |
| MODAL | Mode | 3 | 0.008868 | 2.563E-06 | 0 | 0 |
| MODAL | Mode | 4 | 0.008642 | 0 | 0 | 0.61293 |

Figure 89. Simulation of the frame with tapered members in SAP2000 and modal shapes

Pushover analysis

Two types of hinges were used in the two types of analysis performed. The first scenario was the use of ductile hinges at the column's ends, that do not take into account the brittle shear failure. The second type of hinge was only brittle shear failure, with the corresponding maximum shear strength resulting from the aforementioned analysis to be incorporated in the hinge's properties, as shown in Figure 90.

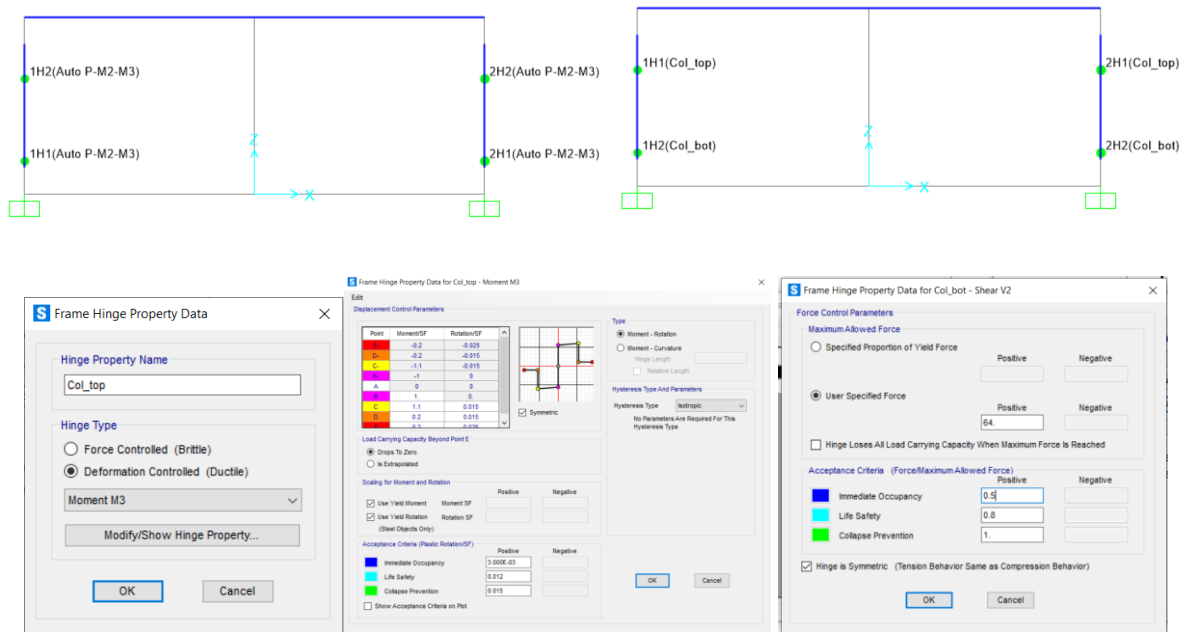


Figure 90. Hinges properties in SAP2000

The pushover curve in the case of the ductile hinges is shown in Figure 91 (top). The frame behaves elastically up to a load of 720 kN, corresponding to yielding of the flexural reinforcement in the columns, while after that a plateau appears, suggesting a great amount of ductility for the frame up to the failure of the hinges. The actual behavior of the frame is depicted in the bottom part of the same figure, where the brittle lap splice failure was incorporated in the properties of the hinges. In this case, the frame was not able to reach its yield load as before, since the columns failed at a Base Shear of 120 kN, and after that the frame's capacity to transfer loads dropped to zero.

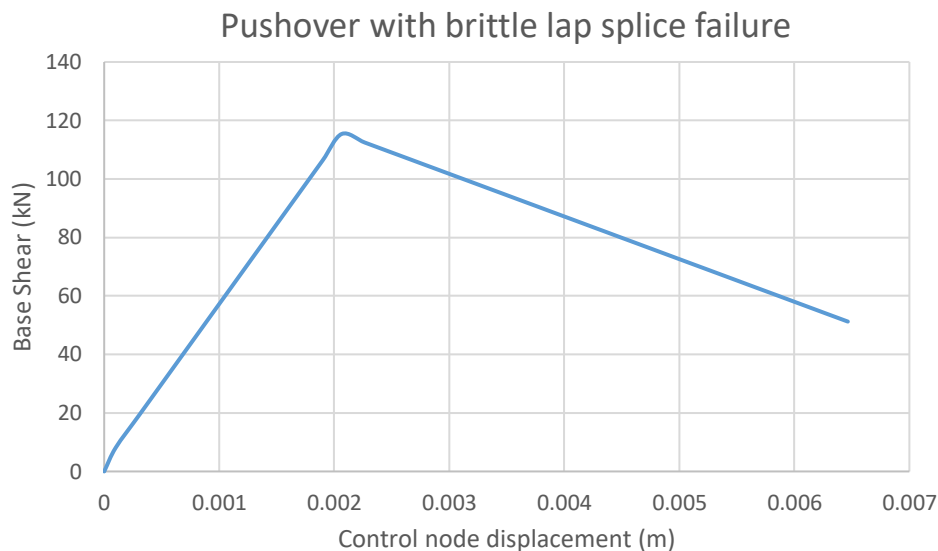
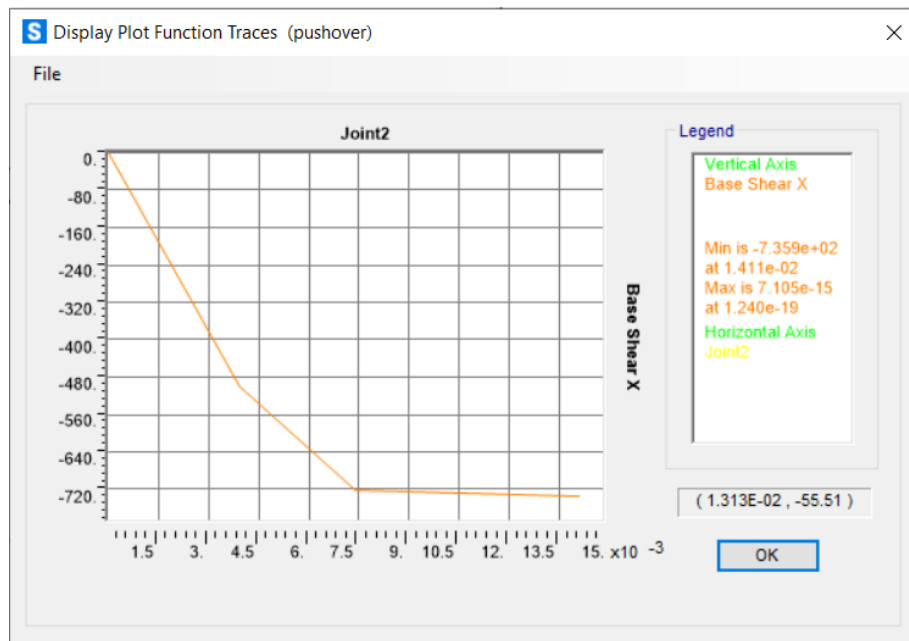


Figure 91. Pushover curve with ductile hinges (top) and brittle hinges (bottom)

Conclusions

The structural assessment of buildings requires good understanding of the various components of the structure, their interconnection and material mechanical properties, and of the global behaviour under seismic excitation. In the local components level, the task of assessing the properties of members is becoming even more challenging in the case of historic structures. In such cases, thorough member analysis has to be explicitly performed and all possible failure mechanisms must be taken under consideration.

This case study explored a cultural heritage listed reinforced concrete structure that underwent some strengthening. Non-linear pushover analysis was used for assessing the capacity of one external frame. The results from the assessment procedures show the brittle lap splice failure in the columns due to their intrinsic characteristics: sparse

stirrups, low concrete strength, no ribs. The report highlights that this type of failure must be incorporated in the analysis in order to assess the actual behavior of the structure and the brittle failures.

References

- [1] Architektoniki_issue_55_on_Cyprus.pdf n.d.
- [2] Docomomo Cyprus. Cyprus 100 [most] Important Buildings, Sites and Neighbourhoods. Nicosia: 2014.
- [3] Αιμίλιος Μιχαήλ. Ιστορική αναδρομή στο μοντερνισμό – Το μοντέρνο στην Κύπρο. Συνθέσεις 2013:86–9.
- [4] Michael, A. 18th January 2021. Personal Communication. n.d.
- [5] Ierides V, Michael E, Christofilopoulou S. Modernism second youth reserves: The example of Alexandros Demetriou Tower. Cyprus Archit Assoc Vol 6 2009:78.
- [6] Michael A, Christofilopoulou S, Ierides V. Conservation and Modern Architecture Reserves: The Alexander Demetriou Building Case, Nicosia, Cyprus. 12th Int. Docomomo Conf. Surviv. Mod. from Coffee Cup to Gen. Plan, Espoo, Finland: 2012.
- [7] Nicosia Municipality. Building Permit File of “Alexandros Demetriou Tower” 2012.
- [8] CEN. EN1998-3. Eurocode 8 : Design of structures for earthquake resistance — Part 3: Assessment and retrofitting of buildings. European Committee for Standardization, Bruxelles 2004;3.
- [9] BS EN 12390-3:2009. Testing hardened concrete, Part 3: Compressive strength of test specimens (2009). Br Stand Inst 2009.
- [10] Pardalopoulos SJ, Thermou GE, Pantazopoulou SJ. Screening criteria to identify brittle R.C. structural failures in earthquakes. Bull Earthq Eng 2013;11:607–36. <https://doi.org/10.1007/s10518-012-9390-7>.
- [11] Evan C Bentz MPC. RESPONSE2000 Reinforced Concrete Sectional Analysis using the Modified Compression Field Theory 2000.
- [12] Syntzirma D V., Pardalopoulos SI, Pantazopoulou SJ. Experimental evaluation of strength assessment procedures for R.C. elements with sub-standard details. Eng Struct 2020;224. <https://doi.org/10.1016/j.engstruct.2020.111191>.
- [13] CSI. SAP2000: Static and Dynamic Finite Element Analysis of Structures 14.0 2009.
- [14] Standard E. EUROPEAN STANDARD Eurocode 1 - Actions on structures Part 4 : Silos and tanks European Committee for Standardization 2003:1–110.

Discussion and Conclusions

Historic concrete structures are resilient at many levels. Even abandoned structures constructed over 115 years ago, like the Hennebique Silos, are still capable to perform structurally. Of course, there are damages and local failures that have to be addressed, but even in a marine environment, which is proven to be one of the worst environments for concrete, most of the structure is still salvable.

The research has shown that, in terms of structural damage, a main issue from which the historic concrete buildings can suffer are the forces derived from seismic events. As seen in the cases of Cyprus, the issues derive from the poor detailing of the reinforcement, insufficient lap splice in the joints between components and lack of shear reinforcement. Also, the strength of concrete is in some cases insufficient. Interventions, aiming at increasing its strength and ductility of the structure, are often done, when a new function is planned for the buildings.

The reports show that the quality of the reinforced concrete slightly differs among the countries, in terms of detailing and composition. The difference can be explained on the basis of the experimental character of the historic concrete, the fabrication entrusted to handicraft, and the fact that the norms on concrete fabrication and use changed in time with the acquisition of more knowledge on the new material. It should be also noticed that not always were the norms followed, as it is clearly stated by the research on the Fruit and Vegetable market in Genoa.

Two of the three buildings selected in Cyprus are an example of a late use of reinforced concrete (later than 1960); however, also on these buildings still detailing mistakes were made, which in other countries with longer concrete tradition were already resolved.

Carbonation induced corrosion of the reinforcement leading to spalling of the concrete cover and superficial damage due to moisture are the most common damage types found across the case studies. This is in agreement with the literature on the conservation of historic concrete. Besides, interventions done in the course of time may have introduced damage or have failed.

A lack of proper detailing is also commonly found in building pre-1930s like the Fenix II in Rotterdam and the market and silos of Genoa. Although this is not particularly worrisome if the building in question is not located in a seismic area.

Regarding the restored buildings, most relevant aspects for a successfully restoration seem to be the co-operation of experts, the selection of building contractors guaranteeing good quality work and a well-planned intervention. Engaging contractors, architects and engineers specialized in concrete restoration contributes to obtaining a good result, i.e. interventions technically, historically and aesthetically compatible. A precise damage mapping and detailing for each damage according to current norms, as found in the Timber factory in Vlissingen, guarantees a proper quality of the intervention and makes monitoring possible.

Specific guidelines are needed to direct the development of a consistent plan of conservation and also transformation of buildings in historic concrete in view of the (re)use. Due to their experimental character each of these buildings should be considered as a unique case, and the guidelines should be flexible enough to be applicable to different situations, though providing the basis for an integral and homogeneous approach.